Holocene Precipitation Variability, Prehistoric Agriculture, and Natural and Human-Set Fires in Costa Rica

A Dissertation Presented for the
Doctor of Philosophy
Degree
The University of Tennessee, Knoxville

Matthew Timothy Kerr
August 2019

Copyright © 2019 by Matthew Timothy Kerr

All rights reserved.

DEDICATION

This dissertation is dedicated to the memory of Leonard Nimoy [1931–2015],
who reminded us all to live long and prosper. We will, God willing.
And to my dear friends Andy Kaylor and Joe Doty,
who didn't make it. I will always miss you.
1-800-273-8255

ACKNOWLEDGEMENTS

I thank my advisor, Dr. Sally Horn, and my committee members, Drs. Chad Lane, David Anderson, and Yingkui Li, for all their support, advice, and encouragement during my time in graduate school and throughout my dissertation research and writing. Sally, I would not be who I am today without your guidance and mentoring. Chad, you are the reason I came to geography in the first place. I look forward to continuing our research and to seeing what post-graduate life brings. David, you have always been quick to provide helpful advice and a listening ear. Philip, your optimism over the years has always helped to keep my spirits up.

I owe a debt of gratitude to many faculty and friends who provided valuable consultation, encouragement, and advice over the years, including Drs. Derek Alderman, Liem Tran, Carol Harden, Melissa Hinten, and Kelsey Ellis in UT Geography, Dr. Anna Szynkiewicz in Earth and Planetary Sciences, Dr. Roger Horn in Electrical Engineering and Computer Science, and Dr. Micheline van Riemsdijk who reminded me to always celebrate the small victories.

Some of the analyses that I describe here were carried out in part at the University of North Carolina Wilmington Isotope Ratio Mass Spectrometry facility under the direction of Dr. Chad Lane and with assistance from Kim Duernberger Rosov. Chad has been instrumental in driving my learning and love of mass spectrometry. Many people from the UNCW isotope lab helped me over the years, including Amy Wagner, Elizabeth Yanuskiewicz, Krysden Schantz, Audrey Taylor, and David Coggins.

I give special thanks to Dr. Nora Reber in the UNCW Department of Anthropology. Nora was my undergraduate mentor and over the years has remained a mentor and become a friend. I don’t know where I would be today without her decade of support, but I certainly wouldn’t be finishing a PhD degree. Dr. Bill Alexander instilled in me a love of culture and theory that has

always helped me to remember that this isn't all about numbers, but also the human side. Drs. Michaela Howells and James Loudon shared their home with me during several research trips, for which I am grateful.

Many fellow UT students helped me over the years of my graduate research and studies. I thank my current and former lab mates Joanne Ballard, Erik Johanson, Mathew Boehm, Lizzie MacLennan, Jacob Cecil, and Luke Blentlinger. I thank many undergraduate students who helped me in the lab during both my MS and PhD work, including Sarah Bleakney, Paul Lemieux, Damani Driver, Leslie Muller, Justin Grabowski, Taylor Tieche, Jonathan Unger, Trell Stroud, Morgan Steckler, Julie Coulombe, Akhil Gosai, and Wesleigh Wright.

Many friends helped me with support and advice over the years. I particularly thank Katie Corcoran, Tyler Sonnichsen, Sam Williams, and Stewart Richardson. Anna Agosta G'Meiner has provided much-needed friendship and help with organizing meeting sessions over the years. Zack Taylor has remained oddly optimistic and supportive over the years, reminding me that I can do this and that sometimes it's ok to just write something ok.

Over my years at UT, I have been supported as a graduate teaching assistant and teaching associate in the Department of Geography, and by a Phi Kappa Phi Dissertation Fellowship, the UT Oscar Roy Ashley Graduate Fellowship, a research assistantship from the UT Initiative for Quaternary Paleoclimate Research, a research assistantship from UT-SARIF, and by a research assistantship supported by National Science Foundation grant #1660185 awarded to Sally Horn, Chad Lane, and Douglas Gamble. My dissertation research has been funded by National Science Foundation grants #1657170 awarded to Sally Horn and myself and grant #1660185 awarded to Horn, Lane, and Gamble. Additional support has come from the Biogeography Specialty Group of the American Association of Geographers, multiple awards from the Stewart K. McCroskey

memorial fund, and additional funds from the University of Tennessee and the University of North Carolina Wilmington.

I thank Maureen Sánchez of the University of Costa Rica for providing consultation over the years and showing me archaeological sites in the Diquís region. I also acknowledge the many former students and others who assisted Sally Horn with recovery of the lake-sediment cores that I investigated, and who carried out analyses of pollen and other proxies. I likewise acknowledge support from NSF, the National Geographic Society, The A.W. Mellon Foundation, the University of Tennessee, the University of Costa Rica, and other sponsors that made this earlier work possible, and the government of Costa Rica for granting permission for the work.

Lastly, I thank my family for all their love and support over the years. First, my wife Dr. Jacqueline Kerr, who was a year ahead of me in graduate school. She always gave me personal insight into what I would soon face. Second, to my parents Jane and Tim Kerr, who have always loved me unconditionally. They sacrificed an unmeasurable amount of family time when I couldn't be there, was there but had to work, and was there but was preoccupied. And to my sister, Emily, and her family, Shawn, Ashlyn, and Hailey. This hasn't been fair to any of you and I'm sorry. It's over now and I hope I can do better.

Finally, I thank my grandmothers, who are strong and educated women. Marjorie Kerr made me who I am today—curious, tenacious, dedicated. She was strong when most people would break. She reminded me that whenever I am lonely, I can look up at the moon and she will be looking, too. And lastly, Francis Kiskaddon, who always said "You need to get that lambskin!" Now I have a whole flock of diplomas and I hope I have made you proud.

To anyone I have overlooked, I apologize.

ABSTRACT

This dissertation presents the results of compound-specific stable hydrogen isotope analysis of *n*-alkanes from terrestrial leaf waxes preserved in sediment cores from three lakes in Costa Rica to reconstruct variations in paleohydrology during the Holocene. Results were compared with pollen and charcoal data from the same cores to examine relationships between paleohydrology, vegetation change, prehistoric agriculture, and fire, and with archaeological evidence in the watersheds of two lakes to better understand prehistoric human-environment interactions.

Lago de las Morrenas 1 (9.4925 °N, 83.4848 °W, 3480 m) is in the Chirripó páramo of Costa Rica, which was never permanently occupied by prehistoric people. The analyses demonstrate 10,000 years of millennial-scale variations in hydroclimate at Morrenas 1, which was dry during the Early Holocene, mesic during the Middle Holocene, and dry over the Late Holocene. The Morrenas sediments record local manifestations of the 8200 BP event, the 5200 BP event, the Terminal Classic Drought (TCD), and the Little Ice Age (LIA).

Laguna Bonillita (9.9921 °N, 83.6114 °W, 450 m), in the Caribbean lowlands of central Costa Rica, has a 2700-year history of continuous maize agriculture. The alkane data show variations in paleohydrology over the Late Holocene and local manifestations of the TCD and the LIA that match patterns throughout the circum-Caribbean. The Bonillita watershed was intensively farmed across the entire history of the lake. Changes in prehistoric culture and maize farming are temporally linked to climate change at Bonillita. The data indicate that maize agriculture benefitted from episodes of drier climate in this lowland rainforest environment.

Laguna Santa Elena (8.9290 °N, 82.9257 °W, 1055 m), in the Diquís archaeological subregion of southern Pacific Costa Rica, has a 2000-year history of maize agriculture. The

analyses document variations in Late Holocene paleohydrology, including local manifestations of the TCD and the LIA, that had important consequences for prehistoric people. Santa Elena may have experienced a decrease in rainfall during the TCD, but unlike the Caribbean side of the Isthmus, the amplitude of this drought event does not appear abnormal on centennial to millennial timescales. Two population collapses inferred to take place during dry periods instead happened during wet intervals at Santa Elena.

TABLE OF CONTENTS

Chapter 1 Introduction..... 1

1.1 Introduction..... 2

1.2 Research Objectives..... 4

1.3 Research Goals..... 5

1.4 Research Questions..... 6

1.5 Dissertation Organization..... 6

1.6 References..... 8

Chapter 2 Compound-Specific Stable Isotope Analysis of Holocene Paleohydrology on Cerro Chirripó, Costa Rica..... 13

2.1 Abstract..... 14

2.2 Introduction..... 15

2.3 Background..... 17

2.3.1 Extreme Climate Events..... 17

2.3.2 The Compound-Specific Stable Hydrogen Isotope (δD) Proxy..... 21

2.3.3 Geographical Setting and Lake-Sediment Research on Cerro Chirripó..... 23

2.3.4 Previous Proxy Work at Lago de las Morrenas 1..... 25

2.4 Methods..... 27

2.4.1 Radiocarbon Calibration and Age-Depth Modeling..... 27

2.4.2 Sample Preparation..... 28

2.4.3 GC Quantification and Identification..... 29

2.4.4 Isotope Ratio Mass Spectrometry..... 30

2.4.5 Data Processing and Analysis..... 31

2.5 Results....34

2.5.1 Zone 4: ca. 10,000–8600 cal yr BP....38

2.5.2 Zone 3: ca. 8600–5400 cal yr BP....38

2.5.3 Zone 2: ca. 5400–3200 cal yr BP....39

2.5.4 Zone 1: ca. 3200 cal yr BP to the Present....39

2.6 Discussion....40

2.6.1 Millennial-Scale Paleohydrology at Lago de las Morrenas 1....40

2.6.2 Local Response to Broad-Scale Climate Events....46

2.6.3 $\delta^{13}C$ and Vegetation Change....48

2.7 Conclusion....50

2.8 Acknowledgements....51

2.9 References....52

2.10 Appendix....73

2.11 Supplemental Information....85

Chapter 3 A 2700-Year History of Precipitation and Maize Agriculture in the Caribbean Lowlands of Costa Rica....87

3.1 Abstract....88

3.2 Introduction....89

3.3 Background....90

3.3.1 The Compound-Specific Stable Hydrogen Isotope (δD) Proxy....90

3.3.2 Extreme Climate Events....91

3.3.3 Geography and Archaeology of the Central Atlantic Watershed....92

3.3.4 Geography and Archaeology of Laguna Bonillita....95

3.3.5 Previous Paleoenvironmental Work at Laguna Bonillita.....98

3.4 Methods..... 101

3.4.1 Radiocarbon Calibration and Age-Depth Modeling.....101

3.4.2 Sample Preparation..... 102

3.4.3 Identification, Quantification, and Isotope Ratio Mass Spectrometry.....103

3.4.4 Data Processing and Analysis.....103

3.5 Results.....105

3.5.1 La Montaña: 2660–2250 BP..... 108

3.5.2 El Bosque: 2250–1450 BP.....109

3.5.3 La Selva: 1450–950 BP..... 110

3.5.4 La Cabaña: 950–400 BP..... 111

3.5.5 Post-Contact: 400 BP to the Present..... 112

3.6 Discussion.....112

3.6.1 Paleohydrology at Laguna Bonillita..... 112

3.6.2 Prehistoric Human-Environment Interactions..... 115

3.6.3 Extreme Climate Events: the TCD and the LIA..... 119

3.7 Conclusions.....121

3.8 Acknowledgements.....121

3.9 References.....123

3.10 Appendix.....136

3.11 Supplemental Information..... 151

Chapter 4 A 2000-Year History of Precipitation and Maize Agriculture in Southern Pacific Costa Rica.....153

4.1 Abstract.....154

4.2 Introduction.....155

4.3 Background.....156

4.3.1 The Compound-Specific Stable Hydrogen Isotope (δD) Proxy.....156

4.3.2 Extreme Climate Events.....157

4.3.3 Geography and Archaeology of Greater Chiriquí.....159

4.3.4 Geography and Archaeology of Laguna Santa Elena.....162

4.3.5 Previous Paleoenvironmental Work at Laguna Santa Elena.....163

4.4 Methods.....164

4.4.1 Radiocarbon Calibration and Age-Depth Modeling.....164

4.4.2 Sample Preparation.....164

4.4.3 Quantification, Identification, and Isotope Ratio Mass Spectrometry.....165

4.4.4 Data Processing and Analysis.....165

4.5 Results.....168

4.5.1 Zone 3: ca. 1780–1590 cal yr BP.....171

4.5.2 Zone 2c: ca. 1590–1150 cal yr BP.....171

4.5.3 Zone 2b: ca. 1150–880 cal yr BP.....172

4.5.4 Zone 2a: ca. 880–450 cal yr BP.....172

4.5.5 Zone 1: ca. 450 cal yr BP to the present.....173

4.6 Discussion.....174

4.6.1 Paleohydrology at Laguna Santa Elena.....174

4.6.2 Prehistoric Human-Environment Interactions.....178

4.6.3 Extreme Climate Events: the TCD and the LIA.....180

4.7 Conclusions....182

4.8 Acknowledgements....183

4.9 References....185

4.10 Appendix....202

4.11 Supplemental Information.... 215

Chapter 5 Summary and Conclusions....216

5.1 Summary of Research....217

5.2 Major Conclusions....217

5.2.1 Hydrogen Isotope Analysis of Holocene Paleohydrology on Cerro Chirripó.....217

5.2.2 Precipitation and Maize Agriculture in the Caribbean Lowlands of Costa Rica....218

5.2.3 Precipitation and Maize Agriculture in Southern Pacific Costa Rica....219

5.3 Future Work....219

Vita....221

LIST OF TABLES

Table 2.1 Radiocarbon determinations for Lago de las Morrenas 1.....73

Table 2.2 Plant taxa represented in the Morrenas 1 pollen assemblages.....74

Table 2.3 Global average apparent fractionation factors (ε) at Morrenas..... 75

Table 2.4 Expected δD values for modern precipitation at Morrenas..... 75

Table 3.1 Reventazón Valley cultural chronology..... 136

Table 3.2 Radiocarbon determinations for the Laguna Bonillita sediment core..... 137

Table 3.3 Plant taxa represented in the Bonillita pollen assemblages..... 138

Table 3.4 Global average apparent fractionation factors (ε) for Bonillita..... 140

Table 3.5 Expected δD values for modern precipitation at Bonillita.....140

Table 4.1 Greater Chiriquí cultural chronology.....202

Table 4.2 Radiocarbon determinations for the Laguna Santa Elena sediment core..... 203

Table 4.3 Plant taxa represented in the Santa Elena pollen assemblages..... 204

Table 4.4 Global average apparent fractionation factors (ε) for Santa Elena..... 206

Table 4.5 Expected δD values for modern precipitation at Santa Elena.....206

LIST OF FIGURES

Figure 2.1 Location of Lago de las Morrenas 1.....76

Figure 2.2 Age-depth models for Lago de las Morrenas 1.....77

Figure 2.3 Regression analyses of stratigraphically coeval bulk $\delta^{13}C$ and *n*-alkane $\delta^{13}C$.....78

Figure 2.4 Alkane distributions, CPI, and ACL for selected samples.....79

Figure 2.5 Plants represented in the LM1 pollen record.....80

Figure 2.6 Morrenas isotope data.....81

Figure 2.7 Fractionation factors (ε) between plants and precipitation.....82

Figure 2.8 Comparison of new and existing isotope data.....83

Figure 2.9 Select proxy data for Morrenas 1.....84

Figure S2.1 *n*-alkane δD values for odd numbered homologues C_{23} to C_{33}.....85

Figure S2.2 *n*-alkane $\delta^{13}C$ values for odd numbered homologues C_{23} to C_{33}.....86

Figure 3.1 Location of Laguna Bonillita and nearby Laguna Bonilla.....141

Figure 3.2 Pollen and stable carbon isotope diagram for Laguna Bonillita.....142

Figure 3.3 Data from Fig. 3.2 replotted by age.....143

Figure 3.4 Age-depth model for Laguna Bonillita.....144

Figure 3.5 Regression analyses of stratigraphically coeval bulk $\delta^{13}C$ and *n*-alkane $\delta^{13}C$.....145

Figure 3.6 Alkane distributions, CPI, and ACL for selected samples.....146

Figure 3.7 Plants represented in the Bonillita pollen record.....147

Figure 3.8 Bonillita isotope data.....148

Figure 3.9 Fractionation factors (ε) between plants and precipitation.....149

Figure 3.10 Select proxy data for Bonillita.....150

Figure S3.1 *n*-alkane δD values for odd numbered homologues C_{23} to C_{33}.....151

Figure S3.2 *n*-alkane $\delta^{13}C$ values for odd numbered homologues C_{23} to C_{31}.....152

Figure 4.1 Location of Laguna Santa Elena.....207

Figure 4.2 Age-depth model for Laguna Santa Elena.....208

Figure 4.3 Regression analyses of stratigraphically coeval bulk $\delta^{13}C$ and *n*-alkane $\delta^{13}C$.....209

Figure 4.4 Alkane distributions, CPI, and ACL for selected samples.....210

Figure 4.5 Plants represented in the Santa Elena pollen record.....211

Figure 4.6 Santa Elena isotope data.....212

Figure 4.7 Fractionation factors (ε) between plants and precipitation.....213

Figure 4.8 Select proxy data for Laguna Santa Elena.....214

Figure S4.1 *n*-alkane $\delta^{13}C$ values for odd numbered homologues C_{25} to C_{33}.....215

CHAPTER 1

INTRODUCTION

1.1 Introduction

The study of Central American lake sediments as archives of paleoenvironmental history is a powerful tool for reconstructing spatial and temporal variability in climate, ecology, and human-environment interactions during the Holocene (Horn 2007). Many microfossil and geochemical signals preserved in sediments provide evidence of vegetation changes, fire regimes, and human activity around lakes. For example, decreasing abundances of tree pollen coupled with the appearance of maize pollen in a sedimentary record is used as a marker for the arrival of prehistoric agriculture in watersheds (Goman and Byrne 1998; Clement and Horn 2001; Dull 2007; Wahl et al. 2007). Additionally, the abundance of sedimentary charcoal is used as an indicator of the scale of biomass burning (Whitlock and Larsen 2001; Walsh et al. 2014). While pollen and charcoal proxies provide important evidence for understanding paleoenvironmental history, their signals are confounded by human activity: changes in both vegetation and fire regimes can be caused by natural or anthropogenic drivers, or a combination of the two, particularly in small Neotropical watersheds that were home to increasingly complex groups of prehistoric maize agriculturalists (Bradbury 1982; Hodell et al. 1995; Haberyan and Horn 1999). Reconstructing the causes of environmental change and the degree to which those changes are related to climate versus human activity requires a proxy that is unaffected by anthropogenic landscape modification.

This dissertation research uses compound-specific stable hydrogen isotope (δD) analyses of *n*-alkanes from terrestrial leaf waxes preserved in sediment cores from three lakes to reconstruct variations in precipitation across the Holocene and compares those variations to patterns of fire, vegetation change, and prehistoric agriculture in Costa Rica. Variations in δD in sediments reflect changes in precipitation that are unaffected by human activity and can be used

to reconstruct variations in hydrology and climate change (Sachse and Gleixner 2004; Liu and Huang 2005; Sachse et al. 2006, 2010; Xia et al. 2008; Kahmen et al. 2013a, 2013b). Recent work from the Yucatan demonstrated a temporal relationship between a series of severe droughts that occurred between ca. 1200 and 850 cal yr BP, collectively known as the Terminal Classic Drought, and the collapse of Maya civilization (Hodell et al. 1995, 2005; Webster et al. 2007; Medina-Elizalde et al. 2010; Kennett et al. 2012; Douglas et al. 2015). Additionally, there is currently debate over the causes and consequences of the Little Ice Age, a multi-century cooling event that occurred ca. 550 to 100 cal yr BP, and its relationship to the Spanish Conquest, population reductions, and changes in global carbon emissions from biomass burning (Nevle and Bird 2008; Dull et al. 2010; Nevle et al. 2011; Power et al. 2013). The only way we can come to fully understand the relationships between climate, environment, and human activity is by developing proxy records that unambiguously reflect climate. This dissertation presents the first long records of precipitation variability from lake sediments in Costa Rica and explores how those records relate to evidence of vegetation, fire history, and prehistoric agriculture from the same cores, and to local and regional archaeological evidence of prehistoric human activity.

The results and interpretations in this dissertation improve understanding of the critical issue of how climate change affects human society. Researchers have demonstrated links between climate change and the collapse of Maya civilization using δD and other isotopic records (Douglas et al. 2015), but few studies have been conducted in Costa Rica on how past climate affected people. Earth is currently undergoing major changes in climate due to unprecedented anthropogenic forcing. Documenting spatial and temporal variations in precipitation and relating them to natural forcing mechanisms such as Intertropical Convergence Zone (ITCZ) migration provides crucial information regarding complex earth-system processes.

Additionally, linking reconstructions of climate variation to environmental and archaeological evidence of prehistoric human activity yields insight into the range of possible responses to climate stress and to the conditions under which prehistoric civilizations declined. Understanding the possibilities inherent in both climate and human response systems is critical to accurately predicting and planning for future change and for the resiliency of our own modern civilizations. The δD records presented here provide some of the first long-term climate reconstructions from Costa Rica and have allowed investigation of the effects of climate on vegetation, fire, and human activity, as has been done for the Maya region (Kennett et al. 2012; Douglas et al. 2015).

1.2 Research Objectives

This dissertation research investigated compound-specific stable hydrogen isotope (δD) ratios of terrestrial leaf waxes preserved in sediment cores from three small lakes in Costa Rica. These lakes are Lago de las Morrenas 1 (9.4925 °N, 83.4848 °W, 3480 m) in the Chirripó highlands straddling the continental divide in the Cordillera de Talamanca of southern Costa Rica, Laguna Bonillita (9.9921 °N, 83.6114 °W, 450 m) in the Caribbean lowlands of the Central Atlantic Watershed archaeological region, and Laguna Santa Elena (8.9290 °N, 82.9257 °W, 1055 m) in the Diquís archaeological subregion of southern Pacific Costa Rica near the border with Panama.

When compared with other indicators of past watershed conditions such as pollen and charcoal, the δD proxy of past precipitation reveals the effects of climate versus human activity on vegetation and ecosystems. For example, this method helps to determine whether changes in the amount of charcoal in sediments are due to changes in human use of fire, or whether they are also (or instead) associated with past droughts that could have led to more wildfires (Power et al.

2013). Analysis of δD signals in cores from different slopes and elevations in Costa Rica allowed the reconstruction of temporal variability in precipitation over the late Holocene from the Bonillita and Santa Elena cores, and nearly the entire Holocene from the Morrenas 1 core. The δD reconstructions of precipitation variability presented in this dissertation provide some of the first long climate records from Costa Rica and make a significant contribution toward a broader, generalizable understanding of Holocene climate variability in Central America.

1.3 Research Goals

The lake-sediment research that I present in this dissertation proceeded with three broad goals in mind:

(1) To use compound-specific stable hydrogen (δD) isotope analysis of odd-numbered *n*-alkanes of carbon chain lengths $C_{27–31}$, produced primarily by terrestrial plants as leaf waxes and preserved in lake sediment cores, to reconstruct variations in paleohydrology across the Late Holocene at Laguna Bonillita and Laguna Santa Elena and nearly the entire Holocene at Lago de las Morrenas 1.

(2) To develop paleoenvironmental reconstructions that unambiguously reflect climate to better understand relationships between climate, environment, and human activity in prehistory.

(3) To develop long records of paleoprecipitation from Costa Rica and to compare those records with paired evidence of vegetation change and fire history from the same sediment cores for all three lakes and with archaeological records of prehistoric human activity at Bonillita and Santa Elena.

1.4 Research Questions

I asked the following questions in this dissertation research:

(1) What patterns and variations in Holocene hydroclimate are recorded in the Lago de las Morrenas 1, Laguna Bonillita, and Laguna Santa Elena sediments?

(2) How do variations in precipitation over time at Bonillita and Santa Elena relate to evidence of prehistoric human activity?

(3) How are extreme climate events, such as the Terminal Classic Drought (ca. 1200–850 cal yr BP) and the Little Ice Age (ca. 550–100 cal yr BP) represented in different environments of Costa Rica?

(4) How does isotopic evidence of vegetation change relate to moist and dry conditions at the research sites?

1.5 Dissertation Organization

Chapter 2 focuses on Lago de las Morrenas 1 in highland Costa Rica. The Morrenas 1 sediment core records 10,000 years of environmental history from a watershed with no evidence of permanent prehistoric settlement and provides a valuable contrast to the lowland sites that experienced thousands of years of maize agriculture. The Morrenas 1 record shows millennial-scale variations in paleohydrology that match with patterns seen at other sites in Central America and the broader circum-Caribbean, demonstrating that climate and environmental change on the high peaks of the Cordillera de Talamanca is linked primarily to Atlantic climate forcing mechanisms.

Chapter 3 focuses on Laguna Bonillita in the Caribbean lowland rainforest of central Costa Rica. The Bonillita sediment core records 2700 years of climate and vegetation change,

prehistoric maize agriculture, and fire history in a region populated by increasingly complex groups of prehistoric people. Unlike sites in the Yucatan far to the north, the Bonillita watershed was not abandoned during events like the Terminal Classic Drought (TCD). While the Bonillita sediments record several episodes of dry conditions throughout the record, the results show that drying in the Caribbean lowlands was linked to increased settlement and maize agriculture, rather than decline. Additionally, Bonillita served as a refuge for native people moving inland as Europeans settled the Caribbean coast. The Bonillita record shows that some drying was good for maize agriculture in the generally wet Caribbean lowlands and that the site provided an attractive location for settlement with a permanent source of water over a long duration.

Chapter 4 focuses on Laguna Santa Elena at mid-elevation in southern Pacific Costa Rica. The Santa Elena sediments record 2000 years of climate and vegetation change, prehistoric maize agriculture, and fire history at varying scales and intensities. As at the other sites, Santa Elena experienced episodes of dry and wet climate over its history, including local manifestations of the Terminal Classic Drought and the Little Ice Age. The interval of the TCD was a time of major culture change at Santa Elena and, more broadly, in southern Costa Rica and western Panama, but our new data show that the TCD was not nearly as dry at Santa Elena as it was on the Caribbean side of the Isthmus. Rather, the TCD at Santa Elena was a time of climate instability that had episodes of both dry and wet conditions. As at Bonillita, the data show that some drying was good for maize agriculture at Santa Elena and that two major periods of population decline happened during wet conditions—first during the TCD and again prior to the LIA—contrary to findings far to the north in the Yucatan.

1.6 References

Bradbury JP (1982) Holocene chronostratigraphy of Mexico and Central America. *Striae* 16: 46–48.

Clement RM and Horn SP (2001) Pre-Columbian land-use history in Costa Rica: a 3000-year record of forest clearance, agriculture and fires from Laguna Zoncho. *The Holocene* 11(4): 419–426.

Douglas PMJ, Pagani M, Canuto MA, Brenner M, Hodell DA, Eglinton TI and Curtis JH (2015) Drought, agricultural adaptation, and sociopolitical collapse in the Maya Lowlands. *PNAS* 112(18): 5607–5612.

Dull RA (2007) Evidence for forest clearance, agriculture, and human-induced erosion in Precolumbian El Salvador. *Annals of the Association of American Geographers* 97: 127–141.

Dull RA, Nevle RJ, Woods WI, Bird DK, Avnery S and Denevan WM (2010) The Columbian Encounter and the Little Ice Age: abrupt land use change, fire, and greenhouse forcing. *Annals of the Association of American Geographers* 100(4): 755–771.

Goman M and Byrne R (1998) A 5000-year record of agriculture and tropical forest clearance in the Tuxtlas, Veracruz, Mexico. *The Holocene* 8: 83–89.

Haberyan KA and Horn SP (1999) A 10,000 year diatom record from a glacial lake in Costa Rica. *Mountain Research and Development* 19(1): 63–70.

Hodell DA, Brenner M, Curtis JH, Medina-González R, Ildefonso-Chan Can E, Albornaz-Pat A and Guilderson TP (2005) Climate change on the Yucatan Peninsula during the Little Ice Age. *Quaternary Research* 63: 109–121.

Hodell DA, Curtis JH and Brenner M (1995) Possible role of climate in the collapse of Classic Maya civilization. *Nature* 375: 391–394.

Horn SP (2007) Late Quaternary lake and swamp sediments: recorders of climate change and environment. In: Bundschuh J and Alvarado GE (eds) *Central America: Geology, Resources and Hazards*, Volume 1. London: Taylor and Francis, pp. 427–445.

Kahmen A, Hoffmann B, Schefuß E, Arndt SK, Cernusak LA, West JB and Sachse D (2013a) Leaf water deuterium enrichment shapes leaf wax *n*-alkane δD values of angiosperm plants II: observational evidence and global implications. *Geochimica et Cosmochimica Acta* 111: 50–63.

Kahmen A, Schefuß E and Sachse D (2013b) Leaf water deuterium enrichment shapes leaf wax *n*-alkane δD values of angiosperm plants I: experimental evidence and mechanistic insights. *Geochimica et Cosmochimica Acta* 111: 39–49.

Kennett DJ, Breitenbach SFM, Aquino VV, Asmerom Y, Awe J, Baldini JUL, Bartlein P, Culleton BJ, Evert C, Jazwa C, Macri MJ, Marwan N, Polyak V, Prufer KM, Ridley HE, Sodemann H, Winterhalder B and Haug GH (2012) Development and disintegration of Maya political systems in response to climate change. *Science* 338: 788–791.

Liu W and Huang Y (2005) Compound specific *D*/*H* ratios and molecular distributions of higher plant leaf waxes as novel paleoenvironmental indicators in the Chinese Loess Plateau. *Organic Geochemistry* 26: 851–860.

Medina-Elizalde M, Burns SJ, Lea DW, Asmerom Y, von Gunten L, Polyak V, Vuille M and Karmalkar A (2010) High resolution stalagmite climate record from the Yucatán Peninsula spanning the Maya terminal classic period. *Earth and Planetary Science Letters* 298: 255–262.

Nevle RJ and Bird DK (2008) Effects of syn-pandemic fire reduction and reforestation in the tropical Americas on atmospheric CO_2 during European conquest. *Palaeogeography, Palaeoclimatology, Palaeoecology* 264: 25–38.

Nevle RJ, Bird DK, Ruddiman WF and Dull RA (2011) Neotropical human-landscape interactions, fire, and atmospheric CO_2 during European conquest. *The Holocene* 21(5): 853–864.

Power MJ, Mayle FE, Bartlein PJ, Marlon JR, Anderson RS, Behling H, Brown KJ, Carcaillet C, Colombaroli D, Gavin DG, Hallett DJ, Horn SP, Kennedy LM, Lane CS, Long CJ, Moreno PI, Paitre C, Robinson G, Taylor Z and Walsh MK (2013) Climate control of the biomass-burning decline in the Americas after AD 1500. *The Holocene* 23(1): 3–13.

Sachse D and Gleixner G (2004) Hydrogen isotope ratios of recent lacustrine sedimentary *n*-alkanes record modern climate variability. *Geochimica et Cosmochimica Acta* 68(23): 4877–4889.

Sachse D, Gleixner G, Wilkes H and Kahmen A (2010) Leaf wax *n*-alkane δD values of field-grown barley reflect leaf water δD values at the time of leaf formation. *Geochimica et Cosmochimica Acta* 74: 6741–6750.

Sachse D, Radke J and Gleixner G (2006) *δ*D values of individual *n*-alkanes from terrestrial plants along a climate gradient – implications for the sedimentary biomarker record. *Organic Geochemistry* 37: 469–483.

Wahl D, Schreiner T, Byrne R and Hansen R (2007) A paleoecological record from a Late Classic Maya reservoir in the north Petén. *Latin American Antiquity* 18: 212–222.

Walsh MK, Prufer KM, Culleton BJ and Kennett DJ (2014) A Late Holocene paleoenvironmental reconstruction from Agua Caliente, southern Belize, linked to regional climate variability and cultural change at the Maya polity of Uxbenká. *Quaternary Research* 82: 38–50.

Webster JW, Brook GA, Railsback LB, Cheng H, Edwards RL, Alexander C and Reeder PP (2007) Stalagmite evidence from Belize indicating significant droughts at the time of the Preclassic Abandonment, the Maya Hiatus, and the Classic Maya collapse. *Palaeogeography, Palaeoclimatology, Palaeoecology* 250: 1–17.

Whitlock C and Larsen C (2001) Charcoal as a fire proxy. In: Smol JP, Birks HJB and Last WM (eds) *Tracking Environmental Change Using Lake Sediments. Volume 3: Terrestrial, Algal, and Siliceous Indicators*. Dordrecht: Kluwer Academic Publishers, pp. 75–97.

Xia Z-H, Xu B-Q, Mügler I, Wu G-J, Gleixner G, Sachse D and Zhu L-P (2008) Hydrogen isotope ratios of terrigenous *n*-alkanes in lacustrine surface sediment of the Tibetan Plateau record the precipitation signal. *Geochemical Journal* 42: 331–33.

CHAPTER 2

COMPOUND-SPECIFIC STABLE ISOTOPE ANALYSIS OF HOLOCENE PALEOHYDROLOGY ON CERRO CHIRRIPO, COSTA RICA

This chapter is in preparation for submission to a journal. The use of "we" in the text refers to me and my co-authors, Sally Horn and Chad Lane. As first author, I led on study design, data collection and analyses, and writing the manuscript.

2.1 Abstract

Lago de las Morrenas 1 (9.4925 °N, 83.4848 °W, 3480 m) is the largest lake on the northern slope of Cerro Chirripó in the Cordillera de Talamanca of Costa Rica. We conducted compound-specific stable hydrogen (δD) and carbon ($\delta^{13}C$) isotope analysis on *n*-alkanes from terrestrial leaf waxes preserved in a 10,000-year long profile of sediments that accumulated in the lake. Our results demonstrate millennial-scale variations in hydroclimate on Cerro Chirripó across the Holocene, with dry conditions during the Early Holocene but gradually increasing precipitation, mesic conditions during the Middle Holocene and a gradual drying trend, and highly variable conditions over the Late Holocene. This general pattern is punctuated by several centennial-scale manifestations of global extreme climate events, including dry conditions during the 8200 cal yr BP event, the 5200 cal yr BP event, and the Terminal Classic Drought, and by wet conditions during the Little Ice Age. Our $\delta^{13}C$ analyses demonstrate that carbon isotope signals are responding to changes in hydroclimate at the site and reinforce prior interpretations of a stable páramo vegetation community that established following deglaciation and persisted throughout the Holocene.

2.2 Introduction

The study of Central American lake sediments as archives of paleoenvironmental history is a powerful tool for reconstructing spatial and temporal variability in climate and ecology during the Holocene (Horn 2007). Many microfossil and geochemical signals preserved in sediments provide evidence of environmental change around lakes. For example, variations in sedimentary pollen allow researchers to reconstruct changes in vegetation (Seppä 2013), abundances of charcoal are used as an indicator of the frequency and scale of biomass burning (Whitlock and Larsen 2001), and chironomid remains provide evidence of temperature variation (Porinchu and MacDonald 2003). While pollen, charcoal, and chironomid proxies provide important evidence for understanding paleoenvironmental history, they can only provide indirect evidence of climate change. For example, an increased abundance of sedimentary charcoal at a given point in time indicates a period of increased fire, which researchers may infer to represent a time of relatively drier climate. Reconstructing the *causes* of environmental change and the degree to which those changes are related to climate events such as extreme drought requires a proxy that directly measures the variable of interest.

Our research presented here uses compound-specific stable hydrogen isotope (δD) analyses of *n*-alkanes from terrestrial leaf waxes preserved in a sediment core from Lago de las Morrenas 1 (LM1), a small glacial lake in the Chirripó páramo of highland Costa Rica (Kappelle and Horn 2016), to reconstruct variations in paleohydrology across the Holocene. Additionally, we compare those variations to patterns of fire and vegetation change recorded in the same lake. Variations in δD in sediments reflect changes in paleoprecipitation that can be used to reconstruct timelines of paleohydrology and climate change, including the occurrence and timing of extreme climate events (Sachse and Gleixner 2004; Liu and Huang 2005; Sachse et al. 2006,

2010; Xia et al. 2008; Kahmen et al. 2013a, 2013b). For example, recent work from the Yucatan has demonstrated a temporal relationship between a series of severe droughts that occurred between ca. 1200 and 850 cal yr BP, collectively known as the Terminal Classic Drought (TCD), and the collapse of Maya civilization (Hodell et al. 1995, 2005; Webster et al. 2007; Medina-Elizalde et al. 2010; Kennett et al. 2012; Douglas et al. 2015). Investigations by our research group and others have reported proxy evidence of local manifestations of the TCD in Costa Rica and concluded that the effects of those droughts had important implications for the environment and for prehistoric civilizations in the region (Anchukaitis and Horn 2005; Taylor et al. 2013; Wu et al. 2017, 2019b; Johanson et al. forthcoming; Kerr et al. forthcoming). However, the only way we can come to fully understand the relationships between climate and environment in the past is by developing proxy records that unambiguously reflect climate. In this project, we present the first long record of paleoprecipitation variability from lake sediments in Costa Rica and explore how that variation relates to evidence of local vegetation and fire history.

Documenting spatial and temporal variations in precipitation and relating them to teleconnected forcing mechanisms such as shifts in the mean annual position of the Intertropical Convergence Zone (ITCZ) provides crucial information regarding complex earth-system processes. Understanding the possibilities inherent in climate systems is critical for accurately predicting and planning for future change. The δD record that we present here provides a climate reconstruction from Costa Rica covering nearly the entire Holocene, showing the effects of climate on vegetation and fire and local manifestations of global-scale extreme climate events. While precipitation reconstructions from isotopic signatures in speleothems and sediments exist from the Yucatan (Hodell et al. 2005) and the Cariaco Basin (Haug et al. 2003; Peterson and Haug 2006), such reconstructions are just now beginning to emerge from Central America and

Costa Rica (Lachniet et al. 2004a, 2004b, 2007, 2009), making this an open area of research in a region with complex atmospheric dynamics.

We asked three questions in our research: (1) what patterns and variations in Holocene paleohydrology are recorded in the Lago de las Morrenas 1 sediments, (2) how are global-scale extreme climate events such as the 8200 cal yr BP event and the Terminal Classic Drought represented in highland Costa Rica, and (3) how does isotopic evidence of vegetation change relate to moist and dry conditions at our research site?

2.3 Background

2.3.1 Extreme Climate Events

The last several decades have seen a significant rise in scholarship on climate change and extreme events, with particular interest in the widespread effects of major shifts to Earth's climate that are globally coincident, yet locally asynchronous. For example, analyses of speleothems and lake sediments from the Yucatan have linked the decline of Maya civilization to a series of severe droughts (Hodell et al. 1995, 2005; Webster et al. 2007; Medina-Elizalde et al. 2010; Kennett et al. 2012; Douglas et al. 2015). Collectively called the Terminal Classic Drought (TCD), these multi-decadal droughts occurred between ca. 1200 and 850 cal yr BP (Hodell et al. 2005; Lane et al. 2014) across the circum-Caribbean region and largely overlap with the wider effects of the Medieval Climate Anomaly (MCA) between ca. 1000 and 700 cal yr BP (Mann et al. 2008, 2009).

We have reported evidence of similarly intense drought during the TCD on Hispaniola using δD analysis of lake sediments (Lane et al. 2014), while Wu et al. (2019b) reported dry conditions at Laguna Zoncho in southern Pacific Costa Rica and at Lago de las Morrenas 3C (ca.

100 m from Morrenas 1) in the Costa Rican highlands from analyses of subfossil chironomids at both sites and bulk sedimentary stable carbon isotopes ($\delta^{13}C$) at Morrenas 3C. Additional evidence of dry conditions comes from a distinct charcoal layer in sediments from Lago Chirripó (Horn and Sanford 1992; Horn 1993) and from increased $\delta^{18}O$ values in a speleothem from Panama (Lachniet et al. 2004b). Marine sediments from the Cariaco Basin off northern Venezuela provide some of the most robust evidence for widespread effects of the TCD. Changes in the mean annual position of the Intertropical Convergence Zone (ITCZ) have been linked to variations in rainfall over northern South America recorded by amounts of titanium in laminated sediments from this anoxic basin (Haug et al. 2003; Peterson and Haug 2006). These findings from Cariaco, along with terrestrial evidence from the broader circum-Caribbean, point to a more southerly mean annual position of the ITCZ as a likely cause of the TCD (Haug et al. 2003; Hodell et al. 2005; Peterson and Haug 2006; Kennett et al. 2012; Luzzadder-Beach et al. 2012).

Evidence for the Little Ice Age (LIA), a widespread multi-century cooling event that occurred between ca. 550 and 100 cal yr BP, likewise appears in the Cariaco sediments. Decreases in titanium content indicate decreased rainfall and increased aridity in the region during this time (Haug et al. 2001; Peterson and Haug 2006; Black et al. 2007). Terrestrial records also indicate widespread drought during the LIA in the broader circum-Caribbean. For example, Hodell et al. (2005) reported aridity in the Yucatan based on oxygen isotope ($\delta^{18}O$) analysis of carbonates from lake-sediment cores. Similarly, Lane et al. (2011b) used $\delta^{18}O$ analysis of sedimentary ostracod valves to demonstrate LIA aridity on Hispaniola. Wu et al. (2019b) reported high-resolution data showing evidence of warm and wet conditions during the first part of the LIA ca. 550–350 cal yr BP followed by cooling and drying during the latter part

ca. 350–100 cal yr BP at Lago de las Morrenas 3C, along with cooling at Laguna Zoncho but with mixed evidence for moisture conditions there. Taylor et al. (2013) reported sedimentary pollen and stable isotope evidence of agricultural decline at Laguna Zoncho that corresponds to LIA drought, while Kerr et al. (forthcoming) reported similar evidence for agricultural decline and hypothesized climate deterioration at nearby Laguna Santa Elena in Costa Rica.

Somewhat less research has been conducted in the Neotropics on the effects of the 8200 cal yr BP event, which manifested globally ca. 8400–8000 cal yr BP as a period of generally cool and dry climate that was less severe than the previous Younger Dryas event but more pronounced than the later LIA (Stuiver et al. 1995; Alley et al. 1997; Alley and Ágústsdóttir 2005; Kobashi et al. 2007). Most terrestrial evidence for the effects of the 8200 cal yr BP event comes from Europe and North America, but several studies have reported dry conditions from tropical Africa and the Americas. Proxy data from Cariaco Basin sediment cores indicate dry conditions and a more southerly mean annual position for the ITCZ, resulting in decreased rainfall in Central America, as with the later TCD and LIA (Hughen et al. 1996; Haug et al. 2001). Gasse (2000) reported lower lake levels in Africa, while Thompson et al. (2002) reported evidence of regional drying from ice cores on Mt. Kilimanjaro. In northern central Costa Rica, Lachniet et al. (2004a) found evidence of dry conditions and a weakened monsoon during the 8200 cal yr BP event using $\delta^{18}O$ analysis of a speleothem from Venado Cave. Additionally, League and Horn (2000) and Watson (2011) reported increased charcoal in sediments from Lago de las Morrenas 1 and 4, respectively, which could indicate a dry period coincident with the 8200 cal yr BP event (Watson 2011).

Evidence also exists for a similarly abrupt global climate event that occurred ca. 5400–5000 cal yr BP, albeit with differing regional manifestations (Magny et al. 2006; Thompson et al.

2006; Brooks 2010). Research from the low latitudes (ca. 30 °N and S) of Asia and Africa shows significant climate variability during this event, recorded in speleothems from Israel (Bar-Matthews et al. 1997, 1999), signals of abrupt drying in marine sediments off the coast of Mauritania (DeMenocal et al. 2000) and lake sediments from Ethiopia (Chalié and Gasse 2002), and rapid cooling in ice core $\delta^{18}O$ data from Mt. Kilimanjaro (Thompson et al. 2006). In the Americas, researchers have suggested that the 5200 cal yr BP event manifested as either cool and dry (Street-Perrott and Perrott 1990; Thompson et al. 1995, 2006; Keigwin 1996) or warm and wet (Clausen et al. 1979; Moy et al. 2002; Stríkis et al. 2011; Atwood 2015). Importantly, Wu et al. (2019a) reported rapid warming, increased moisture, and intense wildfire centered on ca. 5200 cal yr BP from analyses of subfossil chironomids, sedimentary charcoal, and bulk $\delta^{13}C$ from Lago Ditkebi in highland Costa Rica, ca. 2.8 km from our Morrenas site.

Considerable work remains to understand the teleconnections, forcing mechanisms, causes, and consequences of these abrupt, global climate events. Disentangling proxy evidence for these events in Central America is difficult due to a long history of human disturbance and becomes even more difficult later in the Holocene when complex civilizations developed in the Americas (Bradbury 1982; Haberyan and Horn 1999). For example, researchers have documented reduced charcoal in lake sediments from sites in Central America, which they have interpreted as evidence of population collapse brought on by Spanish Conquest during the LIA (Bush and Colinvaux 1994; Behling 2000; Clement and Horn 2001; Dull et al. 2010). Recently, investigators have begun reexamining possible relationships between the temporally synchronous Spanish Conquest and the Little Ice Age. Power et al. (2013) synthesized sedimentary charcoal records for the last ca. 2000 years and found that fires declined globally during the LIA. They concluded that global cooling, rather than European contact, may have

driven the shifts in burning indicated by charcoal records. Conversely, other researchers have suggested that LIA cooling was not the driver of reduced burning, but rather the reduction in burning that resulted from Spanish Conquest and population collapse reduced global carbon dioxide levels, which in turn caused the LIA (Nevle and Bird 2008; Dull et al. 2010; Nevle et al 2011). Sorting out causes and consequences of extreme climate events from proxy records remains challenging, particularly for the Neotropics—an area that was profoundly influenced by prehistoric human activity. Developing long proxy records from sites such as the Chirripó highlands of Costa Rica, which have yielded no evidence of permanent settlement by prehistoric people, using new techniques such as compound-specific isotope analysis has high potential to contribute to this debate.

2.3.2 The Compound-Specific Stable Hydrogen Isotope (δD) Proxy

Compound-specific stable hydrogen isotope (δD) analyses of lipids preserved in lake-sediment cores has emerged in recent years as a powerful means for reconstructing past temporal and spatial variation in precipitation. The oxygen isotope ($\delta^{18}O$) composition of biogenic carbonates is more widely used as a precipitation proxy (Hodell et al. 1995; Huang et al. 2004; Lane et al. 2014; Wahl et al. 2014), but low pH levels in many tropical lakes prevent carbonate preservation, making $\delta^{18}O$ analyses impossible at such sites. The δD proxy shows significant promise for producing records of paleoprecipitation variability from sites such as ours in the Chirripó highlands of Costa Rica where carbonate preservation is poor.

Research has shown that the δD composition of sedimentary *n*-alkane components of terrestrial leaf waxes serve as indicators of watershed hydrology. Sachse and Gleixner (2004) collected lake sediments along a climate transect and assessed δD values of terrestrial *n*-alkanes.

They documented a strong correlation between δD values of C_{31} *n*-alkane and the δD composition of meteoric water. The δD signal from meteoric water is locked into leaf waxes at the time of formation. The resulting biogeochemical signal from this plant matter is then incorporated into lakes through processes of transportation and sedimentation, preserving a stratigraphic record of watershed hydrology (Sachse et al. 2010). Thus, the sedimentary δD record serves as a proxy for precipitation variability through time (Stuiver 1970; Cohen 2003; Sachse and Gleixner 2004).

Increased *n*-alkane δD values in terrestrial plant waxes are interpreted as signals of aridity due to preferential evapotranspiration of the lighter protium (^{1}H) hydrogen isotope from water relative to deuterium (^{2}H), which results in enrichment of the heavier isotope in remaining groundwater available to plants. Conversely, decreased δD values indicate more humid conditions due to a greater abundance of ^{1}H isotopes in available water. Importantly, understanding the specific precipitation and evapotranspiration components of the hydrologic cycle is not necessary for using the δD proxy in the Neotropics, as both decreased precipitation and increased evaporation result in aridity and relatively higher δD values in leaves and sediments (Douglas et al. 2015). Other studies have reported that the amount of precipitation is the primary control on meteoric water δD values in Central America (Dansgaard 1964; Lachniet and Patterson 2002) and that evaporation of water prior to uptake by plants is the main driver of δD enrichment in páramo ecosystems (Polissar and Freeman 2010), and have confirmed the sensitivity of terrestrial *n*-alkane δD values to meteoric δD (Liu and Huang 2005; Sachse et al. 2006; Xia et al. 2008; Kahmen et al. 2013a, 2013b). This biomarker signal of drought has been used to develop paleoclimate records from late Quaternary sediments by multiple research

groups (Tierny et al. 2008; Niedermeyer et al. 2010; Schefuß et al. 2011; Lane and Horn 2013; Lane et al. 2014).

2.3.3 Geographical Setting and Lake-Sediment Research on Cerro Chirripó

Lago de las Morrenas 1 (LM1; Fig. 2.1; 9.4925 °N, 83.4848 °W, elevation 3480 m, area 5.2 ha, maximum depth 8.3 m) is the largest lake on the northern slope of Cerro Chirripó in the Cordillera de Talamanca of Costa Rica (Horn and Haberyan 2016). LM1 formed following deglaciation at the end of the Pleistocene like most other lakes in the Chirripó páramo, including those in adjacent valleys (Orvis and Horn 2000; Lachniet and Seltzer 2002; Horn et al. 2005). Basal sediments date to ca. 13,000 cal yr BP, with the organic portion of the record dating to ca. 10,000 cal yr BP (Horn 1993; Lane et al. 2011a). The site is surrounded by treeless páramo vegetation comprising evergreen shrubs, grasses, and perennial herbs (Kappelle and Horn 2016). The C_3 dwarf bamboo *Chusquea subtessellata* Hitch. dominates much of the páramo, including the area surrounding LM1 and other lakes in the cirque at the head of the Valle Morrenas. Grasses in the genus *Muhlenbergia* along with sedges compose the C_4 component of vegetation at the site. Unlike the vast majority of lake sites in Costa Rica, archaeologists have found no evidence that prehistoric people permanently occupied the watershed of LM1 or adjacent upland areas.

Data spanning the years 1971–2000 from the Cerro Páramo meteorology station (9.5600 °N, 83.7531 °W, 3466 m) ca. 30 km west of Cerro Chirripó in the Buenavista páramo record mean annual temperatures averaging ca. 8.5 °C with little intra-annual variation and distinctly seasonal rainfall with ca. 2300 mm of precipitation falling between May and November and ca. 300 mm from December to April (Horn 1993; Lane et al. 2011a; Kappelle and Horn 2016).

However, precipitation on Cerro Chirripó may be lower, averaging ca. 1000–2000 mm annually (Barquero 2006; Kappelle and Horn 2016; Esquivel-Hernández et al. 2018). Low rainfall during the dry season allows ground litter to dry and promotes wildfires (Kerr et al. 2018). This pattern is strongly linked to Intertropical Convergence Zone dynamics (Lane et al. 2011a). During the boreal winter, the ITCZ is in its southernmost position, which allows for intensification and lowering of the trade wind inversion (TWI). This, in turn, weakens atmospheric convection, decreases cloud formation, and decreases precipitation on Cerro Chirripó. During the boreal spring and summer, northward migration of the ITCZ weakens and raises the TWI, allowing for stronger convection and increased precipitation (Dohrenwend 1972; Coen 1983; Stadtmüller 1987; Hastenrath 1991; Waylen et al. 1996; Lane and Horn 2013; Esquivel-Hernández et al. 2018; Maldonado et al. 2018). Researchers have attempted to link precipitation dynamics on Cerro Chirripó to other forcing mechanisms within Walker cell circulation and beyond, including the El Niño Southern Oscillation (ENSO), the Atlantic Multi-Decadal Oscillation (AMO), the Pacific Decadal Oscillation (PDO), and others, but so far no clear relationships have been established (Wu et al. 2019b).

A considerable amount of research has been conducted on lake sediments from Cerro Chirripó. Horn and colleagues previously analyzed Morrenas 1 sediments for pollen, microscopic and macroscopic charcoal, and diatoms (Horn 1993; Haberyan and Horn 1999; League and Horn 2000). These records show a relatively stable environment over the Holocene at the Morrenas site; however, the macroscopic charcoal record indicates millennial-scale changes in the fire regime, with more fire activity in the Early- and Late Holocene and reduced burning during the Middle Holocene. More recently, Lane and colleagues (2011a, 2013) conducted coarse-resolution compound-specific $\delta^{13}C$ and δD analyses of *n*-alkanes on LM1

sediments. They concluded that changes in the mean northerly position of the ITCZ led to these millennial-scale changes, with dry conditions prevailing in the Early- and Late Holocene and relatively moist conditions in the Middle Holocene, corresponding to the time of reduced burning (Lane et al. 2011a; Lane and Horn 2013). Sediment cores have been recovered and studied from other lakes in the upper Valle de las Morrenas. Watson (2011) examined loss-on-ignition, pollen, and charcoal in a core from Morrenas 4 (lake numbering system from Orvis and Horn 2000). More recently, Wu et al. (2019b) examined chironomids, charcoal, and bulk $\delta^{13}C$ in a short core from Morrenas 3C dating to ca. 1650 cal yr BP. Beyond Morrenas, Horn (1993) studied sedimentary charcoal evidence from Lago Chirripó in the adjacent Valle de las Lagos that supports interpretations of fire history from Morrenas, while Wu et al. (2015, 2019a) reported findings from chironomids, macroscopic charcoal, and bulk $\delta^{13}C$ from nearby Lago Ditkebi in the Valle Ditkebi that are broadly similar to previous work, but differ in some ways (see below).

2.3.4 Previous Proxy Work at Lago de las Morrenas 1

Horn and colleagues recovered two sediment cores from LM1 in 1989 using a square-rod piston corer (Wright et al. 1984) and a plastic tube fitted with a rubber piston for the uppermost, watery sediments (Horn 1993). The core sections were extruded in the field and returned to the Laboratory of Paleoenvironmental Research at the University of Tennessee where they were photographed and described. The organic portion of LM1 core 1 comprises ca. 5.41 m of sediments, while core 2 contains ca. 5.27 m of organic sediments. The organic portions of both cores are underlain by transition sediments and glacial flour. Horn (1993) reported six conventional radiocarbon dates on bulk sediments from core 2 with a basal calibrated age of ca.

12,163–11,270 cal yr BP at 534.75 cm. Lane et al. (2011a) reported six AMS ^{14}C dates on bulk sediments from core 1 with a basal age of ca. 11,313–11,170 cal yr BP at 541 cm.

Horn (1993) sampled 30 stratigraphic levels of core 2 for pollen and microscopic charcoal analysis and reported a stable vegetation assemblage with little variation from the time of deglaciation to the present. Haberyan and Horn (1999) sampled core 2 for diatom analysis at similar depths to the previous pollen work. They reported a stable diatom community with little variation across the entire Holocene, similar to the findings for pollen, although the authors did find increased abundances of diatom valves at ca. 2430 ^{14}C yr BP that they interpreted as evidence of dry conditions matching findings at other sites in Costa Rica (Horn and Sanford 1992) and in the Yucatan (Curtis and Hodell 1996). At ca. 1200 ^{14}C yr BP, a time of drought elsewhere, they found only a broad increase in diatom valve abundance (Haberyan and Horn 1999). League and Horn (2000) sampled 345 levels of core 2 for high-resolution macroscopic charcoal analysis and reported millennial-scale variation in fire regimes, with some occurrences of fire in the Early Holocene, little to no fire in the Middle Holocene, and sustained high levels of fire in the Late Holocene.

More recently, Lane et al. (2011a) sampled core 1 at 47 depths for bulk $\delta^{13}C$, including 37 samples in the organic sediments and 10 in the underlying transition sediments and glacial flour, and at 12 depths (9 organics, 3 transition) for compound-specific $\delta^{13}C$ analysis. From those $\delta^{13}C$ data, Lane et al. (2011a) reported aridity at the Morrenas site during the Early- and Late Holocene and more mesic conditions during the Middle Holocene. Following that work, Lane and Horn (2013) reported compound-specific δD data for 10 samples in core 1 (8 organics, 2 transition) that support the earlier findings of millennial-scale variations in paleohydrology based on $\delta^{13}C$ analysis. Our new work reported here, involving many more sample analyses and based

on new understanding of sedimentation and age-depth relationships, extends the δD and compound-specific $\delta^{13}C$ record for Morrenas 1 and revises previous interpretations of the δD record by Lane and Horn (2013). Our findings confirm and extend the evidence of ITCZ dynamics as a driver of changes to paleohydrology on Cerro Chirripó.

2.4 Methods

2.4.1 Radiocarbon Calibration and Age-Depth Modeling

We recalibrated the radiocarbon dates reported by Lane et al. (2011a) for core 1 and by Horn (1993) for core 2, produced updated age-depth models, and generated point estimates for our sampled levels using the 'clam' package (v. 2.3.2; Blaauw 2019) for the R Statistical Environment (v. 3.5.2; R Core Team 2019) and the IntCal13 radiocarbon calibration curve (Reimer et al. 2013). Lane et al. (2011a) and Horn (1993) originally used linear interpolation to develop age models for the Morrenas 1 cores. Here we also use linear interpolation. We experimented with Bayesian methods of creating age models using the 'rbacon' package for R (v. 2.3.6; Blaauw and Christen 2019), but those models were unable to produce satisfactory depositional histories for the Morrenas 1 cores, given the complex nature of the shift from inorganic glacial flour, to transition sediments, to organic gyttja. We are aware of the limitations of linear interpolation, primarily that it forces unrealistic breakpoints on the radiocarbon dates in the age-depth curve; nevertheless, we find linear interpolation to be a satisfactory model for the site history at Lago de las Morrenas 1 that allows us to directly compare our results from the organic lake sediments in the cores with previous studies (Kerr et al. forthcoming). We used one date from core 1 (AA-52074, 541 cm) in the core two age model and two dates from core 2

(Beta-30435, 521 cm; Beta-31787, 534.75 cm) in the core 1 age model to better constrain the timing of the change from transitional to organic sedimentation in the basin.

2.4.2 Sample Preparation

We sampled the upper organic section of Morrenas 1 core 1 (0–541 cm) for compound-specific isotope analysis at depth intervals of 4–32 cm, corresponding to time intervals of ca. 50–775 calibrated years, guided by our age-depth model and constrained by the availability of sediments remaining from previous studies. Two large gaps exist in our sampling scheme, one between 162 and 127 cm because of sediment loss during core recovery and another between 30 and 2 cm, a portion of the core that was heavily sampled for previous hydrogen isotope analysis (Lane and Horn 2013).

We oven-dried our sediments at 50 °C, then ground them to a fine powder with a mortar and pestle. Sample dry masses ranged from ca. 2.3 to 8.4 g. Samples were extracted three times by sonication for 1 hour with 2:1 by volume dichloromethane and methanol (Fisher Scientific, Optima grade; 150-100-50 mL, total solvent volume 300 mL). The samples were centrifuged after each extraction and the solvent was filtered through glass fiber filters (Whatman GF/A, pore size 1.6 μm), collected in round-bottom flasks, concentrated by rotary evaporation, and blown dry under N_2 gas at 50 °C. Samples were then saponified in an 80 °C oven for two hours with 3 mL of 5% KOH by volume in a solution of 80:20 methanol and purified water. The saponification reaction was quenched with water and the neutral fraction recovered from the total lipids with 3 x 3 mL hexane rinses, and then blown dry. The neutral fraction was further cleaned on silica gel columns (Supelclean LC-Si, particle size 45 μm) under vacuum with dichloromethane as the mobile phase and blown dry. *n*-Alkanes were isolated from the cleaned

neutral fraction by urea adduction. The samples were dissolved in 1.5 mL of 2:1 by volume hexane and acetone, treated with 1.0 g of urea in 4.0 mL of warm methanol, and cooled in a freezer at –10 °C for one hour. The solvent was blown dry and branched and cyclic alkanes were rinsed from the precipitated urea with 3 x 3 mL dichloromethane. The urea was dissolved in 10 mL purified water and *n*-alkanes were recovered with 3 x 3 mL rinses of hexane to yield the adducted fraction. The adducts were blown dry, transferred to GC vial inserts, spiked with a squalane isotope standard (provided by A. Schimmelmann, Indiana University) to monitor instrument precision, and dissolved in 200 μL of hexane. At this point, the *n*-alkane samples were ready for analysis.

2.4.3 GC Quantification and Identification

We quantified alkane abundances and confirmed compound identifications using a Thermo Fisher Trace 1310 gas chromatograph (GC) flame ionization detector (FID) system equipped with a Thermo TriPlus RSH autosampler and interfaced to a Thermo ISQ LT single quadrupole mass spectrometer (MS). Tandem injections of 1.0 μL volume in hexane were introduced into the GC-MS-FID system by splitless injection through PTV inlets at 300 °C with a head pressure of 70 kPa until 0.05 min and a total flow of 50 mL/min. The chromatographic columns were Thermo Scientific TG-5MS (length 30 m, diameter 0.25 mm, film thickness 0.25 μm) using helium as the carrier gas set to a constant flow of 1.5 mL/min, resulting in an average velocity of 44.6 cm/sec. The GC oven program was 60 °C isothermal for 1 min, then 16 °C/min to 160 °C, followed by 8 °C/min to 320 °C, and finally isothermal at 320 °C for 12 minutes. The MS transfer line was set to 300 °C. The MS was operated in electron impact (EI) mode and scanned the total ion current (TIC) from 50–550 AMU with a source temperature of 300 °C and

a quad temperature of 300 °C. The FID was set to 300 °C, with a flow of hydrogen at 30 mL/min, zero air at 350 mL/min, and N_2 makeup gas at 40 mL/min. Alkanes were quantified by an external calibration curve built using 0.50, 0.75, 1.00, 1.25, and 1.50 μg/mL of an *n*-alkane standard (Supelco #49452-U, C_7–C_{40} saturated alkanes) in hexane. Compounds were identified by elution time vs. the Supelco *n*-alkane standard and confirmed by comparing sample mass spectra to the NIST 11 mass spectral database.

2.4.4 Isotope Ratio Mass Spectrometry

We analyzed compound-specific δD and $\delta^{13}C$ using a Thermo Fisher Trace 1310 gas chromatograph (GC) system equipped with an AI/AS 1310 autosampler interfaced to a Thermo DELTA V Plus continuous flow isotope ratio mass spectrometer (IRMS) through a ConFlo IV interface and a GC IsoLink II device. Injections of 1.0 μL were introduced into the GC-IRMS system by splitless injection through a split/splitless inlet at 350 °C with a total flow of 6 mL/min. Reactor temperatures were 1420 °C for hydrogen and 1000 °C for carbon. The chromatographic column was a Thermo Scientific TG-5MS (length 60 m, diameter 0.25 mm, film thickness 0.25 μm) using helium as the carrier gas set to a constant flow of 1.0 mL/min, resulting in an average velocity of 25.9 cm/sec. The GC oven program was 70 °C isothermal for 1 min, then 20 °C/min to 180 °C, followed by 5 °C/min to 320 °C with a 15 min hold, and finally 30 °C/min to 350 °C with a 1 min hold. All samples were analyzed in duplicate and data from the replicate runs were averaged to produce a single value for each datum. ^3H factors were assessed daily. An external isotope standard (*n*-alkane mixture B4, supplied by A. Schimmelmann, Indiana University) was analyzed between every four sample runs to monitor instrument accuracy and precision.

2.4.5 Data Processing and Analysis

We quantified abundances for all alkane homologues of carbon chain lengths C_{21} to C_{33} as μg/gram of dry sediment. Alkane distributions of terrestrial organic matter have a strong odd-over-even dominance in carbon chain lengths. Additionally, longer carbon chain lengths (≥27 carbon atoms) indicate terrestrial organic matter from higher plants, while relatively shorter carbon chain lengths (≤25 carbon atoms) indicate organic matter produced by algae and aquatic plants (Marzi et al. 1993). To assess the strength of the terrestrial signal in our data, we calculated the carbon preference index (CPI) for each of our samples, following Marzi et al. (1993), as:

$$CPI_{C21-33} = \frac{\left(\sum_{i=n}^{m} C_{2i+1}\right)+\left(\sum_{i=n+1}^{m+1} C_{2i+1}\right)}{2\left(\sum_{i=n+1}^{m+1} C_{2i}\right)} \quad \text{(Eq. 1)}$$

where n = the starting alkane number/2, m = the ending alkane number/2, and i = index. Additionally, we calculated average carbon chain length (ACL), following Feakins et al. (2016), as:

$$ACL_{C21-33} = \frac{\sum(C_n * n)}{\sum(C_n)} \quad \text{(Eq. 2)}$$

where n = carbon number ranges and C_n = the concentration of the homologues containing n carbon atoms.

We analyzed isotope data for all odd chain alkane homologues from C_{23} to C_{33}. Here we focus on δD and $\delta^{13}C$ data for C_{27}, C_{29}, and C_{31} alkanes because they are reliable indicators of terrestrial vegetation and fractionation factors (ε) between plants and mean annual precipitation for these homologues are available in the published literature (Sachse et al. 2012). Isotope data for C_{23} and C_{25} homologues, which can function as biomarkers for aquatic plants, along with data for the C_{33} homologue, are in the supplemental information for this chapter (Fig. S2.1). We quantified analytical uncertainty in our compound-specific δD and $\delta^{13}C$ data following the

methods of Polissar and D'Andrea (2014). In addition to terrestrial leaf wax δD and $\delta^{13}C$ values, we also present z-scored, vegetation-corrected δD values for paleoprecipitation (δD_{PP}), following Feakins (2013). Vegetation change can shift the balance of δD fractionation factors (ε) for land cover in a watershed, thus affecting the composition of plant-wax δD signals recorded in lake sediments without necessarily requiring changes to δD in regional paleohydrology. To account for this possible bias in the plant-based δD proxy, we combined pollen data for Morrenas 1 core 2 (Horn 1993), the supplementary dataset of Sachse et al. (2012) comprising a survey of published vegetation fractionation factors, and a two-endmember linear mixing model for grasses and sedges assuming average $\delta^{13}C$ values of –34.0‰ for C_3 and –20.1‰ for C_4 to produce an unbiased, ε-corrected paleoprecipitation reconstruction for the Morrenas site. The mixing model was calculated following Lane et al. (2009) as:

$$\delta_m = f_A\delta_A + f_B\delta_B \qquad \text{(Eq. 3)}$$

and:

$$1 = f_A + f_B \qquad \text{(Eq. 4)}$$

and:

$$f_A = \frac{(\delta_M - \delta_B)}{(\delta_A - \delta_B)} \qquad \text{(Eq. 5)}$$

where δ_M represents the mean isotopic composition of C_{27}, C_{29}, or C_{31} leaf wax *n*-alkanes, δ_A and δ_B represent the mean isotopic composition of carbon sources A and B, and f_A and f_B are the proportion of sources A and B in the mixture. The vegetation-corrected fractionation factors were then calculated as:

$$\varepsilon_{corr} = \sum_i^n [f_n * \varepsilon_n] \qquad \text{(Eq. 6)}$$

where f_n represents the fraction for a given plant life form and ε_n represents the mean global fractionation factor between leaf wax and precipitation for that life form.

Hydrogen and carbon isotope compositions are reported in standard δ-per mil notation, with hydrogen values relative to Vienna Standard Mean Ocean Water (VSMOW) and carbon values relative to the Vienna Pee Dee Belemnite (VPDB) marine carbonate standard, where:

$$\mathrm{R} = {}^{2}\mathrm{H}/{}^{1}\mathrm{H} \text{ or } {}^{13}\mathrm{C}/{}^{12}\mathrm{C} \qquad \text{(Eq. 7)}$$

and:

$$\delta D \text{ or } \delta^{13}C = \left[\frac{R_{sample} - R_{standard}}{R_{standard}}\right] * 1000 \qquad \text{(Eq. 8)}$$

Repeated analyses of our squalane internal standard indicated that instrument precision for our samples (1 SD) averaged ca. 2.5‰ for hydrogen and 1.3‰ for carbon. Repeated analyses of our external isotope standard indicated that propagated error for our dataset (1 SEM) averaged ca. 6.5‰ for hydrogen and 0.8‰ for carbon.

We plotted our new z-scored, ε-corrected δD values for paleoprecipitation (δD_{PP}) for the $C_{27\text{-}31}$ odd *n*-alkanes, along with select pollen, spore, and microscopic charcoal data from Horn (1993), vegetation categorized by life form (following Sachse et al. 2012; Feakins 2013), macroscopic charcoal data from League and Horn (2000), bulk $\delta^{13}C$ from Lane et al. (2011a), and Cariaco Basin titanium data tuned by Kennett et al. (2012) using C2 (v. 1.7.7; Juggins 2007). We plotted proxy data by calibrated age, with all previous data replotted following our new age-depth models. Stratigraphic diagrams are divided into informal zones based on major changes in proxy data.

Pollen percentages for *Alnus* and Poaceae are calculated based on pollen sums for each sampled level (excluding spores and indeterminates; Horn 1993). Counts of spores of the quillwort *Isoetes* (probably *I. storkii* T.C. Palmer, which occurs today in the glacial lakes of the Chirripó massif) are expressed as a ratio of spores to total pollen. For our vegetation correction to δD values, plants represented in the pollen record are categorized by taxonomy and life form

as pteridophytes (excluding *Isoetes*), forbs (non-graminoid herbs), total graminoids (Poaceae and Cyperaceae), C_3 and C_4 graminoids (calculated as a percentage of total graminoids using our mixing model), angiosperm shrubs of the páramo or adjacent subalpine forest, angiosperm trees of the subalpine or montane forest, and gymnosperms of the montane forest (*Prumnopitys*, formerly *Podocarpus*). Microscopic and macroscopic charcoal data are presented as influx values (fragments/cm^2/yr).

Bulk and compound-specific $\delta^{13}C$ and δD plant wax values originally reported in Lane et al. (2011a) and Lane and Horn (2013) are presented here in standard δ-per mil notation, as above, alongside our new plant wax $\delta^{13}C$ and δD data for comparison. Some depths from previous isotope work were adjusted slightly based on a new depth model.

2.5 Results

Our recalibration of previous radiocarbon dates (Table 2.1) and new age modeling (Figure 2.2) indicate that the organic sediments of Lago de las Morrenas 1, extending to 541 cm in core 1 and to 527 cm in core 2, began accumulating ca. 10,000 cal yr BP. The transition sediments below are modeled to contain a hiatus toward the end of deglaciation, but modeled ages for these sediments and for the underlying glacial flour, which are not included in our study, are tentative and may be too old as shown based on cosmogenic isotope dating of moraines in the valley (Potter et al. 2019). Regression analysis comparing bulk and compound-specific $\delta^{13}C$ values indicates minimal pre-aging of alkanes prior to sedimentation (Fig. 2.3; Lane et al. 2016).

The upper 541 cm of Morrenas 1 core 1 on which we focus here is composed of homogenous organic gÿttja (Lane et al. 2011a). High-resolution analysis of the organic content of the corresponding portion of Morrenas 1 core 2 showed an average organic content of ca.

41.4% (range ca. 29.5–49.4%) and an average inorganic content of ca. 58.6% (range ca. 50.6–70.5%), as estimated by loss-on-ignition (LOI) at 550 °C (Dean 1974; League 1998, unpublished dataset). LOI at 1000 °C by Horn (1993) suggested carbonate contents of no more than ca. 2–5% in gÿttja and underlying mineral sediments; however, the loss of interstitial water in clays between 550 °C and 1000 °C (Dean 1974) could have inflated reported carbonate values.

Alkane homologue distributions for all samples display a consistent odd-over-even carbon chain pattern, which is expected of terrestrial organic matter (Fig. 2.4). Carbon preference indices (CPI), which provide a measure of the relative abundances of even- and odd-chain length compounds, average 4.4 (range 2.6–5.4) in the core (Fig. 2.4). Even-carbon *n*-alkanes are typical of microbes and other non-terrestrial organisms (CPI ca. 1.0), while odd-carbon *n*-alkanes are typical of terrestrial vegetation (CPI >3) (Bray and Evans 1961; Eglinton and Hamilton 1963, 1967; Marzi et al. 1993). CPI values for all samples in core 1, excepting the lowest one, are >3, indicating a predominantly terrestrial organic matter source over the past ca. 9700 cal years. The bottom sample at 531.5 cm (ca. 9890 cal yr BP) has a slightly lower CPI value of 2.6, consistent with a lower relative importance of terrestrial carbon sources immediately post deglaciation as plants recolonized newly deposited glacial till surrounding the lake.

Average chain lengths (ACL) range from 26.7–28.6 ($\bar{x}$ = 28.0) through the core (Fig. 2.4). Relatively shorter odd-numbered *n*-alkanes (≤25 carbon atoms) are typical of algae and aquatic vegetation, while relatively longer *n*-alkanes (≥27 carbon atoms) are typical of terrestrial organic matter (Han et al. 1968; Cranwell et al. 1987; Poynter et al. 1989; Poynter and Eglinton 1990; Ficken et al. 2000; Meyers 2003; Feakins et al. 2016; Lane 2017). ACL values for all samples in core 1 except for the lowest two are >27, indicating a predominantly terrestrial origin for sedimentary *n*-alkanes. The bottom two samples at 523.5 and 531.5 cm (9691 and 9890 cal yr

BP, respectively) have ACL values of 26.7 and 26.9 (Fig. 2.4), indicating an increased importance of autochthonous carbon early in the lake's history. Increased abundances of C_{23} and C_{25} homologues in the alkane distributions for these two samples (Fig. 2.4) support this finding.

Based on pollen assemblages in core 2, Horn (1993) determined that treeless páramo vegetation established shortly following deglaciation on Cerro Chirripó and persisted to the present. Shifts in percentages of pollen and spores from páramo taxa and those of adjacent subalpine and montane forests indicated a possible upslope shift in tree line position over the Holocene and some possible variations in forest and páramo composition resulting from changes in climate or from human disturbance at lower elevation. Our categories for plant life forms and their respective fractions of total vegetation include: gymnosperms (0–1.3%, $\bar{x}$ = 0.5), angiosperm trees (42.2–63.0%, $\bar{x}$ = 57.3), angiosperm shrubs (2.1–12.8%, $\bar{x}$ = 5.4), total graminoids (14.5–39.5%, $\bar{x}$ = 23.2), forbs (0–4.0%, $\bar{x}$ = 2.0), and pteridophytes (7.3–17.7%, $\bar{x}$ = 11.8) (Fig. 2.5, Table 2.2). Our mixing model for C_{27}, C_{29}, and C_{31} *n*-alkanes allowed us to estimate the relative abundances and contributions of C_3 grasses dominated by *C. subtessellata* and C_4 grasses comprising mostly *Muhlenbergia* spp., yielding values of ca. 11.7–26.3% for C_3 grasses and sedges ($\bar{x}$ = 17.7%) and 0.9–27.7% for C_4 grasses and sedges ($\bar{x}$ = 2.0%). Our apparent fractionation factors between alkane homologues and mean annual precipitation ($\varepsilon_{C27-31/MAP}$) for C_{27}, C_{29}, and C_{31} *n*-alkanes for each vegetation category (Sachse et al. 2012) are in Table 2.3.

Values for $\delta D_{PP/C27}$ ranged from –72.6‰ to –7.8‰ VSMOW ($\bar{x}$ = –53.5‰), while $\delta D_{PP/C29}$ ranged from –68.6‰ to –22.2‰ ($\bar{x}$ = –55.7‰) and $\delta D_{PP/C31}$ ranged from –76.4‰ to –7.9‰ ($\bar{x}$ = –60.2‰). Mean δD_{PP} values for the Morrenas 1 record are within the hypothesized range of δD for meteoric water at our site location and elevation predicted by the OIPC3.1

(Bowen 2019), ranging from –95‰ to –52‰, and averaging –80‰ (Table 2.4). Likewise, our δD_{PP} values match well with precipitation δD data reported by Esquivel-Hernández et al. (2018) for the period of September 2015 to July 2017 ranging –155.5‰ to –10.6‰ ($\bar{x}$ = –72.4‰). Z-scores of our δD_{PP} values (Fig. 2.6) reveal the timing of millennial-scale changes in paleohydrology, albeit with two large gaps in data for the uppermost sediments deposited during the Late Holocene. Patterns in our leaf wax $\delta^{13}C$ values closely parallel values for δD (Fig. 2.6). Values for $\delta^{13}C_{C27}$ range from –33.53‰ to –20.53‰ VPDB ($\bar{x}$ = –29.70‰), while $\delta^{13}C_{C29}$ ranged from –33.42‰ to –24.24‰ ($\bar{x}$ = –31.02‰) and $\delta^{13}C_{C31}$ ranged from –33.60‰ to –28.91‰ ($\bar{x}$ = –31.13‰). Fractionation factors (ε) between plants and precipitation vary through time with changes in vegetation composition (Fig. 2.7), demonstrating the importance of the vegetation correction to the δD proxy (Feakins 2013).

The overall patterns of compound-specific δD and $\delta^{13}C$ for plant waxes reported by Lane et al. (2011a) and Lane and Horn (2013) from the organic section of the LM1 core match the patterns in our new isotope data; however, we were unable to integrate the datasets because the values appear incompatible (Fig. 2.8). Combining the old data with our new data introduced unrealistic variations in the isotope proxies that are not supported by other proxy data. The small number of samples from the older work (n = 8 for δD; n = 9 for $\delta^{13}C$ in the organic sediments) precludes accurate statistical testing, but visual assessment supports our interpretation that the earlier data are incompatible with our newer data (Fig. 2.8). We attribute this incompatibility in the isotope datasets to advances in analytical technology during the years between research projects.

2.5.1 Zone 4: ca. 10,000–8600 cal yr BP

Zone 4 begins with the driest period in the Morrenas 1 record, with z-scores for δD_{PP} at ca. +4 SD for C_{27} and C_{29}, and ca. +3 for C_{31} at 9890 cal yr BP (Fig. 2.6). Compound-specific $\delta^{13}C$ values are also relatively high at the beginning of the record, as are δD values for leaf waxes. A high contribution of C_4 plants to the proxy record in zone 4 suggests an increased importance of taxa favoring cool and dry conditions, such as *Muhlenbergia* spp., in the watershed. Moving upward in zone 4, values for δD_{PP}, δD and $\delta^{13}C$ of leaf waxes, and bulk $\delta^{13}C$ all steadily decrease, indicating gradual change toward a less arid climate across this period. The contribution of C_4 plants to sedimentary organic matter also declines toward the top of zone 4, after which the relative proportion of C_4 plants never again rises above 8%. Proxy data in zone 4 show relatively low percentages of *Alnus* pollen blowing upslope from montane forests at lower elevation, increased percentages of Poaceae pollen from the surrounding páramo, low ratios of *Isoetes* spores to pollen, high influx of macroscopic charcoal particles >500 μm, and relatively high bulk $\delta^{13}C$ values (Fig. 2.9).

2.5.2 Zone 3: ca. 8600–5400 cal yr BP

Zone 3 begins with a wet interval indicated by decreased δD_{PP} z-scores and δD values for leaf waxes. This is followed by an increase in isotope values at ca. 8200 cal yr BP and a brief period of increased macroscopic charcoal influx. An extended period of average to slightly moist conditions then persists until ca. 7100 cal yr BP, after which z-scores for δD_{PP} and leaf wax δD and $\delta^{13}C$ values decline sharply. The z-score for $\delta D_{PP/C29}$ reaches the lowest value in the record of –1.5 at ca. 6900 cal yr BP, while $\delta D_{PP/C31}$ declines to –2.0. Conditions briefly return to average ca. 6750 cal yr BP, only to fall sharply again into another pronounced wet period at ca.

6175 cal yr BP. Following the second dip to very wet conditions, isotope values begin increasing at the top of zone 3, indicating the onset of a drying trend. Zone 3 shows higher percentages of *Alnus* pollen, low ratios of *Isoetes* spores to pollen, relatively low bulk $\delta^{13}C$ values, and little to no charcoal influx.

2.5.3 Zone 2: ca. 5400–3200 cal yr BP

The bottom of zone 2 begins with an episode of pronounced drying at ca. 5300 cal yr BP, indicated by relatively higher δD values for leaf waxes and increased δD_{PP} z-scores across all three *n*-alkane homologues. Notably, the z-score for $\delta D_{PP/C31}$ of 1.5 is the highest for the record, excepting the lowest sample near the bottom of the core. A*lnus* pollen decreases, while Poaceae pollen, ratios of *Isoetes* spores to pollen, and charcoal influx all increase during a major drying episode centered on ca. 5300 cal BP. Following this 400-year dry period, δD and δD_{PP} values indicate mixed and highly variable moisture conditions for the next ca. 3100 years. Compound-specific $\delta^{13}C$ values remain steady across this zone, indicating stability in terrestrial vegetation. Bulk $\delta^{13}C$ values peak in the middle of zone 2 at ca. 4300 cal yr BP and then decline, following Poaceae pollen percentages. High influx of charcoal in both micro- and macroscopic size classes shows the occurrence of frequent fires throughout zone 2. Ratios of *Isoetes* spores to pollen are relatively high in zone 2.

2.5.4 Zone 1: ca. 3200 cal yr BP to the Present

Sample availability resulted in two large gaps in our new compound-specific isotope dataset, one from ca. 3250–1500 and the second from ca. 900–50 cal yr BP. The interval for which we *do* have new isotope data covers ca. 1500 to 900 cal yr BP and overlaps with the

Terminal Classic Drought and the broader Medieval Warm Period. Values for δD and $\delta^{13}C$ of leaf waxes, z-scores for δD_{PP}, and microscopic charcoal influx are all higher during a drier than average period. No macroscopic charcoal data exist for this interval due to the placement of a radiocarbon date in core 2, but microscopic charcoal reaches its apex here. During this period, Cariaco basin titanium percentages generally decline and become highly variable due to decreased precipitation in northern South America. Bulk $\delta^{13}C$ values increase toward the middle of zone 1. Micro- and macroscopic charcoal influx remains high and steady, showing the occurrence of frequent fires. *Alnus* pollen percentages are generally low across zone 1, while ratios of *Isoetes* spore to pollen are high.

2.6 Discussion

2.6.1 Millennial-Scale Paleohydrology at Lago de las Morrenas 1

The δD_{PP} record from Morrenas 1 demonstrates millennial-scale variations in paleohydrology that were likely controlled by changes in the mean annual position of the Intertropical Convergence Zone, which itself was driven by changes in location of the subsolar point and the thermal equator due to orbital precession (Hodell et al. 1991; Haug et al. 2001; Peterson and Haug 2006; Yancheva et al. 2007; Lane et al. 2011a; Lane and Horn 2013). Our data show generally dry conditions on Cerro Chirripó during the latter part of the Early Holocene, mesic conditions throughout the Middle Holocene, and dry, but highly variable conditions in the late Holocene, supporting previous findings in sediments from the same lake (Horn 1993; League and Horn 2000; Lane et al. 2011a; Lane and Horn 2013).

At the bottom of our sediment core in zone 4, z-scores for δD_{PP} are the highest in the record indicating very dry conditions following deglaciation. Values for δD and $\delta^{13}C$ of leaf

waxes are both high at the bottom of zone 4 and decline moving upward indicating dry conditions when organic sedimentation began at the lake and becoming less dry moving toward the Middle Holocene. Macroscopic charcoal influx is relatively high in zone 4, indicating frequent fires. Bulk $\delta^{13}C$ values are also high at the bottom of the core and trend toward more negative values moving upward. These shifts indicate aridity early in the lake's history, possibly with an increased importance of C_4 *Muhlenbergia* growing on recently exposed coarse glacial till (Lane et al. 2011a). Alternatively, the bulk $\delta^{13}C$ signal may reflect a higher initial contribution of aquatic and emergent *Isoetes* to the sedimentary organic matter prior to full establishment of the modern vegetation assemblage on till deposits surrounding the basin. The quillwort *Isoetes* uses CAM photosynthesis (Keeley 2014), which could have contributed to the relatively higher $\delta^{13}C$ values in the lower sediments. *Alnus* pollen percentages are low in zone 4, while Poaceae pollen percentages are relatively high, indicating an increased importance of grasses at the lake supporting an interpretation of aridity in zone 4 (Horn 1993). *Isoetes* ratios are low in zone 4, but in this case may not indicate lake level, but rather smaller populations of these plants that were just becoming established following deglaciation.

Zone 3, broadly covering the end of the Late Holocene and the majority of the Middle Holocene, represents a period of very wet climate on Cerro Chirripó. The bottom of zone 3 begins with z-scores for δD_{PP} indicating one of the wettest times in the record but then trending sharply upward toward a relatively drier signal, albeit represented by average conditions for the record. We interpret this shift toward drier conditions as a local manifestation of the 8200 cal yr BP event (see below), which is further supported by a spike in macroscopic charcoal indicating increased fires in the watershed at that time. Z-scores for δD_{PP} then indicate ca. 1100 years of average moisture conditions, followed by multiple excursions to very wet conditions, and then

gradually trending back toward average conditions at the top of the zone. Values for δD and $\delta^{13}C$ of leaf waxes trend relatively more negative across zone 3, supporting an interpretation of mesic climate in this zone. Charcoal values are low through zone 3, indicating less burning and, by extension, more moisture. *Alnus* pollen percentages are relatively high and Poaceae pollen percentages are low, while *Isoetes* ratios are lower, indicating wetter conditions and higher lake levels at the site. Values for bulk $\delta^{13}C$ are generally steady across zone 3, but with a peak toward the middle of the zone that is not reflected in compound-specific $\delta^{13}C$, possibly due to an increased importance of autochthonous organic matter in the sediments at that time.

Zone 2, covering the end of the Middle Holocene and the beginning of the Late Holocene, was a time of increased variability in hydroclimate, with z-scores for δD_{PP} indicating oscillations between arid and mesic conditions over a span of ca. 2200 cal yrs. This zone begins with very dry conditions coincident with the broader 5200 cal yr BP event (see below) and ends slightly wetter than average at the top of the zone and the bottom of the first break in our data. Values for δD of leaf waxes are similarly variable across the zone, while leaf wax $\delta^{13}C$ values indicate stable vegetation. Bulk $\delta^{13}C$ values move relatively higher in the middle of zone 2 and then decline to more negative values. This trend is not seen in compound-specific $\delta^{13}C$ values and likely indicates an increased importance of autochthonous material to the sedimentary organic matter. *Alnus* pollen percentages are low in zone 2, while *Isoetes* ratios are higher, indicating overall drier conditions and reduced lake levels. Macroscopic and microscopic charcoal influx both increase in zone 2 relative to previously, indicating increased fire linked to aridity. Cariaco Basin titanium percentages trend toward a drier signal across zone 2, supporting an interpretation of gradual drying during the Late Holocene on Cerro Chirripó.

Zone 1 contains two gaps in our data. Where we do have data covers ca. 1500–900 cal yr BP and a final datapoint at ca. 36 cal yr BP at the top of the core. The period of 1500–900 cal yr BP, including the Terminal Classic Drought, was generally dry on Cerro Chirripó, an interpretation that agrees with other proxy records from the circum-Caribbean (Hodell et al. 1995, 2005; Webster et al. 2007; Medina-Elizalde et al. 2010; Kennett et al. 2012; Lane et al. 2014; Douglas et al. 2015; Wu et al. 2019b). Z-scores for δD_{PP} are positive in the middle of zone 1, indicating aridity. More positive bulk $\delta^{13}C$ values likewise indicate aridity or a trend toward slightly more C_4 vegetation. Charcoal influx values are high across zone 1, indicating frequent fires. The increased burning seen in zone 1 may represent a trend toward drier climate but may also have been affected by fires spreading upslope from lower elevations where groups of prehistoric people were increasing in both number and cultural complexity (Horn 1993; League and Horn 2000). During the TCD, *Alnus* pollen is low and Poaceae pollen is relatively high, while *Isoetes* ratios are also higher, supporting an interpretation of aridity and lower lake levels.

Given the close correspondence between our new isotope data and proxy data reported in previous studies, we can speculate on conditions across the gaps in our data. The interval of ca. 3200–1500 cal yr BP shows high influx of macro- and microscopic charcoal particles and relatively higher bulk $\delta^{13}C$ values and *Isoetes* ratios, indicating dry climate at that time. Interpolating across the upper gap ca. 900–35 cal yr BP, lower macro- and microscopic charcoal influx, lower *Isoetes* ratios, along with higher *Alnus* and lower Poaceae pollen percentages indicate generally wetter climate during the Little Ice Age. However, Cariaco Basin titanium data indicate dry conditions in the region during the LIA (Haug et al. 2001; Peterson and Haug 2006; Black et al. 2007), as do other studies (Hodell et al. 2005; Lane et al. 2011b). New high-resolution data reported by Wu et al. (2019b) from sediments of Morrenas 3C show warm and

wet conditions ca. 550–350 cal yr BP during the first part of the LIA and cooler, drier conditions ca. 350–100 cal yr BP during the latter part. Our interpretation is that wet conditions prevailed on Cerro Chirripó during the LIA, but that finding would be strengthened by developing compound-specific isotope data covering that interval, possibly by analyzing contemporaneous sediments from other lakes in the Chirripó highlands.

Our interpretations of Holocene paleohydrology on Cerro Chirripó differ from findings reported by other researchers in two key ways. First, Wu et al. (2019a) reported cold conditions at Lago Ditkebi for the interval of ca. 8100–5270 cal yr BP based on subfossil chironomid data. Additionally, they reported low fire activity from charcoal data, but dry conditions with low lake levels based on increased bulk $\delta^{13}C$ values that the authors interpreted as an increased importance of C_4 grasses of the *Muhlenbergia* genus at the time. Rather than associating low fire activity with wetter conditions, they suggested reduced convective activity led to dry conditions and lower lake levels and that reduced lightning-induced ignition resulted in fewer fires (Wu et al. 2019a). Low charcoal values in our sediments from the Morrenas site for the period of ca. 8600–5400 cal yr BP support the interpretation of low fire on Cerro Chirripó during that interval; however, our new compound-specific isotope data, including z-scores for δD_{PP} combined with δD and $\delta^{13}C$ values for leaf waxes, indicate wetter than average conditions across this interval punctuated by several episodes of extremely wet climate and no major changes in leaf wax δD values that would correspond to the Wu et al. (2019a) interpretations of the bulk $\delta^{13}C$ record from Ditkebi. Likewise, low *Isoetes* ratios indicate high lake levels during this interval, and *Alnus* pollen shows peak percentages, both of which we interpret to represent overall wetter climate. We believe the interpretations of bulk $\delta^{13}C$ values as representing relatively drier conditions ca. 8100–5720 cal yr BP by Wu et al. (2019a) are unwarranted, given our new direct

δD evidence of paleohydrology. Wu et al. (2019a) may be correct that increased $\delta^{13}C$ values reflect an increased abundance of *Muhlenbergia* (or perhaps C_4 sedges) in the Ditkebi watershed, but they are incorrect in interpreting increased $\delta^{13}C$ values as indicating substantial aridity at this time.

And second, while our work supports the finding of millennial-scale variations in hydroclimate reported by Lane et al. (2011a) and by Lane and Horn (2013), our new findings differ in some ways from the latter study. Lane and Horn (2013) reported a disconnect between millennial-scale variations in δD data for their $C_{25–27}$ versus $C_{29–33}$ odd numbered *n*-alkanes. In that work the authors hypothesized that data for the $C_{25–27}$ *n*-alkane homologues represented a local vegetation signal in the Chirripó páramo, while signals from the $C_{29–33}$ homologues represented signals of paleohydrology from *n*-alkanes blowing upslope from lower elevations due to the different patterns observed in their δD dataset (Lane and Horn 2013, Fig. 2). This contrasts with the results of compound-specific carbon isotopes analyses by Lane et al. (2011a), for which the authors reported a local signal recorded in all *n*-alkane homologues investigated and little evidence suggesting upslope movement of biomarkers.

In our new depth and age model for the Morrenas 1 cores, we now recognize a hiatus in sedimentation of ca. 1100 years between the underlying inorganic transition sediments and the beginning of organic sedimentation ca. 10,000 cal yr BP. Ignoring the bottom two samples reported by Lane and Horn (2013, Fig. 2), patterns of temporal variation for all *n*-alkane homologues match well in that study and with our new δD and $\delta^{13}C$ data (Fig. 2.8). The biogeochemical signals from the underlying transition sediments in the Morrenas 1 cores likely represent fundamentally different environmental conditions and processes from those recorded in the overlying organic sediments and we now think that Lane and Horn (2013) erred in

interpolating environmental change across that hiatus. Thus, our new data do not include samples from the underlying transition sediments in the Morrenas 1 cores. For the organic portion of the Morrenas 1 sediments our data do pair well with the overall patterns of coarse-resolution variations seen in δD and $\delta^{13}C$ for all *n*-alkane homologues reported by Lane et al. (2011a) and Lane and Horn (2013; Fig. 2.8). Our relatively high CPI and ACL values and strong odd-over-even predominance of *n*-alkane homologues reinforce the findings of Lane et al. (2011a), which concluded that the sedimentary *n*-alkane record at Morrenas 1 represents a local signal of vegetation and paleohydrology across the Holocene.

2.6.2 Local Response to Broad-Scale Climate Events

The Lago de las Morrenas 1 sediments record local manifestations of four global-scale extreme climate events, including the 8200 cal yr BP event, the 5200 cal yr BP event, the Terminal Classic Drought, and the Little Ice Age. The 8200 cal yr BP event (ca. 8400–8000 cal yr BP; Alley et al. 1997; Kobashi et al. 2007) appears as a distinct drying event in the LM1 proxy data, in agreement with other research indicating arid conditions at the time (Hodell et al. 1995; Hughen et al. 1996; Gasse 2000; League and Horn 2000; Haug et al. 2001; Thompson et al. 2002; Lachniet et al. 2004a; Watson 2011). Z-scores for δD_{PP} move sharply more positive, albeit this change is from very wet to average conditions. The shift to a relatively drier climate is likewise reflected in δD and $\delta^{13}C$ values of leaf waxes, decreased percentages of *Alnus* pollen blowing upslope from lower elevations, and spikes in macro- and microscopic charcoal indicating increased fire ca. 8200 cal yr BP.

The 5200 cal yr BP event (ca. 5400–5000 cal yr BP; Magney et al. 2006; Thompson et al 2006; Brooks 2010) also appears in the Morrenas 1 sediments as a distinct drying event,

supporting other research in the circum-Caribbean (Street-Perrott and Perrott 1990; Thompson et al. 1995, 2006; Keigwin 1996). Z-scores for δD_{PP} again move sharply more positive toward a signal of the highest aridity in the record excepting the bottommost samples from zone 4. This drying is also seen in δD values of leaf waxes. A spike in macro- and microscopic charcoal indicates more fires. Decreased percentages of *Alnus* pollen and increased Poaceae pollen indicate aridity at this time, while increased *Isoetes* ratios indicate lower lake levels coincident with the 5200 cal yr BP event. This contrasts with findings from Lago Ditkebi reported by Wu et al. (2019a), who interpreted bulk $\delta^{13}C$ and charcoal data at that site to indicate warmer, wetter conditions coincident with a severe fire event. Compound-specific isotope analysis of *n*-alkanes from the Ditkebi sediments could help clarify this discrepancy.

The LM1 sediments reveal evidence of a third major drying episode coincident with the Terminal Classic Drought ca. 1200–850 cal yr BP (Hodell et al. 2005; Lane et al. 2014), which agrees with other findings from the Morrenas lakes (Wu et al. 2019b) and in the broader region (Hodell et al. 1996, 2005; Haug et al. 2003; Lachniet et al. 2004b; Peterson and Haug 2006; Webster et al. 2007; Medina-Elizalde et al. 2010; Luzzadder-Beach et al. 2012; Douglas et al. 2015). Z-scores for δD_{PP} trend higher during this time, indicating aridity. Values for δD and $\delta^{13}C$ of leaf waxes show a slight move toward relatively more positive values. Microscopic charcoal influx greatly increases, signaling the highest level of fire in the record. Macroscopic charcoal data are largely missing from the interval of the TCD due to the location of a radiocarbon date in the sediment core. Decreased *Alnus* and increased Poaceae pollen percentages indicate dry conditions, while increased *Isoetes* ratios show lower lake levels during the TCD, in agreement with other studies.

We do not have new isotope data covering the interval of the Little Ice Age (ca. 550–100 cal yr BP), however, with some caution we can infer conditions during that time from other proxy data. Microscopic and macroscopic charcoal influx decreases across the LIA interval. *Alnus* pollen increases and Poaceae pollen decrease signaling wetter conditions, while *Isoetes* ratios decrease, indicating higher lake levels. Altogether, the proxy signals indicate a wetter Little Ice Age at the Morrenas site compared to the preceding TCD interval. Our findings of relatively wet LIA conditions contrast with dry conditions in the circum-Caribbean reported by other researchers (Haug et al. 2001; Hodell et al. 2005; Peterson and Haug 2006; Black et al. 2007; Lane et al. 2011b; Taylor et al. 2013). On the other hand, Wu et al. (2019b) reported warm and wet conditions at the Morrenas site ca. 550–350 cal yr BP followed by cool and dry conditions ca. 350–100 cal yr BP during the LIA. The temporal resolution of our LM1 data is too coarse to allow interpretations on a centennial scale across the interval of the Little Ice Age, but the data we do have is not entirely inconsistent with the findings of Wu et al. (2019b) regarding different climate conditions across the LIA.

2.6.3 $\delta^{13}C$ and Vegetation Change

Our new compound-specific $\delta^{13}C$ leaf wax values track well with our δD values for all odd numbered *n*-alkane homologues ranging C_{23}–C_{33} (Fig. 2.6; also see supplemental information for this chapter, Figs. S2.1 and S2.2), indicating that carbon isotope ratios in longer chain $C_{27–33}$ *n*-alkanes from terrestrial plants and relatively shorter chain $C_{23–25}$ *n*-alkanes from aquatic plants are responding to aridity on Cerro Chirripó. Relatively positive shifts in δD values of leaf waxes and corresponding shifts toward aridity in z-scores for δD_{PP} are matched by shifts toward relatively more positive values for $\delta^{13}C$ of leaf waxes. Conversely, lower hydrogen

values are tracked by lower carbon values. Horn (1993) reported a stable vegetation community on Cerro Chirripó following deglaciation, with pollen data indicating very little change over ca. 10,000 ^{14}C years; however, pollen analysis cannot differentiate between C_3 grasses such as *Chusquea subtessellata* and C_4 *Muhlenbergia* spp. at the site. Our new compound-specific $\delta^{13}C$ leaf wax data agree with the findings of little vegetation change at the site following deglaciation and establishment of páramo. Lane et al. (2011a) reported that $\delta^{13}C$ values indicate moisture signals at the Morrenas site during the Holocene, rather than vegetation change. The temporal patterns of variation in our new isotope data agree well with the overall patterns seen in the organic sediments from the LM1 core reported by Lane and coauthors (2011a; Fig. 2.8).

Conversely, Wu et al. (2019a) interpreted changes in bulk $\delta^{13}C$ from the sediments of Lago Ditkebi as representing changing abundances of C_4 grasses in the *Muhlenbergia* genus in the watershed. In their interpretation, relatively more positive bulk $\delta^{13}C$ values represent the presence of more *Muhlenbergia*, which indicates lower lake levels and drier conditions at the site. *Muhlenbergia* prefers cool and dry conditions (Schwarz and Redmann 1988; Sage et al. 1999) and flourishes on dry microhabitats with coarse substructure in the Valle de las Morrenas (Chaverri and Cleef 2005; Lane et al. 2011a), which led Wu et al. (2019a, p.181) to conclude that "relatively enriched $\delta^{13}C$ values during [the interval of] DKB-I indicate that *Muhlenbergia* expanded along the margin of the lake as a result of lowered lake levels and an expansion of suitable habitat, likely driven by relatively cold and dry conditions."

An increased presence of C_4 grasses could produce relatively higher bulk $\delta^{13}C$ values in the lake sediments, as suggested by Wu et al. (2019a). However, carbon isotopes in C_3 plants can also shift to relatively more positive values under dry conditions and to more negative values under moist conditions (Farquhar and Richards 1984; Read et al. 1992; Stevenson et al. 2005;

Diefendorf et al. 2010; Kohn 2010; Lane et al. 2011a). Variability in $\delta^{13}C$ also could be caused by changes in temperature, but water stress is a more important control (Stewart et al. 1995; Miller et al. 2001; Leffler and Enquist 2002; Stevenson et al. 2005; Song et al. 2008). While increasing and decreasing the relative abundance of C_4 plants in a watershed does change $\delta^{13}C$ values, the values for our $\delta^{13}C$ leaf wax proxy across zones 3–1 range ca. 6.2‰ for C_{27}, 3.7‰ for C_{29}, and 3.5‰ for C_{31}, which are reasonable biogeochemical responses to changing hydroclimate in an otherwise stable vegetation community. While changes in $\delta^{13}C$ in lake sediments from Chirripó may be driven in part by changes to the C_4 component of vegetation, we view our compound-specific $\delta^{13}C$ data from Morrenas to primarily reflect changes in moisture in otherwise stable vegetation, following the initial period of lake formation. Wu et al. (2019a) may be correct regarding bulk $\delta^{13}C$ signals and the possibility of increased or decreased abundances of *Muhlenbergia* on Cerro Chirripó, but their interpretation of wetter conditions during the 5200 cal yr BP event differ from our direct evidence of drier conditions at that same time seen in our δD, $\delta^{13}C$, and z-scored δD_{PP} data.

2.7 Conclusion

Our compound-specific δD analyses revealed millennial-scale patterns and variations in hydroclimate on Cerro Chirripó across the Holocene. The period of ca. 10,000–8600 cal yr BP was characterized by dry climate, frequent fires, increased C_4 plants, and high lake levels. For the period of ca. 8600–5400 cal yr BP, the Morrenas site was marked by a relatively wetter climate with little fire and continued high lake levels. During the period of ca. 5400–3200 cal yr BP, the site experienced gradual drying and highly variable conditions, with low lake levels and considerably more frequent fires than before. Finally, the period of ca. 3200 cal yr BP to the

present was generally dry, with low lake levels and sustained frequent fires. This overall pattern is interrupted by several centennial-scale manifestations of global extreme climate events, including dry conditions during the 8200 cal yr BP event, the 5200 cal yr BP event, and the Terminal Classic Drought, and possibly by wet conditions during the Little Ice Age. Our $\delta^{13}C$ analyses demonstrate that carbon isotope signals are responding to changes in hydroclimate at the site and reinforce prior interpretations of a stable páramo vegetation community that established following deglaciation and persisted throughout the Holocene.

2.8 Acknowledgements

Core recovery and analyses of pollen, charcoal, and diatoms were funded by a grant from the National Geographic Society to SPH. Macroscopic charcoal work was supported by an REU supplement to NSF grant SBR-9512484 awarded to Carol Harden, Ken Orvis, and SPH. Previous stable isotope analyses and related fieldwork were funded by grants from the National Geographic Society and The A.W. Mellon Foundation awarded to SPH, by NSF grants EAR-0004104 awarded to Claudia Mora and BCS-0550382 awarded to SPH, Kenneth Orvis, and Claudia Mora, and by additional funds from the University of Tennessee and the University of North Carolina Wilmington. The new analyses reported here were supported by NSF grant #1657170 awarded to SPH and MTK, NSF grant #1660185 awarded to SPH, CSL, and Douglas Gamble, and by funds from the University of Tennessee and the University of North Carolina Wilmington. We thank Luke Blentlinger, Trell Stroud, and Jonathan Unger for assistance in the laboratory.

2.9 References

Alley RB and Ágústsdóttir AM (2005) The 8k event: cause and consequence of a major Holocene abrupt climate change. *Quaternary Science Reviews* 24: 1123–1149.

Alley RB, Mayewski PA, Sowers T, Stuiver M, Taylor KC and Clark PU (1997) Holocene climatic instability: a prominent, widespread event 8200 yr ago. *Geology* 25(6): 483–486.

Anchukaitis KJ and Horn SP (2005) A 2000-year reconstruction of forest disturbance from southern Pacific Costa Rica. *Palaeogeography, Palaeoclimatology, Palaeoecology* 221: 35–54.

Atwood AR (2015) *Mechanisms of tropical Pacific climate change during the Holocene*. PhD Thesis, University of Washington, USA.

Bar-Matthews M, Ayalon A and Kaufman A (1997) Late Quaternary paleoclimate in the Eastern Mediterranean region from stable isotope analysis of speleothems at Soreq cave, Israel. *Quaternary Research* 47: 155–168.

Bar-Matthews M, Ayalon A, Kaufman A and Wasserburg GJ (1999) The Eastern Mediterranean paleoclimate as a reflection of regional events: Soreq cave, Israel. *Earth and Planetary Science Letters* 166: 85–95.

Barquero J (2006) *La Majestuosa Cima de Costa Rica: el Macizo Chirripó*. San José: [s.n.].

Behling H (2000) A 2860-year high-resolution pollen and charcoal record from the Cordillera de Talamanca in Panama: a history of human and volcanic forest disturbance. *The Holocene* 10(3): 387–393.

Blaauw M (2019) clam: classical age-depth modeling of cores from deposits. R package version 2.3.2. Available at: https://CRAN.R-project.org/package=clam (accessed 23 January 2019).

Blaauw M and Christen JA (2019) rbacon: age-depth modeling using Bayesian statistics. R package version 2.3.6. Available at: http://CRAN.R-project.org/package=rbacon (accessed 23 January 2019).

Black DE, Abahazi MA, Thunell RC, Kaplan A, Tappa EJ and Peterson LC (2007) An 8-century tropical Atlantic SST record from the Cariaco Basin: baseline variability, twentieth-century warming, and Atlantic hurricane frequency. *Paleoceanography* 22: PA4204.

Bowen GJ (2019) The Online Isotopes in Precipitation Calculator, v.3.1. Available at: http://www.waterisotopes.org (accessed 7 May 2019).

Bradbury JP (1982) Holocene chronostratigraphy of Mexico and Central America. *Striae* 16: 46–48.

Bray EE and Evans ED (1961) Distribution of *n*-paraffins as a clue to recognition of source beds. *Geochimica et Cosmochimica Acta* 22: 2–15.

Brooks N (2010) Human responses to climatically-driven landscape change and resource scarcity: learning from the past and planning for the future. In: Martini IP and Chesworth W (eds) *Landscapes and Societies*. Dordrecht: Springer, pp. 43–66.

Bush MB and Colinvaux PA (1994) Tropical forest disturbance: paleoecological records from Darien, Panama. *Ecology* 75(6): 1761–1768.

Chalié F and Gasse F (2002) Late Glacial-Holocene diatom record of water chemistry and lake level change from the tropical East African Rift Lake Abiyata (Ethiopia). *Palaeogeography, Palaeoclimatology, Palaeoecology* 187: 259–283.

Chaverri A and Cleef AM (2005) Comunidades vegetales de los páramos de los macizos de Chirripó y Buenavista, Costa Rica. In: Kappelle M and Horn SP (eds) *Páramos de Costa Rica*. Santo Domingo: INBio Press, pp. 577–592.

Clement RM and Horn SP (2001) Pre-Columbian land-use history in Costa Rica: a 3000-year record of forest clearance, agriculture and fires from Laguna Zoncho. *The Holocene* 11(4): 419–426.

Clausen CJ, Cohen AD, Emiliani C, Holman JA and Stipp JJ (1979) Little Salt Spring, Florida: a unique underwater site. *Science* 203: 609–614.

Coen E (1983) Climate. In: Janzen DH (ed) *Costa Rican Natural History*. Chicago: University of Chicago Press, pp. 35–46.

Cohen AS (2003) *Paleolimnology: The History and Evolution of Lake Systems*. Oxford: Oxford University Press.

Cranwell PA, Eglinton G and Robinson N (1987) Lipids of aquatic organisms as potential contributors to lacustrine sediments—II. *Organic Geochemistry* 11(6): 513–527.

Curtis JH and Hodell DA (1996) Climate variability on the Yucatan Peninsula (Mexico) during the past 3500 years, and implications for Maya cultural evolution. *Quaternary Research* 46: 37–47.

Dansgaard W (1964) Stable isotopes in precipitation. *Tellus* 16(4): 436–468.

Dean WE (1974) Determination of carbonate and organic matter in calcareous sediments and sedimentary rocks by loss on ignition: comparison with other methods. *Journal of Sedimentary Petrology* 44(1): 242–248.

DeMenocal P, Ortiz J, Guilderson T, Adkins J, Sarnthein M, Baker L and Yarusinsky M (2000) Abrupt onset and termination of the African Humid Period: rapid climate responses to gradual insolation forcing. *Quaternary Science Reviews* 19: 347–361.

Diefendorf AF, Mueller KE, Wing SL, Koch PL and Freeman KH (2010) Global patterns in leaf ^{13}C discrimination and implications for studies of past and future climate. *PNAS* 107(13): 5738–5743.

Dohrenwend RE (1972) *The energetic role of the trade wind inversion in a tropical alpine ecosystem*. PhD Thesis, Syracuse University, USA.

Douglas PMJ, Pagani M, Canuto MA, Brenner M, Hodell DA, Eglinton TI and Curtis JH (2015) Drought, agricultural adaptation, and sociopolitical collapse in the Maya Lowlands. *PNAS* 112(18): 5607–5612.

Dull RA, Nevle RJ, Woods WI, Bird DK, Avnery S and Denevan WM (2010) The Columbian Encounter and the Little Ice Age: abrupt land use change, fire, and greenhouse forcing. *Annals of the Association of American Geographers* 100(4): 755–771.

Eglinton G and Hamilton RJ (1963) The distribution of alkanes. In: Swain T (ed) *Chemical Plant Taxonomy*. London: Academic Press, pp. 187–217.

Eglinton G and Hamilton RJ (1967) Leaf epicuticular waxes. *Science* 156: 1322–1335.

Esquivel-Hernández G, Sánchez-Murillo R, Quesada-Román A, Mosquera GM, Birkel C and Boll J (2018) Insight into the stable isotopic composition of glacial lakes in a tropical alpine ecosystem: Chirripó, Costa Rica. *Hydrological Processes* 32: 3588–3603.

Farquhar GD and Richards RA (1984) Isotopic composition of plant carbon correlates with water-use efficiency of wheat genotypes. *Australian Journal of Plant Physiology* 11(6): 539–552.

Feakins SJ (2013) Pollen-corrected leaf wax D/H reconstructions of northeast African hydrological changes during the late Miocene. *Palaeogeography, Palaeoclimatology, Palaeoecology* 374: 62–71.

Feakins SJ, Peters T, Sin Wu M, Shenkin A, Salinas N, Girardin CAJ, Patrick Bentley L, Blonder B, Enquist BJ, Martin RE, Asner GP and Malhi Y (2016) Production of leaf wax *n*-alkanes across a tropical forest elevation transect. *Organic Geochemistry* 100: 89–100.

Ficken KJ, Li B, Swain DL and Eglinton G (2000) An *n*-alkane proxy for the sedimentary input of submerged/floating freshwater aquatic macrophytes. *Organic Geochemistry* 31: 745–749.

Gasse F (2000) Hydrological changes in the African tropics since the Last Glacial Maximum. *Quaternary Science Reviews* 19: 189–211.

Haberyan KA and Horn SP (1999) A 10,000 year diatom record from a glacial lake in Costa Rica. *Mountain Research and Development* 19(1): 63–68.

Han JH, McCarthy ED, Van Hoeven W, Calvin M and Bradley WH (1968) Organic geochemical studies, II. a preliminary report on the distribution of aliphatic hydrocarbons in algae, in bacteria, and in a recent lake sediment. *PNAS* 59: 29–33.

Hastenrath S (1991) *Climate Dynamics of the Tropics*. Dordrecht: Kluwer Academic Publishers.

Haug GH, Günther D, Peterson LC, Sigman DM, Hughen KA and Aeschlimann B (2003) Climate and the collapse of Maya civilization. *Science* 299: 1731–1735.

Haug GH, Hughen KA, Sigman DM, Peterson LC and Röhl U (2001) Southward migration of the Intertropical Convergence Zone through the Holocene. *Science* 293: 1304–1308.

Hodell DA, Brenner M, Curtis JH, Medina-González R, Ildefonso-Chan Can E, Albornaz-Pat A and Guilderson TP (2005) Climate change on the Yucatan Peninsula during the Little Ice Age. *Quaternary Research* 63: 109–121.

Hodell DA, Curtis JH and Brenner M (1995) Possible role of climate in the collapse of Classic Maya civilization. *Nature* 375: 391–394.

Hodell DA, Curtis JH, Jones GA, Higuera-Grundy A, Brenner M, Binford MW and Dorsey KT (1991) Reconstruction of Caribbean climate change over the past 10,500 years. *Nature* 352: 790–793.

Horn SP (1993) Postglacial vegetation and fire history in the Chirripó Páramo of Costa Rica. *Quaternary Research* 40: 107–116.

Horn SP (2007) Late Quaternary lake and swamp sediments: recorders of climate and environment. In: Bundschuh JB and Alvarado GE (eds) *Central America: Geology, Resources, Hazards*, Vol. 1. London: Taylor and Francis, pp. 423–441.

Horn SP and Haberyan KA (2016) Lakes of Costa Rica. In: Kappelle M (ed) *Costa Rican Ecosystems*. Chicago: University of Chicago Press, pp. 656–682.

Horn SP and Sanford RL (1992) Holocene fires in Costa Rica. *Biotropica* 24(3): 354–361.

Horn SP, Orvis KH and Haberyan KA (2005) Limnología de las lagunas glaciales en el páramo del Chirripó, Costa Rica. In: Kappelle M and Horn SP (eds) *Páramos de Costa Rica*. Santo Domingo: INBio Press, pp. 161–181.

Huang Y, Shuman B, Wang Y and Webb T III (2004) Hydrogen isotope ratios of individual lipids in lake sediments as novel tracers of climatic and environmental change: a surface sediment test. *Journal of Paleolimnology* 31: 363–375.

Hughen KA, Overpeck JT, Peterson LC and Trumbore S (1996) Rapid climate changes in the tropical Atlantic region during the last deglaciation. *Nature* 380: 51–54.

Johanson EN, Horn SP and Lane CS (forthcoming) Pre-Columbian agriculture, fire, and Spanish contact: a 4200-year record from Laguna Los Mangos, Costa Rica. *The Holocene*.

Juggins S (2007) C2: software for ecological and palaeoecological data analysis and visualization (user guide version 1.5). Newcastle upon Tyne: Newcastle University, UK.

Kahmen A, Hoffmann B, Schefuß E, Arndt SK, Cernusak LA, West JB and Sachse D (2013a) Leaf water deuterium enrichment shapes leaf wax *n*-alkane δD values of angiosperm plants II: observational evidence and global implications. *Geochimica et Cosmochimica Acta* 111: 50–63.

Kahmen A, Schefuß E and Sachse D (2013b) Leaf water deuterium enrichment shapes leaf wax *n*-alkane δD values of angiosperm plants I: experimental evidence and mechanistic insights. *Geochimica et Cosmochimica Acta* 111: 39–49.

Kappelle M and Horn SP (2016) The *Páramo* grasslands of Costa Rica's highlands. In: Kappelle M (ed) *Costa Rican Ecosystems*. Chicago: University of Chicago Press, pp. 492–523.

Keeley JE (2014) Aquatic CAM photosynthesis: a brief history of its discovery. *Aquatic Botany* 118: 38–44.

Keigwin LD (1996) The Little Ice Age and the Medieval Warm Period in the Sargasso Sea. *Science* 274: 1504–1508.

Kennett DJ, Breitenbach SFM, Aquino VV, Asmerom Y, Awe J, Baldini JUL, Bartlein P, Culleton BJ, Evert C, Jazwa C, Macri MJ, Marwan N, Polyak V, Prufer KM, Ridley HE, Sodemann H, Winterhalder B and Haug GH (2012) Development and disintegration of Maya political systems in response to climate change. *Science* 338: 788–791.

Kerr MT, Horn SP, Grissino-Mayer HD and Stachowiak LA (2018) Annual growth zones in stems of *Hypericum irazuense* (Guttiferae) in the Costa Rican páramos. *Physical Geography* 39(1): 38–50.

Kerr MT, Horn SP and Lane CS (forthcoming) Stable isotope analysis of vegetation history and land-use change at Laguna Santa Elena in southern Pacific Costa Rica. *Vegetation History and Archaeobotany*.

Kobashi T, Severinghaus JP, Brook EJ, Barnola J-M and Grachev AM (2007) Precise timing and characterization of abrupt climate change 8200 years ago from air trapped in polar ice. *Quaternary Science Reviews* 26: 1212–1222.

Kohn MJ (2010) Carbon isotope compositions of terrestrial C3 plants as indicators of (paleo)ecology and (paleo)climate. *PNAS* 107(46): 19691–19695.

Lachniet MS and Patterson WP (2002) Stable isotope values of Costa Rican surface waters. *Journal of Hydrology* 260: 135–150.

Lachniet MS and Seltzer GO (2002) Late Quaternary glaciation of Costa Rica. *GSA Bulletin* 114(5): 547–558.

Lachniet MS, Asmerom Y, Burns SJ, Patterson WP, Polyak VJ and Seltzer GO (2004a) Tropical response to the 8200 yr B.P. cold event? Speleothem isotopes indicate a weakened early Holocene monsoon in Costa Rica. *Geology* 32(11): 957–960.

Lachniet MS, Burns SJ, Piperno DR, Asmerom Y, Polyak VJ, Moy CM and Christenson K (2004b) A 1500-year El Niño/Southern Oscillation and rainfall history for the Isthmus of Panama from speleothem calcite. *Journal of Geophysical Research* 109: D20117.

Lachniet MS, Johnson L, Asmerom Y, Burns SJ, Polyak V, Patterson WP, Burt L and Azouz A (2009) Late Quaternary moisture export across Central America and to Greenland: evidence for tropical rainfall variability from Costa Rican stalagmites. *Quaternary Science Reviews* 28: 3348–3360.

Lachniet MS, Patterson WP, Burns S, Asmerom Y and Polyak V (2007) Caribbean and Pacific moisture sources on the Isthmus of Panama revealed from stalagmite and surface water δ^{18}O gradients. *Geophysical Research Letters* 34: L01708.

Lane CS (2017) Modern *n*-alkane abundances and isotopic composition of vegetation in a gymnosperm-dominated ecosystem of the southeastern U.S. coastal plain. *Organic Geochemistry* 105: 33–36.

Lane CS and Horn SP (2013) Terrestrially derived n-alkane δD evidence of shifting Holocene paleohydrology in highland Costa Rica. *Arctic, Antarctic, and Alpine Research* 45(3): 342–349.

Lane CS, Horn SP and Kerr MT (2014) Beyond the Mayan Lowlands: impacts of the Terminal Classic Drought in the Caribbean Antilles. *Quaternary Science Reviews* 86: 89–98.

Lane CS, Horn SP, Mora CI, Orvis KH and Finkelstein DB (2011a) Sedimentary stable carbon isotope evidence of late Quaternary vegetation and climate change in highland Costa Rica. *Journal of Paleolimnology* 45: 323–338.

Lane CS, Horn SP, Orvis KH and Thomason JM (2011b) Oxygen isotope evidence of Little Ice Age aridity on the Caribbean slope of the Cordillera Central, Dominican Republic. *Quaternary Research* 75: 461–470.

Lane CS, Horn SP, Taylor ZP and Kerr MT (2016) Correlation of bulk sedimentary and compound-specific $\delta^{13}C$ values indicates minimal pre-aging of *n*-alkanes in a small tropical watershed. *Quaternary Science Reviews* 145: 238–242.

Lane CS, Horn SP, Taylor ZP and Mora CI (2009) Assessing the scale of prehistoric human impact in the neotropics using stable carbon isotope analyses of lake sediments: a test case from Costa Rica. *Latin American Antiquity* 20(1): 120–133.

League BL (1998) *Sedimentary charcoal, magnetic susceptibility, and Páramo fires in Chirripó National Park, Costa Rica*. Senior Honors Thesis, University of Tennessee, USA.

League BL and Horn SP (2000) A 10 000 year record of Páramo fires in Costa Rica. *Journal of Tropical Ecology* 16: 747–752.

Leffler AJ and Enquist BJ (2002) Carbon isotope composition of tree leaves from Guanacaste, Costa Rica: a comparison across tropical forests and tree life history. *Journal of Tropical Ecology* 18: 151–159.

Liu W and Huang Y (2005) Compound specific *D*/*H* ratios and molecular distributions of higher plant leaf waxes as novel paleoenvironmental indicators in the Chinese Loess Plateau. *Organic Geochemistry* 26: 851–860.

Luzzadder-Beach S, Beach TP and Dunning NP (2012) Wetland fields as mirrors of drought and the Maya abandonment. *PNAS* 109(10): 3646–3651.

Magny M, Leuzinger U, Bortenschlager S and Haas JN (2006) Tripartite climate reversal in Central Europe 5600–5300 years ago. *Quaternary Research* 65: 3–19.

Maldonado T, Alfaro EJ and Hidalgo HG (2018) A review of the main drivers and variability of Central America's climate and seasonal forecast system. *Revista Biología Tropical* 66 (Supplement 1): S153–S175.

Mann ME, Zhang Z, Hughes MK, Bradley RS, Miller SK, Rutherford S and Ni F (2008) Proxy-based reconstructions of hemispheric and global surface temperature variations over the past two millennia. *PNAS* 105(36): 13252–13257.

Mann ME, Zhang Z, Rutherford S, Bradley RS, Hughes MK, Shindell D, Ammann C, Faluvegi G and Ni F (2009) Global signatures and dynamical origins of the Little Ice Age and Medieval Climate Anomaly. *Science* 326: 1256–1260.

Marzi R, Torkelson BE and Olson RK (1993) A revised carbon preference index. *Organic Geochemistry* 20(8): 1303–1306.

Medina-Elizalde M, Burns SJ, Lea DW, Asmerom Y, von Gunten L, Polyak V, Vuille M and Karmalkar A (2010) High resolution stalagmite climate record from the Yucatán Peninsula spanning the Maya terminal classic period. *Earth and Planetary Science Letters* 298: 255–262.

Meyers PA (2003) Applications of organic geochemistry to paleolimnological reconstructions: a summary of examples from the Laurentian Great Lakes. *Organic Geochemistry* 34: 261–289.

Miller JM, Williams RJ and Farquhar GD (2001) Carbon isotope discrimination by a sequence of *Eucalyptus* species along a subcontinental rainfall gradient in Australia. *Functional Ecology* 15: 222–232.

Moy CM, Seltzer GO, Rodbell DT and Anderson DM (2002) Variability of El Niño/Southern Oscillation activity at millennial timescales during the Holocene epoch. *Nature* 420: 162–165.

Nevle RJ and Bird DK (2008) Effects of syn-pandemic fire reduction and reforestation in the tropical Americas on atmospheric CO_2 during European conquest. *Palaeogeography, Palaeoclimatology, Palaeoecology* 264: 25–38.

Nevle RJ, Bird DK, Ruddiman WF and Dull RA (2011) Neotropical human-landscape interactions, fire, and atmospheric CO_2 during European conquest. *The Holocene* 21(5): 853–864.

Niedermeyer EM, Schefuß E, Sessions AL, Mulitza S, Mollenjauer G, Schultz M and Wefer G (2010) Orbital- and millennial-scale changes in the hydrologic cycle and vegetation in the western African Sahel: insights from individual plant wax δD and δ^{13}C. *Quaternary Science Reviews* 29: 2996–3005.

Orvis KH and Horn SP (2000) Quaternary glaciers and climate on Cerro Chirripó, Costa Rica. *Quaternary Research* 54: 24–37.

Peterson LC and Haug GH (2006) Variability in the mean latitude of the Atlantic Intertropical Convergence Zone as recorded by riverine input of sediments to the Cariaco Basin (Venezuela). *Palaeogeography, Palaeoclimatology, Palaeoecology* 234: 97–113.

Polissar PJ and D'Andrea WJ (2014) Uncertainty in paleohydrologic reconstructions from molecular δ*D* values. *Geochimica et Cosmochimica Acta* 129: 146–156.

Polissar PJ and Freeman KH (2010) Effects of aridity and vegetation on plant-wax δD in modern lake sediments. *Geochimica et Cosmochimica Acta* 74: 5785–5797.

Porinchu DF and MacDonald GM (2003) The use and application of freshwater midges (Chironomidae: Insects: Diptera) in geographical research. *Progress in Physical Geography* 27(3): 378–422.

Potter R, Li Y, Horn SP and Orvis KH (2019) Cosmogenic Cl-36 surface exposure dating of late Quaternary glacial events in the Cordillera de Talamanca, Costa Rica. *Quaternary Research* 92: 216–231.

Power MJ, Mayle FE, Bartlein PJ, Marlon JR, Anderson RS, Behling H, Brown KJ, Carcaillet C, Colombaroli D, Gavin DG, Hallett DJ, Horn SP, Kennedy LM, Lane CS, Long CJ, Moreno PI, Paitre C, Robinson G, Taylor Z and Walsh MK (2013) Climate control of the biomass-burning decline in the Americas after AD 1500. *The Holocene* 23(1): 3–13.

Poynter J and Eglinton G (1990) Molecular composition of three sediments from Hole 717C: the Bengal Fan. *Proceedings of the Ocean Drilling Program, Scientific Results* 116: 155–161.

Poynter JG, Farrimond P, Robinson N and Eglinton G (1989) Aeolian-derived higher plant lipids in the marine sedimentary record: links with palaeoclomate. In: Leinen M and Sarnthein M (eds) *Paleoclimatology and Paleometerology: Modern and Past Patterns of Global Atmospheric Transport*. Dordrecht: Kluwer Academic Publishers, pp. 435–462.

R Core Team (2019) R: a language and environment for statistical computing. R Foundation for Statistical Computing, Vienna. Available at: https://www.r-project.org (accessed 23 January 2019).

Read JJ, Johnson DA, Asay KH and Tieszen LL (1992) Carbon isotope discrimination: relationship to yield, gas exchange, and water-use efficiency in field-grown crested wheatgrass. *Crop Science* 32(1): 168–175.

Reimer PJ, Bard E, Bayliss A, Beck JW, Blackwell PG, Ramsey CB, Buck CE, Cheng H, Edwards RL, Friedrich M, Grootes PM, Guilderson TP, Haflidason H, Hajdas I, Hatté C, Heaton TJ, Hoffmann DL, Hogg AG, Hughen KA, Kaiser KF, Kromer B, Manning SW, Niu M, Reimer RW, Richards DA, Scott EM, Southon JR, Staff RA, Turney CSM and van der Plicht J (2013) IntCal13 and Marine13 radiocarbon age calibration curves 0-50,000 years cal BP. *Radiocarbon* 55(4): 1869–1887.

Sachse D and Gleixner G (2004) Hydrogen isotope ratios of recent lacustrine sedimentary n-alkanes record modern climate variability. *Geochimica et Cosmochimica Acta* 68(23): 4877–4889.

Sachse D, Billault I, Bowen GJ, Chikaraishi Y, Dawson TE, Feakins SJ, Freeman KH, Magill CR, McInerney FA, van der Meer MTJ, Polissar P, Robins RJ, Sachs JP, Schmidt H-L, Sessions AL, White JWC, West JB and Kahmen A (2012) Molecular paleohydrology: interpreting the hydrogen-isotopic composition of lipid biomarkers from photosynthesizing organisms. *Annual Review of Earth and Planetary Sciences* 40: 221–249.

Sachse D, Gleixner G, Wilkes H and Kahmen A (2010) Leaf wax *n*-alkane δD values of field-grown barley reflect leaf water δD values at the time of leaf formation. *Geochimica et Cosmochimica Acta* 74: 6741–6750.

Sachse D, Radke J and Gleixner G (2006) δD values of individual *n*-alkanes from terrestrial plants along a climate gradient – implications for the sedimentary biomarker record. *Organic Geochemistry* 37: 469–483.

Sage RF, Wedin DA and Li M (1999) The biogeography of C_4 photosynthesis: patterns and controlling factors. In: Sage RF and Monson RK (eds) *C_4 Plant Biology*. San Diego: Academic Press, pp. 313–373.

Schefuß E, Kuhlmann H, Mollenhauer G, Prange M and Pätzold J (2011) Forcing of wet phases in southeast Africa over the past 17,000 years. *Nature* 480: 509–512.

Schwarz AG and Redmann RE (1988) C_4 grasses from the boreal forest region of northwestern Canada. *Canadian Journal of Botany* 66: 2424–2430.

Seppä H (2013) Pollen analysis, principles. In: Elias SA and Mock CJ (eds) *Encyclopedia of Quaternary Science*. Amsterdam: Elsevier, pp. 794–804.

Song M, Duan D, Chen H, Hu Q, Zhang F, Xu X, Tian Y, Ouyang H and Peng C (2008) Leaf δ^{13}C reflects ecosystem patterns and responses of alpine plants to the environments on the Tibetan Plateau. *Ecography* 31: 499–508.

Stadtmüller T (1987) *Cloud Forests in the Humid Tropics: a Bibliographic Review*. Tokyo: United Nations University.

Stevenson BA, Kelly EF, McDonald EV and Busacca AJ (2005) The stable carbon isotope composition of soil organic carbon and pedogenic carbonates along a bioclimatic gradient in the Palouse region, Washington State, USA. *Geoderma* 124: 37–47.

Stewart GR, Turnbull MH, Schmidt S and Erskine PD (1995) ^{13}C natural abundance in plant communities along a rainfall gradient: a biological integrator of water availability. *Australian Journal of Plant Physiology* 22: 51–55.

Street-Perrott FA and Perrott RA (1990) Abrupt climate fluctuations in the tropics: the influence of Atlantic Ocean circulation. *Nature* 343: 607–612.

Stríkis NM, Cruz FW, Cheng H, Karmann I, Edwards RL, Vuille M, Wang X, De Paula MS, Novello VF and Auler AS (2011) Abrupt variations in South American monsoon rainfall during the Holocene based on a speleothem record from central-eastern Brazil. *Geology* 39(11): 1075–1078.

Stuiver M (1970) Oxygen and carbon isotope ratios of fresh-water carbonates as climatic indicators. *Journal of Geophysical Research* 75(27): 5247–5257.

Stuvier M, Grootes PM and Braziunas TF (1995) The GISP2 $\delta^{18}O$ climate record of the past 16,500 years and the role of the sun, ocean, and volcanoes. *Quaternary Research* 44: 341–354.

Taylor ZP, Horn SP and Finkelstein DB (2013) Pre-Hispanic agricultural decline prior to the Spanish Conquest in southern Central America. *Quaternary Science Reviews* 73: 196–200.

Thompson LG, Moseley-Thompson E, Brecher H, Davis M, León B, Les D, Lin P-N, Mashiotta T and Mountain K (2006) Abrupt tropical climate change: past and present. *PNAS* 103(28): 10536–10543.

Thompson LG, Moseley-Thompson E, Davis ME, Henderson KA, Brecher HH, Zagorodnov VS, Mashiotta TA, Lin P-N, Mikhalenko VN, Hardy DR and Beer J (2002) Kilimanjaro ice core records: evidence of Holocene climate change in tropical Africa. *Science* 298: 589–593.

Thompson LG, Moseley-Thompson E, Davis ME, Lin P-N, Henderson KA, Cole-Dai J, Bolzan JF and Liu K-B (1995) Late Glacial Stage and Holocene tropical ice core records from Huascarán, Peru. *Science* 269: 46–50.

Tierney JE, Russell JM, Huang Y, Sinninghe Damsté JS, Hopmans EC and Cohen AS (2008) Northern Hemisphere controls on tropical Southeast African climate during the past 60,000 years. *Science* 322: 252–255.

Wahl D, Byrne R and Anderson L (2014) An 8700 year paleoclimate reconstruction from the southern Maya lowlands. *Quaternary Science Reviews* 103: 19–25.

Watson BT (2011) *An investigation of stratigraphic evidence for an abrupt climatic event 8200 yr BP in Valle de las Morrenas, Costa Rica*. MS Thesis, University of Tennessee, USA.

Waylen PR, Caviedes CN and Quesada ME (1996) Interannual variability of monthly precipitation in Costa Rica. *Journal of Climate* 9: 2606–2613.

Webster JW, Brook GA, Railsback LB, Cheng H, Edwards RL, Alexander C and Reeder PP (2007) Stalagmite evidence from Belize indicating significant droughts at the time of the Preclassic Abandonment, the Maya Hiatus, and the Classic Maya collapse. *Palaeogeography, Palaeoclimatology, Palaeoecology* 250: 1–17.

Whitlock C and Larsen C (2001) Charcoal as a fire proxy. In: Smol JP, Birks HJB and Last WM (eds) *Tracking Environmental Change Using Lake Sediments, Vol. 3: Terrestrial, Algal, and Siliceous Indicators*. Dordrecht: Kluwer Academic Publishers, pp. 75–97.

Wright HE Jr., Mann DH and Glaser PH (1984) Piston corers for peat and lake sediments. *Ecology* 65(2): 657–659.

Wu J, Porinchu DF, Campbell NL, Mordecal TM and Alden EC (2019a) Holocene hydroclimate and environmental change inferred from a high-resolution multi-proxy record from Lago Ditkebi, Chirripó National Park, Costa Rica. *Palaeogeography, Palaeoclimatology, Palaeoecology* 518: 172–186.

Wu J, Porinchu DF and Horn SP (2017) A chironomid-based reconstruction of late-Holocene climate and environmental change for southern Pacific Costa Rica. *The Holocene* 27(1): 73–84.

Wu J, Porinchu DF and Horn SP (2019b) Late Holocene hydroclimate variability in Costa Rica: signature of the Terminal Classic Drought and the Medieval Climate Anomaly in the northern tropical Americas. *Quaternary Science Reviews* 215: 144–159.

Wu J, Porinchu DF, Horn SP and Haberyan KA (2015) The modern distribution of chironomid sub-fossils (Insecta: Diptera) in Costa Rica and the development of a regional chironomid-based temperature inference model. *Hydrobiologia* 742: 107–127.

Xia Z-H, Xu B-Q, Mügler I, Wu G-J, Gleixner G, Sachse D and Zhu L-P (2008) Hydrogen isotope ratios of terrigenous *n*-alkanes in lacustrine surface sediment of the Tibetan Plateau record the precipitation signal. *Geochemical Journal* 42: 331–338.

Yancheva G, Nowaczyk NR, Mingram J, Dulski P, Schettler G, Negendank JFW, Liu J, Sigman DM, Peterson LC and Haug GH (2007) Influence of the intertropical convergence zone on the East Asian monsoon. *Nature* 445: 74–77.

2.10 Appendix

Table 2.1. Radiocarbon determinations for Lago de las Morrenas 1. Core 1 (top) and core 2 (bottom).[a]

Lab Number[b]	Depth (cm)	$\delta^{13}C$	Uncalibrated ^{14}C Age (^{14}C yr BP)	±2σ Range (cal yr BP)	Probability
AA-52069	83	–19.6	1236 ± 31	1163–1072 1263–1169	40.1 54.7
AA-52070	181	–20.9	3397 ± 34	3719–3566	94.3
AA-52071	333	–20.6	4511 ± 37	5209–5047 5303–5211	61.9 32.9
AA-52072	389	–19.2	5611 ± 38	6454–6307 6465–6457	93.1 1.7
AA-52073	430	–18.4	6444 ± 40	7428–7287	94.8
AA-52074[c]	541	–15.5	9811 ± 50	11313–11170	95.0
Beta-30431	96	–	1230 ± 170	1416–795 1481–1463 1516–1495	93.5 0.7 0.8
Beta-30432	225.5	–	3100 ± 90	3484–3063 3493–3486 3506–3504 3554–3533	93.4 0.3 0.1 1.1
Beta-30433	325	–	4250 ± 90	5039–4528	95.0
Beta-30434	425	–	6830 ± 120	7876–7492 7929–7892	91.3 3.7
Beta-30435[d]	521	–	8900 ± 100	10232–9688	95.0
Beta-31787[d]	534.87	–	10140 ± 120	12163–11270 12228–12212 12366–12357	94.2 0.5 0.3

[a] Dates calibrated using the 'clam' package (v. 2.3.2; Blaauw 2019) for the R Statistical Environment (v. 3.5.2; R Core Team 2019) and the IntCal13 radiocarbon calibration curve (Reimer et al. 2013).
[b] Analyses performed by the Arizona Accelerator Mass Spectrometry Lab (AA #) and Beta Analytic, Inc (Beta #). All dates are on bulk sediment. Depths are midpoints for intervals of 2 cm in core 1 and 12–30 cm in core 2.
[c] Date from core 1 used in core 2 age model to constrain the hiatus.
[d] Date from core 2 used in core 1 age model to constrain the hiatus.

Table 2.2. Plant taxa represented in the Morrenas 1 pollen assemblages. Categorized by most likely life form at our research site.[a]

Taxon[b]	Vegetation Zone	Life Form Category[c]
Myrtaceae	Tropical to lower montane	Angiosperm tree
Urticales	Tropical to lower montane	Angiosperm tree
Acalypha	Tropical to lower montane	Angiosperm tree
Alchornea	Tropical to lower montane	Angiosperm tree
Alfaroa	Tropical to lower montane	Angiosperm tree
Alnus	Montane	Angiosperm tree
Bocconia	Tropical to lower montane	Angiosperm tree
Cecropia	Tropical to lower montane	Angiosperm tree
Celtis	Tropical to lower montane	Angiosperm tree
Clethra	Montane	Angiosperm tree
Cornus	Montane	Angiosperm tree
Drimys	Montane	Angiosperm tree
Hedyosmum	Montane	Angiosperm tree
Myrica	Montane	Angiosperm tree
Piper	Tropical to lower montane	Angiosperm tree
Quercus	Montane	Angiosperm tree
Ulmus	Tropical to lower montane	Angiosperm tree
Asteraceae	Subalpine	Angiosperm shrub
Ericaceae	Subalpine	Angiosperm shrub
Liguliflorae	Subalpine	Angiosperm shrub
Melastomataceae	Subalpine	Angiosperm shrub
Diplostephium	Subalpine	Angiosperm shrub
Garrya	Subalpine	Angiosperm shrub
Myrsine	Subalpine	Angiosperm shrub
Weinmannia	Subalpine	Angiosperm shrub
Caryophyllaceae	Páramo	Forb
Umbelliferae	Páramo	Forb
Acaena	Páramo	Forb
Geranium	Páramo	Forb
Valeriana	Páramo	Forb
Cyperaceae	Páramo	Graminoid
Poaceae	Páramo	Graminoid
Prumnopitys (formerly *Podocarpus*)	Montane	Gymnosperm
Mono- and trilete spores[d]	Páramo	Pteridophytes

[a] Pollen identification and taxonomy follows Horn (1993). We excluded indeterminate pollen grains and spores and taxa that could not be reliably classified.

[b] In many cases, pollen can only be identified to the family level or to the order for some pollen types in the Urticales group.

[c] Many taxa listed include species with more than one life form. Here we categorize plants into the life forms that are most likely represented at the Morrenas site.

[d] Includes all mono- and trilete spores except *Isoetes*.

Table 2.3. Global average apparent fractionation factors (ε) at Morrenas. Fractionations between plants and meteoric water for $C_{27–31}$ odd *n*-alkanes. Compiled from the supplementary data in Sachse et al. (2012).

Plant Type	$\varepsilon_{C27/MAP}$	$\varepsilon_{C29/MAP}$	$\varepsilon_{C31/MAP}$
Gymnosperms	–112‰	–110‰	–103‰
Angiosperm trees	–107‰	–122‰	–114‰
Angiosperm shrubs	–110‰	–101‰	–95‰
C_3 Graminoids	–127‰	–149‰	–157‰
C_4 Graminoids	–131‰	–132‰	–136‰
Forbs	–124‰	–128‰	–130‰
Pteridophytes[a]	–103‰	–108‰	–114‰

[a] Excludes *Isoetes* spores.

Table 2.4. Expected δD values for modern precipitation at Morrenas. Location: 9.4925 °N, 83.4848 °W, 3480 m. From the Online Isotopes in Precipitation Calculator (OIPC v. 3.1; Bowen 2019).

	Jan	Feb	Mar	Apr	May	Jun	Jul	Aug	Sep	Oct	Nov	Dec	Year
δD (‰)	–55	–52	–68	–61	–95	–87	–78	–66	–72	–92	–79	–74	–80

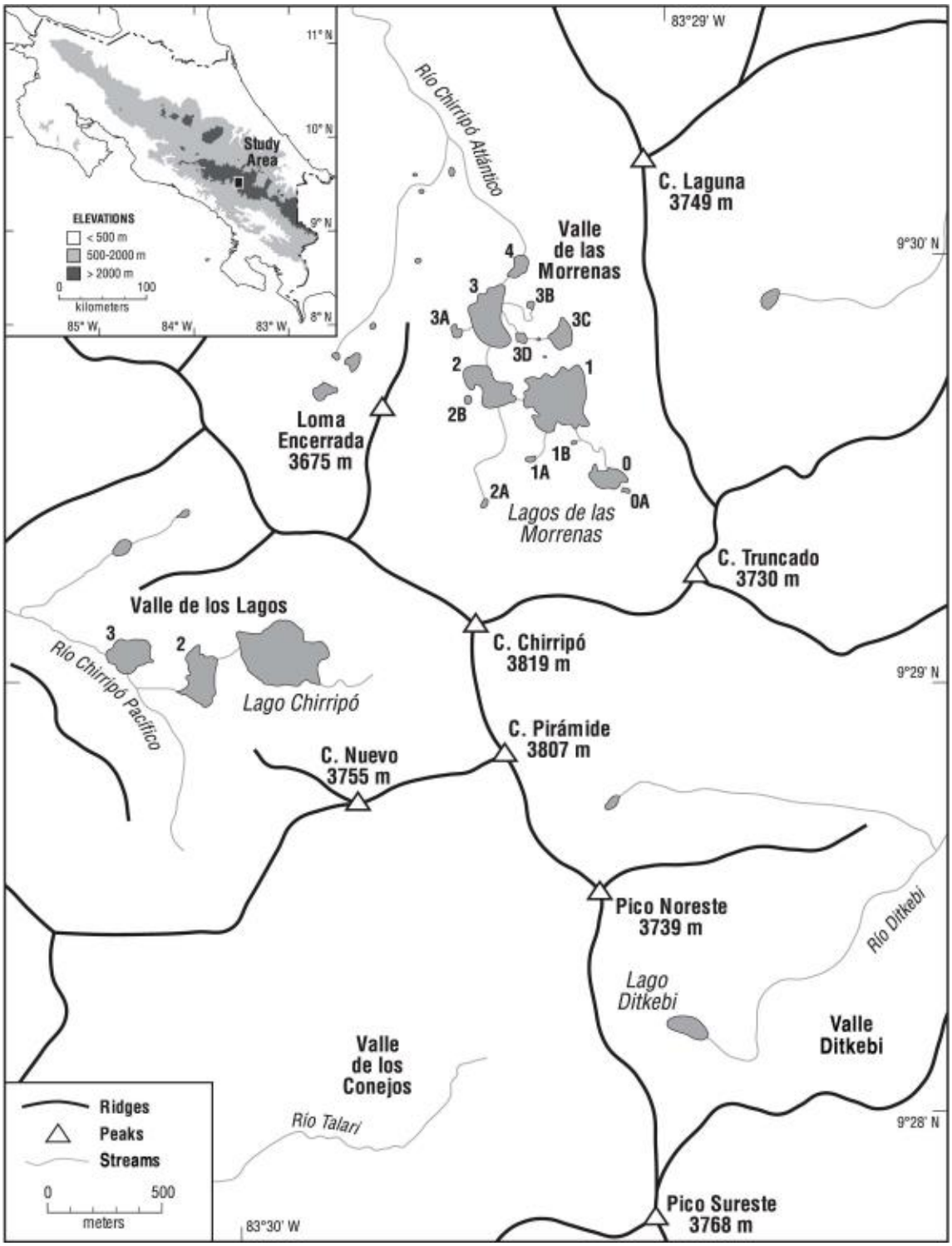

Fig 2.1. Location of Lago de las Morrenas 1. Includes other sites in Costa Rica mentioned in the text. Map modified from Fig. 1 in Orvis and Horn (2000). Lake numbering follows Orvis and Horn (2000) and Horn et al. (2005).

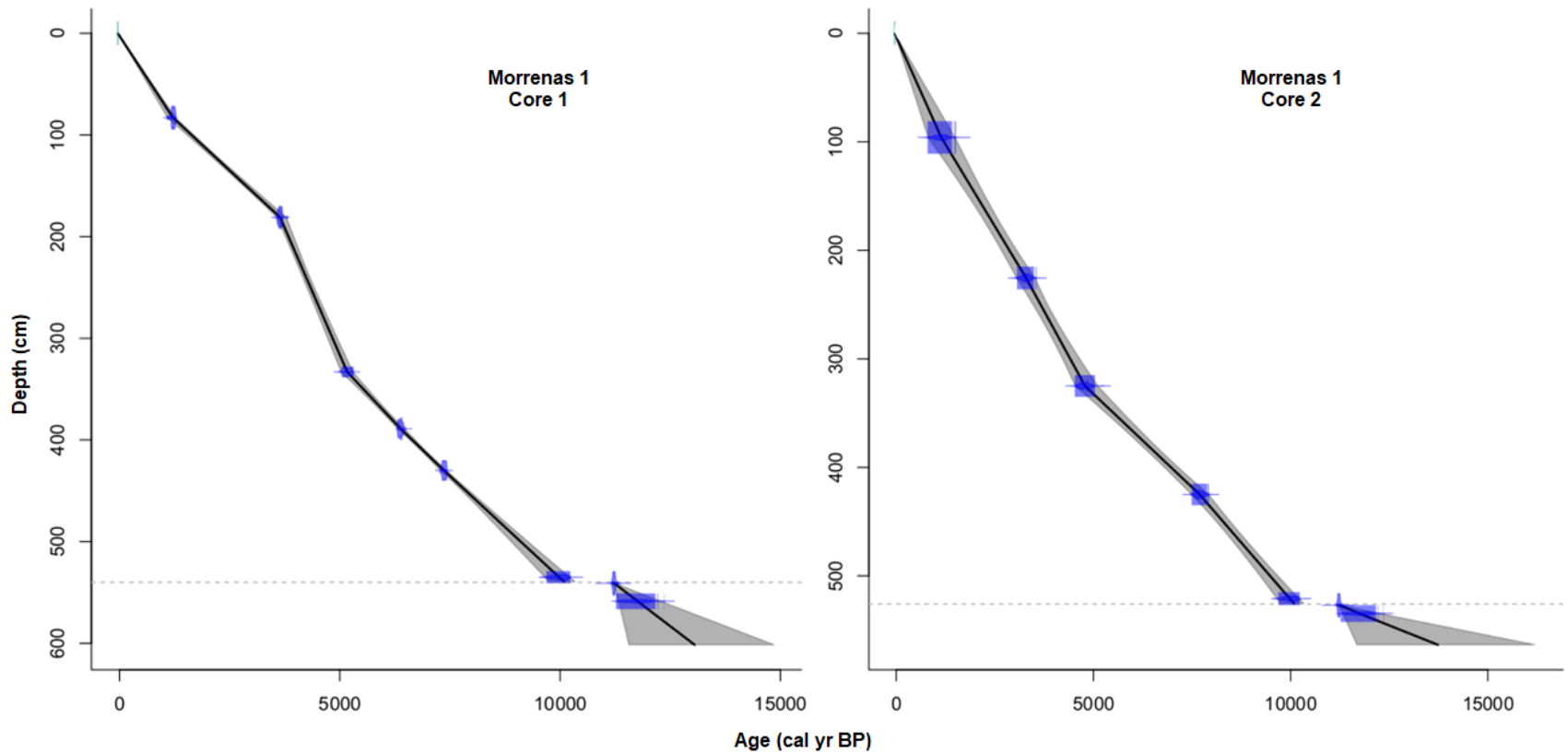

Fig. 2.2. Age-depth models for Lago de las Morrenas 1. Core 1 (left) and core 2 (right). The dashed horizontal lines show the location of a hiatus in sedimentation. The organic sediments above the hiatus are the focus of this study. The models were created using linear interpolation with the 'clam' package (Blaauw 2019) for the R Statistical Environment (R Core Team 2019). Blue rectangles indicating positions of radiocarbon dates are larger for core 2 as the dates for that core were conventional radiocarbon dates on bulk sediment that required larger sections of sediment than the AMS radiocarbon dates obtained for core 1.

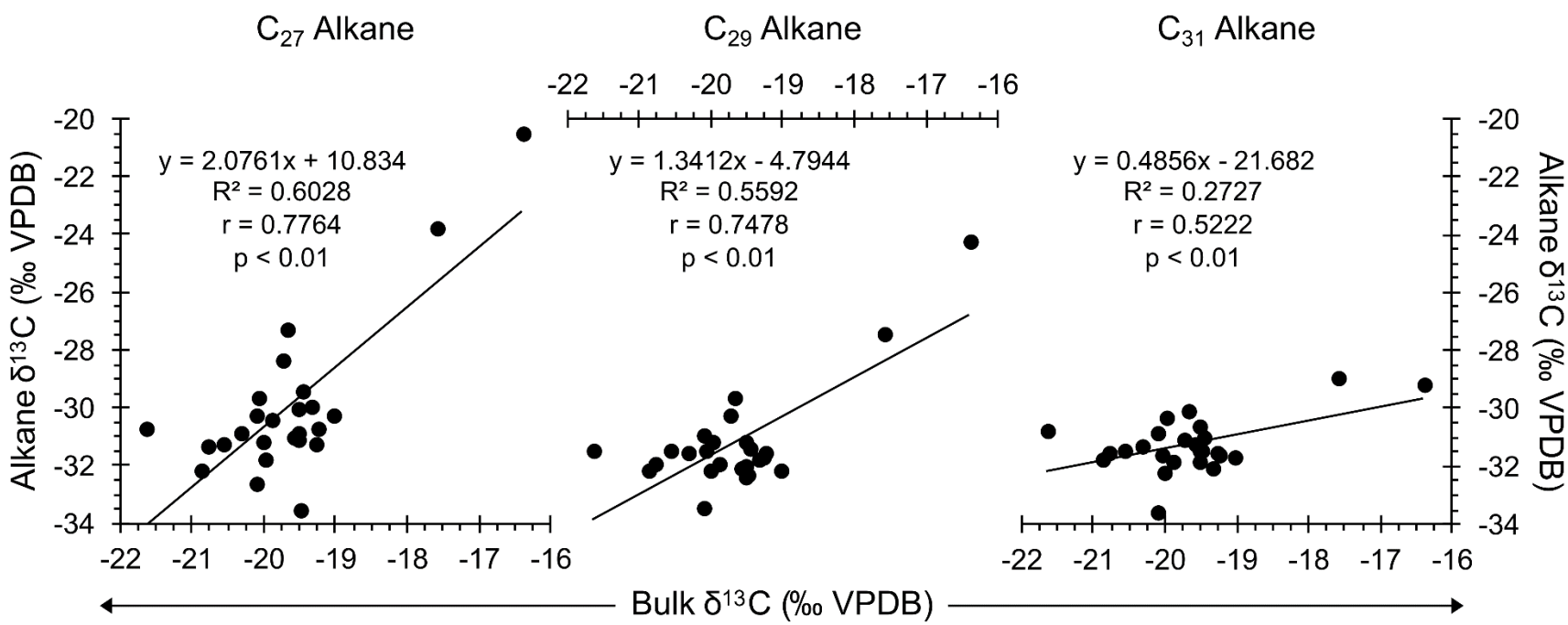

Fig. 2.3. Regression analyses of stratigraphically coeval bulk $\delta^{13}C$ and *n*-alkane $\delta^{13}C$.

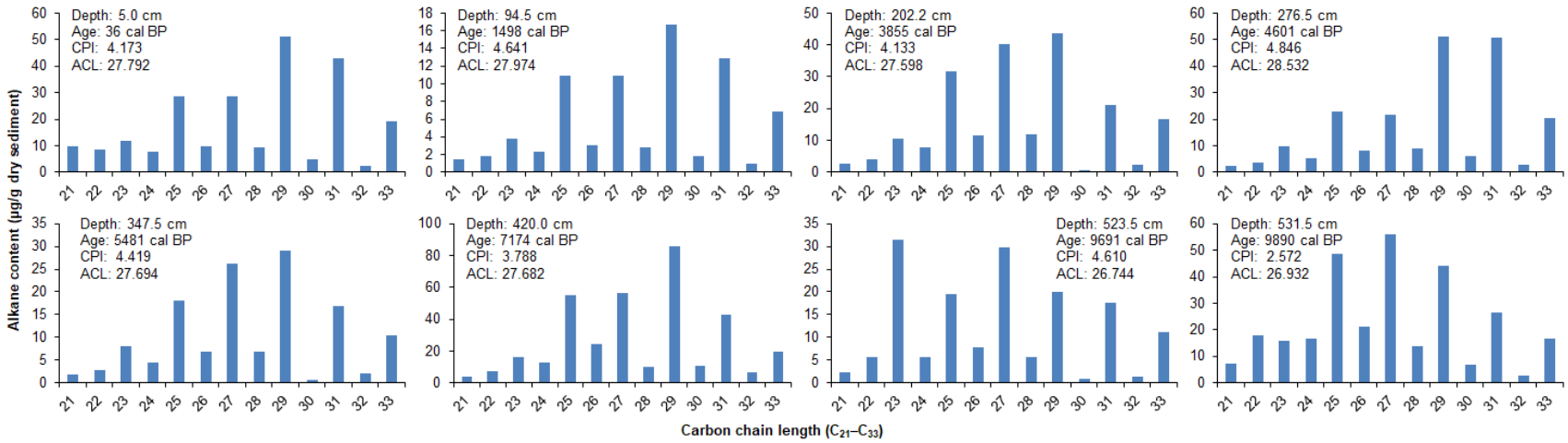

Fig. 2.4. Alkane distributions, CPI, and ACL for selected samples. Note scale changes on the y-axes.

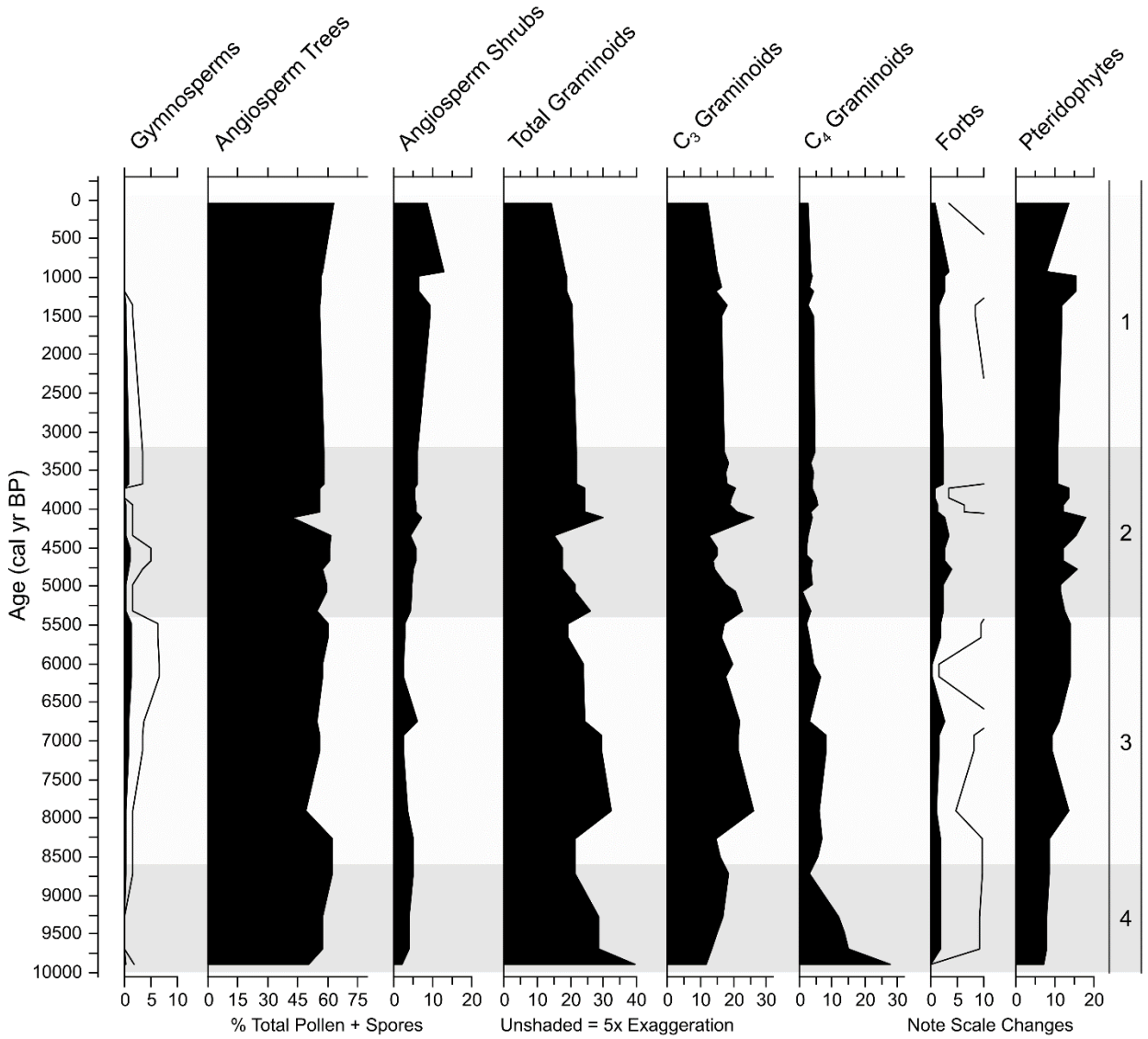

Fig. 2.5. Plants represented in the LM1 pollen record. Categorized by taxonomy and life form following Feakins (2013). Percentages for gymnosperms, angiosperm trees and shrubs, total graminoids, forbs (non-graminoid herbaceous taxa), and pteridophytes (excluding *Isoetes*) are calculated based on a sum of pollen and spore counts for all included taxa. Percentages for C_3 and C_4 graminoids are calculated from total graminoids using a two-endmember mixing model (see text) representing an average of $C_{29–31}$ odd numbered *n*-alkane homologues. Zones are informally delineated based on major changes in proxy data seen in Figs. 2.6 and 2.9.

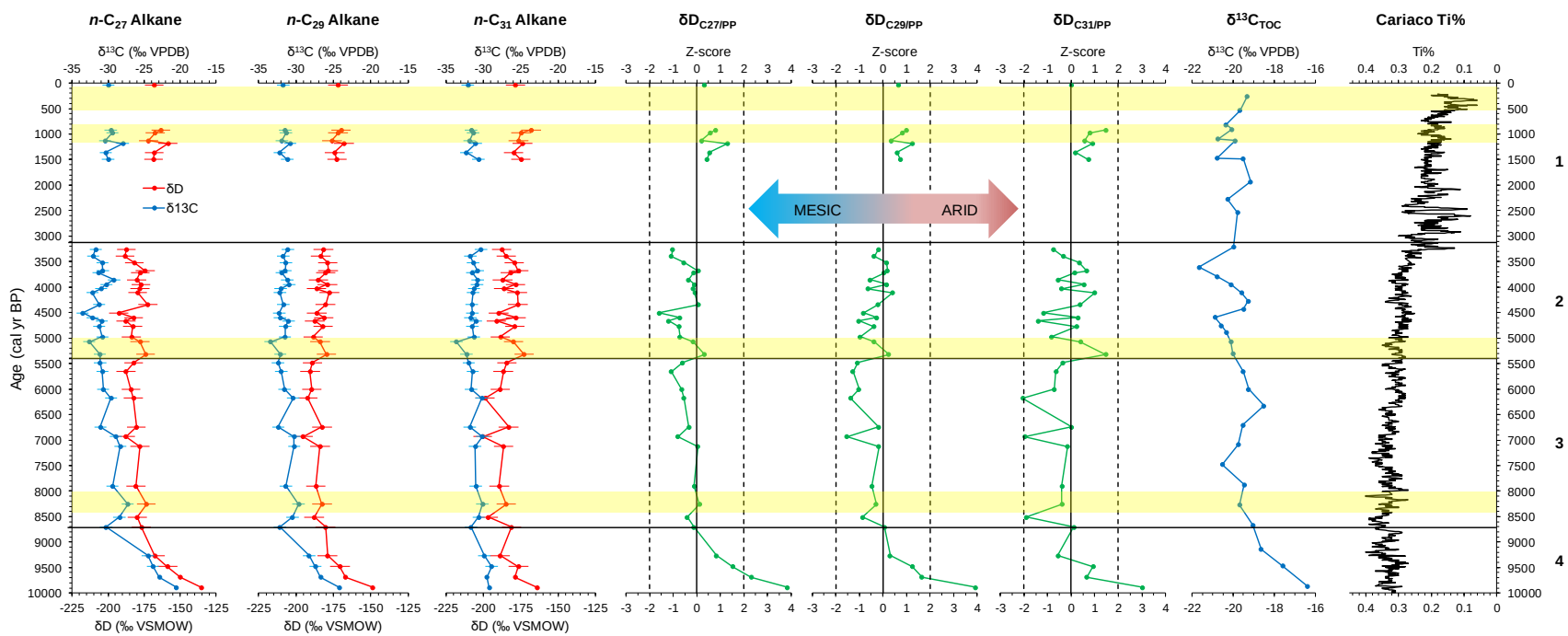

Fig. 2.6. Morrenas isotope data. Includes leaf wax δD and $\delta^{13}C$ data and z-scores for δD_{PP} for odd numbered *n*-alkanes $C_{27–31}$. Bulk $\delta^{13}C_{TOC}$ data are from Lane et al. (2011a). Cariaco Basin titanium values are from the dataset tuned by Kennett et al. (2012). Note scale changes on the x-axes. Zones 1–4 are delineated informally based on major changes in the proxy data and correspond to the same zones in Figs. 2.5, 2.8, and 2.9. Yellow bands cover periods of global extreme climate events, including the 8200 BP event (ca. 8400–8000 cal yr BP), the 5200 BP event (ca. 5400–5000 cal yr BP), the TCD (ca. 1200–850 cal yr BP), and the LIA (ca. 550–100 cal yr BP). Data trending toward the left on the x-axes represent mesic conditions, while data trending to the right represent arid conditions for all proxy data curves. VPDB = Vienna Pee Dee Belemnite. VSMOW = Vienna Standard Mean Ocean Water. The two gaps in the stratigraphic record are gaps in sediment availability for the analyses reported here, not gaps in sedimentation at the lake.

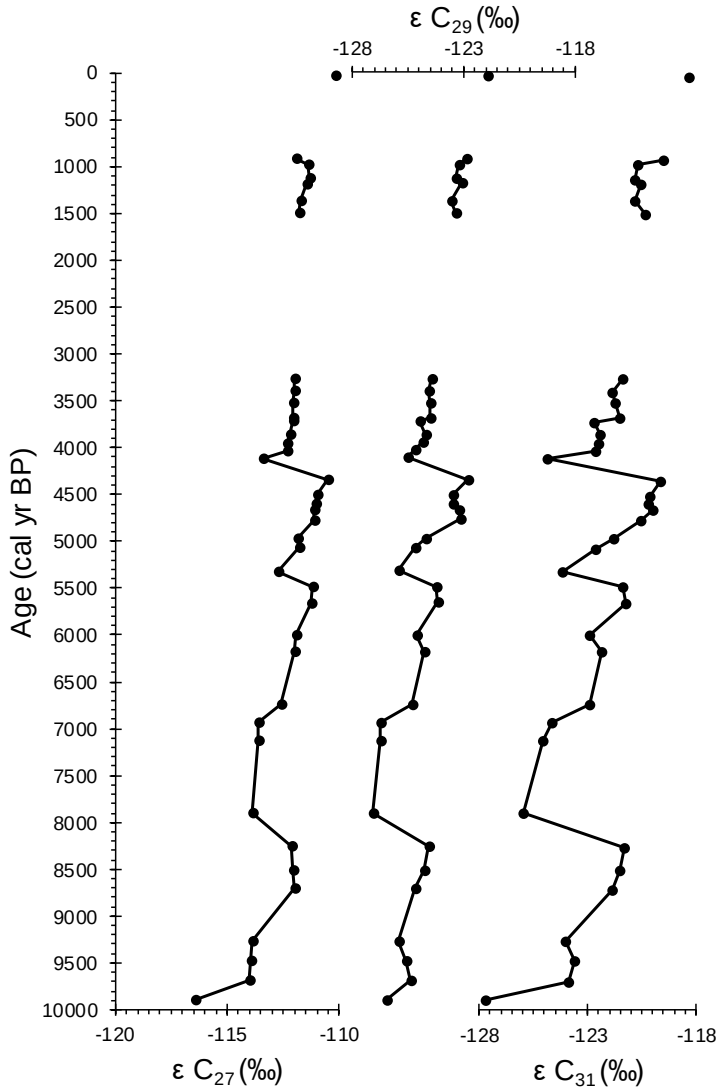

Fig. 2.7. Fractionation factors (ε) between plants and precipitation. Note changes in scale on the x-axes. Breaks in the curves indicate two intervals of the core with no samples.

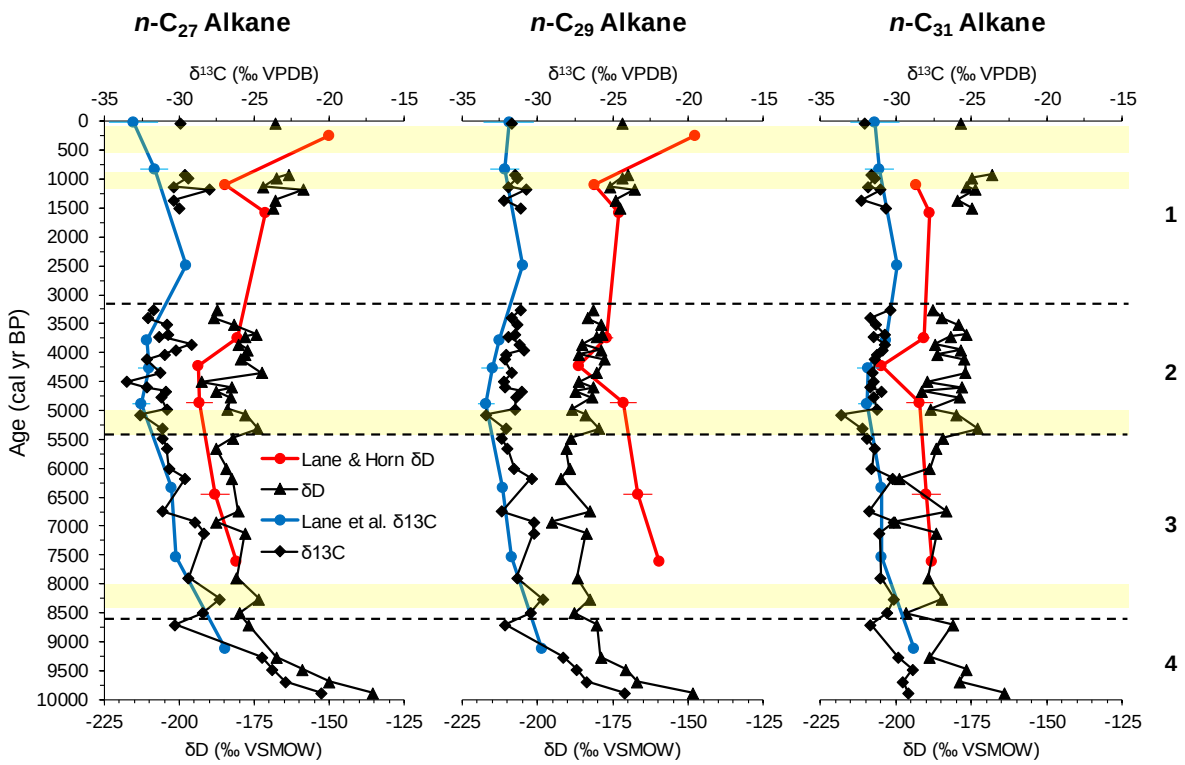

Fig. 2.8. Comparison of new and existing isotope data. Data for compound-specific δD (red curves) from Lane and Horn (2013) and $\delta^{13}C$ (blue curves) from Lane et al. (2011a) plotted over data for δD and $\delta^{13}C$ from this study for odd numbered *n*-alkanes $C_{27–31}$. Yellow bands represent the intervals of the 8200 BP event, the 5200 BP event, the TCD, and the LIA, as in Fig. 2.6. Zones 1–4 (dashed lines) are delineated informally by major changes in the proxy data and correspond to the same zones in other figures.

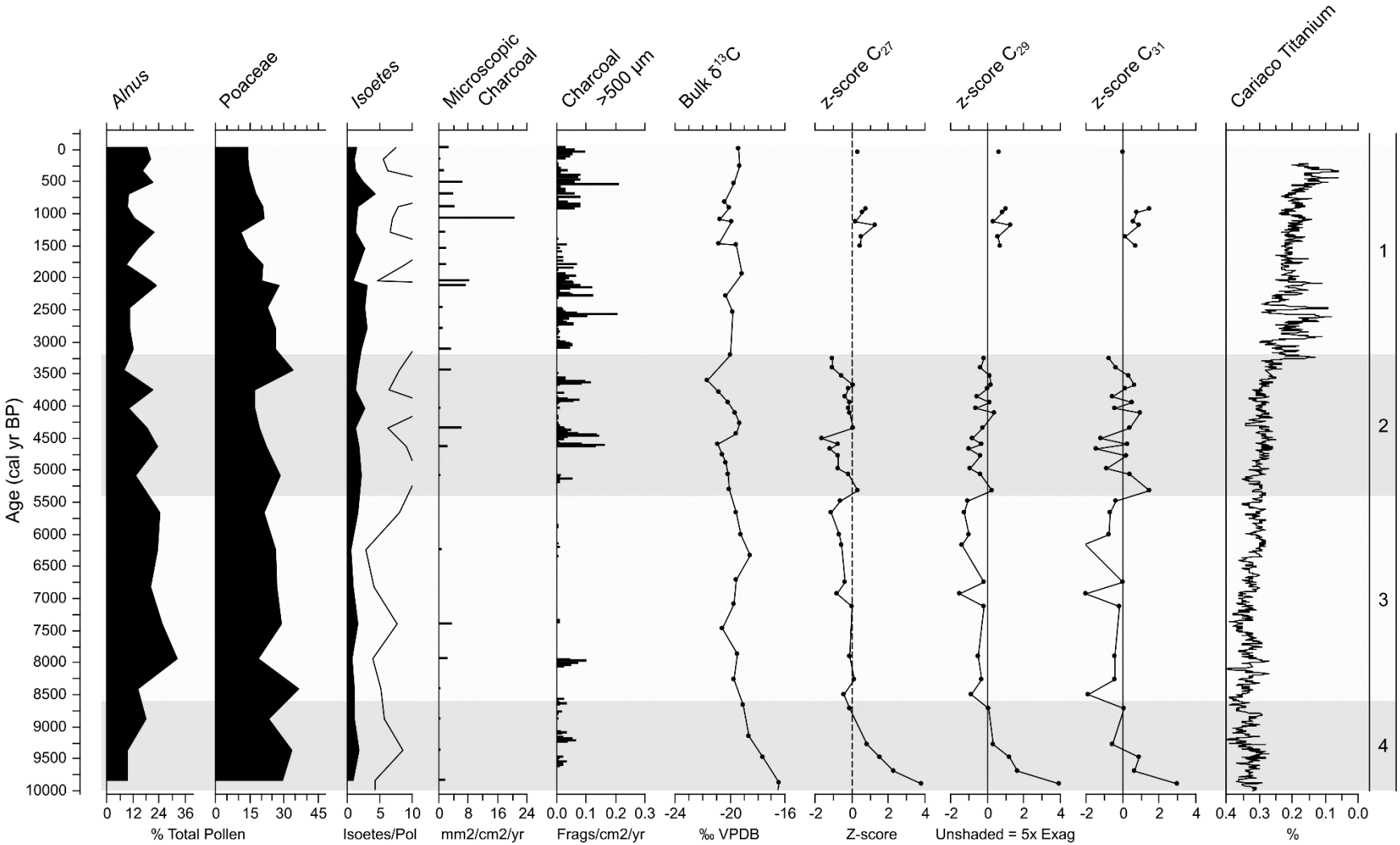

Fig. 2.9. Select proxy data for Morrenas 1. Pollen and spore data and microscopic charcoal fragments (<125 µm) are from Horn (1993), macroscopic charcoal fragments (>500 µm) from League and Horn (2000), bulk $\delta^{13}C$ data from Lane et al. (2011a), z-scores for δD_{PP} for odd numbered *n*-alkanes $C_{27–33}$ from this study, and Cariaco Basin titanium data tuned by Kennett et al. (2012). Zones 1–4 are delineated informally by major changes in the proxy data and match zones in other figures in this study.

2.11 Supplemental Information

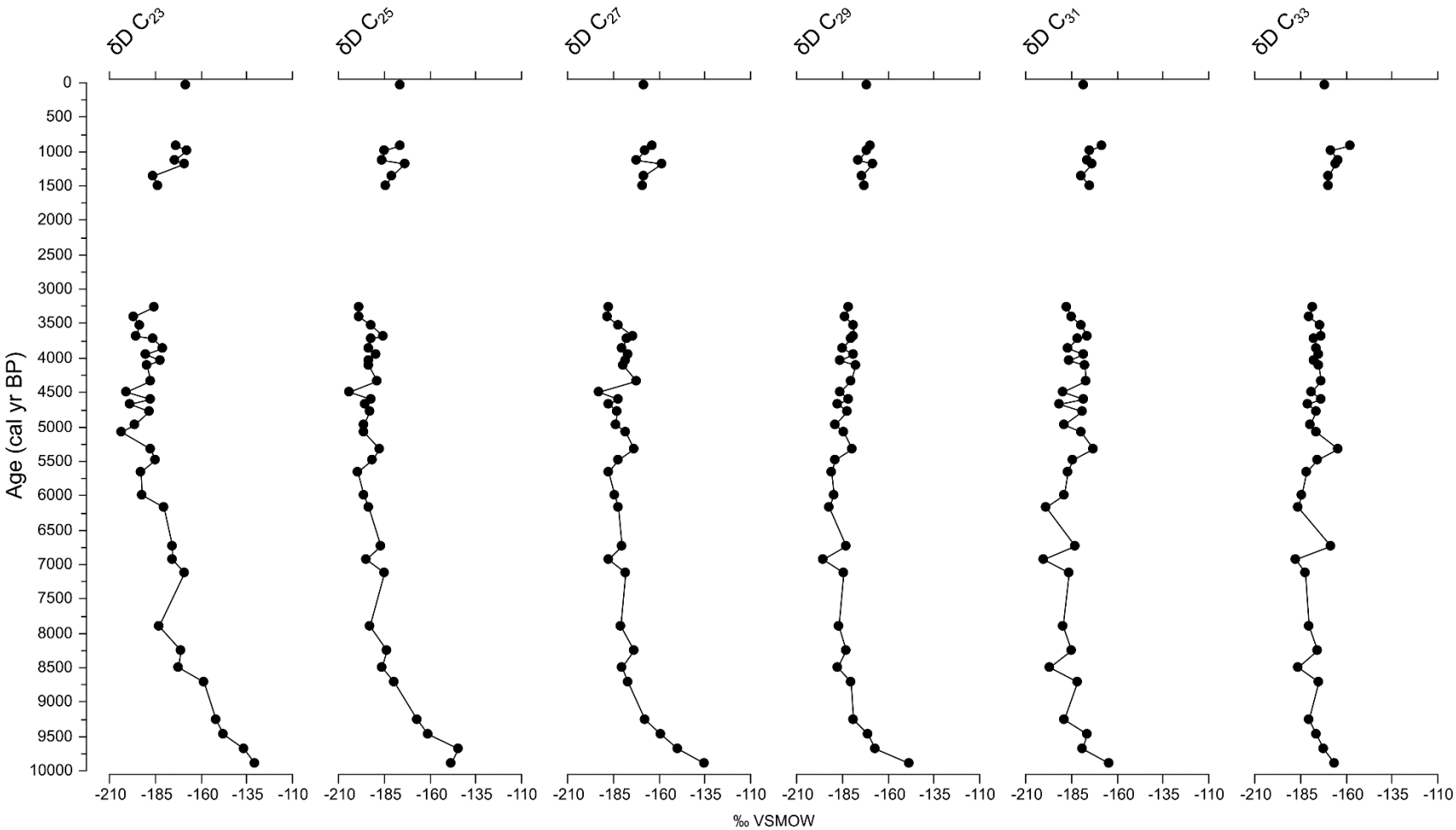

Fig. S2.1. *n*-alkane δD values for odd numbered homologues C_{23} to C_{33}.

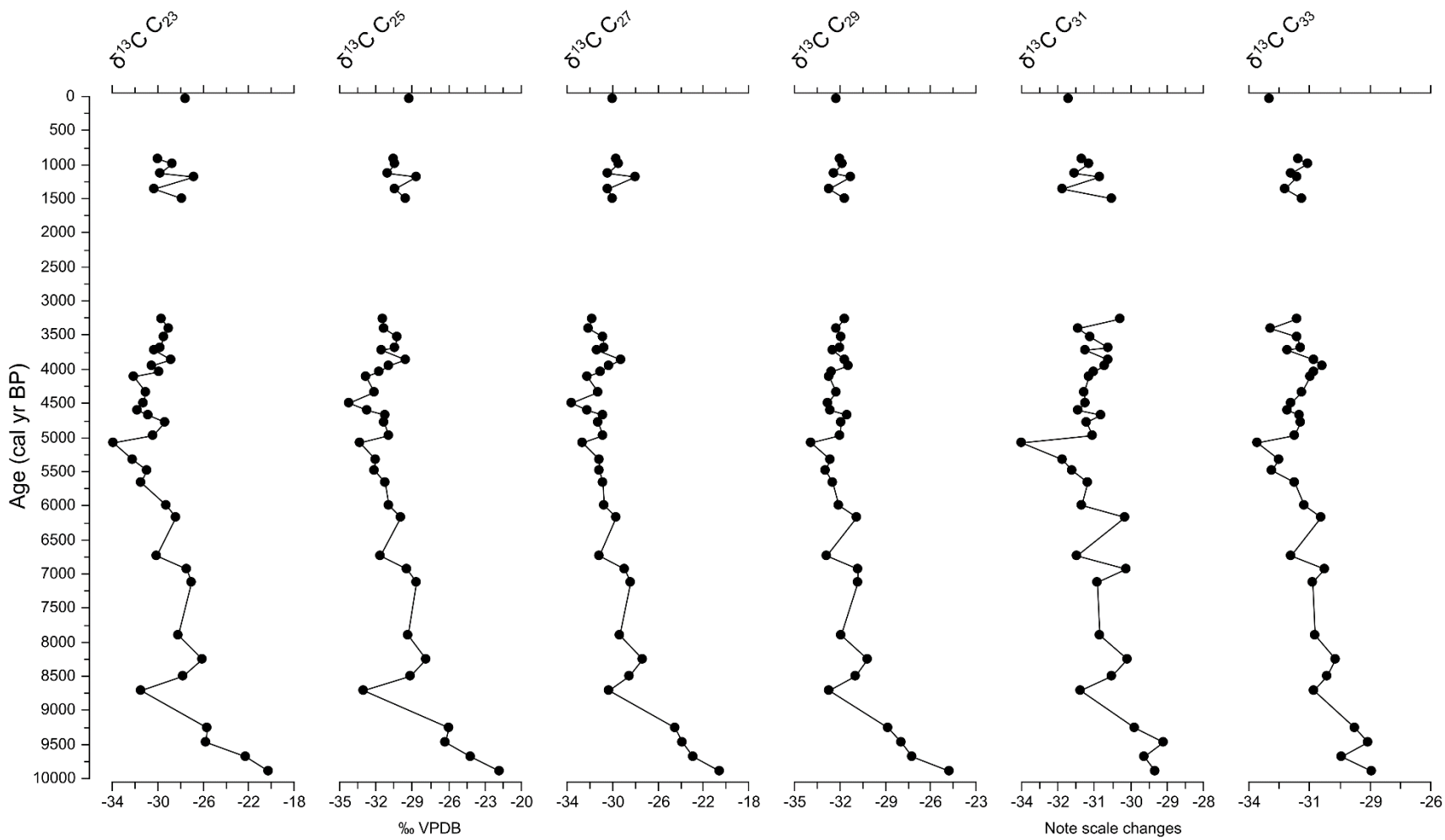

Fig. S2.2. *n*-alkane $\delta^{13}C$ values for odd numbered homologues C_{23} to C_{33}. Note changes to the scale on the x-axes.

CHAPTER 3

A 2700-YEAR HISTORY OF PRECIPITATION AND MAIZE AGRICULTURE IN THE CARIBBEAN LOWLANDS OF COSTA RICA

This chapter is in preparation for submission to a journal. The use of "we" in the text refers to me and my co-authors, Sally Horn and Chad Lane. As first author, I led on study design, data collection and analyses, and writing the manuscript.

3.1 Abstract

We conducted compound-specific stable hydrogen (δD) and carbon ($\delta^{13}C$) isotope analysis of *n*-alkanes from terrestrial leaf waxes in a sediment core from Laguna Bonillita (9.9921 °N, 83.6114 °W, 450 m) to reconstruct variations in late Holocene precipitation in the Caribbean lowlands of Costa Rica. We compared our new record with paired evidence of vegetation and fire history from the same sediment core and with archaeological evidence of prehistoric human activity in the area around Laguna Bonillita to better understand relationships between climate, environment, and human activity. Our new data show variation in Holocene hydroclimate at Bonillita consistent with evidence from the wider circum-Caribbean, including local manifestations of aridity and climate instability during the Terminal Classic Drought (ca. 1200–850 cal yr BP) and a 350-year period of sustained aridity during the Little Ice Age (ca. 550–100 cal yr BP). Our paired paleoenvironmental and archaeological findings indicate that some drying at Bonillita may have been beneficial for maize agriculture at a site that is generally wet throughout the year.

3.2 Introduction

Laguna Bonillita (9.9921 °N, 83.6114 °W, 450 m) is a small lake on the lower Caribbean slope of Volcán Turrialba in the Cordillera Central of Costa Rica. Paleoecological analyses of a 9.5 m sediment core from the lake revealed a history of land use and maize agriculture at varying scales and intensities from ca. 2700 cal yr BP to the present (Northrop and Horn 1996; Lane et al. 2009). Archaeological surveys of the area around Bonillita and nearby Laguna Bonilla demonstrate that the area was continuously occupied by sophisticated and increasingly complex prehistoric people from the La Montaña phase (ca. 2950–2250 cal yr BP) until late in the timeline of Spanish settlement of the Caribbean interior of Costa Rica, with maximum site occupation during the El Bosque phase ca. 2250–1650 cal yr BP (Kennedy 1968, 1976; Snarskis 1981, 1984; Bustos Ramos 2007).

We conducted compound-specific stable hydrogen (δD) and carbon ($\delta^{13}C$) isotope analysis of *n*-alkanes from terrestrial leaf waxes preserved in the Laguna Bonillita sediment core to reconstruct variations in precipitation in the Caribbean lowlands during the Late Holocene. Our goals were to develop a paleoenvironmental reconstruction that unambiguously reflects climate and to compare that record with paired evidence of vegetation and fire history from the same sediment core and with local archaeological evidence to better understand relationships between climate, environment, and human activity in Costa Rican prehistory.

We asked three questions in our research: (1) what patterns and variations in Late Holocene hydroclimate are recorded in the Laguna Bonillita sediments; (2) how do variations in precipitation over time at Bonillita relate to evidence of prehistoric human activity; and (3) how are global-scale extreme climate events, such as the Terminal Classic Drought (TCD; ca. 1200–

850 cal yr BP) and the Little Ice Age (LIA; ca. 550–100 cal yr BP) represented in the Caribbean lowlands of Costa Rica?

3.3 Background

3.3.1 The Compound-Specific Stable Hydrogen Isotope (δD) Proxy

Compound-specific stable hydrogen isotope (δD) analyses of lipids preserved in lake-sediment cores is a powerful tool for reconstructing past temporal and spatial variation in precipitation. The δD composition of sedimentary *n*-alkane components of terrestrial leaf waxes serves as an indicator of watershed hydrology (Sachse and Gleixner 2004; Sachse et al. 2010) and the sedimentary δD record serves as a proxy for precipitation variability through time (Stuiver 1970; Cohen 2003; Sachse and Gleixner 2004).

The δD composition of meteoric water in the tropics is controlled by the amount effect and evapotranspiration. Increased precipitation results in relatively lower δD values, and vice versa (Dansgaard 1964; Lachniet and Patterson 2002), while evaporation and transpiration preferentially remove the lighter protium (^{1}H) isotope from water relative to deuterium (^{2}H), which results in enrichment of the heavier isotope in remaining groundwater available to plants (Polissar and Freeman 2010). Increased δD values in terrestrial plant waxes indicate aridity due to the additive effects of amount effect and evapotranspiration, while decreased δD values indicate more humid conditions due to a greater abundance of ^{1}H isotopes in available water (Liu and Huang 2005; Sachse et al. 2006; Xia et al. 2008; Kahmen et al. 2013a, 2013b). Both decreased precipitation and increased evapotranspiration result in aridity and relatively higher δD values in leaves and sediments (Douglas et al. 2015). This biomarker signal of drought has been used to develop paleoclimate records from late Quaternary sediments by multiple research

groups (Tierny et al. 2008; Niedermeyer et al. 2010; Schefuß et al. 2011; Lane and Horn 2013; Lane et al. 2014).

3.3.2 Extreme Climate Events

The last several decades have seen significant interest and scholarship on climate change and extreme events (see Chapter 2 of this dissertation). Analyses of speleothems and lake sediments from the Yucatan have linked the decline of Maya civilization to the Terminal Classic Drought (TCD), a series of severe, multi-decadal droughts that occurred between ca. 1200 and 850 cal yr BP (Hodell et al. 2005; Lane et al. 2014) across the circum-Caribbean region (Hodell et al. 1995, 2005; Webster et al. 2007; Medina-Elizalde et al. 2010; Kennett et al. 2012; Douglas et al. 2015; Bhattacharya et al. 2017). Researchers studying titanium content in sediments from the Cariaco basin have linked changes in the mean annual position of the Intertropical Convergence Zone (ITCZ) to variations in rainfall over northern South America (Haug et al. 2003; Peterson and Haug 2006). These findings point to a more southerly mean annual position of the ITCZ as a likely cause of the TCD (Haug et al. 2003; Hodell et al. 2005; Peterson and Haug 2006; Kennett et al. 2012; Luzzadder-Beach et al. 2012).

We have reported evidence of similarly intense drought during the TCD at Laguna Castilla on Hispaniola (Lane et al. 2014) and at Lago de las Morrenas 1 in highland Costa Rica (Kerr et al. this dissertation) using δD analysis of lake sediments. Other evidence of dry conditions during the TCD on the Panamanian Isthmus comes from analyses of subfossil chironomids and bulk sedimentary stable carbon isotopes ($\delta^{13}C$) at Laguna Zoncho in southern Pacific Costa Rica and at Lago de las Morrenas 3C (Wu et al. 2017, 2019), from a distinct charcoal layer in sediments from Lago Chirripó (Horn 1989, 1993) and increased diatom valves

in sediments from Lago de las Morrenas 1 in the Chirripó highlands of Costa Rica (Haberyan and Horn 1999), and from increased $\delta^{18}O$ values in a speleothem from Panama (Lachniet et al. 2004).

Evidence for the Little Ice Age (LIA; ca. 550–100 cal yr BP) likewise appears in the Cariaco sediments. Decreased titanium content indicates decreased rainfall in northern South America and the broader circum-Caribbean region (Haug et al. 2001; Peterson and Haug 2006; Black et al. 2007). Terrestrial records also indicate widespread drought during the LIA, including aridity in the Yucatan based on oxygen isotope ($\delta^{18}O$) analysis of sedimentary carbonates (Hodell et al. 2005) and on Hispaniola based on sedimentary ostracod valves (Lane et al. 2011). Wu et al. (2019) reported evidence of warm and wet conditions during the first part of the LIA ca. 550–350 cal yr BP followed by cooling and drying during the latter part ca. 350–100 cal yr BP at Lago de las Morrenas 3C. Taylor et al. (2013) reported evidence of agricultural decline at Laguna Zoncho that corresponds to LIA drought. We reported similar evidence for agricultural decline and hypothesized climate deterioration at nearby Laguna Santa Elena (Kerr et al. forthcoming, chapter 4 of this dissertation).

Sorting out causes and consequences of extreme climate events from proxy records remains challenging, particularly for the Neotropics—an area that was profoundly influenced by prehistoric human activity. Developing long proxy records from sites such as Laguna Bonillita in central Atlantic Costa Rica, which was inhabited by prehistoric maize agriculturalists at varying intensities for at least 2700 years, has high potential to contribute to this debate.

3.3.3 Geography and Archaeology of the Central Atlantic Watershed

The Río Reventazón Valley served for millennia as a cultural conduit between the central highland basin and the Atlantic coast of Costa Rica. While archaeological investigations have

been conducted in the Valley and surrounding central Atlantic watershed, comparatively little is known about past environmental conditions and how prehistoric people affected their environment. The earliest excavated site in Costa Rica is the Turrialba Paleoindian quarry in the upper Río Reventazón Valley, which yielded Clovis and Magellan points dated to the earliest Holocene (Snarskis 1979), but the beginnings of sedentism in the central Atlantic region came much later, with sites no older than ca. 3000 BP (Snarskis 1984). The prehistoric Reventazón chronology comprises four phases of increasing social complexity, all of which are represented to varying degrees in the archaeological record near our research site at Laguna Bonillita (Table 3.1).

The La Montaña phase (2950–2250 BP) was characterized by small, dispersed sites preferentially located near hunting and gathering resources. Archaeological and paleoecological evidence from this phase indicates swidden root cropping, likely supplemented by gathered wild resources and incipient maize agriculture. The artifact assemblage is noted for containing griddles (*budares*) for processing bitter manioc late in the cultural chronology of the wider region, even after adoption of maize agriculture in other areas. Snarskis (1984) noted that the La Montaña phase represents a “fluctuating cultural frontier” in eastern central Costa Rica, incorporating elements of both Mesoamerican and South American cultures.

The El Bosque phase (2250–1450 cal yr BP) was a time of cultural fluorescence in the Atlantic watershed. Sites were numerous and large, yet still dispersed on the landscape. This period saw explosive population growth, possibly owing to a modified agricultural system incorporating expansion and intensification of maize, plus expanded availability of farmland (Snarskis 1984). Settlements were preferentially located near farmland on alluvial plains and terraces and show the adoption of full-scale maize agriculture. Societies became considerably

more complex in the El Bosque phase, incorporating craft specialization in ceramic, lithic, and lapidary industries, ceremonial grave goods and elaborate burials, a distinct architectural style, and extensive cemeteries that may have been organized by clan, lineage, or social group. The El Bosque complex represents ranked societies at or near the chiefdom level, likely incorporating control and redistribution of resources (Snarskis 1984).

The La Selva phase (1450–950 cal yr BP) was a time of rapid culture change (Snarskis 1984). Archaeological evidence indicates a cultural decline from the El Bosque phase, although comparatively less is known about La Selva compared to the previous two phases and the subsequent La Cabaña phase. The subsistence strategy continued to incorporate maize agriculture, likely supplemented with gathered wild resources. Architecture began to change from rectangular to circular structures, incorporating influences from farther south in the region, including elements of South American culture. Metallurgy was introduced to the area, while the lapidary industry saw a general decline in quality.

The La Cabaña phase (950–400 cal yr BP), which was in place at the time of Spanish arrival, saw further significant culture change. Settlement patterns became nucleated and oriented around small ceremonial centers, and possibly focused on socio-political boundaries and defense. Snarskis (1984) referred to these settlements as “city-states.” The ceramic industry generally declined in quality and ceremonial ceramics declined in number. Lithics, and notably *metates*, became more utilitarian in nature. Human images increased in artwork and incorporated more images of violence and warfare. Architecture of the La Cabaña phase is noted for clearly defined activity areas and buildings, including plazas possibly for ritual or civic use. Large sites, such as Guayabo, Nájera, and La Zoila appeared during the La Cabaña phase and may have been part of a network of important centers (Snarskis 1984).

The central Atlantic watershed, including the area around Laguna Bonillita, is wet and warm all year, which is important for understanding the development and trajectory of prehistoric culture and maize agriculture in eastern Costa Rica. Maize appears to have been adopted relatively late compared to other regions of Costa Rica (Horn 2006) and to adjacent Nicaragua and Panama, but once maize arrived at sites like Laguna Bonillita, agriculture became a continuous feature on the landscape even during times of global-scale climate change that led to abandonment at other sites on the Isthmus (Taylor et al. 2013; Kerr et al. forthcoming). Evidence from the Bonillita site indicates an increase and change in the character of site use during the widespread Terminal Classic Drought (ca. 1200–850 cal yr BP), despite severe drying of climate in the circum-Caribbean. Snarskis (1984, p. 231) noted that "[h]uge expanses of extremely arid land that characterize parts of Mesoamerica and the west coast of South America do not exist in Central America, and even the regions which are somewhat arid today were probably less so in the past before most of the forest cover was altered." Indeed, Bonillita and the wider central Atlantic region may have been so wet in prehistory that *some drying* may have been *good* for maize agriculture, leading to continued resource extraction from sites like Bonillita even while the region was undergoing significant settlement and cultural reorganization.

3.3.4 Geography and Archaeology of Laguna Bonillita

Laguna Bonillita (9.9921 °N, 83.6114 °W, 450 m; Fig. 3.1) is a small (6 ha) deep (20 m) lake occupying a terrace of the Río Reventazón where it crosses the lower southeastern slope of Volcán Turrialba in the central Atlantic watershed archaeological subregion of Costa Rica (Horn and Haberyan 2016). Bonillita lies in the tropical wet forest life zone of the Holdridge

bioclimatic classification system (Tosi 1969; Holdridge et al. 1971) and in the Afw′ climate zone (tropical rainy without prolonged periods of drought) of the Köppen system (Gómez 1986). Data from nearby meteorological stations indicate that annual precipitation at Bonillita averages ca. 3100–3200 mm with slightly lower amounts of precipitation falling between February and April (Northrop and Horn 1996). Mean monthly temperatures show little variation over the year, with lows ranging 18–20 °C and highs ranging 26–28.5 °C (Coen 1983; Northrop and Horn 1996; Lane et al. 2009).

Kennedy (1968, 1976) conducted limited archaeological reconnaissance of the area near Laguna Bonillita and hypothesized that the site was occupied sporadically ca. 1950–1100 BP; however, the presence of maize pollen dated to ca. 2660 cal yr BP in the lowest sediments of Laguna Bonillita show that the site was settled much earlier and was continuously occupied by prehistoric people engaged in maize agriculture as part of their subsistence strategy (Northrop and Horn 1996). Previously, researchers had hypothesized that the La Montaña phase was marked by dependence on cultivated tubers and gathered wild resources (Snarskis 1984; Quintanilla 1990), but the Bonillita pollen record shows that maize was part of the strategy earlier (Northrop and Horn 1996). Maize is the only cultigen clearly represented in the Bonillita sediment record, but *Sechium* pollen may indicate the presence of cultivated *Sechium edule* (chayote). Potential wild food resources represented in the pollen assemblage include *Iriartea* and other palms, and fruit-bearing shrubs and trees including *Anacardium*, *Byrsonima*, and possibly *Brosimum alicastrum* (Northrop and Horn 1996).

Bustos Ramos (2007) conducted a detailed archaeological survey of the area surrounding Laguna Bonillita and nearby Laguna Bonilla with a goal of understanding the spatial and temporal aspects of archaeological evidence at the “Hacienda Dos Lagunas” site (LB-118) and to

reconstruct and explain the nature of social and cultural change represented therein. Permanent water sources would have been attractive to prehistoric people, plus the presence of both uplands and alluvial farmland at lower elevations may have been important to early settlers in both conceptual and utilitarian senses (Bustos Ramos 2007).

All four phases of the Reventazón chronology are represented at Bonillita to varying degrees. Archaeological evidence indicates that La Montaña was a transitional phase at the site, represented by a very small fraction of artifacts and evidence recovered (Bustos Ramos 2007). The El Bosque phase was the time of maximum site occupation at Bonillita. Archaeological evidence demonstrates significant population growth during El Bosque that brought elaborate craft specialization to the site. Burials and ceremonial grave goods demonstrate the importance of social or political status. Overall, the El Bosque phase at Bonillita was a period of increasing social complexity moving toward a hierarchical society in which the development of maize agriculture led to a population increase and competition for control of the land (Bustos Ramos 2007).

Evidence from the subsequent La Selva phase shows a decrease in occupation and a drawdown of the Bonillita site as population centers shifted toward areas of higher elevation in the Reventazón Valley and surrounding area. The final La Cabaña phase is represented by only a very small fraction of archaeological evidence recovered, but paleoecological evidence indicates continued maize agriculture at Bonillita well into Spanish settlement of the Atlantic watershed (Northrop and Horn 1996; Lane et al. 2009). It may be the case that people were maintaining the area around Bonillita as an agricultural outpost, even as populations moved toward larger, regional centers such as Guayabo, Najera, and La Zoila, as hypothesized for the southern Pacific region of Costa Rica (Kerr et al. forthcoming). Nevertheless, all current archaeological and

paleoecological evidence supports the conclusion that the Bonillita site was continuously occupied to varying degrees by hierarchical maize farmers who were linked into to a broader complex social organization over ca. 2700 years of Costa Rican prehistory (Snarskis 1984; Northrop and Horn 1996; Bustos Ramos 2007; Lane et al. 2009).

3.3.5 Previous Paleoenvironmental Work at Laguna Bonillita

Horn and students recovered a sediment core from Laguna Bonillita in 1991 using a square-rod piston corer (Wright et al. 1984) and a PVC tube fitted with a rubber piston for the uppermost watery sediments. The coring site was located on a relatively shallow shelf in 6.10 m of water offshore from known archaeological sites with the goal of recovering evidence of prehistoric human presence (Burden et al. 1986; Northrop and Horn 1996). Coring continued to bedrock, but older sediments may exist in deeper parts of the lake. The core sections were extruded in the field and returned to the Laboratory of Paleoenvironmental Research at the University of Tennessee for analysis.

The Bonillita core consists of 9.59 m of dark (Munsell 10YR 2/1), highly organic lacustrine sediments with abundant woody fragments and larger nonwoody plant remains. Despite being located on a slope of Volcán Turrialba, no ash layers are evident visually or in magnetic susceptibility readings for the Bonillita core. Northrop and Horn (1996) obtained five conventional radiocarbon (^{14}C) dates on bulk sediments from the core and two AMS ^{14}C dates on wood fragments. They conducted loss-on-ignition (LOI; Dean 1974) analysis and counted pollen and microscopic charcoal from 30 sampled intervals of the core.

The pollen and charcoal data reported by Northrop and Horn (1996) from Laguna Bonillita provided some of the first evidence of prehistoric human impacts in the lowland

rainforests of Costa Rica and led to a reassessment of culture and prehistory in the area (Lane et al. 2009). Their data revealed permanent settlement of the lakeshore by ca. 2660 cal yr BP at the latest. The presence of pollen of *Zea mays* subsp. *mays* and microscopic charcoal fragments in the deepest sediments from Bonillita shows a prehistoric subsistence strategy in central Atlantic Costa Rica that incorporated maize agriculture and fire much earlier than previously known at the time (Fig. 3.2; Northrop and Horn 1996). That same study also showed a steep decline in sedimentary pollen of the genus *Myrsine* at ca. 1300 cal yr BP, which the authors interpreted as near-eradication of the taxon at the Bonillita site due to land clearance and preferential use of *Myrsine* wood as a construction material (Pittier 1908; Northrop and Horn 1996).

The Bonillita pollen and charcoal record shows a strong signal of human disturbance and reflects localized vegetation change from forest clearance and maize agriculture in the basin (Fig. 3.2). Northrop and Horn (1996) divided their paleoenvironmental reconstruction into three stratigraphic zones based on the presence of maize pollen and major trends in other plant taxa, including a "*Myrsine*-*Zea*" zone in which both genera were abundant, a "Disturbance-*Zea*" zone in which maize agriculture continued following near eradication of *Myrsine* from the site, and a subsequent "Post-*Zea*" zone reflecting possible indigenous abandonment of the site late in the chronology, at or just before European settlement of this part of Costa Rica. The timing of events discussed by Northrop and Horn (1996) and Lane et al. (2009) differs somewhat with the new age model we created, in which we recognize and remove two slumps of sediment deposited out of sequence (see below), but the presence and sequence of events remains relatively unchanged (Fig. 3.3).

Snarskis (1984) hypothesized that a regional population explosion took place around 2250 BP in the Atlantic watershed accompanied by wider adoption of maize agriculture. The

Bonillita proxy record supports that hypothesis, showing increased input of inorganic matter to the lake along with declines in pollen from arboreal taxa and increased pollen from *Zea* and other potential crops and wild resources at that time (Northrop and Horn 1996). While the Bonillita record clearly shows evidence of forest clearance and maize agriculture corresponding temporally to Snarskis' hypothesized period of regional population growth, Northrop and Horn (1996) concluded that the LOI, pollen, and charcoal record placed the period of maximum population growth at ca. 1300–1100 BP, at the bottom of their "Disturbance-*Zea*" zone (Figs. 3.2 and 3.3).

Lane et al. (2009) analyzed bulk sedimentary stable carbon isotopes ($\delta^{13}C$) in the Bonillita core to determine the relative contribution of plants using the C_3 photosynthetic pathway and plants using the less common C_4 pathway to the sedimentary organic matter (Fig. 3.2). They interpreted changes in $\delta^{13}C$ values as an indicator of changes in the scale of maize agriculture in the Bonillita watershed. Their bulk $\delta^{13}C$ record indicated that the period of maximum prehistoric agriculture and inferred maximum population took place at ca. 2250 cal yr BP at Bonillita (Lane et al. 2009), consistent with archaeological evidence of rapid population growth and expansion of maize agriculture during the El Bosque phase (Snarskis 1981, 1984; Bustos Ramos 2007). Relatively higher bulk $\delta^{13}C$ values in the lower part of the Bonillita core ca. 2660–1300 cal yr BP are associated with pollen from taxa representing landscape disturbance, including Asteraceae, Poaceae, and *Zea*, indicating increased site use and larger-scale maize agriculture in the early half of the site history (Fig. 3.3). Relatively lower $\delta^{13}C$ values in the Bonillita sediments after ca. 1300 cal yr BP are associated with pollen from taxa representing increased forest cover, including *Cecropia*, other Urticales, and other lowland tropical taxa, in addition to decreased abundances of disturbance taxa and maize pollen,

indicating a decrease in the scale or intensity of maize agriculture and site use in the latter half of the record (Northrop and Horn 1996; Lane et al. 2009).

Our new work at the Bonillita site identified two levels of sedimentary material deposited out of temporal sequence in the Bonillita core (see below), the lower of which contains the interval that Northrop and Horn (1996) hypothesized as their period of major population growth and site use. As part of this study, we present an updated proxy record and chronology of land use and maize agriculture (Fig. 3.3) that more closely agrees with available archaeological evidence and other paleoenvironmental interpretations, which place the period of major population growth earlier in the site history during the El Bosque phase ca. 2250–1450 BP (Snarskis 1984; Bustos Ramos 2007; Lane et al. 2009). Our reinterpretation of paleoenvironmental history at Laguna Bonillita still recognizes the significant change in site use later in the record originally reported by Northrop and Horn (1996), but with a revised interpretation informed by our new precipitation record.

3.4 Methods

3.4.1 Radiocarbon Calibration and Age-Depth Modeling

We obtained new AMS ^{14}C dates on macrofossils from seven stratigraphic levels in the Bonillita sediment core, recalibrated the radiocarbon dates originally reported by Northrop and Horn (1996), produced an updated age-depth model, and generated point estimates for our sampled levels using the 'clam' package (v. 2.3.2; Blaauw 2019) for the R Statistical Environment (v. 3.5.2; R Core Team 2019) and the IntCal13 radiocarbon calibration curve (Reimer et al. 2013). Northrop and Horn (1996) originally used linear interpolation to develop an age model for the Bonillita core, as did Lane et al. (2009). Here we also use linear interpolation.

Our new ^{14}C dates allowed us to identify two intervals of redeposited, out of sequence sediment (slumps) in the Bonillita core. We constrained the interval of the upper slump using a ^{14}C date at 107.5 cm for the top and a second date at 145.5 cm for the bottom. For the lower slump, we were similarly guided by a ^{14}C date reported by Northrop and Horn (1996) at 470.75 cm and by one new ^{14}C date at 557.5 cm, but we tuned the interval of the lower slump using a series of unusually low bulk $\delta^{13}C$ values originally reported by Lane et al. (2009) that also appear in our new compound-specific $\delta^{13}C$ data. We removed data in the two slump intervals from our dataset and plotted previous and new proxies by age to reexamine the paleoenvironmental history of the Bonillita site following this new understanding of depositional history and informed by our new work on Holocene hydroclimate.

3.4.2 Sample Preparation

We sampled the Bonillita core for compound-specific stable isotope analysis at depth intervals of 8–37 cm, corresponding to time intervals of ca. 16–423 calibrated years, guided by our age-depth model and previous proxy work (Northrop and Horn 1996; Lane et al. 2009) and constrained by the availability of sediments remaining from previous studies. A large gap exists in our compound-specific isotope data between 222.5 and 255.5 cm because of prior use of a wide section of sediment for a bulk ^{14}C date. Sample dry masses ranged from ca. 0.6 g in highly organic sediments to 15.9 g in sediments with higher mineral content.

Sample preparation followed the methods detailed in Chapter 2 of this dissertation. Briefly, we oven-dried sediments, ground them to a fine powder, and extracted them with dichloromethane and methanol. The samples were centrifuged, and the solvent was filtered, concentrated, and blown dry. Samples were then saponified and the neutral fraction was

recovered from the total lipids with hexane. The neutral fraction was cleaned on silica gel columns and *n*-alkanes were isolated by urea adduction. Lastly, the adducts were spiked with a squalane isotope standard (provided by A. Schimmelmann, Indiana University) to monitor instrument precision.

3.4.3 Identification, Quantification, and Isotope Ratio Mass Spectrometry

We identified and quantified compounds using tandem gas chromatography mass spectrometry (GCMS) and flame ionization detection (FID). Instrument parameters were identical to those presented in Chapter 2 of this dissertation.

We analyzed compound-specific δD and $\delta^{13}C$ using gas chromatography – isotope ratio mass spectrometry (GC-IRMS). Instrument parameters were again identical to those in Chapter 2 of this dissertation. An external isotope standard (*n*-alkane mixture B4, supplied by A. Schimmelmann, Indiana University) was analyzed between every four sample runs to monitor instrument accuracy and precision.

3.4.4 Data Processing and Analysis

Methods and equations for data analysis follow those presented in Chapter 2 of this dissertation. Briefly, we quantified abundances for all alkane homologues of carbon chain lengths C_{20} to C_{33} as μg/gram of dry sediment. To assess the strength of the terrestrial signal in our data, we calculated the carbon preference index (CPI) for each of our samples, following Marzi et al. (1993) and average carbon chain length (ACL), following Feakins et al. (2016).

We analyzed isotope data for all odd chain alkane homologues from C_{23} to C_{33} for δD and C_{23} to C_{31} for $\delta^{13}C$. We were unable to use the $\delta^{13}C$ values for the C_{33} homologue due to the

presence of a triterpenoid compound that had a similar elution time and interfered with the C_{33} peak in our carbon runs. Here we focus on δD and $\delta^{13}C$ data for C_{27}, C_{29}, and C_{31} alkanes because they are reliable indicators of terrestrial vegetation and fractionation factors (ε) between plants and mean annual precipitation for these homologues are available in the published literature (Sachse et al. 2012). We quantified analytical uncertainty in our δD and $\delta^{13}C$ data following Polissar and D'Andrea (2014).

In addition to terrestrial leaf wax δD and $\delta^{13}C$ values, we present z-scored, vegetation-corrected δD values for paleoprecipitation (δD_{PP}), following Feakins (2013). We combined pollen data from the Bonillita core (Northrop and Horn 1996), the supplementary dataset of Sachse et al. (2012) comprising a global survey of published fractionation factors (ε) for many plant taxa, and a two-endmember linear mixing model for grasses assuming average $\delta^{13}C$ values of –38.3‰, –35.0‰, and –35.5‰ for C_3 grasses in our C_{27}, C_{29}, and C_{31} alkane data, respectively, and –21.3‰ for C_4 grasses across all homologues to produce an unbiased ε-corrected paleoprecipitation reconstruction for the Bonillita site.

Hydrogen and carbon isotope compositions are reported in standard δ-per mil notation, with hydrogen values relative to Vienna Standard Mean Ocean Water (VSMOW) and carbon values relative to the Vienna Pee Dee Belemnite (VPDB) marine carbonate standard. Repeated analyses of our squalane internal standard indicated that instrument precision for our samples (1 SD) averaged ca. 5.9‰ for hydrogen and 2.1‰ for carbon. Repeated analyses of our external isotope standard indicated that propagated error for our dataset (1 SEM) averaged ca. 9.0‰ for hydrogen and 0.5‰ for carbon.

We plotted our new z-scored, ε-corrected δD of paleoprecipitation (δD_{PP}) for the $C_{27\text{-}31}$ odd *n*-alkanes, along with select pollen, spore, and microscopic charcoal data from Northrop and

Horn (1996), vegetation categorized by life form (following Sachse et al. 2012; Feakins 2013), bulk $\delta^{13}C$ from Lane et al. (2009), and Cariaco Basin titanium data tuned by Kennett et al. (2012) using C2 (v. 1.7.7; Juggins 2007). We plotted proxy data by calibrated age, with all previous data replotted following our new age-depth model. Stratigraphic diagrams are divided into informal zones based on the Río Reventazón Valley cultural chronology (Snarskis 1984).

Methods for loss-on-ignition, pollen, and charcoal analyses are in Northrop and Horn (1996). Pollen percentages for all taxa except Cyperaceae are calculated based on pollen sums for each sampled level excluding Cyperaceae, fern spores, and indeterminates. Percentages for Cyperaceae are based on counts that exclude spores and indeterminates. Fern spores are expressed as a percentage of total pollen plus spores, excluding indeterminates. For our vegetation correction to δD values, plants represented in the pollen record are categorized by taxonomy and life form as pteridophytes, forbs (non-graminoid herbs), total graminoids (Poaceae and Cyperaceae), C_3 and C_4 graminoids (calculated as a percentage of total graminoids using our mixing model), angiosperm shrubs and trees, and gymnosperms of the montane forest (*Prumnopitys*, formerly *Podocarpus*). Microscopic charcoal data are presented as influx values (fragments/cm^2/yr). Methods for bulk $\delta^{13}C$ analysis are in Lane et al. (2009). Bulk $\delta^{13}C$ values originally reported in Lane et al. (2009) are presented here in standard δ-per mil notation alongside our new plant wax $\delta^{13}C$ and δD data.

3.5 Results

Our new radiocarbon dates, recalibration of previous dates (Table 3.2), and new age modeling (Figure 3.4) confirm that organic sediments at Laguna Bonillita began accumulating ca. 2700 cal yr BP. The stratigraphy is interrupted by two slump intervals of redeposited material

that we removed from our new age-depth model and our proxy record. At this point, we are unable to fully explain the processes that led to these slump intervals, but we can speculate that the location of the coring site on a relatively shallow shelf offshore from known archaeological sites may have resulted in capturing intervals of intense forest clearance that led to significant landscape instability and rapid movement of disturbed material into the lake from the surrounding forest and fields. Regression analysis comparing bulk and compound-specific $\delta^{13}C$ values indicates minimal pre-aging of alkanes prior to sedimentation (Fig. 3.5; Lane et al. 2016).

The Bonillita core is composed of dark, homogenous, organic lake sediments containing high amounts of macrobotanical materials. Analysis showed an average organic content of ca. 81.5% (range ca. 27.0–97.4%) and an average total inorganic content of ca. 18.5% (range ca. 2.6–73.0%), as estimated by loss-on-ignition (LOI) at 550 °C (Dean 1974; Northrop and Horn 1996). LOI at 1000 °C by Northrop and Horn (1996) suggested carbonate contents of no more than ca. 0.5–4.5%; however, the loss of interstitial water in clays between 550 °C and 1000 °C (Dean 1974) could have inflated reported carbonate values.

Alkane homologue distributions for all our samples display a consistent odd-over-even carbon chain pattern, which is expected of terrestrial organic matter (Fig. 3.6). Carbon preference indices (CPI), which provide a measure of the relative abundances of even- and odd-chain length compounds, average 6.7 (range 3.1–10.7) throughout the core (Fig. 3.6). Even-carbon *n*-alkanes are typical of microbes and other non-terrestrial organisms (CPI ca. 1.0), while odd-carbon *n*-alkanes are typical of terrestrial vegetation (CPI >3) (Bray and Evans 1961; Eglinton and Hamilton 1963, 1967; Marzi et al. 1993). CPI values for all samples in the Bonillita core are >3, indicating a predominantly terrestrial organic matter source over the past ca. 2700 cal years.

Average chain lengths (ACL) in the Bonillita sediments range 26.2–30.6 ($\bar{x}$ = 28.1) through the core (Fig. 3.6). Relatively shorter odd-numbered *n*-alkanes (≤25 carbon atoms) are typical of algae and aquatic vegetation, while relatively longer *n*-alkanes (≥27 carbon atoms) are typical of terrestrial organic matter (Han et al. 1968; Cranwell et al. 1987; Poynter et al. 1989; Poynter and Eglinton 1990; Ficken et al. 2000; Meyers 2003; Feakins et al. 2016; Lane 2017). Eleven of our samples (ca. 26%) have ACL values ranging ca. 26.2–27.0 and alkane distributions in several samples (Fig. 3.6) display an increased importance of the C_{25} *n*-alkane homologue. This may indicate an increased importance of aquatic plant material in the sediments at those intervals, including contributions from emergent plants near the lakeshore. The Bonillita sediments contain high amounts of macrobotanical remains from aquatic plants, which can explain increased abundances of C_{23} and C_{25} *n*-alkanes in the sediments. Nevertheless, our samples contained longer-chain $C_{27–31}$ odd *n*-alkanes in abundances sufficient for analysis.

The plant life form categories and their respective fractions of total vegetation that we used to calculate our vegetation-corrected paleoprecipitation values (δD_{PP}; Feakins 2013) included: gymnosperms (0–1.1%, $\bar{x}$ = 0.1), angiosperm trees and shrubs (16.4–76.6%, $\bar{x}$ = 50.9), total graminoids (9.5–67.6%, $\bar{x}$ = 26.5), forbs (1.8–14.6%, $\bar{x}$ = 6.2), and pteridophytes (4.2–55.4%, $\bar{x}$ = 11.8) (Fig. 3.7, Table 3.3). Our mixing model estimates for the relative abundances and contributions of C_3 and C_4 graminoids yielded values of ca. 5.9–44.2% for C_3 plants ($\bar{x}$ = 16.3%) and 0.6–25.0% for C_4 plants ($\bar{x}$ = 6.8%). Apparent fractionation factors (ε) between alkane homologues and mean annual precipitation ($\varepsilon_{C27–31/MAP}$) for C_{27}, C_{29}, and C_{31} *n*-alkanes for each vegetation category are in Table 3.4.

Values for $\delta D_{PP/C27}$ ranged from –97.4‰ to –17.5‰ VSMOW ($\bar{x}$ = –59.9‰), while $\delta D_{PP/C29}$ ranged from –71.8‰ to –25.9‰ ($\bar{x}$ = –45.9‰) and $\delta D_{PP/C31}$ ranged from –71.6‰ to

–18.9‰ ($\bar{x}$ = –46.4‰) (Fig. 3.8). Mean δD_{PP} values for the Bonillita record are within the hypothesized range of δD for meteoric water at our site location and elevation predicted by the OIPC3.1 (Bowen 2019), ranging from –57‰ to –9‰, and averaging –39‰ (Table 3.5). Z-scores of our δD_{PP} values (Fig. 3.8) reveal the timing of decadal- to centennial-scale changes in paleohydrology at Bonillita, albeit with a large gap in data between ca. 545 and 970 cal yr BP.

Patterns in our leaf wax $\delta^{13}C$ values frequently diverge from values for δD, indicating that $\delta^{13}C$ and δD are responding to different forcing mechanisms (Fig. 3.8), with δD responding primarily to changes in moisture availability and $\delta^{13}C$ responding to changes in vegetation composition, likely driven by the relative scale and intensity of forest clearance and maize agriculture. Values for $\delta^{13}C_{C27}$ range from –38.2‰ to –28.3‰ VPDB ($\bar{x}$ = –33.1‰), while $\delta^{13}C_{C29}$ range from –35.0‰ to –24.7‰ ($\bar{x}$ = –31.2‰) and $\delta^{13}C_{C31}$ from –35.5‰ to –29.3‰ ($\bar{x}$ = –32.3‰) (Fig. 3.8). Fractionation factors (ε) between plants and precipitation vary through time with changes to the vegetation composition (Fig. 3.9), demonstrating the importance of the vegetation correction to the δD proxy (Feakins 2013). Hydrogen and carbon isotope data for C_{23} and C_{25} homologues, which can function as biomarkers for aquatic plants, along with hydrogen data for the C_{33} homologue, are in the supplemental information for this chapter (Figs. S3.1 and S3.2).

3.5.1 La Montaña: 2660–2250 BP

The Bonillita sediments began accumulating ca. 2660 cal yr BP during the La Montaña phase with positive z-scores for δD_{PP} indicating dry conditions at the time. Values for $\delta^{13}C$ in *n*-alkanes are relatively low, corresponding with high pollen percentages for trees and other taxa representing intact native C_3 forest, including *Ficus*, other Urticales, and *Myrsine* (Fig. 3.10).

Inorganic content reaches the highest level in the record at ca. 73%, indicating significant landscape disturbance. The presence of microscopic charcoal, pollen of *Sechium* in the Cucurbitaceae family (a potential wild food crop or cultigen), and high amounts of *Zea* pollen shows that maize farming was taking place at the Bonillita site during the La Montaña phase, as it was at other sites in the Caribbean lowlands (Horn and Kennedy 2001; Horn 2006). Urticales pollen declines across the interval, in response to forest clearance and conversion of land to agricultural fields. This is supported by an increase in pollen of weedy taxa, including Poaceae, Amaranthaceae, and Asteraceae.

3.5.2 El Bosque: 2250–1450 BP

The El Bosque phase begins with a multi-century period of average to wet conditions indicated by slightly negative z-scores for δD_{PP}. High percentages of *Zea* pollen show continued agriculture in the watershed. Bulk $\delta^{13}C$ reaches the highest value in the record at ca. –24.3‰ consistent with increasing $\delta^{13}C$ values in *n*-alkanes and increasing *Zea* pollen, indicating expansion or intensification of C_4 maize agriculture ca. 1900 cal yr BP. Inorganic content and charcoal influx decrease toward the middle of the phase, indicating stabilization of the local agricultural system. In the middle of the El Bosque phase, negative z-scores for δD_{PP} show a period of significantly wet conditions ca. 1815–1780 cal yr BP, followed by a return to average- to dry conditions shortly thereafter. Toward the end of the El Bosque phase, inorganic content and charcoal influx declines. Pollen of weedy taxa and cultigens likewise decline, while pollen of forest and successionary taxa, including *Myrsine*, *Trema*, *Ficus*, *Cecropia*, and other Urticales increases. Taken together, the proxy record indicates a peak in site use and agriculture in the

middle of the El Bosque phase, followed by a possible drawdown of human activity in the watershed throughout the second half of the phase.

3.5.3 La Selva: 1450–950 BP

The La Selva phase is marked by a high sedimentation rate (Fig. 3.4), which allowed sampling at finer time intervals than in other parts of the profile. Values for δD_{PP} vary over a wider range, with differences accentuated by the closer sampling versus lower zones in the core. This phase begins dry with positive z-scores for δD_{PP}, but then climate becomes much wetter indicated by the most negative z-scores for δD_{PP} in the record. Values for both bulk and *n*-alkane $\delta^{13}C$ increase at the beginning of La Selva, showing more maize agriculture in the Bonillita watershed. This is supported by declining pollen of forest taxa and increasing pollen percentages for weedy disturbance taxa, including Poaceae, Amaranthaceae, and Asteraceae. Pollen percentages for *Zea* and *Sechium* likewise increase at the beginning of La Selva.

Beginning ca. 1300 cal yr BP, the Bonillita sediments record a major change in the watershed indicating a second period of significant forest clearance and reestablishment of large-scale maize agriculture. Pollen percentages for forest taxa decline, while *Myrsine* nearly disappears from the site. Poaceae pollen and fern spores spike, indicating significant ecosystem disturbance. Charcoal influx reaches a remarkably high level in the middle of La Selva, indicating charcoal production and transport on an unprecedented scale at Bonillita, perhaps indicating a severe fire or series of fires. The lower of the two slump intervals occurs in the Bonillita core during this period, indicating that a major destabilization event took place in the watershed that resulted in redeposition of older material out of sequence in the lake. This may

correspond to widespread deforestation indicated by declining pollen percentages for forest taxa and greatly increased charcoal influx seen immediately up-core.

The later half of the La Selva phase overlaps with the Terminal Classic Drought in the wider circum-Caribbean region. Z-scores for δD_{PP} show three periods of dry climate interrupted by wetter periods between. Overall, the Bonillita δD_{PP} record indicates hydroclimate instability during the TCD. Values for bulk and *n*-alkane $\delta^{13}C$ decline before the TCD ca. 1210 cal yr BP, but then increase again shortly after. Pollen percentages for *Zea mays* remain relatively high through the end of the La Selva phase, indicating continued maize agriculture at Bonillita well into the TCD.

3.5.4 La Cabaña: 950–400 BP

We have fewer data for the La Cabaña phase compared to other times at Bonillita due to low sample resolution and the gap in the core. The very slow sediment accumulation at this time may indicate low landscape disturbance in conjunction with reduced agriculture in the watershed. Archaeological evidence from Bonillita indicates a low human presence during La Cabaña, supporting an interpretation of reduced human activity.

The end of the La Cabaña phase overlaps with the beginning of the widespread Little Ice Age event, beginning ca. 550 cal yr BP. Values for δD_{PP} show average conditions ca. 550 cal yr BP, but values increase sharply at ca. 450 cal yr BP to one of the driest signals in the record at the end of La Cabaña. Values for $\delta^{13}C$ decline toward the end of this phase, as do pollen percentages for *Zea mays*, indicating a decline in agriculture. Pollen percentages for *Iriartea*, *Trema*, *Ficus*, and *Cecropia* increase, indicating forest regrowth.

3.5.5 Post-Contact: 400 BP to the Present

Dry LIA conditions continue through ca. 260 cal yr BP, well into the Post-Contact period. Values for bulk and *n*-alkane $\delta^{13}C$ increase toward the middle of the LIA and Post-Contact period, while pollen percentages for forest taxa decline. Poaceae pollen increases and pollen percentages for *Zea mays* also increases notably. Taken together, the proxy record indicates a return of maize agriculture to the watershed at the height of LIA aridity and coinciding with increasing European colonization of the Caribbean region. The end of the record shows *Zea* pollen disappearing from the sediments after ca. 125 cal yr BP, indicating the end of indigenous maize agriculture at the Bonillita site. Pollen percentages of Urticales and other forest taxa increase at the top of this zone. Values for δD_{PP} decline moving out of the LIA, indicating the return of wet conditions moving toward the present.

3.6 Discussion

3.6.1 Paleohydrology at Laguna Bonillita

Hydroclimate in the Caribbean lowlands of Costa Rica and broader Central America is controlled by several forcing mechanisms operating at different timescales. Southern Central America receives a mixture of ITCZ moisture from both Caribbean and Pacific sources, but the Caribbean lowlands receive moisture predominantly from the east and contributions from the Pacific, while thought to be small, are nevertheless poorly understood (Lachniet et al. 2007). Precipitation amounts are controlled by ITCZ migration on an intra-annual timescale (Hastenrath 2002; Poveda et al. 2006), by the El Niño Southern Oscillation (ENSO) on an interannual scale (Poveda et al. 2006; Lachniet et al. 2007), by the Atlantic Multidecadal Oscillation (AMO) on an interdecadal scale (Knight et al. 2005), and by orbital forcing and variations in the subsolar point

(Haug et al. 2003), changing sea-surface temperatures (SSTs; Black et al. 2007), and variability in the Atlantic Thermohaline Circulation (THC; Alley et al. 1999) on a Quaternary timescale.

The Panamanian Isthmus, including Costa Rica, receives moisture from the Atlantic and Caribbean that is advected onshore by the Northeast Trade Winds and sites like Bonillita at 450 m elevation have increased rainfall with strengthening of the NE Trades due to orographic uplift (Lachniet et al. 2007). Additionally, Lachniet et al. (2007) found that variations in moisture delivery on the Isthmus over the Late Holocene are linked to variations in the Central American Monsoon (CAM), which itself is modulated by ENSO variability. Strengthened El Niño events result in a weakened CAM, which reduce precipitation on the Isthmus. The Late Holocene has experienced increased ENSO variability, which has resulted in increased precipitation variability in Central America with approximately 100-year pulsing (Lachniet et al. 2007).

The record of paleohydrology from in the Laguna Bonillita sediments reveals patterns of variability similar to those seen at other sites in Central America and the wider circum-Caribbean over the Late Holocene. Sediment began accumulating at our coring location during a period of dry climate in the Caribbean lowlands, matched by a dry interval seen elsewhere in Costa Rica (Horn 1989, 1993; Horn and Sanford 1992; Haberyan and Horn 1999), in the Cariaco Basin (Haug et al. 2003), and in Haiti (Hodell et al 1991) and the Yucatan (Hodell et al. 1995). The El Bosque phase, which was the time of maximum maize agriculture and settlement at the Bonillita site (Snarskis 1984; Bustos Ramos 2007; Lane et al. 2009), was marked by average moisture conditions, with a notable period of very wet conditions ca. 1760 cal yr BP marked by the beginning of an agricultural decline at Bonillita. The subsequent La Selva phase, largely overlapping with the Terminal Classic Drought, was a time of hydroclimate variability, with several dry intervals interspersed by wet conditions corresponding to findings at other sites in

Costa Rica (Horn 1989, 1993; Haberyan and Horn 1999; Wu et al. 2019) and Panama (Lachniet et al. 2004), the Yucatan (Hodell et al. 2005; Kennett et al. 2012; Douglas et al. 2015), and the Dominican Republic (Lane et al. 2014). The end of the La Cabaña phase and most of the Post-Contact period overlap with the Little Ice Age and are marked by extremely dry conditions in the Caribbean lowlands, matching reduced titanium input in the Cariaco sediments (Haug et al. 2001) and other evidence of aridity from Costa Rica (Taylor et al. 2013; Wu et al. 2019; Kerr et al. forthcoming), Panama (Stansell et al. 2013), and the Dominican Republic (Lane et al 2011).

While paleoenvironmental records from Central America tend to report periods of dry hydroclimate more noticeably than wet intervals, the wet periods at Bonillita are important to consider. Bonillita is located on the windward eastern slope of the Cordillera Central and receives a significant amount of onshore moisture delivery throughout the year (Northrop and Horn 1996; Lachniet et al. 2007). Essentially, the Bonillita site is very wet all the time. Unlike other areas such as the Mayan Lowlands in the Yucatan to the north, which saw collapse at many sites during regional drying episodes (Hodell et al. 1995, 2005; Kennett et al. 2012; Douglas et al. 2015), some drying may have been beneficial for maize agriculture at Laguna Bonillita. Indeed, our proxy record indicates *increases* in maize agriculture during drying trends at the beginning of the Bonillita record during the La Montaña phase, during drier parts of the El Bosque phase, in the middle- to later part of the La Selva period, and again during the driest part of the Bonillita record at the end of the La Cabaña phase and into the Post-Contact period (Fig. 3.10). By contrast, the wet period in the middle of the El Bosque phase was followed by a slow decline in maize agriculture. Contrary to conventional paleoenvironmental wisdom that predicts circum-Caribbean drought as bad for prehistoric maize agriculture, at Bonillita, extended periods of wet conditions may have made maize farming difficult or impossible (Anderson 1990;

Anderson et al. 1995), while periods of dry conditions made the Bonillita site with permanent water sources attractive to prehistoric maize agriculturalists (Bustos Ramos 2007).

3.6.2 Prehistoric Human-Environment Interactions

Prehistoric human settlement and maize agriculture were in place at the Bonillita site dating to the oldest sediments in our core ca. 2700 cal yr BP, although older sediments may exist in deeper parts of the lake (Northrop and Horn 1996). The Bonillita record began during a dry period in the Caribbean lowlands and our paleoenvironmental record from the watershed indicates significant forest clearance and landscape disturbance during the La Montaña phase early in the site's history. The archaeological record shows La Montaña as a transitional period at Bonillita, with maize agriculture beginning in the Río Reventazón valley and elsewhere in the Caribbean lowlands but continuing to be mixed with root cropping and supplemented by gathered wild resources (Snarskis 1984; Horn and Kennedy 2001; Bustos Ramos 2007). The limited archaeological evidence available from the La Montaña phase at Laguna Bonillita (Bustos Ramos 2007) supports an interpretation of a small human presence on the landscape and indicates that our sediment core captured the initial stages of settlement, forest clearance, and maize agriculture at the site.

The El Bosque phase saw continued forest clearance and maize agriculture that peaked in the middle of the phase at ca. 1850 cal yr BP coincident with average to slightly dry conditions, but then declined during a period of wet conditions beginning ca. 1815 cal yr BP. The inorganic content of the Bonillita sediments declines across the lower half of the El Bosque phase and then stabilizes, and charcoal influx is generally low through this zone, indicating a decline in landscape disturbance and possibly in prehistoric agriculture. Pollen percentages for taxa in the

Urticales group are lower than in the preceding La Montaña phase, but then slowly increase, and pollen percentages for *Myrsine*, *Trema*, *Ficus*, and *Cecropia* increase across this zone, indicating forest recovery. Pollen for *Zea mays* and *Sechium* both peak ca. 1900–1850 cal yr BP along with *Iriartea*, another potential food resource. Amaranthaceae and Asteraceae pollen increase toward the middle of the zone along with other proxy indicators of increased agriculture, but then decline across the upper part of the zone.

Archaeological evidence indicates that the El Bosque phase was the time of maximum population growth and settlement at Laguna Bonillita (Snarskis 1984; Bustos Ramos 2007). Northrop and Horn (1996) regarded the later La Selva phase as the time of maximum site occupation, but our revised chronology for the pollen and bulk isotope records with data from the slump intervals removed confirm the interpretation of Lane et al. (2009) that maximum settlement and maximum maize agriculture occurred during the El Bosque phase. Values for compound-specific $\delta^{13}C$ reach maxima for the record in the middle of the El Bosque phase at ca. 1900–1850 cal yr BP, supporting these interpretations.

Proxy signals of maize agriculture then decline across the top of the El Bosque phase coincident with a distinct wet period shown by z-scores for δD_{PP} across all three of our alkane homologues. Pollen percentages for *Zea mays* and *Sechium* both decline along with *Iriartea*, indicating a decrease in crop cultivation and possibly in tending of wild resources. Pollen percentages for forest taxa increase, while percentages for weedy disturbance taxa decrease. The Bonillita site continued to be occupied through the later part of the El Bosque phase, as indicated by continued deposition of maize pollen in the sediments, but culture, settlement patterns, and subsistence strategies were changing.

The La Selva phase saw another period of significantly increased agriculture at the Bonillita site, but proxy evidence and the archaeological record indicate that this episode was different from those before it (Bustos Ramos 2007). Archaeological evidence indicates that prehistoric people did live at Bonillita during the La Selva phase, but at reduced numbers compared to the preceding El Bosque phase (Bustos Ramos 2007). Our δD_{PP} values show that hydroclimate became more unpredictable than in previous times, with periods that were both notably wet and notably dry, although our higher sampling resolution in this part of the core accentuates this. Pollen percentages for forest taxa decline, while pollen for crop taxa increases, indicating renewed use of the site for agriculture. Charcoal influx spikes in the middle of the La Selva zone, indicating fire in the watershed on a scale not previously seen in the record. Pollen of *Myrsine* drops sharply and may show that people were preferentially harvesting trees of this genus from the Bonillita site for local building projects (Northrop and Horn 1996) or elsewhere in the Río Reventazón Valley.

The La Selva phase was a time of increasing cultural complexity in the Río Reventazón Valley (Snarskis 1984; Bustos Ramos 2007). Archaeological evidence indicates that this was a time of rapid culture change, with increasing social differentiation and highly organized chiefdoms controlled by powerful *caciques*. La Selva may have also seen the beginning of cultural centers that became a feature of the subsequent La Cabaña phase. While paleoecological evidence shows that agriculture increased and continued at the Bonillita site, archaeological evidence indicates that the local population was decreasing at Bonillita in conjunction with other changes to demography and subsistence systems in the wider region.

The La Cabaña phase saw continued increases in cultural complexity in the Caribbean lowlands. The regional settlement pattern became nucleated, with small ceremonial centers

connected in a network of larger regional centers such as Guayabo, Najera, and La Zoila (Snarskis 1984). Boundaries may have been established around socio-political or defensive concerns. Archaeological evidence from Bonillita shows a reduced population at the site during the La Cabaña phase (Bustos Ramos 2007). Slow sediment accumulation at this time may indicate decreased agricultural activity in the Bonillita watershed. Building on evidence from the previous La Selva phase and regional archaeology and interpreting from patterns seen in the southern Pacific region of Costa Rica (Kerr et al. forthcoming), a reasonable interpretation is that prehistoric people were aggregating into regional population centers, possibly as violence and centralized control increased, and maintaining sites like Bonillita as agricultural hinterlands.

The end of the La Cabaña phase saw significant drying with the onset of the Little Ice Age that continued into the Post-Contact period. The Bonillita sediments record yet another increase in agriculture at the site, peaking at ca. 175 cal yr BP with a spike in pollen percentages for *Zea mays*, *Sechium*, and *Iriartea*. Pollen percentages for forest taxa decline, indicating a renewed episode of forest clearance. While other sites in Costa Rica, Central America, and the wider circum-Caribbean experienced population collapse and site abandonment somewhat before or during Spanish settlement (Taylor et al. 2013; Kerr et al. forthcoming), Bonillita appears to have been a refuge for people moving inland as Spanish settlement began along the Caribbean coast and moved inward (Northrop and Horn 1996; Lane et al. 2009). Bonillita would have been an attractive site during this pressure, much as it would have been centuries earlier as a permanent site for initial settlement and maize agriculture during the La Montaña phase. Maize disappears from the sedimentary record after ca. 125 cal yr BP coincident with forest regrowth, indicating the end of indigenous agriculture in the Bonillita watershed.

3.6.3 Extreme Climate Events: the TCD and the LIA

The Terminal Classic Drought (ca. 1200–850 cal yr BP) manifested as a period of climate instability and unpredictability at Laguna Bonillita with episodes of drying like those as seen at other sites in Costa Rica and nearby Panama (Horn 1989, 1993; Horn and Sanford 1992; Haberyan and Horn 1999; Lachniet et al. 2004; Wu et al. 2017, 2019) and throughout the circum-Caribbean (Hodell et al. 1995, 2005; Curtis et al. 1996; Haug et al. 2001, 2003; Peterson and Haug 2006; Webster et al. 2007; Medina Elizalde et al. 2010; Kennett et al. 2012; Luzzadder-Beach et al. 2012; Lane et al. 2014; Douglas et al. 2015). High z-scores for our δD_{PP} reconstructions across all three alkane homologues indicate unusually dry conditions at ca. 1195 and ca. 1105 cal yr BP during the "early" TCD, followed by a transition to wet conditions lasting nearly a century ca. 1070–980 cal yr BP, only to return to dry conditions again at ca. 965 cal yr BP during the "late" TCD (Hodell et al. 2005).

The TCD was not a 350-year period of sustained drought, but rather a series of severe droughts that have been implicated in the collapse of Maya civilization on the Yucatan Peninsula far to the north of our Bonillita sites (Hodell et al. 2005; Kennett et al. 2012; Douglas et al. 2015). Our proxy data from the Bonillita sediments confirm a similar pattern at the local scale that likely resulted from southward displacement of the Intertropical Convergence Zone and related reductions in rainfall, as demonstrated for Costa Rica, the Cariaco Basin, and the wider circum-Caribbean (Haug et al. 2001; Lane et al. 2011, 2013, 2014). This matches patterns in paleohydrology seen at our other study sites, including Laguna Santa Elena in southern pacific Costa Rica and Lago de las Morrenas 1 in the Costa Rican highlands (this dissertation, chapters 2 and 4). Importantly, forest clearance, landscape disturbance, and prehistoric agriculture continued at Laguna Bonillita during TCD drying, supporting our hypothesis that some drying

was beneficial for maize agriculture at the generally wet Bonillita site. In contrast to the Mayan Lowlands, populations in Costa Rica, Panama, and the Dominican Republic grew after 1150 cal yr BP near permanent water sources, indicating different cultural responses to rainfall variability across the region (Lane et al. 2014).

Like the TCD, the effects of Little Ice Age are clearly visible in our reconstructed paleohydrology data from the Bonillita sediments. Z-scores for δD_{PP} indicate a multi-century period of pronounced aridity lasting ca. 540–260 cal yr BP spanning the later part of the La Cabaña phase and lasting well into the Post-Contact period. Again like the TCD, this Little Ice Age drying at Bonillita matches significant drying seen in other records from Costa Rica, Central America, and the wider circum-Caribbean (Curtis et al. 1996; Haug et al. 2001; Hodell et al. 2005; Peterson and Haug 2006; Black et al. 2007; Lane et al. 2011; Stansell et al. 2013; Taylor et al. 2013; Wu et al. 2019; Kerr et al. forthcoming). The LIA was a time of population collapse and site abandonment in southern Pacific Costa Rica (Taylor et al. 2013; Kerr et al. forthcoming), but the Bonillita site saw a period of renewed maize agriculture despite significantly drier hydroclimate. Laguna Bonillita would have been an attractive site for indigenous people moving inland as Spanish settlement began in earnest along the Caribbean coast and pushed into the Costa Rican interior (Northrop and Horn 1996; Lane et al. 2009). Although more evidence is needed, a reasonable interpretation of the available paleoecological, paleoenvironmental, and archaeological evidence indicates that Bonillita was one of the last bastions of indigenous settlement in the Caribbean lowlands of Costa Rica, having been occupied by indigenous maize agriculturalists until at least ca. 75 cal yr BP, which is quite late in the chronology of the Spanish Conquest.

3.7 Conclusions

Compound-specific stable hydrogen and carbon isotope analysis of terrestrial leaf waxes preserved in the Laguna Bonillita sediment core provided a 2700-year history of paleohydrology that unambiguously reflects climate in the Caribbean lowlands of Costa Rica and provides one of the first long records of paleoprecipitation reconstructed using lake sediments from Central America. Our data show that the Bonillita site experienced multiple episodes of significantly wetter and significantly drier than average hydroclimate during the late Holocene, the timing of which matches other records from Costa Rica, Central America, and the wider circum-Caribbean. Unlike at other sites, prehistoric settlement and maize agriculture apparently benefitted from periods of drying at Bonillita and the proxy record indicates increases in maize agriculture at or around times of drier hydroclimate instead of declines like at other sites. The Terminal Classic Drought (ca. 1200–850 cal yr BP) and the Little Ice Age (ca. 550–100 cal yr BP) are both well-represented in the Bonillita proxy record. The TCD manifested as a period of climate instability marked by multiple episodes of dry conditions, while the LIA was marked by a multi-century, sustained period of unusually dry hydroclimate at Bonillita, matching other records from the circum-Caribbean.

3.8 Acknowledgements

Recovery of the Bonillita sediment core and prior pollen and radiocarbon analyses were supported by NSF grant SES-9111588 awarded to Sally Horn and by additional funding from the National Geographic Society, the Association of American Geographers, and the University of Tennessee. Bulk carbon isotope analysis was funded by NSF grant EAR-0004104 awarded to Claudia Mora and by additional funding from the University of Tennessee. The new analyses

reported here were supported by NSF grant #1657170 awarded to SPH and MTK, NSF grant #1660185 awarded to SPH, CSL, and Douglas Gamble, NSF grant #1600376 awarded to Larry McKay and SPH, and by funds from the University of Tennessee and the University of North Carolina Wilmington. We thank Leslie Muller, Justin Grabowski, Julie Coulombe, and Trell Stroud for assistance in the laboratory.

3.9 References

Alley RB and Clark PU (1999) The deglaciation of the Northern Hemisphere: a global perspective. *Annual Review of Earth and Planetary Sciences* 27: 149–182.

Anderson DG (1990) *Political change in chiefdom societies: cycling in the late prehistoric Southeastern United States*. PhD Thesis, University of Michigan, USA.

Anderson DG, Stahle, DW and Cleaveland MK (1995) Paleoclimate and the potential food reserves of Mississippian societies: a case study from the Savannah River Valley. *American Antiquity* 60(2): 258–286.

Bhattacharya T, Chiang JCH and Cheng W (2017) Ocean-atmosphere dynamics linked to 800–1050 CE drying in Mesoamerica. *Quaternary Science Reviews* 169: 263–277.

Blaauw M (2019) clam: classical age-depth modeling of cores from deposits. R package version 2.3.2. Available at: https://CRAN.R-project.org/package=clam (accessed 23 January 2019).

Black DE, Abahazi MA, Thunell RC, Kaplan A, Tappa EJ and Peterson LC (2007) An 8-century tropical Atlantic SST record from the Cariaco Basin: baseline variability, twentieth-century warming, and Atlantic hurricane frequency. *Paleoceanography* 22: PA4204.

Bowen GJ (2019) The Online Isotopes in Precipitation Calculator. Version 3.1. Available at: http://www.waterisotopes.org (accessed 15 April 2016).

Bray EE and Evans ED (1961) Distribution of *n*-paraffins as a clue to recognition of source beds. *Geochimica et Cosmochimica Acta* 22: 2–15.

Burden ET, McAndrews JH and Norris G (1986) Palynology of Indian and European forest clearance and farming in lake sediment cores from Awenda Provincial Park, Ontario. *Canadian Journal of Earth Sciences* 23: 43–54.

Bustos Ramos JC (2007) *Prospección arqueológica en un ambiente lacustre de la Subregión Caribe de Costa Rica, el caso de las Lagunas Bonilla y Bonillita, Siquirres, Provincia de Limón*. Tesis de Licenciatura, Universidad de Costa Rica.

Coen E (1983) Climate. In: Janzen DH (ed) *Costa Rican Natural History*. Chicago: University of Chicago Press, pp. 35–46.

Cohen AS (2003) *Paleolimnology: The History and Evolution of Lake Systems*. Oxford: Oxford University Press.

Cranwell PA, Eglinton G and Robinson N (1987) Lipids of aquatic organisms as potential contributors to lacustrine sediments—II. *Organic Geochemistry* 11(6): 513–527.

Curtis JH, Hodell DA and Brenner M (1996) Climate variability on the Yucatan Peninsula (Mexico) during the past 3500 years, and implications for Maya cultural evolution. *Quaternary Research* 46: 37–47.

Dansgaard W (1964) Stable isotopes in precipitation. *Tellus* 16(4): 436–468.

Dean WE (1974) Determination of carbonate and organic matter in calcareous sediments and sedimentary rocks by loss on ignition: comparison with other methods. *Journal of Sedimentary Petrology* 44(1): 242–248.

Douglas PMJ, Pagani M, Canuto MA, Brenner M, Hodell DA, Eglinton TI and Curtis JH (2015) Drought, agricultural adaptation, and sociopolitical collapse in the Maya Lowlands. *PNAS* 112(18): 5607–5612.

Eglinton G and Hamilton RJ (1963) The distribution of alkanes. In: Swain T (ed) *Chemical Plant Taxonomy*. London: Academic Press, pp. 187–217.

Eglinton G and Hamilton RJ (1967) Leaf epicuticular waxes. *Science* 156: 1322–1335.

Feakins SJ (2013) Pollen-corrected leaf wax D/H reconstructions of northeast African hydrological changes during the late Miocene. *Palaeogeography, Palaeoclimatology, Palaeoecology* 374: 62–71.

Feakins SJ, Peters T, Sin Wu M, Shenkin A, Salinas N, Girardin CAJ, Patrick Bentley L, Blonder B, Enquist BJ, Martin RE, Asner GP and Malhi Y (2016) Production of leaf wax *n*-alkanes across a tropical forest elevation transect. *Organic Geochemistry* 100: 89–100.

Ficken KJ, Li B, Swain DL and Eglinton G (2000) An *n*-alkane proxy for the sedimentary input of submerged/floating freshwater aquatic macrophytes. *Organic Geochemistry* 31: 745–749.

Gómez LD (1986) *Vegetación de Costa Rica: Apuntes para una Biogeografía Costarricense*. San José: Editorial Universidad Estatal a Distancia.

Haberyan KA and Horn SP (1999) A 10,000 year diatom record from a glacial lake in Costa Rica. *Mountain Research and Development* 19(1): 63–68.

Han JH, McCarthy ED, Van Hoeven W, Calvin M and Bradley WH (1968) Organic geochemical studies, II. a preliminary report on the distribution of aliphatic hydrocarbons in algae, in bacteria, and in a recent lake sediment. *PNAS* 59: 29–33.

Hastenrath S (2002) The Intertropical Convergence Zone of the eastern Pacific revisited. *International Journal of Climatology* 22: 347–356.

Haug GH, Günther D, Peterson LC, Sigman DM, Hughen KA and Aeschlimann B (2003) Climate and the collapse of Maya civilization. *Science* 299: 1731–1735.

Haug GH, Hughen KA, Sigman DM, Peterson LC and Röhl U (2001) Southward migration of the Intertropical Convergence Zone through the Holocene. *Science* 293: 1304–1308.

Hodell DA, Brenner M, Curtis JH, Medina-González R, Ildefonso-Chan Can E, Albornaz-Pat A and Guilderson TP (2005) Climate change on the Yucatan Peninsula during the Little Ice Age. *Quaternary Research* 63: 109–121.

Hodell DA, Curtis JH and Brenner M (1995) Possible role of climate in the collapse of Classic Maya civilization. *Nature* 375: 391–394.

Hodell DA, Curtis JH, Jones GA, Higuera-Grundy A, Brenner M, Binford MW and Dorsey KT (1991) Reconstruction of Caribbean climate change over the past 10,500 years. *Nature* 352: 790–793.

Holdridge LR, Grenke WC, Hatheway WH, Laing T and Tosi JA Jr. (1971) *Forest Environments in Tropical Life Zones: a Pilot Study*. Oxford: Pergamon Press.

Horn SP (1989) Prehistoric fires in the Chirripó highlands of Costa Rica: sedimentary charcoal evidence. *Revista de Biologia Tropical* 37(2): 139–148.

Horn SP (1993) Postglacial vegetation and fire history in the Chirripó Páramo of Costa Rica. *Quaternary Research* 40: 107–116.

Horn SP (2006) Pre-Columbian maize agriculture in Costa Rica: pollen and other evidence from lake and swamp sediments. In: Staller JE, Tykot RH and Benz BF (eds) *Histories of Maize: Multidisciplinary Approaches to the Prehistory, Linguistics, Biogeography, Domestication, and Evolution of Maize*. Amsterdam: Elsevier, pp. 367–380.

Horn SP and Haberyan KA (2016) Lakes of Costa Rica. In: Kappelle M (ed) *Costa Rican Ecosystems*. Chicago: University of Chicago Press, pp. 656–682.

Horn SP and Kennedy LM (2001) Pollen evidence of maize cultivation 2700 B.P. at La Selva Biological Station, Costa Rica. *Biotropica* 33(1): 191–196.

Horn SP and Sanford RL (1992) Holocene fires in Costa Rica. *Biotropica* 24(3): 354–361.

Juggins S (2007) C2: software for ecological and palaeoecological data analysis and visualization (user guide version 1.5). Newcastle upon Tyne: Newcastle University, UK.

Kahmen A, Hoffmann B, Schefuß E, Arndt SK, Cernusak LA, West JB and Sachse D (2013a) Leaf water deuterium enrichment shapes leaf wax *n*-alkane δD values of angiosperm plants II: observational evidence and global implications. *Geochimica et Cosmochimica Acta* 111: 50–63.

Kahmen A, Schefuß E and Sachse D (2013b) Leaf water deuterium enrichment shapes leaf wax *n*-alkane δD values of angiosperm plants I: experimental evidence and mechanistic insights. *Geochimica et Cosmochimica Acta* 111: 39–49.

Kennedy WJ (1968) *Archaeological investigations in the Reventazón River drainage area, Costa Rica*. PhD Thesis, Tulane University, USA.

Kennedy WJ (1976) Prehistory of the Reventazón River drainage area, Costa Rica. *Vínculos* 2(1): 87–100.

Kennett DJ, Breitenbach SFM, Aquino VV, Asmerom Y, Awe J, Baldini JUL, Bartlein P, Culleton BJ, Evert C, Jazwa C, Macri MJ, Marwan N, Polyak V, Prufer KM, Ridley HE, Sodemann H, Winterhalder B and Haug GH (2012) Development and disintegration of Maya political systems in response to climate change. *Science* 338: 788–791.

Kerr MT, Horn SP and Lane CS (forthcoming) Stable isotope analysis of vegetation history and land-use change at Laguna Santa Elena in southern Pacific Costa Rica. *Vegetation History and Archaeobotany*.

Knight JR, Allan RJ, Folland CK, Vellinga M and Mann ME (2005) A signature of persistent natural thermohaline circulation cycles in observed climate. *Geophysical Research Letters* 32: L20708.

Lachniet MS and Patterson WP (2002) Stable isotope values of Costa Rican surface waters. *Journal of Hydrology* 260: 135–150.

Lachniet MS, Burns SJ, Piperno DR, Asmerom Y, Polyak VJ, Moy CM and Christenson K (2004) A 1500-year El Niño/Southern Oscillation and rainfall history for the Isthmus of Panama from speleothem calcite. *Journal of Geophysical Research* 109: D20117.

Lachniet MS, Patterson WP, Burns S, Asmerom Y and Polyak V (2007) Caribbean and Pacific moisture sources on the Isthmus of Panama revealed from stalagmite and surface water δ^{18}O gradients. *Geophysical Research Letters* 34: L01708.

Lane CS (2017) Modern *n*-alkane abundances and isotopic composition of vegetation in a gymnosperm-dominated ecosystem of the southeastern U.S. coastal plain. *Organic Geochemistry* 105: 33–36.

Lane CS and Horn SP (2013) Terrestrially derived *n*-alkane δD evidence of shifting Holocene paleohydrology in highland Costa Rica. *Arctic, Antarctic, and Alpine Research* 45(3): 342–349.

Lane CS, Horn SP and Kerr MT (2014) Beyond the Mayan Lowlands: impacts of the Terminal Classic Drought in the Caribbean Antilles. *Quaternary Science Reviews* 86: 89–98.

Lane CS, Horn SP, Orvis KH and Thomason JM (2011) Oxygen isotope evidence of Little Ice Age aridity on the Caribbean slope of the Cordillera Central, Dominican Republic. *Quaternary Research* 75: 461–470.

Lane CS, Horn SP, Taylor ZP and Kerr MT (2016) Correlation of bulk sedimentary and compound-specific $\delta^{13}C$ values indicates minimal pre-aging of *n*-aklanes in a small tropical watershed. *Quaternary Science Reviews* 145: 238–242.

Lane CS, Horn SP, Taylor ZP and Mora CI (2009) Assessing the scale of prehistoric human impact in the Neotropics using stable carbon isotope analysis of lake sediments: a test case from Costa Rica. *Latin American Antiquity* 20(1): 120–133.

Liu W and Huang Y (2005) Compound specific *D*/*H* ratios and molecular distributions of higher plant leaf waxes as novel paleoenvironmental indicators in the Chinese Loess Plateau. *Organic Geochemistry* 26: 851–860.

Luzzadder-Beach S, Beach TP and Dunning NP (2012) Wetland fields as mirrors of drought and the Maya abandonment. *PNAS* 109(10): 3646–3651.

Marzi R, Torkelson BE and Olson RK (1993) A revised carbon preference index. *Organic Geochemistry* 20(8): 1303–1306.

Medina-Elizalde M, Burns SJ, Lea DW, Asmerom Y, von Gunten L, Polyak V, Vuille M and Karmalkar A (2010) High resolution stalagmite climate record from the Yucatán Peninsula spanning the Maya terminal classic period. *Earth and Planetary Science Letters* 298: 255–262.

Meyers PA (2003) Applications of organic geochemistry to paleolimnological reconstructions: a summary of examples from the Laurentian Great Lakes. *Organic Geochemistry* 34: 261–289.

Niedermeyer EM, Schefuß E, Sessions AL, Mulitza S, Mollenjauer G, Schultz M and Wefer G (2010) Orbital- and millennial-scale changes in the hydrologic cycle and vegetation in the western African Sahel: insights from individual plant wax δD and δ^{13}C. *Quaternary Science Reviews* 29: 2996–3005.

Northrop LA and Horn SP (1996) PreColumbian agriculture and forest disturbance in Costa Rica: palaeoecological evidence from two lowland rainforest lakes. *The Holocene* 6(3): 289–299.

Peterson LC and Haug GH (2006) Variability in the mean latitude of the Atlantic Intertropical Convergence Zone as recorded by riverine input of sediments to the Cariaco Basin (Venezuela). *Palaeogeography, Palaeoclimatology, Palaeoecology* 234: 97–113.

Pittier H (1908) *Ensayo sobre las Plantas Usuales de Costa Rica*. Washington, DC: HL & JB McQueen, Inc.

Polissar PJ and D'Andrea WJ (2014) Uncertainty in paleohydrologic reconstructions from molecular δ*D* values. *Geochimica et Cosmochimica Acta* 129: 146–156.

Polissar PJ and Freeman KH (2010) Effects of aridity and vegetation on plant-wax δD in modern lake sediments. *Geochimica et Cosmochimica Acta* 74: 5785–5797.

Poveda G, Waylen PR and Pulwarty RS (2006) Annual and inter-annual variability of the present climate in northern South America and southern Mesoamerica. *Palaeogeography, Palaeoclimatology, Palaeoecology* 234: 3–27.

Poynter J and Eglinton G (1990) Molecular composition of three sediments from Hole 717C: the Bengal Fan. *Proceedings of the Ocean Drilling Program, Scientific Results* 116: 155–161.

Poynter JG, Farrimond P, Robinson N and Eglinton (1989) Aeolian-derived higher plant lipids in the marine sedimentary record: links with palaeoclimate. In: Leinen M and Sarnthein M (eds) *Paleoclimatology and Paleometerology: Modern and Past Patterns of Global Atmospheric Transport*. Dordrecht: Kluwer Academic Publishers, pp. 435–462.

Quintanilla I (1990) *Ocupaciones precolumbinas en el bosque tropical lluvioso: evaluación arqueológica de la Estación Biológica La Selva*. Unpublished report on file at the La Selva Biological Station, Puerto Viejo de Sarapiquí, Costa Rica.

R Core Team (2019) R: a language and environment for statistical computing. R Foundation for Statistical Computing, Vienna. Available at: https://www.r-project.org (accessed 23 January 2019).

Reimer PJ, Bard E, Bayliss A, Beck JW, Blackwell PG, Ramsey CB, Buck CE, Cheng H, Edwards RL, Friedrich M, Grootes PM, Guilderson TP, Haflidason H, Hajdas I, Hatté C, Heaton TJ, Hoffmann DL, Hogg AG, Hughen KA, Kaiser KF, Kromer B, Manning SW, Niu M, Reimer RW, Richards DA, Scott EM, Southon JR, Staff RA, Turney CSM and van der Plicht J (2013)

IntCal13 and Marine13 radiocarbon age calibration curves 0-50,000 years cal BP. *Radiocarbon* 55(4): 1869–1887.

Sachse D and Gleixner G (2004) Hydrogen isotope ratios of recent lacustrine sedimentary *n*-alkanes record modern climate variability. *Geochimica et Cosmochimica Acta* 68(23): 4877–4889.

Sachse D, Billault I, Bowen GJ, Chikaraishi Y, Dawson TE, Feakins SJ, Freeman KH, Magill CR, McInerney FA, van der Meer MTJ, Polissar P, Robins RJ, Sachs JP, Schmidt H-L, Sessions AL, White JWC, West JB and Kahmen A (2012) Molecular paleohydrology: interpreting the hydrogen-isotopic composition of lipid biomarkers from photosynthesizing organisms. *Annual Review of Earth and Planetary Sciences* 40: 221–249.

Sachse D, Gleixner G, Wilkes H and Kahmen A (2010) Leaf wax *n*-alkane δD values of field-grown barley reflect leaf water δD values at the time of leaf formation. *Geochimica et Cosmochimica Acta* 74: 6741–6750.

Sachse D, Radke J and Gleixner G (2006) *δ*D values of individual *n*-alkanes from terrestrial plants along a climate gradient – implications for the sedimentary biomarker record. *Organic Geochemistry* 37: 469–483.

Schefuß E, Kuhlmann H, Mollenhauer G, Prange M and Pätzold J (2011) Forcing of wet phases in southeast Africa over the past 17,000 years. *Nature* 480: 509–512.

Snarskis MJ (1979) Turrialba: a Paleo-Indian quarry and workshop site in eastern Costa Rica. *American Antiquity* 44(1): 125–138.

Snarskis MJ (1981) The archaeology of Costa Rica. In: Benson EP (ed) *Between Continents/Between Seas: Precolumbian Art of Costa Rica*. New York: Harry N Abrams, pp. 15–84.

Snarskis MJ (1984) Central America: the Lower Caribbean. In: Lange FW and Stone DL (eds) *The Archaeology of Lower Central America*. Albuquerque: University of New Mexico Press, pp. 195–232.

Stansell ND, Steinman BA, Abbott MB, Rubinov M and Roman-Lacayo M (2013) Lacustrine stable isotope record of precipitation changes in Nicaragua during the Little Ice Age and the Medieval Climate Anomaly. *Geology* 41(2): 151–154.

Stuiver M (1970) Oxygen and carbon isotope ratios of fresh-water carbonates as climatic indicators. *Journal of Geophysical Research* 75(27): 5247–5257.

Taylor ZP, Horn SP and Finkelstein DB (2013) Pre-Hispanic agricultural decline prior to the Spanish Conquest in southern Central America. *Quaternary Science Reviews* 73: 196–200.

Tierney JE, Russell JM, Huang Y, Sinninghe Damsté JS, Hopmans EC and Cohen AS (2008) Northern Hemisphere controls on tropical Southeast African climate during the past 60,000 years. *Science* 322: 252–255.

Tosi JA Jr. (1969) *Republica de Costa Rica: Mapa Ecológico*. 1:750,000. San José: Centro Cientifico Tropical.

Webster JW, Brook GA, Railsback LB, Cheng H, Edwards RL, Alexander C and Reeder PP (2007) Stalagmite evidence from Belize indicating significant droughts at the time of the Preclassic Abandonment, the Maya Hiatus, and the Classic Maya collapse. *Palaeogeography, Palaeoclimatology, Palaeoecology* 250: 1–17.

Wright HE Jr., Mann DH and Glaser PH (1984) Piston corers for peat and lake sediments. *Ecology* 65(2): 657–659.

Wu J, Porinchu DF and Horn SP (2017) A chironomid-based reconstruction of late-Holocene climate and environmental change for southern Pacific Costa Rica. *The Holocene* 27(1): 73–84.

Wu J, Porinchu DF and Horn SP (2019) Late Holocene hydroclimate variability in Costa Rica: signature of the Terminal Classic Drought and the Medieval Climate Anomaly in the northern tropical Americas. *Quaternary Science Reviews* 215: 144–159.

Xia Z-H, Xu B-Q, Mügler I, Wu G-J, Gleixner G, Sachse D and Zhu L-P (2008) Hydrogen isotope ratios of terrigenous *n*-alkanes in lacustrine surface sediment of the Tibetan Plateau record the precipitation signal. *Geochemical Journal* 42: 331–338.

3.10 Appendix

Table 3.1. Reventazón Valley cultural chronology. Following Snarskis (1984).

Phase	Dates (BP)	Key cultural features and developments
La Cabaña	950–400	• Nucleated settlements, small ceremonial centers, city-states • Site location random, socio-political boundaries or defense • Continued maize agriculture, plus roots, tubers, tree crops • Decline in quality of ceramics, fewer ceremonial ceramic items • Metates more utilitarian • Human images increase in artwork, including images of warfare • Appearance of Spanish items in graves • Architecture incorporates defined activity areas and buildings, plazas for ritual or civic use • Network of large centers, including Guayabo, Najera, and La Zoila
La Selva	1450–950	• Time of rapid cultural change • Fewer sites compared to El Bosque, less well-known • Continued maize agriculture • Decline in quality of lapidary industry • Introduction of metallurgy • Increasing social differentiation • Highly organized chiefdoms, powerful *caciques* exercise control
El Bosque	2250–1450	• Large, dispersed sites, competition for land • Site location favors alluvial farmland • Explosive population growth • Expansion/intensification of maize agriculture supplemented by root and tree crops plus riverine resources • Lithics for clearing forests (hafted celts) • Craft specialization – ceramics, lithics, lapidary • Elaboration of ceremonial items, grave goods • Extensive cemeteries, possibly by clan, lineage, or social group • Emerging wealth/class differences • Infrastructure/architecture reflecting status • Elaborate burials and grave goods • Ranked societies at or near chiefdom level
La Montaña	2950–2250	• Small sites, low population • Site location favors hunting and gathering • Swidden root cropping, incipient agriculture, some maize • Subsistence strategy incorporating root and tree crops, gathered wild nuts and fruits late in Central/South American chronology • Griddles (*budares*) for processing bitter manioc • “Fluctuating cultural frontier”

Table 3.2. Radiocarbon determinations for the Laguna Bonillita sediment core.[a]

Lab Number[b]	Material Dated	Depth (cm)	$\delta^{13}C$ (‰)	Uncalibrated ^{14}C Age (^{14}C yr BP)	±2σ Range (cal yr BP)	Probability	Notes
Beta-47263	Bulk sediment	5.0	–	125.2% ± 0.8 Modern	(–30) – (–35) (–12) (–9) – (–10)	81.2 8.9 4.8	
OS-142042	Plant material	107.5	–28.70	975 ± 15	812–802 861–827 932–903	6.2 30.3 58.3	In upper slump
OS-142098	Wood fragments	145.5	–29.37	970 ± 15	813–801 864–826 929–901	8.6 37.2 48.9	In upper slump
OS-142043	Leaf fragments	224.5	–27.05	540 ± 15	555–523 622–609	85.1 9.8	
Beta-65516	Bulk sediment	238.0	–	810 ± 60	803–663 829–810 904–858	84.1 2.7 8.1	
OS-142044	Leaf fragments	249.5	–29.99	1050 ± 20	981–927 1040–1039	94.5 0.4	
OS-142099	Plant material	330.5	–28.88	1190 ± 15	1175–1068	95.0	
Beta-66490	Bulk sediment	470.75	–	1960 ± 60	1761–1738 2055–1722	1.9 93.1	In lower slump
OS-138978	Plant material	557.5	–27.46	2040 ± 25	2063–1927 2105–2085	91.1 3.8	In lower slump
Beta-65518	Bulk sediment	718.0	–	1490 ± 60	1445–1300 1522–1452	72.7 22.2	
Beta-67835	Wood fragments	767.5	–27.60	1835 ± 55	1676–1620 1886–1687	10.2 84.7	
OS-138979	Plant material	864.5	–27.57	1910 ± 20	1895–1820	95.0	
Beta-67836	Wood fragments	952.0	–26.80	1765 ± 65	1826–1546 1859–1852	94.2 0.7	Roots – reject
Beta-47264	Bulk sediment	954.0	–	2560 ± 60	2448–2441 2779–2457	0.5 94.5	

[a] Dates calibrated using the 'clam' package (v. 2.3.2; Blaauw 2019) for the R Statistical Environment (v. 3.5.3; R Core Team 2019) and the IntCal13 radiocarbon calibration curve (Reimer et al. 2013).

[b] Analyses were performed by the National Ocean Sciences Accelerator Mass Spectrometry Lab (OS #) and Beta Analytic, Inc (Beta #).

Table 3.3. Plant taxa represented in the Bonillita pollen assemblages. Categorized by most likely life form at our research site.[a]

Taxon[b]	Life Form Category[c]
Anacardiaceae	Angiosperm tree + shrub
Apocynaceae	Angiosperm tree + shrub
Bignoniaceae	Angiosperm tree + shrub
Bombacaceae	Angiosperm tree + shrub
Ericaceae	Angiosperm tree + shrub
Malvaceae	Angiosperm tree + shrub
Melastomataceae/Combretaceae	Angiosperm tree + shrub
Meliaceae/Sapotaceae	Angiosperm tree + shrub
Mimosoideae	Angiosperm tree + shrub
Myrtaceae	Angiosperm tree + shrub
Palmae	Angiosperm tree + shrub
Rhamnaceae	Angiosperm tree + shrub
Rosaceae	Angiosperm tree + shrub
Rubiaceae	Angiosperm tree + shrub
Sapindaceae	Angiosperm tree + shrub
Solanaceae	Angiosperm tree + shrub
Urticales (di- + triporate)	Angiosperm tree + shrub
Acalypha	Angiosperm tree + shrub
Alchornea	Angiosperm tree + shrub
Alfaroa	Angiosperm tree + shrub
Alnus	Angiosperm tree + shrub
Bunchosia	Angiosperm tree + shrub
Bursera	Angiosperm tree + shrub
Byrsonima	Angiosperm tree + shrub
Cecropia	Angiosperm tree + shrub
Celtis	Angiosperm tree + shrub
Cordia	Angiosperm tree + shrub
Ficus	Angiosperm tree + shrub
Guazuma	Angiosperm tree + shrub
Hedyosmum	Angiosperm tree + shrub
Hura	Angiosperm tree + shrub
Ilex	Angiosperm tree + shrub
Iriartea	Angiosperm tree + shrub
Malpighia	Angiosperm tree + shrub
Mortoniodendron	Angiosperm tree + shrub
Myrica	Angiosperm tree + shrub
Myrsine	Angiosperm tree + shrub
Piper	Angiosperm tree + shrub
Quercus	Angiosperm tree + shrub
Sapium	Angiosperm tree + shrub
Tournefortia	Angiosperm tree + shrub

Table 3.3. Continued.

Taxa	Life Form
Trema	Angiosperm tree + shrub
Ulmus	Angiosperm tree + shrub
Virola	Angiosperm tree + shrub
Weinmannia	Angiosperm tree + shrub
Zanthoxylum	Angiosperm tree + shrub
Amaranthaceae	Forb
Caryophyllaceae	Forb
Asteraceae	Forb
Liguliflorae	Forb
Lentibulariaceae	Forb
Gentianaceae	Forb
Liliaceae	Forb
Onagraceae	Forb
Polygalaceae	Forb
Umbelliferae	Forb
Cucurbitaceae	Forb
Labiatae	Forb
Alternanthera	Forb
Dalechampia	Forb
Dorstenia	Forb
Typha	Forb
Cyperaceae	Graminoid
Poaceae	Graminoid
Zea mays subsp. *mays*	Graminoid
Prumnopitys (formerly *Podocarpus*)	Gymnosperm
Mono- and trilete spores	Pteridophytes

[a] Pollen identification and taxonomy follows Northrop and Horn (1996). We excluded indeterminate pollen grains and spores and taxa that could not be reliably classified.

[b] In many cases, pollen can only be identified to the family level or to the order for some pollen types in the Urticales group.

[c] Many taxa listed include species with more than one life form. Here we categorize plants into the life forms that are most likely represented at the Laguna Bonillita site. We combined angiosperm trees and shrubs because many taxa in the list are found as both in forests of the Caribbean lowlands of Costa Rica.

Table 3.4. Global average apparent fractionation factors (ε) for Bonillita. Fractionation between plants and meteoric water for $C_{27–31}$ odd *n*-alkanes. Compiled from the supplementary data in Sachse et al. (2012).

Plant Type	C_{27}	C_{29}	C_{31}
Gymnosperms	–112‰	–110‰	–103‰
Angiosperm trees and shrubs	–107‰	–111‰	–107‰
C_3 Graminoids	–127‰	–149‰	–157‰
C_4 Graminoids	–131‰	–132‰	–136‰
Forbs	–124‰	–128‰	–130‰
Pteridophytes	–103‰	–108‰	–114‰

Table 3.5. Expected δD values for modern precipitation at Bonillita. Location: 9.9921 °N, 83.6114 °W, 450 m. From the Online Isotopes in Precipitation Calculator (OIPC v. 3.1; Bowen 2019).

	Jan	Feb	Mar	Apr	May	Jun	Jul	Aug	Sep	Oct	Nov	Dec	Year
δD (‰)	–13	–9	–11	–18	–37	–57	–35	–48	–44	–44	–39	–27	–39

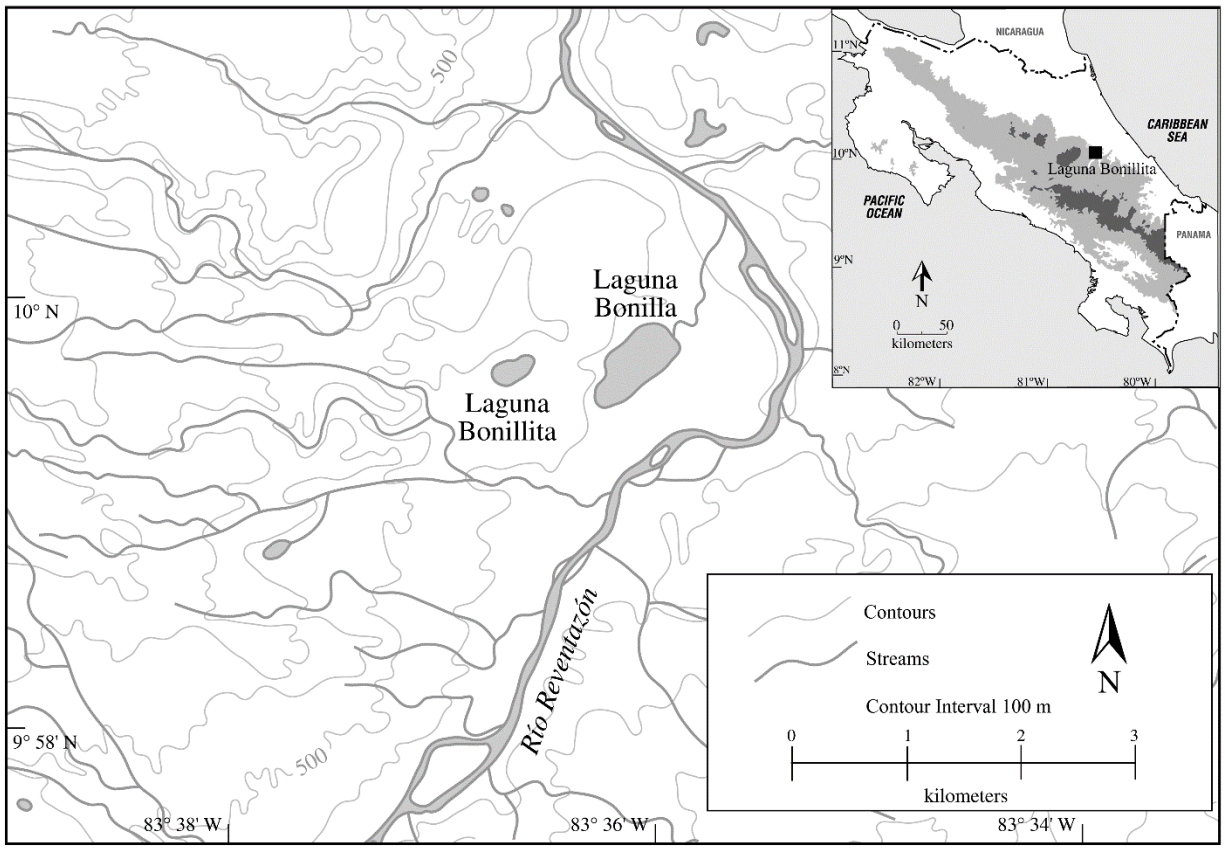

Fig. 3.1. Location of Laguna Bonillita and nearby Laguna Bonilla. Site is along the Río Reventazón in eastern Costa Rica. Inset: unshaded areas are <500 m elevation; areas with intermediate shading are 500–2000 m; areas with darkest shading are >2000 m. Modified from Fig. 1 in Lane et al. (2009).

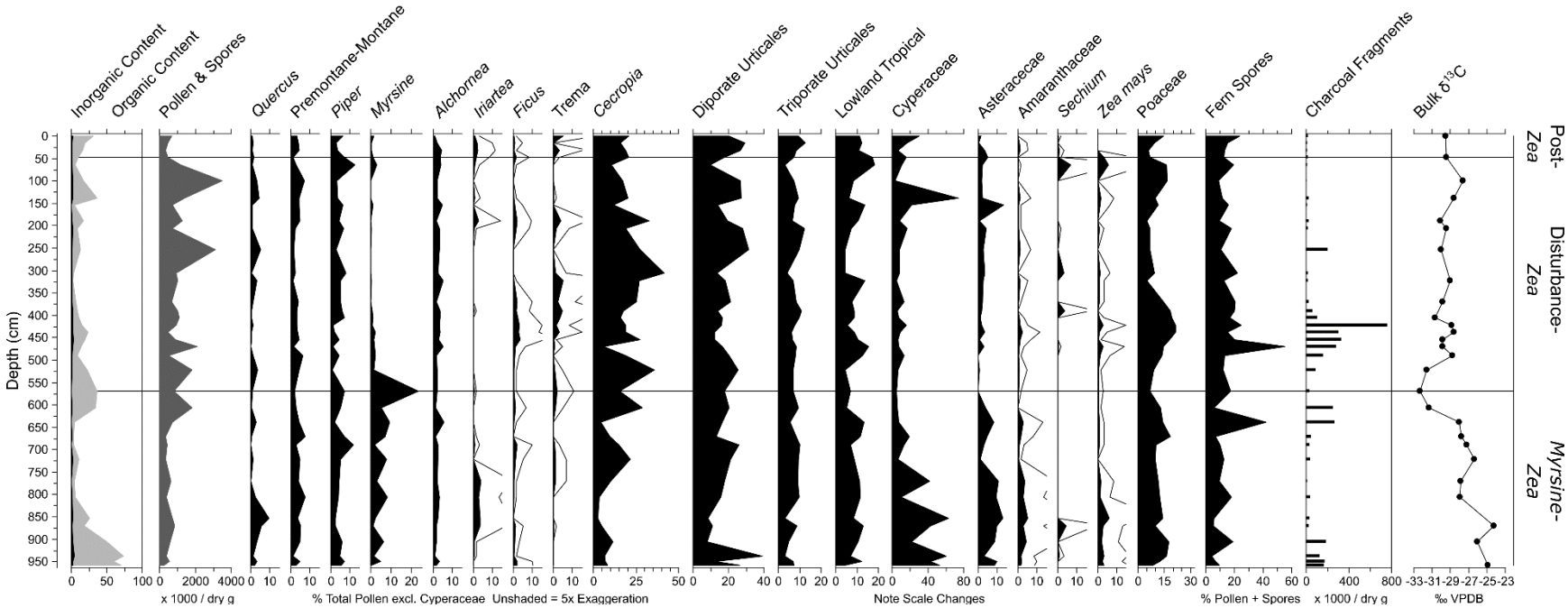

Fig 3.2. Pollen and stable carbon isotope diagram for Laguna Bonillita. The pollen data are from Northrop and Horn (1996) and are plotted to recreate the original diagram. From left the diagram shows sediment composition including carbonate (black curve), non-carbonate inorganic, and organic content; pollen and spore concentrations; pollen and spore percentage curves for major taxa and composite groups; charcoal profile; pollen zones; and bulk $\delta^{13}C$. The composite Premontane-Montane category includes *Alnus*, *Hedyosmum*, *Weinmannia*, *Alfaroa-Oreomunnia*, *Malpighia*, *Myrica*, *Podocarpus*, and *Ulmus*. The composite lowland tropical category includes *Anacardium*, Apocynaceae, *Ilex*, Bignoniaceae, Bombacaceae, *Cordia*, *Tournefortia*, *Bursera*, Ericaceae, *Acalypha*, *Croton*, *Hura*, *Sapium*, Flacourtiaceae, *Hippocratea*, Mimosoidea, other Leguminosae, *Bunchosia*, *Byrsonima*, Malvaceae, Melastomataceae/ Combretaceae, *Virola*, Myrtaceae, Palmae other than *Iriartea*, Rhamnaceae, Rosaceae, Rubiaceae, *Zanthoxylum*, Sapindaceae, Sapotaceae/Meliaceae, *Guazuma*, and *Mortoniodendron*. Cyperaceae pollen is excluded from the pollen sum for the composite percentage curves and all individual percentage curves other than its own, but is included in the pollen concentration curve and in the pollen sum used to plot fern spore percentages. Charcoal concentrations are for fragments ≥25 μm length. Bulk $\delta^{13}C$ data are replotted from Lane et al. (2009). VPDB = Vienna Pee Dee Belemnite. Zones labeled at right follow major changes in the proxy record delineated by Northrop and Horn (1996).

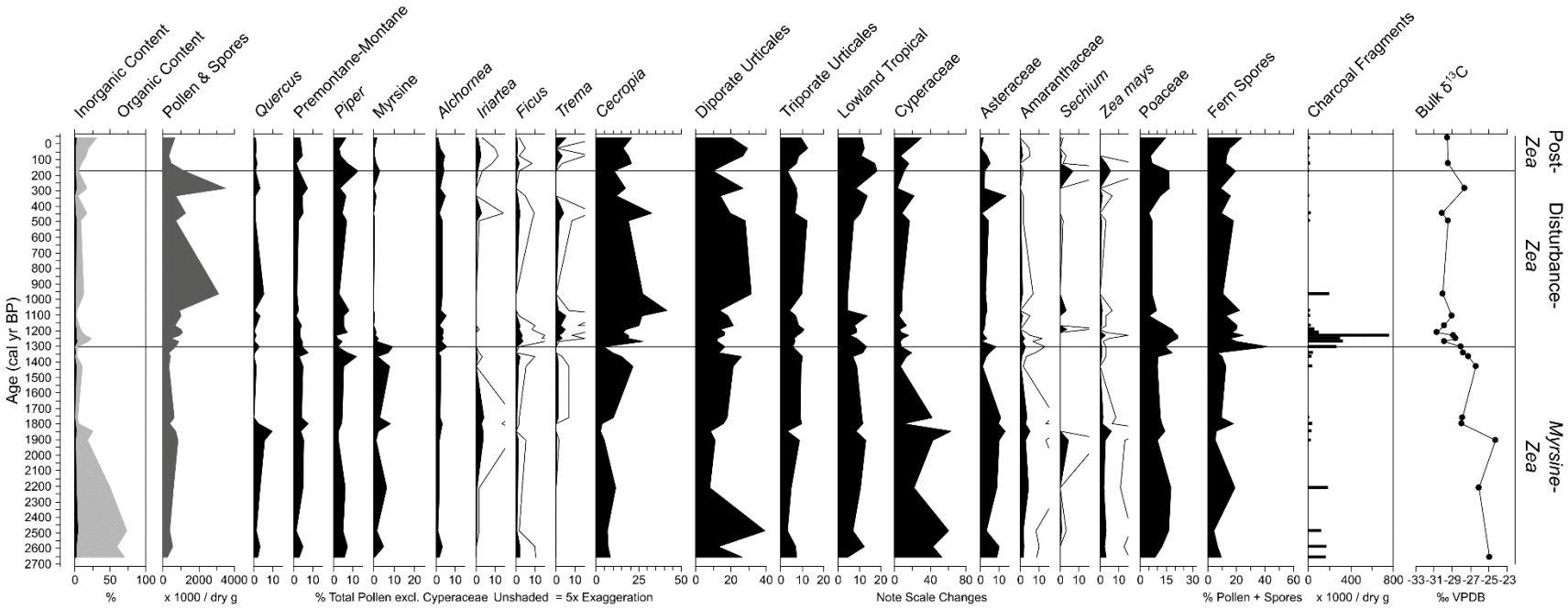

Fig. 3.3. Data from Fig. 3.2 replotted by age. This plot uses our new age-depth model with slump intervals from 108–146 cm and 438–606 cm removed. Notes in the caption for Fig. 3.2 apply here, as well. See text for further details.

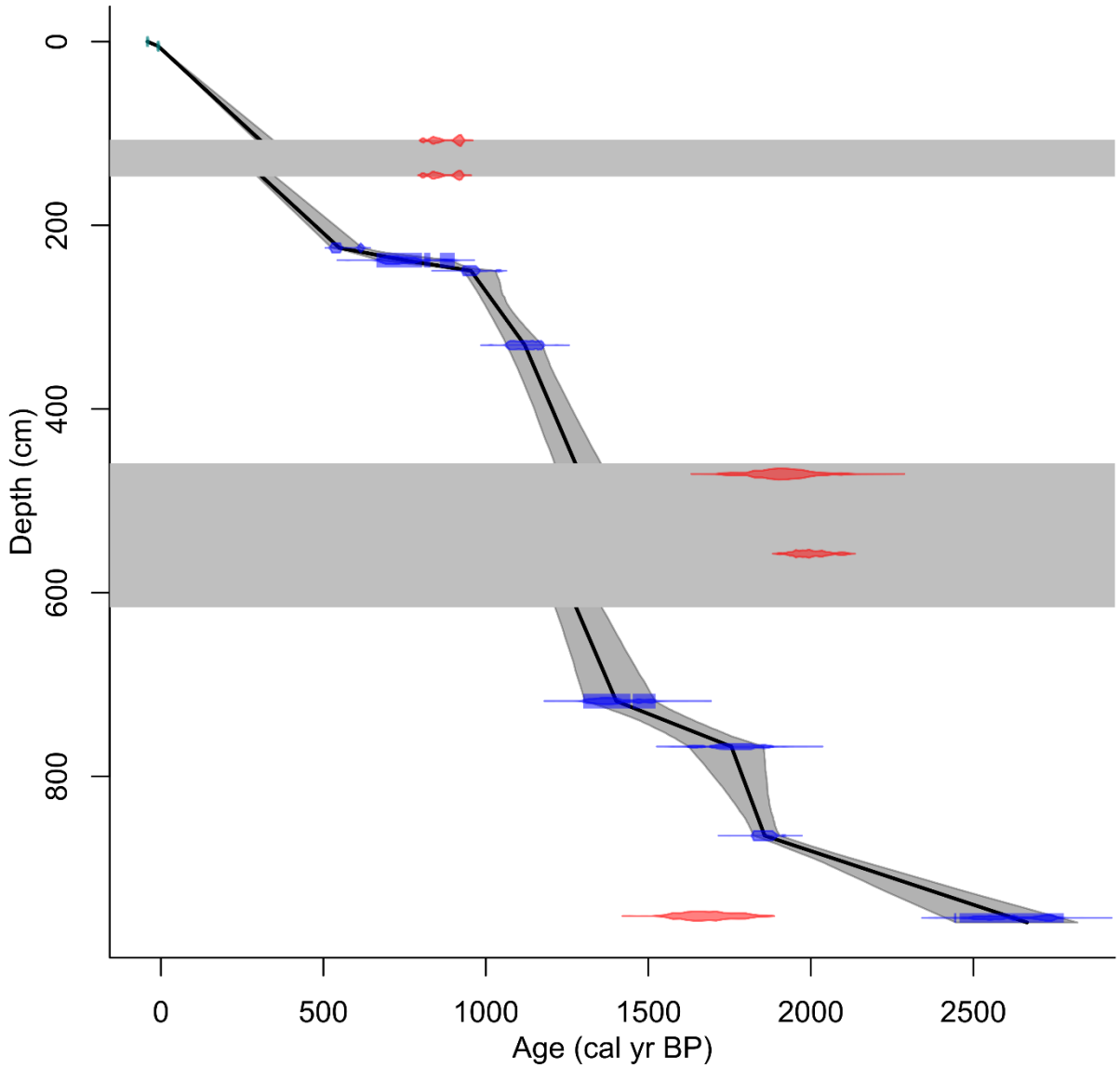

Fig. 3.4. Age-depth model for Laguna Bonillita. Gray bars show locations of two slump intervals. Blue marks represent ^{14}C probability distributions for dates included in the age-depth model, while red marks represent ^{14}C probabilities for dates excluded from the model (see Table 3.2). Model was created using linear interpolation with the 'clam' package (Blaauw 2019) for the R Statistical Environment (R Core Team 2019) and the IntCal13 radiocarbon calibration curve (Reimer et al. 2013).

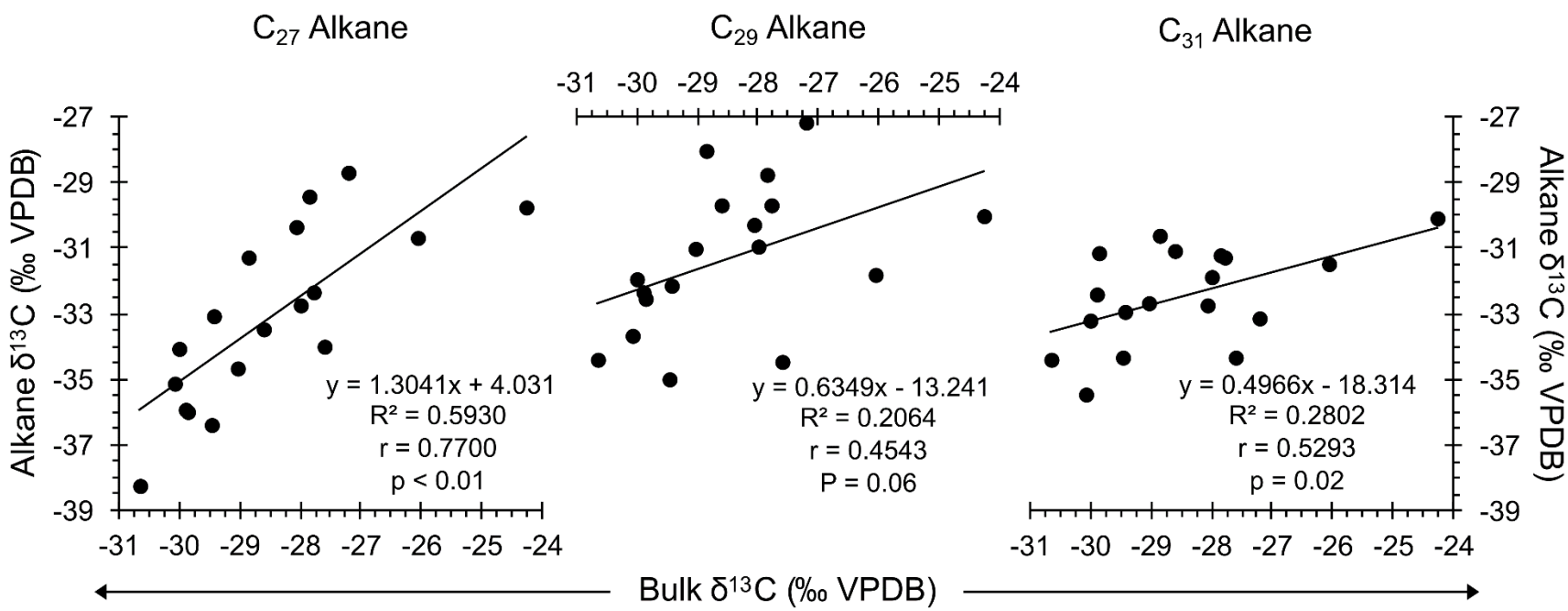

Fig. 3.5. Regression analyses of stratigraphically coeval bulk sedimentary $\delta^{13}C$ and *n*-alkane $\delta^{13}C$ values.

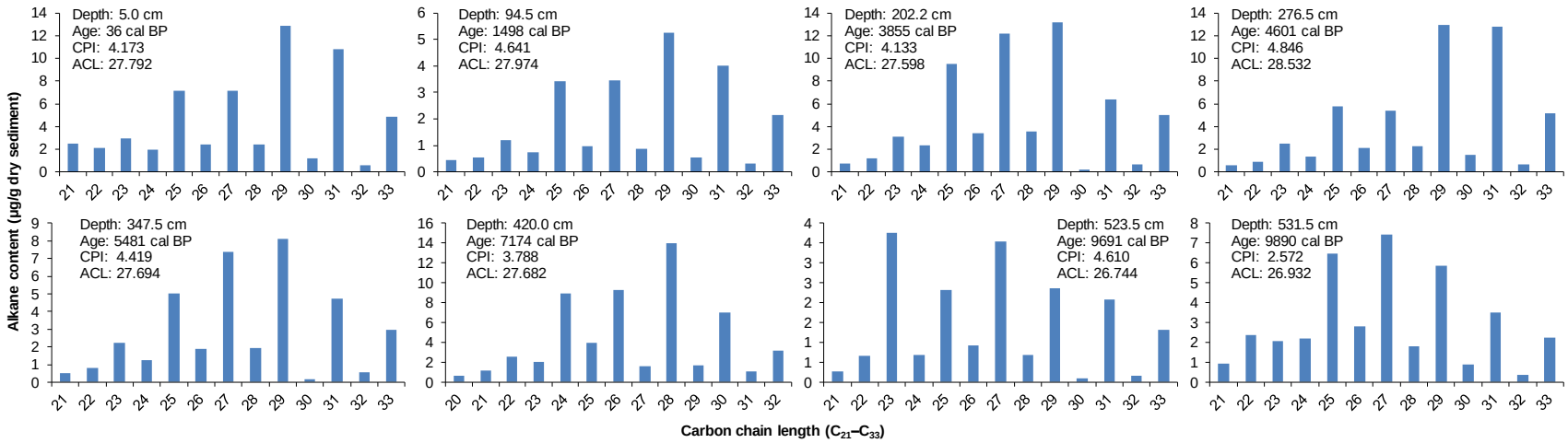

Fig. 3.6. Alkane distributions, CPI, and ACL for selected samples. Note changes in scale on the y-axes.

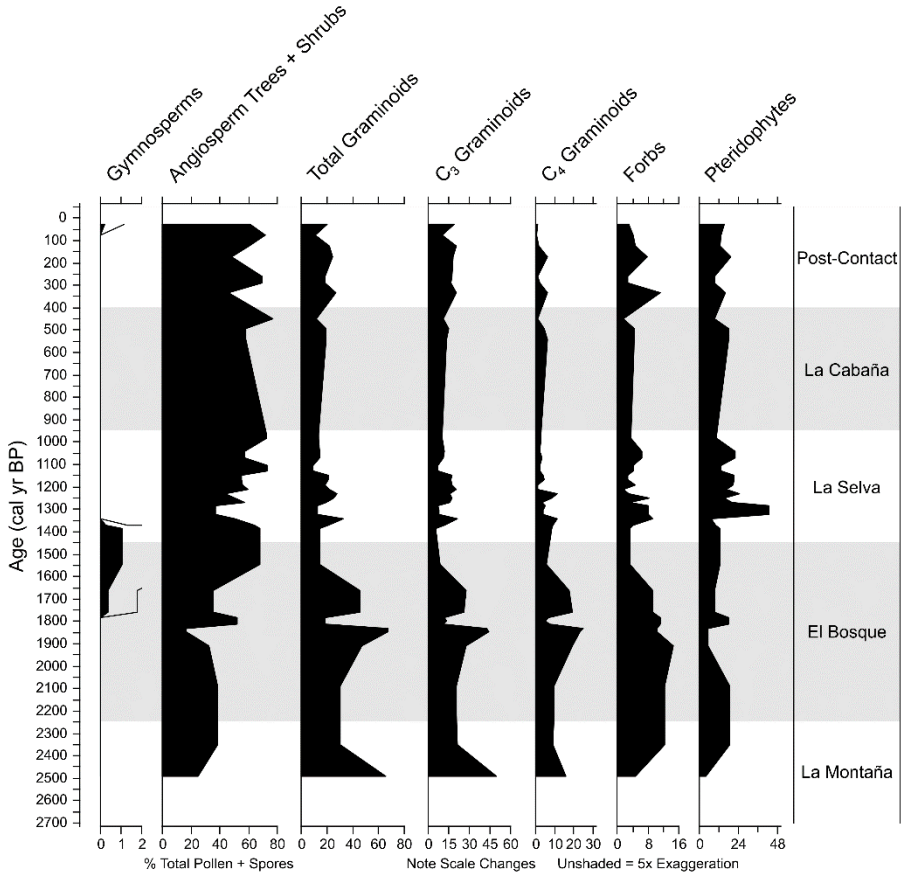

Fig. 3.7. Plants represented in the Bonillita pollen record. Categorized by taxonomy and life form following Feakins (2013). Percentages for gymnosperms, angiosperm trees and shrubs, total graminoids, forbs (non-graminoid herbaceous taxa), and pteridophytes are calculated based on a sum of pollen and spore counts for all included taxa. Percentages for C_3 and C_4 graminoids are calculated from total graminoids using a two-endmember mixing model (see text) representing an average of $C_{29–31}$ odd numbered *n*-alkane homologues. Zones are delineated following the cultural chronology of the Río Reventazón Valley following Snarskis (1984).

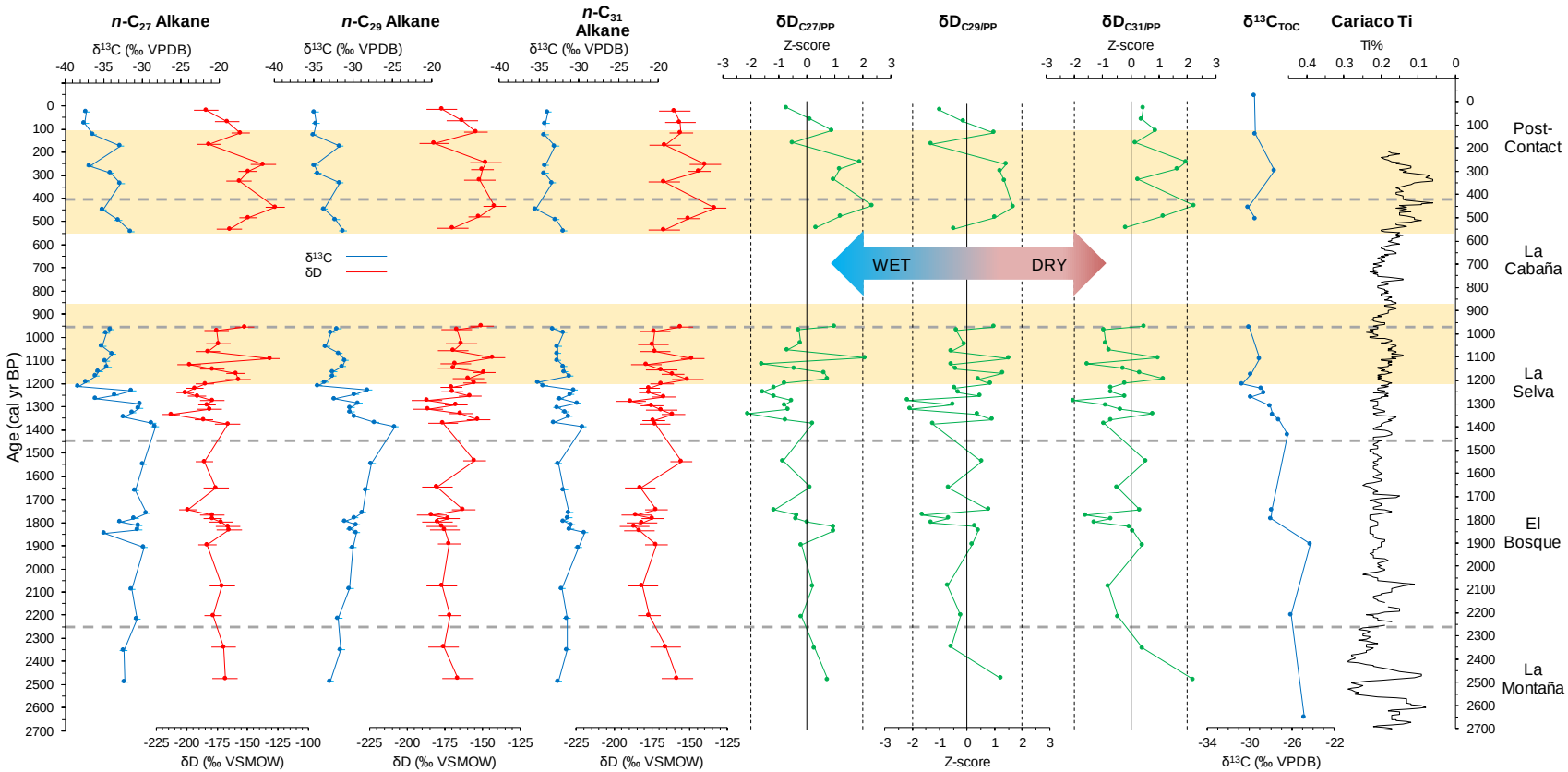

Fig. 3.8. Bonillita isotope data. Includes: leaf wax δD and $\delta^{13}C$ data and z-scores for δD_{PP} for odd numbered *n*-alkanes $C_{27–31}$. Bulk $\delta^{13}C_{TOC}$ data are from Lane et al. (2009). Cariaco Basin titanium values are from the dataset tuned by Kennett et al. (2012). Note scale changes on the x-axes. Zones shown by horizontal gray dashed lines follow the Río Reventazón Valley cultural chronology (Snarskis 1984) as labeled at right. The upper shaded band covers the interval of the Little Ice Age (ca. 550–100 cal yr BP) and the lower band covers the Terminal Classic Drought (ca. 1200–850 cal yr BP). VPDB = Vienna Pee Dee Belemnite. VSMOW = Vienna Standard Mean Ocean Water. The gap in the stratigraphic record is a gap in sediment availability for the analyses reported here, not a gap in sedimentation at the lake.

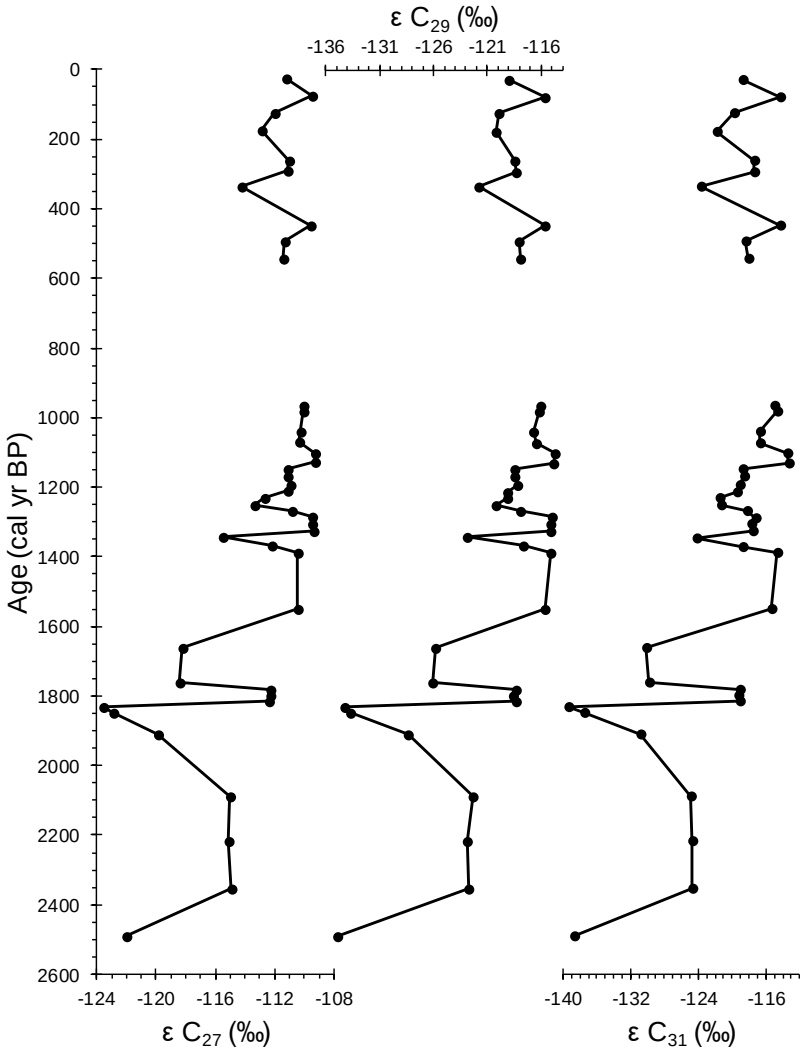

Fig. 3.9. Fractionation factors (ε) between plants and precipitation. Note changes in scale on the x-axes. Breaks in the curves indicate an interval of the core with no samples due to sediment availability.

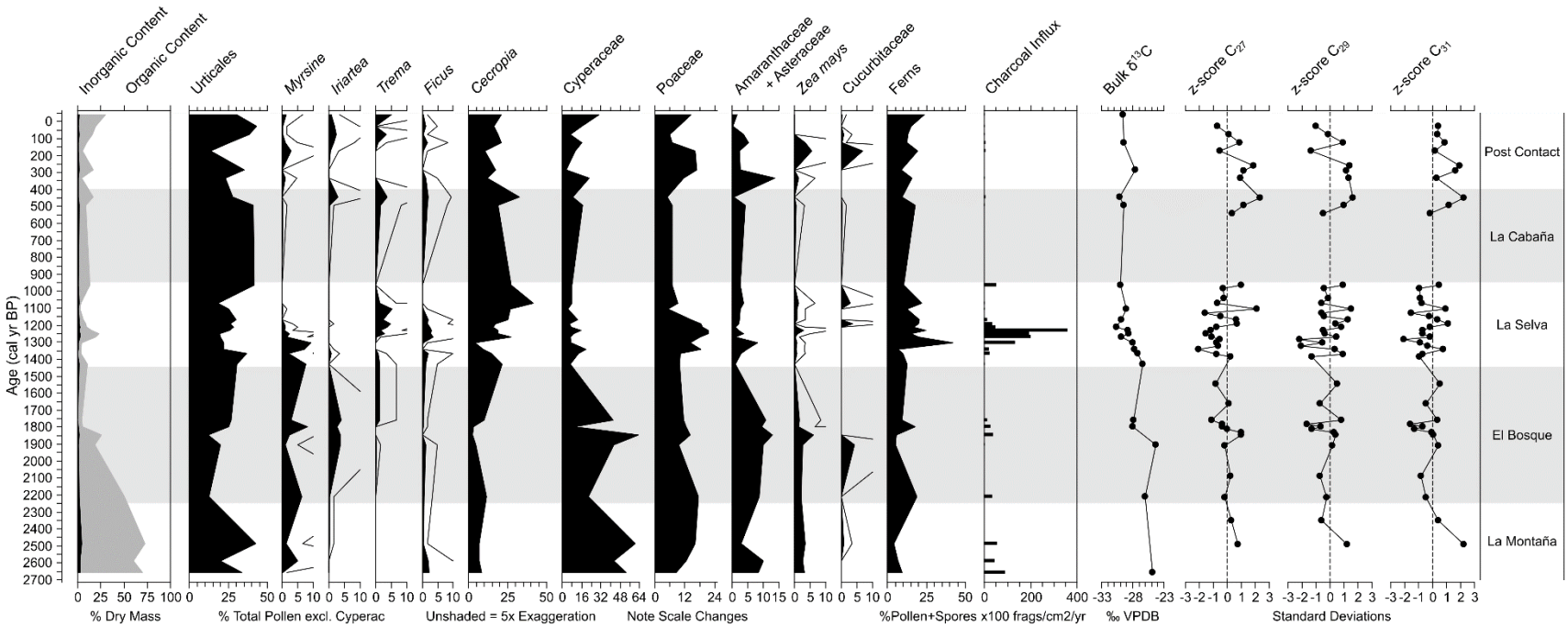

Fig. 3.10. Select proxy data for Bonillita. Includes: sediment composition (black curve = % carbonate), select pollen and spore data, and microscopic charcoal influx (particle size 25–125 μm) from Northrop and Horn (1996), bulk $\delta^{13}C$ data from Lane et al. (2009), and z-scores for δD_{PP} for odd numbered *n*-alkanes $C_{27–33}$ (this study) for Laguna Bonillita. Zones shown at right are delineated following the Río Reventazón Valley cultural chronology (Snarskis 1984). The Urticales group includes all di- and triporate types other than *Trema*, *Cecropia*, and *Ficus*. Cyperaceae pollen is excluded from the pollen sum for all curves other than its own but is included in the sum used for fern spores. Note scale changes. VPDB = Vienna Pee Dee Belemnite.

3.11 Supplemental Information

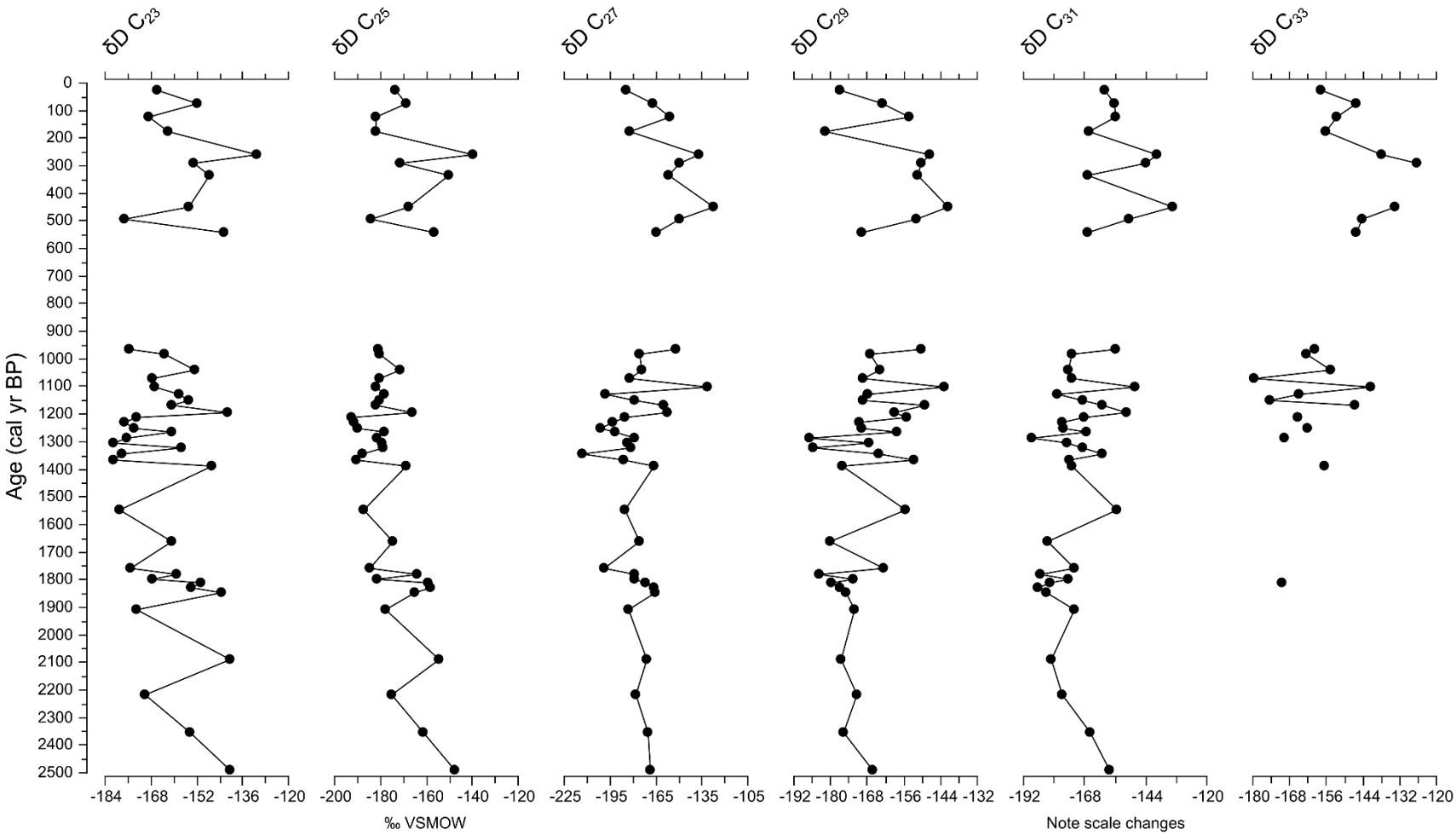

Fig. S3.1. *n*-alkane δD values for odd numbered homologues C_{23} to C_{33}. Note changes to the scale on the x-axes.

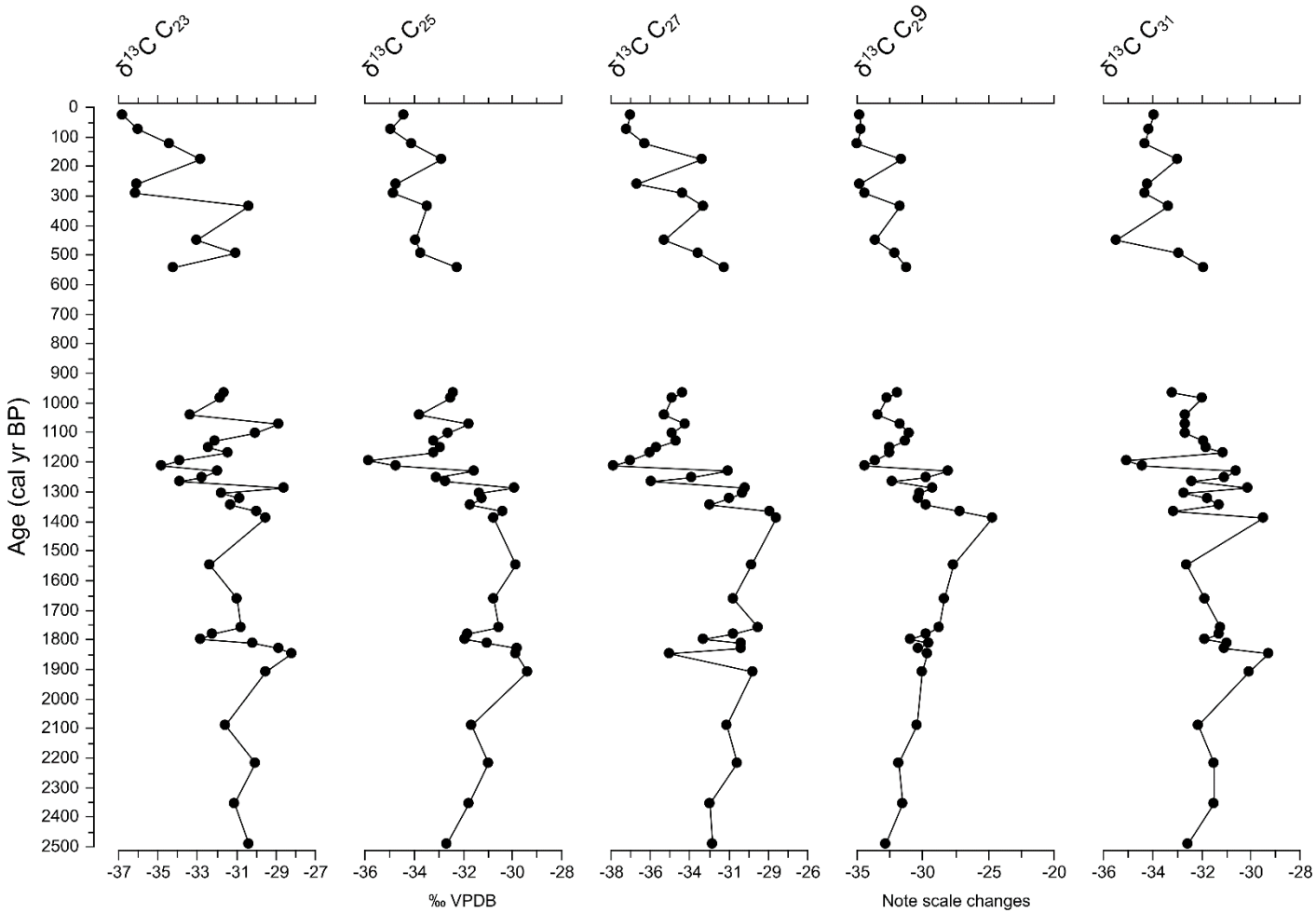

Fig. S3.2. *n*-alkane $\delta^{13}C$ values for odd numbered homologues C_{23} to C_{31}. Note changes to the scale on the x-axes.

CHAPTER 4

A 2000-YEAR HISTORY OF PRECIPITATION AND MAIZE AGRICULTURE IN SOUTHERN PACIFIC COSTA RICA

This chapter is in preparation for submission to a journal. The use of "we" in the text refers to me and my co-authors, Sally Horn and Chad Lane. As first author, I led on study design, data collection and analyses, and writing the manuscript.

4.1 Abstract

We conducted compound-specific stable hydrogen (δD) and carbon ($\delta^{13}C$) isotope analysis of *n*-alkanes from terrestrial leaf waxes in a sediment core from Laguna Santa Elena (8.9290 °N, 82.9257 °W, 1055 m) to reconstruct variations in late Holocene precipitation in southern Pacific Costa Rica. We compared our new record with paired evidence of vegetation and fire history from the same sediment core and with archaeological evidence of prehistoric human activity in the area around Laguna Santa Elena to better understand relationships between climate, environment, and human activity. Our new data show variations in Holocene hydroclimate at Santa Elena broadly consistent with evidence from the wider circum-Caribbean, including local manifestations of the Terminal Classic Drought (ca. 1200–850 cal yr BP) and the Little Ice Age (ca. 550–100 cal yr BP). Unlike sites on the Caribbean side of the Panamanian Isthmus, Santa Elena does not show δD evidence of severe, sustained aridity during the Terminal Classic Drought. Our paired paleoenvironmental and archaeological findings indicate that wet conditions at Santa Elena may be related to declines in maize agriculture and may have driven a population collapse around 700 cal yr BP before the onset of the Little Ice Age and Spanish Conquest.

4.2 Introduction

Laguna Santa Elena (8.9290 °N, 82.9257 °W, 1055 m elevation) is a small lake in the Diquís archaeological subregion of southern Pacific Costa Rica (Horn and Haberyan 2016). Paleoecological and geochemical analyses of a 7.1 m sediment core from the lake revealed a history of land use and maize agriculture at varying scales and intensities from ca. 1800 cal yr BP to the present (Anchukaitis and Horn 2005; Kerr et al. forthcoming). Archaeological surveys of the area around Santa Elena demonstrate that the area was continuously occupied by sophisticated and increasingly complex prehistoric people from the Aguas Buenas period (ca. 2250–1150 cal yr BP; Corrales 2000) until ca. two centuries prior to the arrival of Spanish explorers, although stable carbon isotopes ($\delta^{13}C$) and the presence of maize pollen in the Santa Elena sediments show that the watershed was never completely abandoned (Anchukaitis and Horn 2005; Kerr et al. forthcoming). The history of maize agriculture at Santa Elena includes several episodes of agricultural expansion or intensification and also declines that coincide temporally with both culture change in the Diquís and extreme climate events in the broader circum-Caribbean, including the Terminal Classic Drought (ca. 1200–850 cal yr BP; Hodell et al. 2005; Lane et al. 2014) and the Little Ice Age (ca. 550–100 cal yr BP; Lane et al. 2011).

We conducted compound-specific stable hydrogen (δD) and carbon ($\delta^{13}C$) isotope analysis of *n*-alkanes from terrestrial leaf waxes preserved in the Laguna Santa Elena sediment core to reconstruct variations in precipitation in the southern Pacific region of Costa Rica during the late Holocene. Our goals were to develop a paleoenvironmental reconstruction that unambiguously reflects climate and to compare that record with paired evidence of vegetation change and fire history from the same sediment core and with local archaeological evidence to

better understand relationships between climate, environment, and human activity in Costa Rican prehistory.

We asked three questions in our research: (1) what patterns and variations in Late Holocene hydroclimate are recorded in the Laguna Santa Elena sediments; (2) how do variations in precipitation over time at Santa Elena relate to evidence of prehistoric human activity; and (3) how are global-scale extreme climate events, including the Terminal Classic Drought (TCD; ca. 1200–850 cal yr BP) and the Little Ice Age (LIA; ca. 550–100 cal yr BP), represented at our site in southern Pacific Costa Rica?

4.3 Background

4.3.1 The Compound-Specific Stable Hydrogen Isotope (δD) Proxy

The δD composition of sedimentary *n*-alkanes from terrestrial leaf waxes preserved in lake-sediment cores serves as an indicator of watershed hydrology (Sachse and Gleixner 2004; Sachse et al. 2010). Oxygen isotope ($\delta^{18}O$) analysis of biogenic carbonates is more widely used as a precipitation proxy (Hodell et al. 1995; Huang et al. 2004; Lane et al. 2014; Wahl et al. 2014), but carbonate preservation is poor in many tropical lakes with low pH. The δD proxy shows significant promise for producing records of paleoprecipitation variability from sites such as Laguna Santa Elena in Costa Rica where carbonate preservation is poor (Kerr et al. this dissertation, Chapters 2 and 3).

In the tropics, the δD composition of meteoric water is controlled by the amount effect and evapotranspiration (Dansgaard 1964; Lachniet and Patterson 2002; Polissar and Freeman 2010). More precipitation results in relatively lower δD values and less precipitation yields higher δD values (Dansgaard 1964; Lachniet and Patterson 2002). Evapotranspiration

preferentially removes the ^{1}H isotope from water, leaving the remaining groundwater available for plants enriched in the heavier ^{2}H isotope (Polissar and Freeman 2010). Higher *n*-alkane δD values in plant waxes indicate aridity and lower values indicate more humid conditions (Liu and Huang 2005; Sachse et al. 2006; Xia et al. 2008; Kahmen et al. 2013a, 2013b).

The δD signal from water is locked into leaf waxes at the time of formation and the biogeochemical signal from this plant matter is then incorporated into lake sediments, preserving a stratigraphic record of watershed hydrology (Sachse et al. 2010). This allows the sedimentary δD record to serve as a proxy for precipitation variability through time (Stuvier 1970; Cohen 2003; Sachse and Gleixner 2004).

4.3.2 Extreme Climate Events

The last several decades have seen a rise in scholarship on climate change and extreme events. For example, the Terminal Classic Drought (TCD), a series of severe multi-decadal droughts that occurred between ca. 1200 and 850 cal yr BP (Hodell et al. 2005; Lane et al. 2014) across the circum-Caribbean region have been linked to the decline of Maya civilization (Hodell et al. 1995, 2005; Webster et al. 2007; Medina-Elizalde et al. 2010; Kennett et al. 2012; Douglas et al. 2015). We have reported evidence of drought during the TCD at Laguna Castilla on Hispaniola (Lane et al 2014), at Laguna Bonillita in central Atlantic Costa Rica (Kerr et al. this dissertation), and at Lago de las Morrenas 1 in highland Costa Rica (Kerr et al. this dissertation) using δD analysis of lake sediments.

Additional evidence of dry conditions in Costa Rica and on the Panamanian Isthmus during the TCD comes from analysis of charcoal in sediments from Lago Chirripó (Horn and Sanford 1992; Horn 1993), subfossil chironomids in sediments from Laguna Zoncho and Lago

de las Morrenas 3C (Wu et al. 2017, 2019), stable carbon isotopes ($\delta^{13}C$) at Morrenas 3C (Wu et al. 2019), and $\delta^{18}O$ values in speleothem carbonates from Panama (Lachniet et al. 2004). More broadly, several research groups have reported hypothesized links between titanium content in marine sediments from the Cariaco Basin off northern Venezuela, changes in the mean annual position of the Intertropical Convergence Zone (ITCZ), and culture change in the circum-Caribbean (Haug et al. 2003; Hodell et al. 2005; Peterson and Haug 2006; Kennett et al. 2012; Luzzadder-Beach et al. 2012).

Evidence for the Little Ice Age (LIA), a widespread multi-century cooling event that occurred between ca. 550 and 100 cal yr BP (Lane et al. 2011), also appears in marine and terrestrial records, including the Cariaco Basin sediments (Haug et al. 2001; Peterson and Haug 2006; Black et al. 2007), and in lake-sediment cores from the Yucatan (Hodell et al. 2005) and Hispaniola (Lane et al. 2011). In Costa Rica, Wu et al. (2019) reported warm and wet conditions during the first part of the LIA ca. 550–350 cal yr BP followed by cooling and drying during the latter part ca. 350–100 cal yr BP at Lago de las Morrenas 3C and cooling at Laguna Zoncho but with mixed evidence for moisture conditions there. Taylor et al. (2013) reported evidence of agricultural decline at Laguna Zoncho that corresponds temporally to LIA drought, while we reported similar evidence for agricultural decline and hypothesized climate deterioration at Laguna Santa Elena (Kerr et al. forthcoming).

Considerable work remains to understand the teleconnections, forcing mechanisms, causes, and consequences of these abrupt, global climate events. Disentangling proxy evidence for these events in Central America is difficult due to a long history of human disturbance (Bradbury 1982; Horn 2007) and becomes even more difficult later in the Holocene when complex civilizations developed in the Americas. Developing long proxy records from sites such

as Laguna Santa Elena in southern Pacific Costa Rica, which was inhabited by prehistoric maize agriculturalists at varying intensities for nearly 4000 years (Johanson et al. forthcoming), has high potential to contribute to this debate.

4.3.3 Geography and Archaeology of Greater Chiriquí

The geography and archaeology of southern Pacific Costa Rica and adjacent western Panama have been covered in detail by several researchers (e.g., Anchukaitis and Horn 2005; Palumbo 2009; Kerr 2014; Johanson et al. forthcoming; Kerr et al. forthcoming). Here we provide a brief summary (Table 4.1).

In the broadest context, Laguna Santa Elena is part of the Intermediate Area archaeological region of lower Central America and northwestern South America, which includes parts of Honduras and El Salvador, all of Nicaragua, Costa Rica, and Panama, northern Ecuador and Colombia, and western Venezuela (Lange 1992). Humans have continuously occupied the Intermediate Area for thousands of years (Barrantes et al. 1990; Costenla 1991, 1994; Barrantes 1993; Lange 1993; Corrales 2000) and were more egalitarian than Mesoamerican groups to the north and Andean groups to the south (Sheets 1992). Zooming in, Santa Elena is in the Greater Chiriquí archaeological area that includes closely related cultures in southern Pacific Costa Rica and western Panama, with the Costa Rican portion designated the Diquís archaeological subregion. The chronology of the Diquís is not as well-dated as in other areas in Costa Rica and broader Central America and had been established mostly through pottery seriation and comparison with other areas (Anchukaitis and Horn 2005). It is the least well-known of Costa Rica's archaeological regions (Snarskis 1981).

The Sinancrá period (ca. 3450–2250 BP) was the earliest time of permanent settlement in the Diquís, including at the Curré site in the Diquís Delta (Corrales 1985) and the Nikira site in the Coto Colorado Valley (Corrales 2000). Very little is known about Sinancrá, but the pottery may be related to other contemporaneous styles from southern Pacific Costa Rica and western Panama. Paleoecological and geochemical studies of lake sediments have demonstrated the presence of maize (*Zea mays* subsp. *mays*) in the Diquís dated to the the Sinancrá period, including at Laguna Zoncho (Clement and Horn 2001), Laguna los Mangos (Johanson et al. forthcoming), and Laguna Gamboa (Horn 2006), although the role of maize this early in the chronology remains uncertain (Hoopes 1991, 1996). Researchers have debated whether early maize agriculture developed for use as a subsistence crop (Galinat 1980; Smith 1980), a special-use crop for ritual feasting (Hoopes 1991, 1996), or for use of the sugary stalks in the alcoholic beverage *chicha* (Iltis 2000; Iltis and Benz 2000; Smalley and Blake 2003).

The Aguas Buenas period (ca. 2250–1150 BP) is defined by ceramic types, settlement patterns, and site characteristics. Aguas Buenas was spatially and temporally extensive in Greater Chiriquí and although research has revealed more about this phase versus the preceding Sinancrá, the exact details and timing continue to be debated. Hoopes (1996) argued that populations were small and dispersed in Greater Chiriquí during Aguas Buenas, while Linares et al. (1975) identified chiefdom-level groups in western Panama dated to ca. 2150 BP (Sheets 2001). Maize agriculture was firmly established across southern Pacific Costa Rica and western Panama during the Aguas Buenas period (Behling 2000; Clement and Horn 2001; Anchukaitis and Horn 2005; Taylor et al. 2013; Johanson et al. forthcoming; Kerr et al. forthcoming).

The Chiriquí period (ca. 1150–450 BP) follows Aguas Buenas and lasted until Spanish arrival early in the 16th century. Chiriquí was significantly different from the preceding periods

and was marked by major shifts in culture, settlement, subsistence, and social organization, including the appearance of metallurgy and more elaborate ceramics, larger and more complex sites, increased importance of maize, and hierarchical, ranked societies organized around politically and economically oriented connections (Corrales et al. 1988; Drolet 1992). Site locations shifted toward more consolidated regional centers located in lowland alluvial areas (Linares et al. 1975; Sheets 1980; Drolet 1983, 1984, 1988, 1992), but mid-elevation sites existed contemporaneously with lowland and floodplain sites (Corrales 2000; Sánchez and Rojas 2002). In general, Chiriquí was marked by complex, hierarchical societies with large populations supported by intensive maize agriculture (Corrales 2000).

Columbus explored the Caribbean coast of Central America in 1502 AD and Hernan Ponce de Leon and Juan de Castañeda entered the Golfo Dulce in southern Pacific Costa Rica in 1519 AD (Corrales et al. 1988). Juan Vásquez de Coronado defeated indigenous groups in the Rio Térraba-Coto Brus Valley in 1562–1563 AD, effectively ending the Chiriquí and beginning the post-Contact period. Coronado described large plantations of maize, beans, and fruit trees, and reported the presence of fortifications, conflicts between territorial chieftains, and warfare over territory and property at the time (Fernández Guardia 1913). Indigenous settlement continued through the post-Contact period, albeit at greatly reduced levels, and the presence of European items in native burials demonstrates at least a minor level of coexistence (Corrales 1986; Quintanilla 1990). Southern Pacific Costa Rica then remained only lightly settled well into the 20th century (Hall 1985).

4.3.4 Geography and Archaeology of Laguna Santa Elena

Laguna Santa Elena (8.9290 °N, 82.9257 °W, 1055 m elevation; Fig. 4.1) occupies a landslide-truncated stream channel in southern Pacific Costa Rica near the Térraba-Coto Brus River Valley (Horn and Haberyan 2016). The modern lake is small (0.13 ha) and shallow (3.8 m), but the presence of old shorelines indicates the lake was once larger, possibly ca. 1 ha (Anchukaitis and Horn 2005). Annual rainfall averages ca. 3500–4000 mm with a short but pronounced dry season January–March. Temperature averages ca. 21–23 °C (Herrera 1985). Santa Elena is in the "premontane wet forest transition to rainforest" life zone of the Holdridge bioclimatic classification system (Holdridge 1967; Hartshorn 1983). Taxa expected in mature forest include *Quercus*, Lauraceae, *Hedyosmum*, *Weinmannia*, *Alnus*, and Melastomataceae (Anchukaitis and Horn 2005). Previous paleoecological and geochemical work at Santa Elena has revealed a nearly 2000-year history of forest disturbance, vegetation change, and indigenous maize agriculture dated to the early Aguas Buenas period (Anchukaitis and Horn 2005; Kerr et al. forthcoming).

Archaeologists from the Universidad de Costa Rica have conducted limited reconnaissance, surface collections, and test excavations at mid-elevation sites in the Coto Brus region (Sánchez and Rojas 2002). Test pits and surface collections on the hilltops surrounding Santa Elena showed evidence of dispersed dwelling sites and lithics diagnostic of the Aguas Buenas period, but no artifacts from the later Chiriquí period. A larger site named Fila Tigre is situated ca. 2 km east of Santa Elena. Surface collections there yielded ceramics predominantly from the Aguas Buenas period along with a lesser presence of Chiriquí materials, possible house sites, and potential burials. Sánchez and Rojas (2002) noted that Fila Tigre was likely a significant regional center and a focus for political and economic activity in the area. The Las

Tablas area lies several km to the north of Santa Elena and contains many sites dated to both the Aguas Buenas and the Chiriquí periods (Leon 1986; Corrales 2000). Several more sites exist to the south of Santa Elena, the closest being Piedra Pintada and Rio Negro, both dated to the Aguas Buenas (Sánchez and Rojas 2002).

4.3.5 Previous Paleoenvironmental Work at Laguna Santa Elena

Horn and students recovered a sediment core in 2000 from near the center of Laguna Santa Elena using a Colinvaux-Vohnout locking piston corer (Colinvaux et al. 1999) and a PVC tube fitted with a rubber piston for the uppermost watery sediments (Anchukaitis and Horn 2005). The core sections were returned to the Laboratory of Paleoenvironmental Research at the University of Tennessee, where they were opened, sectioned, photographed, and described. Anchukaitis and Horn (2005) obtained AMS ^{14}C dates on macrofossils from six levels of the Santa Elena sediment core and developed an age-depth model using linear interpolation. They sampled 29 levels of the core for sedimentary pollen and micro- and macroscopic charcoal analyses. Additionally, they scanned prepared slides for maize pollen at low magnification to establish the presence or absence of maize in their sampled levels. The work reported by Anchukaitis and Horn (2005) revealed a nearly continuous 2000-year record of prehistoric and historic human forest disturbance, vegetation change, and maize agriculture, three eruptions of nearby Volcán Barú in Panama, and the timing of an agricultural decline near the arrival of the Spanish in southern Pacific Costa Rica.

More recently, Kerr et al. (forthcoming) conducted geochemical, stable carbon ($\delta^{13}C$) and nitrogen ($\delta^{15}N$) isotope, and loss-on-ignition analyses of sediments from the Santa Elena core to supplement and refine the record reported by Anchukaitis and Horn (2005) from sedimentary

pollen and charcoal. Their work revealed the timing of several episodes of both agricultural intensification and decline in the Santa Elena watershed, including two declines coincident with the onset of the Terminal Classic Drought and the Little Ice Age. Additionally, Kerr et al. (forthcoming) confirmed that the latter decline at Santa Elena occurred prior to the arrival of the Spanish in the region, matching a pre-Hispanic decline reported by Taylor et al. (2013) at nearby Laguna Zoncho.

4.4 Methods

4.4.1 Radiocarbon Calibration and Age-Depth Modeling

We obtained one new AMS ^{14}C date on a macrofossil from the Santa Elena sediment core, recalibrated the radiocarbon dates originally reported by Anchukaitis and Horn (2005), produced an updated age-depth model, and generated point estimates for our sampled levels using the 'clam' package (v. 2.3.2; Blaauw 2019) for the R Statistical Environment (v. 3.5.2; R Core Team 2019) and the IntCal13 radiocarbon calibration curve (Reimer et al. 2013). Anchukaitis and Horn (2005) originally used linear interpolation to develop an age model for the Santa Elena core, as did Kerr et al. (forthcoming). Here we also use linear interpolation.

4.4.2 Sample Preparation

We sampled the Santa Elena core for compound-specific isotope analysis at depth intervals of 11–32 cm, corresponding to time intervals of ca. 12–207 calibrated years, guided by our age-depth model and previous proxy work (Anchukaitis and Horn 2005; Kerr et al. forthcoming) and constrained by the availability of sediments remaining from previous studies.

Sample dry masses ranged from ca. 11.3 g in more organic sediments to 30.2 g in sediments with higher mineral content.

Methods for sample preparation are identical to those presented in Chapters 2 of this dissertation. Briefly, we oven-dried sediment samples, ground them to a fine powder and extracted them by sonication with dichloromethane and methanol. The samples were centrifuged, concentrated by rotary evaporation, and blown dry. Samples were then saponified and the neutral fraction was recovered from the total lipids with hexane. The neutral fraction was further cleaned on silica gel columns and *n*-alkanes were isolated from the cleaned neutral fraction by urea adduction. The adducts were spiked with a squalane isotope standard (provided by A. Schimmelmann, Indiana University) to monitor instrument precision.

4.4.3 Quantification, Identification, and Isotope Ratio Mass Spectrometry

We identified compounds using gas chromatography mass spectrometry (GCMS), quantified compound abundances using flame ionization detection (FID), and analyzed compound-specific isotope ratios using gas chromatography-isotope ratio mass spectrometry (GC-IRMS). Instruments and parameters were identical to those presented in Chapter 2 of this dissertation. An external isotope standard (*n*-alkane mixture B4, supplied by A. Schimmelmann, Indiana University) was analyzed between every four sample runs to monitor instrument accuracy and precision.

4.4.4 Data Processing and Analysis

Data processing methods and equations follow those presented in Chapter 2 of this dissertation. We quantified abundances for all alkane homologues of carbon chain lengths C_{20} to

C_{33}. To assess the strength of the terrestrial signal in our data, we calculated the carbon preference index (CPI) for each of our samples, following Marzi et al. (1993). Additionally, we calculated average carbon chain length (ACL), following Feakins et al. (2016).

We analyzed isotope data for all odd chain alkane homologues from C_{27} to C_{31} for δD and C_{25} to C_{33} for $\delta^{13}C$. Low alkane abundances precluded analysis of other homologues. Here we focus on δD and $\delta^{13}C$ data for C_{27}, C_{29}, and C_{31} alkanes because they are reliable indicators of terrestrial vegetation and fractionation factors (ε) between plants and mean annual precipitation for these homologues are available in the published literature (Sachse et al. 2012).

We quantified analytical uncertainty in our compound-specific δD and $\delta^{13}C$ data following the methods of Polissar and D'Andrea (2014). In addition to terrestrial leaf wax δD and $\delta^{13}C$ values, we present z-scored, vegetation-corrected δD values for paleoprecipitation (δD_{PP}), following Feakins (2013). Vegetation change can shift the balance of δD fractionation factors (ε) for landcover in a watershed, thus affecting the composition of plant-wax δD signals recorded in lake sediments without necessarily requiring changes to δD in regional hydrology. To account for this possible bias in the plant-based δD proxy, we combined pollen data from the Santa Elena sediments (Anchukaitis and Horn 2005), the supplementary dataset of Sachse et al. (2012) comprising a global survey of published fractionation factors (ε) for many plant taxa, and a two-endmember linear mixing model for grasses assuming average $\delta^{13}C$ values of –34.0‰, –34.5‰, and –35.0‰ for C_3 grasses in our C_{27}, C_{29}, and C_{31} alkane data, respectively, and –21.3‰ for C_4 grasses across all homologues to produce an unbiased, ε-corrected paleoprecipitation reconstruction for the Bonillita site.

Hydrogen and carbon isotope compositions are reported in standard δ-per mil notation, with hydrogen values relative to Vienna Standard Mean Ocean Water (VSMOW) and carbon

values relative to the Vienna Pee Dee Belemnite (VPDB) marine carbonate standard. Repeated analyses of our squalane internal standard indicated that instrument precision for our samples (1 SD) averaged ca. 2.9‰ for hydrogen and 0.2‰ for carbon. Repeated analyses of our external isotope standard indicated that propagated error for our dataset (1 SEM) averaged ca. 6.8‰ for hydrogen and 0.7‰ for carbon.

We plotted our new z-scored and ε-corrected δD values for paleoprecipitation (δD_{PP}) for the $C_{27\text{-}31}$ odd *n*-alkanes, along with select pollen, micro-, and macroscopic charcoal data from Anchukaitis and Horn (2005), vegetation categorized by life form (following Sachse et al. 2012; Feakins 2013), bulk $\delta^{13}C$ from Kerr et al. (forthcoming), and Cariaco Basin titanium data tuned by Kennett et al. (2012) using C2 (v. 1.7.7; Juggins 2007). We plotted proxy data by calibrated age, with all previous data replotted following our new age-depth model. Stratigraphic diagrams are divided into informal zones following Anchukaitis and Horn (2005) and Kerr et al. (forthcoming) based on major changes in proxy data.

Methods for pollen and charcoal analyses are in Anchukaitis and Horn (2005). Pollen percentages for all taxa are calculated based on pollen sums for each sampled level excluding Cyperaceae, fern spores, and indeterminates. For our vegetation correction to δD values, plants represented in the pollen record are categorized by taxonomy and life form as pteridophytes, forbs (non-graminoid herbs), total graminoids (Poaceae and Cyperaceae), C_3 and C_4 graminoids (calculated as a percentage of total graminoids using our mixing model), angiosperm shrubs and trees, and gymnosperms of the montane forest (*Prumnopitys*, formerly *Podocarpus*). Charcoal data are presented as influx values (fragments/cm^2/yr). Methods for loss-on-ignition and bulk $\delta^{13}C$ analysis are in Kerr et al. (forthcoming). Bulk $\delta^{13}C$ values originally reported by Kerr et al.

(forthcoming) are presented here in standard δ-per mil notation, as above, alongside our new plant wax $\delta^{13}C$ and δD data.

4.5 Results

Our new radiocarbon date, recalibration of previous dates (Table 4.2), and new age modeling (Fig. 4.2) confirm a normal stratigraphic sequence at Laguna Santa Elena with organic sedimentation beginning ca. 1830 cal yr BP. Regression analysis comparing bulk and compound-speific $\delta^{13}C$ values indicates minimal pre-aging of alkanes prior to sedimentation (Fig. 4.3; Lane et al. 2016).

The Santa Elena core is composed of ca. 6.0 m of lacustrine silts and clays consisting of coarse partially-decomposed organic material underlain by ca. 1.2 m of strongly-weathered mineral soil. The upper 25 samples examined by Anchukaitis and Horn (2005) contained well-preserved pollen and charcoal, while the lower 4 contained few palynomorphs and were not counted. Maize pollen was present in all but three levels. Analysis showed an average organic content of ca. 30.1% (range ca. 15.1–45.6%) and an average total inorganic content of ca. 69.9% (range ca. 54.4–84.9%), as estimated by loss-on-ignition (LOI) at 550 °C (Dean 1974; Kerr et al. forthcoming). Data for LOI at 1000 °C from Kerr et al. (forthcoming) indicates carbonate contents of no more than ca. 2.0–5.5%; however, the loss of interstitial water in clays between 550 °C and 1000 °C (Dean 1974) could have inflated reported carbonate values.

Alkane homologue distributions for all our samples display a consistent odd-over-even carbon chain pattern, which is expected of terrestrial organic matter (Fig. 4.4). Carbon preference indices (CPI), which provide a measure of the relative abundances of even- and odd-chain length compounds, average 4.4 (range 2.4–5.7) throughout the core (Fig. 4.4). Even-carbon *n*-alkanes

are typical of microbes and other non-terrestrial organisms (CPI ca. 1.0), while odd-carbon *n*-alkanes are typical of terrestrial vegetation (CPI >3; Bray and Evans 1961; Eglinton and Hamilton 1963, 1967; Marzi et al. 1993). CPI values for all samples except one in the Santa Elena core are >3, indicating a predominantly terrestrial organic matter source over the past ca. 1800 cal years. The sample from 16.5 cm (ca. –33 cal yr BP) has a CPI value of 2.4, indicating an increased contribution of autochthonous material in these recent sediments.

Average chain lengths (ACL) in the Santa Elena sediments range from 27.6–29.6 ($\bar{x}$ = 28.7) throughout the core (Fig. 4.4). Relatively shorter odd-numbered *n*-alkanes (≤25 carbon atoms) are typical of algae and aquatic vegetation, while relatively longer *n*-alkanes (≥27 carbon atoms) are typical of terrestrial organic matter (Han et al. 1968; Cranwell et al. 1987; Poynter et al. 1989; Poynter and Eglinton 1990; Ficken et al. 2000; Meyers 2003; Feakins et al. 2016; Lane 2017). All our samples have ACL values >27.0, indicating that the Santa Elena sediments are composed primarily of allochthonous terrestrial organic matter from higher plants. Additionally, all our samples contained longer-chain $C_{27–31}$ odd *n*-alkanes in abundances sufficient for analysis.

The plant life form categories and their respective fractions of total vegetation that we used to calculate our vegetation-corrected paleoprecipitation values (δD_{PP}; Feakins 2013) included: gymnosperms (0–0.1%, $\bar{x}$ = 0.04%), angiosperm trees and shrubs (10.4–75.8%, $\bar{x}$ = 37.0%), total graminoids (4.2–64.1%, $\bar{x}$ = 32.4%), forbs (3.9–10.4%, $\bar{x}$ = 7.1%), and pteridophytes (9.0–31.8%, $\bar{x}$ = 23.5%) (Fig. 4.5, Table 4.3). Our mixing model estimates for the relative abundances and contributions of C_3 and C_4 graminoids yielded values of ca. 4.0–30.1% for C_3 plants ($\bar{x}$ = 18.9%) and 0.2–34.0% for C_4 plants ($\bar{x}$ = 13.5%). Apparent fractionation

factors (ε) between alkane homologues and mean annual precipitation ($\varepsilon_{C27–31/MAP}$) for C_{27}, C_{29}, and C_{31} *n*-alkanes for each vegetation category are in Table 4.4.

Values for $\delta D_{PP/C27}$ ranged from –76.1‰ to –39.4‰ VSMOW ($\bar{x}$ = –58.0‰), while $\delta D_{PP/C29}$ ranged from –63.9‰ to –31.4‰ ($\bar{x}$ = –46.2‰) and $\delta D_{PP/C31}$ ranged from –72.5‰ to –28.2‰ ($\bar{x}$ = –45.3‰; Fig. 4.6). Mean δD_{PP} values for the Santa Elena record are within the hypothesized range of δD for meteoric water at our site location and elevation predicted by the OIPC3.1 (Bowen 2019), ranging from –67‰ to –21‰, and averaging –57‰ (Table 4.5). Z-scores of our δD_{PP} values (Fig. 4.6) reveal the timing of decadal- to centennial-scale changes in paleohydrology at Santa Elena.

Patterns in our leaf wax $\delta^{13}C$ values track well with values for δD prior to ca. 700 cal yr BP, indicating that $\delta^{13}C$ and δD are both responding to changing moisture availability in the lower part of the Santa Elena record (Fig. 4.6). After ca. 700 cal yr BP, patterns in $\delta^{13}C$ and δD diverge, with δD responding primarily to changes in moisture availability and $\delta^{13}C$ responding to changes in vegetation composition driven by a reduction in the scale and intensity of maize agriculture and resulting reforestation of the watershed. Values for $\delta^{13}C_{C27}$ range from –33.3‰ to –22.3‰ VPDB ($\bar{x}$ = –28.2‰), while $\delta^{13}C_{C29}$ range from –33.9‰ to –25.6‰ ($\bar{x}$ = –30.4‰) and $\delta^{13}C_{C31}$ from –34.3‰ to –23.7‰ ($\bar{x}$ = –29.7‰) (Fig. 4.6). Fractionation factors (ε) between plants and precipitation vary through time with changes to the vegetation composition (Fig. 4.7), demonstrating the importance of the vegetation correction to the δD proxy (Feakins 2013). Carbon isotope data for C_{25} and C_{33} homologues are in the supplemental information for this chapter (Fig. S4.1).

4.5.1 Zone 3: ca. 1780–1590 cal yr BP

The Santa Elena sediments began accumulating ca. 1780 cal yr BP during the Aguas Buenas period with average to negative z-scores for δD_{PP} indicating moist conditions at the time. Values for $\delta^{13}C$ in *n*-alkanes are relatively low, corresponding with high pollen percentages for trees and other taxa representing intact native C_3 forest, including *Quercus*, *Alchornea*, Melastomataceae, *Weinmannia*, *Myrsine*, and *Cecropia* (Fig. 4.8). Low charcoal influx together with the presence of *Zea mays* pollen shows that maize farming was taking place at the Santa Elena site during the early Aguas Buenas period, as it was at other sites in southern Pacific Costa Rica at the time (Behling 2000; Clement and Horn 2001; Anchukaitis and Horn 2005; Horn 2006; Johanson et al. forthcoming). Pollen percentages for forest taxa decline somewhat across Zone 3, while leaf-wax $\delta^{13}C$ values and pollen percentages for weedy taxa in the Poaceae and Asteraceae families increase slightly in response to initial forest clearance and conversion of land to agricultural fields.

4.5.2 Zone 2c: ca. 1590–1150 cal yr BP

Zone 2c begins with average to slightly dry conditions indicated by positive z-scores for δD_{PP}. Increasing percentages of *Zea* pollen show expansion or intensification of maize agriculture in the watershed. Bulk $\delta^{13}C$ reaches the highest value in the record at ca. –10.3‰ at ca. 1450 cal yr BP consistent with increasing $\delta^{13}C$ values in *n*-alkanes and increasing *Zea* pollen, indicating major expansion or intensification of C_4 maize agriculture. In the middle of Zone 2c, decreasing z-scores for δD_{PP} show a return to wet conditions ca. 1290 cal yr BP. The upper part of Zone 2c shows the highest charcoal influx in the record, along with high percentages of *Zea* pollen and pollen for weedy taxa in the Poaceae and Asteraceae families, indicating a high and

sustained level of forest clearance and maize agriculture in the Santa Elena watershed. The beginning of the Terminal Classic Drought overlaps by ca. 50 years with the top of Zone 2c, with z-scores for δD_{PP} indicating slightly wetter than average conditions.

4.5.3 Zone 2b: ca. 1150–880 cal yr BP

The entirety of Zone 2b overlaps with the Terminal Classic Drought. Z-scores for δD_{PP} indicate drier than average conditions ca. 1085 and 1035 cal yr BP for the C_{27} and C_{29} alkanes, respectively, but δD_{PP} values overall indicate predominantly average to moist conditions at Santa Elena during the TCD interrupted by a brief, punctuated episode of drying. Leaf-wax $\delta^{13}C$ values increase slightly at the bottom of Zone 2b and then stabilize throughout the rest of the zone. Maize pollen percentages and values for bulk $\delta^{13}C$ decline in the bottom of the zone at ca. 1085 cal yr BP and pollen percentages for *Quercus* and *Alnus* increase, indicating a decline in maize agriculture and regrowth of some forest components coincident with slightly dry conditions seen in δD_{PP} values. Following this brief decline in maize agriculture, pollen of forest taxa then declines and *Zea* pollen and bulk $\delta^{13}C$ values again increase to the second highest levels in the core in the middle of zone 2b at ca. 1010 cal yr BP, indicating a resurgence in the scale or intensity of maize agriculture. Charcoal influx and pollen percentages for weedy taxa remain high in zone 2b, indicating continued fire and landscape disturbance in the watershed.

4.5.4 Zone 2a: ca. 880–450 cal yr BP

The bottom of Zone 2a begins with z-scores for δD_{PP} indicating average moisture, but then values decline to the most negative in the record at ca. 720 cal yr BP. Bulk and compound-specific $\delta^{13}C$ values also decline at ca. 720 cal yr BP, indicating a significant shift in vegetation

composition in the Santa Elena watershed. Maize pollen percentages decline, as do pollen percentages for weedy taxa in the middle of Zone 2a, indicating an end to intensive maize agriculture at the site. Pollen percentages for mature and secondary forest taxa, including *Hedyosmum*, *Alchornea*, Melastomataceae, *Weinmannia*, and *Myrsine*, increase in the upper part of Zone 2a, indicating forest recovery. A minor presence of *Zea* pollen and continued charcoal influx shows that maize agriculture continued at Santa Elena, albeit at a greatly reduced level. The beginning of the Little Ice Age overlaps with the top of Zone 2a, but proxy data indicate no major changes in local conditions at the time.

4.5.5 Zone 1: ca. 450 cal yr BP to the present

Most of Zone 1 overlaps with the LIA from ca. 450 to 100 cal yr BP. In the bottom half of the zone, z-scores for δD_{PP} indicate average moisture conditions in the watershed; however, increased δD_{PP} values later show a severe drying trend toward the end of the LIA beginning no later than ca. 215 cal yr BP. After ca. 215 cal yr BP, δD_{PP} values become highly variable and unpredictable, oscillating between wet and dry conditions through the remainder of the record, although some of this variability is likely a function of sampling density in the upper part of the sediment core. Values for bulk and leaf-wax $\delta^{13}C$ remain steady until ca. 50 cal yr BP, indicating stability in the local vegetation composition. After ca. 50 cal yr BP, $\delta^{13}C$ values increase in response to the arrival of modern agriculture in the Santa Elena watershed. Pollen percentages for forest taxa remain relatively high through most of Zone 1, but then decline near the top of the record in response to clearance for modern agriculture. Pollen of weedy taxa are relatively low until the top of the zone, when percentages for Asteraceae, Poaceae, and Amaranthaceae increase in response to modern agriculture. Prior to the modern period, charcoal influx continues across

the zone 2a/zone 1 boundary, along with the presence of *Zea* pollen and relatively elevated bulk $\delta^{13}C$ values. These data indicate that the Santa Elena watershed was never completely abandoned, despite marked population decline in zone 2a.

4.6 Discussion

4.6.1 Paleohydrology at Laguna Santa Elena

Costa Rica receives a mixture of ITCZ moisture from both Caribbean and Pacific sources, with sites to the west of the high cordilleras receiving increased contributions from Pacific airmasses. While considerable research has been conducted on climate change and forcing mechanisms in the circum-Caribbean, the Pacific side has seen far less work and remains poorly understood (Lachniet et al. 2007). Only one prior study has examined hydroclimate on the Pacific side of the Isthmus: Stansell et al. (2013) analyzed $\delta^{18}O$ in ostracods from Lago el Gancho in Pacific Nicaragua. Other researchers working to develop paleoenvironmental reconstructions in southern pacific Costa Rica (e.g., Anchukaitis and Horn 2005; Taylor et al. 2013; Wu et al. 2019; Johanson et al. forthcoming; Kerr et al. forthcoming) have interpreted changes in lake levels as an indicator of hydroclimate. These researchers have extrapolated paleoclimate conditions from the circum-Caribbean side of the cordilleras, noting that the timing of major changes in prehistoric agricultural, cultural, and social systems coincide with the timing of the widespread Terminal Classic Drought and the Little Ice Age. Our new δD reconstruction of hydroclimate at Laguna Santa Elena reported here indicates that, while these events may be synchronous, assuming similar climate conditions between the two coasts of Costa Rica may be unwarranted and that teleconnected forcing mechanisms may be decoupled on the Isthmus. At the least, the situation is far more complicated than once thought.

Hydroclimate in southern Pacific Costa Rica and broader Central America is controlled by several forcing mechanisms, including: ITCZ migration (Hastenrath 2002; Poveda et al. 2006), the El Niño Southern Oscillation (ENSO; Poveda et al. 2006; Lachniet et al. 2007), the Atlantic Multidecadal Oscillation (AMO; Knight et al. 2005), orbital forcing and variations in the subsolar point (Haug et al. 2003), changing sea-surface temperatures (SSTs; Black et al. 2007), and variability in the Atlantic Meridional Overturning Circulation (AMOC; Alley and Clark 1999). Lachniet et al. (2007) found that variations in moisture delivery on the Isthmus over the Late Holocene are linked to variations in the Central American Monsoon (CAM), which itself is modulated by ENSO variability. Strengthened El Niño events result in a weakened CAM, which reduce precipitation on the Isthmus. This is particularly important on the Pacific side of the Isthmus. The Late Holocene has experienced increased ENSO variability, which has resulted in increased precipitation variability in Central America with approximately 100-year pulsing (Lachniet et al. 2007).

The history of hydrology recorded in the Laguna Santa Elena sediments reveals patterns of variability both similar to and different from those seen at other sites in Costa Rica, Central America, and the wider circum-Caribbean over the Late Holocene. Sediment began accumulating at our coring location during a period of average to slightly wet climate in southern Pacific Costa Rica. The Aguas Buenas period, which covers Zones 3 and 2c in our sediment core and was the time of maximum maize agriculture and settlement at the Santa Elena site (Sánchez and Rojas 2002; Kerr et al. forthcoming), had average moisture conditions from ca. 1800 to 1290 cal yr BP, after which time climate turned wet prior to the onset of the TCD.

The subsequent Chiriquí period, the first half of which overlaps with the Terminal Classic Drought in Zone 2b and the second of which covers the intervening years between the TCD and

the LIA in Zone 2a, was a time of increased hydroclimate variability. The interval of the TCD as a whole, ca. 1200–850 cal yr BP (discussed further below) was not notably dry, which differs from other findings from Costa Rica (Horn and Sanford 1992; Horn 1993) including at Laguna Zoncho (Wu et al. 2017, 2019) and Laguna Los Mangos (Johanson et al. forthcoming), Panama (Lachniet et al. 2004), the Yucatan (Hodell et al. 2005; Kennett et al. 2012; Douglas et al. 2015), and the Dominican Republic (Lane et al. 2014). Note that all these study sites except Laguna Zoncho and Laguna Los Mangos are in the Costa Rican highlands and the Caribbean side of Central America and Mexico, where they are affected more strongly by Atlantic climate dynamics. The TCD at Santa Elena began with average to wet conditions, experienced two drying episodes at ca. 1085 and 1035 cal yr BP, and another turn to wet conditions toward the end of the TCD at ca. 940 cal yr BP. These findings show some similarity to those of Hodell et al. (2005) that identified two intervals of extreme drought during the TCD in sediments from Lake Chichancanab on the Yucatan Peninsula, e.g. an "early" TCD ca. 1180–1080 BP and a "late" TCD ca. 1030–850 BP. But in contrast to the situation in the Yucatan, hydroclimate at Santa Elena during this time was *not* remarkably dry, in contrast to conditions expected from extrapolating across the cordilleras from the Caribbean side. The years between the TCD and the LIA were markedly wet, which had important consequences for prehistoric people living at the site, discussed further below.

The post-Contact period covering Zone 1 in the Santa Elena core is overlain by the Little Ice Age and was marked by average moisture conditions until quite late in the LIA around 215 cal yr BP, after which time climate dried significantly and became more variable. These findings largely agree with findings in Costa Rica and the circum-Caribbean, matching reduced titanium input in the Cariaco sediments (Haug et al. 2001) and other evidence of aridity from Costa Rica

(Wu et al. 2017, 2019), Nicaragua (Stansell et al. 2013), and the Dominican Republic (Lane et al 2011).

While paleoenvironmental reconstructions from Central America tend to focus on periods of dry hydroclimate more noticeably than wet intervals, the wet periods at Santa Elena are important to consider. Santa Elena is located on the leeward western slope of the Cordillera de Talamanca, receives a significant amount of moisture from Pacific sources (Lachniet et al. 2007), and is not necessarily controlled by the same teleconnected climate forcing mechanisms as eastern and highland Costa Rica. One surprising result from our research is the finding that Santa Elena was not nearly as dry as expected during the TCD and, in fact, was somewhat wet toward both the beginning and the end of the TCD. Possibly more surprising is our finding that the intervening years between the TCD and the LIA were very wet centered on ca. 720 cal yr BP. Prehistoric populations and maize agriculture declined notably around 700 cal yr BP in southern Pacific Costa Rica at Laguna Santa Elena (Anchukaitis and Horn 2005; Kerr et al. forthcoming) and at nearby Laguna Zoncho (Taylor et al. 2013). Taylor et al. (2013) proposed that population declines in the Diquís may have been accompanied by drying due to the onset of the Little Ice Age, but that is not the case. In fact, the synchronous declines at these sites may be related to a *very wet* period, which could have been as bad for growing maize as very dry conditions.

Unlike other areas such as the Mayan Lowlands in the Yucatan to the north, which saw collapse at many sites during regional drying episodes (Hodell et al. 1995, 2005; Kennett et al. 2012; Douglas et al. 2015), maize agriculture at Laguna Santa Elena appears to have been largely unaffected by dry conditions. Indeed, our proxy record indicates *increases* in maize agriculture during drying trends in Zone 2c of the Santa Elena sediment core and again at the height of the TCD in Zone 2b. By contrast, the *wet* period in the middle of the Chiriquí in Zone 2a saw a

major decline in maize agriculture and population collapse at the site (Anchukaitis and Horn 2005; Kerr et al. forthcoming). Contrary to conventional paleoenvironmental wisdom that predicts circum-Caribbean drought as bad for prehistoric maize agriculture, at Santa Elena, extended periods of wet conditions may have made maize farming difficult or impossible (Anderson 1990; Anderson et al. 1995), while periods of dry conditions made the Santa Elena site with permanent water sources attractive to prehistoric maize agriculturalists.

4.6.2 Prehistoric Human-Environment Interactions

Prehistoric human settlement and maize agriculture were in place at the Santa Elena site at the time of lake formation ca. 1800 cal yr BP (Anchukaitis and Horn 2005; Kerr et al. forthcoming). Laguna Santa Elena formed and began accumulating sediment during an average to wet period in southern Pacific Costa Rica. Our paleoenvironmental record from the site indicates significant forest clearance and landscape disturbance shortly after lake formation during the latter part of the Aguas Buenas period. The archaeological record from Santa Elena shows permanent settlement of the ridgelines around the lake with artifacts diagnostic of the Aguas Buenas period (Sánchez and Rojas 2002), although the Santa Elena timeline begins late in the prehistoric chronology of the Diquís (Clement and Horn 2001; Johanson et al. forthcoming). The limited archaeological evidence available from the Santa Elena site (Sánchez and Rojas 2002) supports an interpretation of a small human presence on the landscape at the time of lake formation and indicates that our sediment core captured the initial stages of settlement, forest clearance, and maize agriculture at the site.

The latter part of the Aguas Buenas period saw continued forest clearance and intensified maize agriculture that peaked toward the middle of the period in Zone 2c of our sediment core at

ca. 1450 cal yr BP, coincident with average to slightly dry conditions, but then declined somewhat during a period of wetter conditions beginning ca. 1260 cal yr BP at the top of Zone 2c just before the onset of the TCD. Bulk $\delta^{13}C$ values decline from a peak at ca. 1450 cal yr BP indicating a reduction of maize agriculture but continued high levels of charcoal influx indicate that burning in the watershed continued. Pollen percentages for weedy taxa in the Poaceae and Asteraceae families remain high at the end of Aguas Buenas, together with high charcoal influx suggesting that fire was used to clear more forest or maintain extensive agricultural fields leading up to the TCD.

Paleoecological and archaeological evidence indicates that the early part of the Chiriquí period and the Terminal Classic Drought was a time of transition at Laguna Santa Elena (Sánchez and Rojas 2002; Anchukaitis and Horn 2005; Kerr et al. forthcoming). Maize agriculture declined at the bottom of Zone 2b at ca. 1140 cal yr BP, coincident with a moderately wet phase, but then recovered to the second highest level in the Santa Elena record at ca. 1010 cal yr BP during a mild drying trend. Following this second peak, maize agriculture then declined again at ca. 995 cal yr BP as another wet interval began in the region.

Following amelioration of the TCD in the wider circum-Caribbean, southern Pacific Costa Rica experienced an interval of extremely wet hydroclimate centered on ca. 720 cal yr BP, coincident with a major decline in prehistoric populations and maize agriculture. Previous research tentatively associated this decline with Spanish arrival in the region at Santa Elena (Anchukaitis and Horn 2005) and nearby Laguna Zoncho (Clement and Horn 2001). Later research by Kerr et al. (forthcoming) at Santa Elena and Taylor et al. (2013) at Zoncho refined the timeline of agricultural decline, reporting that the declines in maize agriculture and population at both sites occurred a few centuries before Spanish expeditions inland. Both Kerr et

al. (forthcoming) and Taylor et al. (2013) speculated that the declines seen at both sites may have been due to early drying as the Little Ice Age began. Our new isotope data demonstrate that was not the case. Rather, population and maize agriculture declined at Santa Elena and Zoncho during a wet interval between the TCD and LIA. As at our Bonillita site in the Caribbean lowlands (Kerr et al. this dissertation), extremely wet conditions in southern Pacific Costa Rica may have been bad for maize agriculture. Contrary to the situation in much drier parts of Central America, some drying may have actually been good for prehistoric people living in southern Pacific Costa Rica.

The centuries following ca. 720 cal yr BP at Santa Elena saw a continued human presence and small-scale maize agriculture shown by continued charcoal influx and the presence of *Zea* pollen. However, the collapse at the site during the wet years between the TCD and the LIA ended significant prehistoric use of the Santa Elena watershed. The top of the sediment core then records the arrival of modern agriculture, with declining pollen percentages of forest taxa and increasing percentages of disturbance taxa, and increased *Zea* pollen.

4.6.3 Extreme Climate Events: the TCD and the LIA

The Terminal Classic Drought (ca. 1200–850 cal yr BP) manifested as a period of climate instability and unpredictability at Laguna Santa Elena, as seen at other sites in Costa Rica and nearby Panama (Horn and Sanford 1992; Horn 1993; Lachniet et al. 2004; Wu et al. 2017, 2019; Kerr et al. this dissertation) and through the circum-Caribbean (Hodell et al. 1995, 2005; Curtis et al. 1996; Haug et al. 2001, 2003; Peterson and Haug 2006; Webster et al. 2007; Medina Elizalde et al. 2010; Kennett et al. 2012; Luzzadder-Beach et al. 2012; Lane et al. 2014; Douglas et al. 2015). However, unlike at other sites, the TCD at Santa Elena was *not* a time of extreme

drought. Rather, the TCD at Santa Elena began wet at ca. 1200 cal yr BP, turned slightly dry ca. 1085–1035 cal yr BP, and then returned to wetter conditions ca. 940 cal yr BP.

The TCD was not a 350-year period of sustained drought in the circum-Caribbean, but rather a series of severe droughts that have been implicated in the collapse of Maya civilization on the Yucatan Peninsula far to the north of our Santa Elena site (Hodell et al. 2005; Kennett et al. 2012; Douglas et al. 2015). Our proxy data from the Santa Elena sediments confirm a similar pattern of variability and unpredictability at the local scale which likely resulted from fluctuations in the mean annual position of the Intertropical Convergence Zone and related reductions in rainfall, as demonstrated for Costa Rica, the Cariaco Basin, and the wider circum-Caribbean (Haug et al. 2001; Lane et al. 2011, 2014), but with further interactions between the ITCZ, ENSO variability, and the Central American Monsoon complicating matters. This matches patterns in paleohydrology seen at our other study sites, including Laguna Bonillita in the Caribbean lowlands and Lago de las Morrenas 1 in the Costa Rican highlands (Kerr et al. this dissertation). Importantly, though, hydroclimate conditions at Santa Elena never reached the level of drought reported from the Caribbean side of the Isthmus. Forest clearance, landscape disturbance, and prehistoric agriculture continued at Laguna Santa Elena during TCD drying, supporting our hypothesis that some drying is beneficial for maize agriculture in Costa Rica. In contrast to the Mayan Lowlands, populations in Costa Rica, Panama, and the Dominican Republic grew after 1150 cal yr BP near permanent water sources, suggesting different cultural responses to rainfall variability throughout the region (Lane et al. 2014).

Like the TCD, the effects of Little Ice Age are clearly visible in our reconstructed paleohydrology data from the Santa Elena sediments. Z-scores for δD_{PP} indicate a period of climate stability and average moisture conditions ca. 550–330 cal yr BP, followed by instability

punctuated by intervals of pronounced aridity lasting ca. 330 cal yr BP through the end of the LIA and into modern times. Again, like the TCD, this drying in the later part of the Little Ice Age at Santa Elena matches significant drying seen in other records from Costa Rica, Central America, and the wider circum-Caribbean (Curtis et al. 1996; Haug et al. 2001; Hodell et al. 2005; Peterson and Haug 2006; Black et al. 2007; Lane et al. 2011; Stansell et al. 2013; Taylor et al. 2013; Wu et al. 2019; Kerr et al. forthcoming). Population collapse and site abandonment preceded the LIA at Santa Elena and Laguna Zoncho in southern Pacific Costa Rica near Panama (Taylor et al. 2013; Kerr et al. forthcoming), but at sites farther to the north in the Diquís, including Lagunas Carse and Danta, the LIA was a period of renewed maize agriculture (Johanson et al. forthcoming), demonstrating that extreme climate events manifested differently at different times throughout the circum-Caribbean at both the regional and local scales. Laguna Santa Elena and nearby Zoncho were mostly abandoned by the time the Spanish arrived in the area and remained so through the end of the LIA until the establishment of modern agriculture in the 20th century. Ironically, it may have been an extremely wet period preceding the LIA that led to collapse and site abandonment rather than dry conditions hypothesized by extrapolating Caribbean climate onto the Pacific side of the high cordilleras.

4.7 Conclusions

Compound-specific stable hydrogen and carbon isotope analysis of terrestrial leaf waxes preserved in the Laguna Santa Elena sediment core provides an 1800-year history of hydrology that unambiguously reflects climate in southern Pacific Costa Rica and provides one of the first long records of precipitation reconstructed using lake sediments from the Pacific side of Central America. Our data show that the Santa Elena site experienced multiple episodes of significantly

wetter and significantly drier than average hydroclimate during the late Holocene, the timing of which match other records from Costa Rica, Central America, and the wider circum-Caribbean. The Terminal Classic Drought (ca. 1200–850 cal yr BP) and the Little Ice Age (ca. 550–100 cal yr BP) are both well-represented in the Santa Elena proxy record. Unlike at other sites, Santa Elena was not extremely dry during the Terminal Classic Drought and, in fact, experienced intervals of wetter than average conditions during the TCD. The LIA at Santa Elena began with ca. 170 years of average moisture conditions followed by ca. 220 years of unpredictable conditions marked by swings between wet and dry. Like at our Bonillita site, prehistoric settlement and maize agriculture may have benefitted from periods of drying at Santa Elena and declined during extremely wet periods. Overall, hydroclimate forcing in southern Pacific Costa Rica over the Late Holocene appears more complicated than previously thought. Fully understanding the causes and consequences of climate conditions and drivers on the Pacific side of the Isthmus will require more records from more sites.

4.8 Acknowledgements

Core recovery, radiocarbon dating, and previous pollen and charcoal analyses were funded by a grant from The A.W. Mellon Foundation to Sally Horn and Robert Sanford, Jr., and by a STAR Fellowship from the U.S. Environmental Protection Agency awarded to Kevin Anchukaitis. A 2013 field visit and our new results reported here were supported by the University of Tennessee, the Center for Marine Science and College of Arts and Sciences at the University of North Carolina Wilmington, NSF grant #1660185 awarded to Sally Horn, Chad Lane, and Doug Gamble, and by NSF grant #1657171 awarded to Horn and Kerr. We thank

Maureen Sánchez for sharing her knowledge on the archaeology of the Santa Elena site and surrounding area, and Paul Lemieux and Sarah Bleakney for laboratory assistance.

4.9 References

Alley RB and Clark PU (1999) The deglaciation of the Northern Hemisphere: a global perspective. *Annual Review of Earth and Planetary Sciences* 27: 149–182.

Anchukaitis KJ and Horn SP (2005) A 2000-year reconstruction of forest disturbance from southern Pacific Costa Rica. *Palaeogeography, Palaeoclimatology, Palaeoecology* 221: 35–54.

Anderson DG (1990) *Political change in chiefdom societies: cycling in the late prehistoric Southeastern United States*. PhD Thesis, University of Michigan, USA.

Anderson DG, Stahle DW and Cleaveland MK (1995) Paleoclimate and the potential food reserves of Mississippian societies. *American Antiquity* 60(2): 258–286.

Barrantes R (1993) Evolución en el Trópico: los Amerindios de Costa Rica y Panamá. Editorial de la Universidad de Costa Rica, San José.

Barrantes R, Smouse PE, Mohrenweiser HW, Gershowitz H, Azofeifa J, Arias TD and Neel JV (1990) Microevolution in lower Central America: genetic characterization of the Chibcha-speaking groups of Costa Rica and Panama, and consensus taxonomy based on genetic and linguistic affinity. *American Journal of Human Genetics* 46: 63–84.

Behling H (2000) A 2860-year high-resolution pollen and charcoal record from the Cordillera de Talamanca in Panama: a history of human and volcanic forest disturbance. *The Holocene* 10(3): 387–393.

Blaauw M (2019) clam: classical age-depth modeling of cores from deposits. R package version 2.3.2. Available at: https://CRAN.R-project.org/package=clam (accessed 23 January 2019).

Black DE, Abahazi MA, Thunell RC, Kaplan A, Tappa EJ and Peterson LC (2007) An 8-century tropical Atlantic SST record from the Cariaco Basin: baseline variability, twentieth-century warming, and Atlantic hurricane frequency. *Paleoceanography* 22: PA4204.

Bowen GJ (2019) The Online Isotopes in Precipitation Calculator. Version 3.1. Available at: http://www.waterisotopes.org (accessed 15 April 2016).

Bradbury JP (1982) Holocene chronostratigraphy of Mexico and Central America. *Striae* 16: 46–48.

Bray EE and Evans ED (1961) Distribution of *n*-paraffins as a clue to recognition of source beds. *Geochimica et Cosmochimica Acta* 22: 2–15.

Clement RM and Horn SP (2001) Pre-Columbian land-use history in Costa Rica: a 3000-year record of forest clearance, agriculture and fires from Laguna Zoncho. *The Holocene* 11(4): 419–426.

Cohen AS (2003) *Paleolimnology: The History and Evolution of Lake Systems*. Oxford: Oxford University Press.

Colinvaux P, De Oliveira PE and Moreno JE (1999) *Amazon Pollen Manual and Atlas*. Amsterdam: Hardwood Academic Publishers.

Constenla A (1991) Las Lenguas del Área Intermedia: Introducción a su Estudio Areal. Editorial de la Universidad de Costa Rica, San José.

Constenla A (1994) Las lenguas de la Gran Nicoya. *Vínculos* 18–19: 209–228.

Corrales F (1985) Prospección y excavaciones estratigráficas en al Sitio Curré (p-64-ce) Valle del Diquís, Costa Rica. *Vínculos* 11(1–2): 1–16.

Corrales F (1986) Prospección arqueológica en Potrero Grande. *Vínculos* 12(1–2): 21–38.

Corrales F (2000) *An evaluation of long-term cultural change in southern Central America: the ceramic record of the Diquís archaeological subregion, southern Costa Rica*. PhD Thesis, University of Kansas, USA.

Corrales F, Quintanilla I and Barrantes O (1988) *Historia Precolombina y de los Siglos XVI y XVII del Sureste de Costa Rica. Proyecto Investigación y Promoción de la Cultura Popular y Tradicional del Pacifico Sur*. San José: OEA/MCJD.

Cranwell PA, Eglinton G and Robinson N (1987) Lipids of aquatic organisms as potential contributors to lacustrine sediments—II. *Organic Geochemistry* 11(6): 513–527.

Curtis JH, Hodell DA and Brenner M (1996) Climate variability on the Yucatan Peninsula (Mexico) during the past 3500 years, and implications for Maya cultural evolution. *Quaternary Research* 46: 37–47.

Dansgaard W (1964) Stable isotopes in precipitation. *Tellus* 16(4): 436–468.

Dean WE (1974) Determination of carbonate and organic matter in calcareous sediments and sedimentary rocks by loss on ignition: comparison with other methods. *Journal of Sedimentary Petrology* 44(1): 242–248.

Douglas PMJ, Pagani M, Canuto MA, Brenner M, Hodell DA, Eglinton TI and Curtis JH (2015) Drought, agricultural adaptation, and sociopolitical collapse in the Maya Lowlands. *PNAS* 112(18): 5607–5612.

Drolet RP (1983) Social groupings and residential activities within a late phase polity network: Diquís Valley, southeastern Costa Rica. *Journal of the Steward Anthropological Society* 14(1–2): 325–338.

Drolet RP (1984) Community life in a late phase agricultural village, southeastern Costa Rica. In: Lange FW (ed) *Recent Developments in Isthmian Archaeology: Advances in the Prehistory of Lower Central America*. BAR International Series 212. Oxford: B.A.R., pp 123–152.

Drolet RP (1988) The emergence and intensification of complex societies in Pacific southern Costa Rica. In: Lange FW (ed) *Costa Rican Art and Archaeology: Essays in Honor of Frederick R. Mayer*. Boulder: University of Colorado, pp. 163–188.

Drolet RP (1992) The house and the territory: the organizational structure for chiefdom art in the Diquís subregion of greater Chiriquí. In: Lange FW (ed) *Wealth and Hierarchy in the Intermediate Area: a Symposium at Dumbarton Oaks 10th and 11th October 1987*. Washington DC: Dumbarton Oaks Research Library and Collection, pp. 207–241.

Eglinton G and Hamilton RJ (1963) The distribution of alkanes. In: Swain T (ed) *Chemical Plant Taxonomy*. London: Academic Press, pp. 187–217.

Eglinton G and Hamilton RJ (1967) Leaf epicuticular waxes. *Science* 156: 1322–1335.

Feakins SJ (2013) Pollen-corrected leaf wax D/H reconstructions of northeast African hydrological changes during the late Miocene. *Palaeogeography, Palaeoclimatology, Palaeoecology* 374: 62–71.

Feakins SJ, Peters T, Sin Wu M, Shenkin A, Salinas N, Girardin CAJ, Patrick Bentley L, Blonder B, Enquist BJ, Martin RE, Asner GP and Malhi Y (2016) Production of leaf wax *n*-alkanes across a tropica forest elevation transect. *Organic Geochemistry* 100: 89–100.

Fernández Guardia R (1913) *History of the Discovery and Conquest of Costa Rica* (translated by Harry Weston Van Dyke). New York: Thomas Crowell Company.

Ficken KJ, Li B, Swain DL and Eglinton G (2000) An *n*-alkane proxy for the sedimentary input of submerged/floating freshwater aquatic macrophytes. *Organic Geochemistry* 31: 745–749.

Galinat WC (1980) The archaeological maize remains from Volcán, Panama – a comparative perspective. In: Linares OF and Ranere AJ (eds) *Adaptive Radiations in Prehistoric Panama*. Peabody Museum Monographs 5. Cambridge: Harvard University, pp. 175–180.

Haberland W (1984) The archaeology of Greater Chiriqui. In: Lange FW and Stone DZ (eds) *The Archaeology of Lower Central America*. Albuquerque: University of New Mexico Press, pp. 233–262.

Hall C (1985) *Costa Rica: A Geographical Interpretation in Historical Perspective*. Boulder: Westview Press.

Han J, McCarthy ED, van Hoeven W, Calvin M and Bradley WH (1968) Organic geochemical studies, II. A preliminary report on the distribution of aliphatic hydrocarbons in algae, in bacteria, and in a recent lake sediment. *PNAS* 59: 29–33.

Hartshorn GS (1983) Plants. In: Janzen DH (ed) *Costa Rican Natural History*. Chicago: University of Chicago Press, pp. 118–350.

Hastenrath S (2002) The Intertropical Convergence Zone of the eastern Pacific revisited. *International Journal of Climatology* 22: 347–356.

Haug GH, Günther D, Peterson LC, Sigman DM, Hughen KA and Aeschlimann B (2003) Climate and the collapse of Maya civilization. *Science* 299: 1731–1735.

Haug GH, Hughen KA, Sigman DM, Peterson LC and Röhl U (2001) Southward migration of the Intertropical Convergence Zone through the Holocene. *Science* 293: 1304–1308.

Herrera W (1985) *Clima de Costa Rica*. Editorial de Universidad Nacional Estatal a Distancia, San Jose, Costa Rica.

Hodell DA, Brenner M, Curtis JH, Medina-González R, Ildefonso-Chan Can E, Albornaz-Pat A and Guilderson TP (2005) Climate change on the Yucatan Peninsula during the Little Ice Age. *Quaternary Research* 63: 109–121.

Hodell DA, Curtis JH and Brenner M (1995) Possible role of climate in the collapse of Classic Maya civilization. *Nature* 375: 391–394.

Holdridge LR (1967) *Life Zone Ecology*. San José: Tropical Science Center.

Hoopes JW (1991) The Isthmian alternative: reconstructing patterns of social organization in formative Costa Rica. In: Fowler WR Jr (ed) *The Formation of Complex Society in Southeastern Mesoamerica*. Boca Raton: CRC Press, pp. 171–192.

Hoopes JW (1996) Settlement, subsistence, and the origins of social complexity in Greater Chiriquí: a reappraisal of the Aguas Buenas tradition. In: Lange FW (ed) *Paths to Central American Prehistory*. Niwot: University Press of Colorado, pp. 15–47.

Horn SP (1993) Postglacial vegetation and fire history in the Chirripó Páramo of Costa Rica. *Quaternary Research* 40: 107–116.

Horn SP (2006) Pre-Columbian maize agriculture in Costa Rica: pollen and other evidence from lake and swamp sediments. In: Staller JE, Tykot RH and Benz BF (eds) *Histories of Maize: Multidisciplinary Approaches to the Prehistory, Linguistics, Biogeography, Domestication, and Evolution of Maize*. Amsterdam: Elsevier, pp. 367–380.

Horn SP (2007) Late Quaternary lake and swamp sediments: recorders of climate change and environment. In: Bundschuh J and Alvarado GE (eds) *Central America: Geology, Resources and Hazards*, Volume 1. London: Taylor and Francis, pp. 427–445.

Horn SP and Haberyan KA (2016) Lakes of Costa Rica. In: Kappelle M (ed) *Costa Rican Ecosystems*. Chicago: University of Chicago Press, pp. 656–682.

Horn SP and Sanford RL (1992) Holocene fires in Costa Rica. *Biotropica* 24(3): 354–361.

Huang Y, Shuman B, Wang Y and Webb T III (2004) Hydrogen isotope ratios of individual lipids in lake sediments as novel tracers of climatic and environmental change: a surface sediment test. *Journal of Paleolimnology* 31: 363–375.

Iltis HH (2000) Homeotic sexual translocations and the origin of maize (*Zea mays*, Poaceae): a new look at an old problem. *Economic Botany* 54(1): 7–42.

Iltis HH and Benz BF (2000) *Zea nicaraguensis* (Poaceae), a new teosinte from Pacific coastal Nicaragua. *Novon* 10(4): 382–390.

Johanson EJ, Horn SP and Lane CS (forthcoming) Pre-Columbian agriculture, fire, and Spanish contact: a 4200-year record from Laguna Los Mangos, Costa Rica. *The Holocene*.

Juggins S (2007) C2: software for ecological and palaeoecological data analysis and visualization (user guide version 1.5). Newcastle upon Tyne: Newcastle University, UK.

Kahmen A, Hoffmann B, Schefuß E, Arndt SK, Cernusak LA, West JB and Sachse D (2013a) Leaf water deuterium enrichment shapes leaf wax *n*-alkane δD values of angiosperm plants II: observational evidence and global implications. *Geochimica et Cosmochimica Acta* 111: 50–63.

Kahmen A, Schefuß E and Sachse D (2013b) Leaf water deuterium enrichment shapes leaf wax *n*-alkane δD values of angiosperm plants I: experimental evidence and mechanistic insights. *Geochimica et Cosmochimica Acta* 111: 39–49.

Kennett DJ, Breitenbach SFM, Aquino VV, Asmerom Y, Awe J, Baldini JUL, Bartlein P, Culleton BJ, Evert C, Jazwa C, Macri MJ, Marwan N, Polyak V, Prufer KM, Ridley HE, Sodemann H, Winterhalder B and Haug GH (2012) Development and disintegration of Maya political systems in response to climate change. *Science* 338: 788–791.

Kerr MT (2014) *Stable isotope analysis of lake sediments from Laguna Santa Elena and Laguna Azul, Costa Rica*. MS Thesis, University of Tennessee Knoxville, USA.

Kerr MT, Horn SP and Lane CS (forthcoming) Stable isotope analysis of vegetation history and land-use change at Laguna Santa Elena in southern Pacific Costa Rica. *Vegetation History and Archaeobotany*.

Knight JR, Allan RJ, Folland CK, Vellinga M and Mann ME (2005) A signature of persistent natural thermohaline circulation cycles in observed climate. *Geophysical Research Letters* 32: L20708.

Lachniet MS and Patterson WP (2002) Stable isotope values of Costa Rican surface waters. *Journal of Hydrology* 260: 135–150.

Lachniet MS, Burns SJ, Piperno DR, Asmerom Y, Polyak VJ, Moy CM and Christenson K (2004) A 1500-year El Niño/Southern Oscillation and rainfall history for the Isthmus of Panama from speleothem calcite. *Journal of Geophysical Research* 109: D20117.

Lachniet MS, Patterson WP, Burns S, Asmerom Y and Polyak V (2007) Caribbean and Pacific moisture sources on the Isthmus of Panama revealed from stalagmite and surface water $\delta^{18}O$ gradients. *Geophysical Research Letters* 34: L01708.

Lane CS (2017) Modern *n*-alkane abundances and isotopic composition of vegetation in a gymnosperm-dominated ecosystem of the southeastern U.S. coastal plain. *Organic Geochemistry* 105: 33–36.

Lane CS, Horn SP and Kerr MT (2014) Beyond the Mayan Lowlands: impacts of the Terminal Classic Drought in the Caribbean Antilles. *Quaternary Science Reviews* 86: 89–98.

Lane CS, Horn SP, Orvis KH and Thomason JM (2011) Oxygen isotope evidence of Little Ice Age aridity on the Caribbean slope of the Cordillera Central, Dominican Republic. *Quaternary Research* 75: 461–470.

Lane CS, Horn SP, Taylor ZP and Kerr MT (2016) Correlation of bulk sedimentary and compound-specific $\delta^{13}C$ values indicates minimal pre-aging of *n*-alkanes in a small tropical watershed. *Quaternary Science Reviews* 145: 238–242.

Lange FW (1992) The intermediate area: an introductory overview of wealth and hierarchy issues. In: Lange FW (ed) *Wealth and Hierarchy in the Intermediate Area: a Symposium at*

Dumbarton Oaks 10th and 11th October 1987. Washington DC: Dumbarton Oaks Research Library and Collection, pp. 1–14.

Lange FW (1993) The conceptual structure in lower Central American studies: a Central American view. In: Graham MM (ed) *Reinterpreting Prehistory of Central America*. Niwot: University Press of Colorado, pp. 277–324.

Leon M (1986) Análisis functional de sitios arqueológicos en La Zona Protectora Las Tablas, sur-este de Costa Rica. *Vínculos* 12(1–2), 83–120.

Linares OF and Sheets PD (1980) Highland agricultural villages in the Volcán Barú region. In: Linares OF and Ranere AJ (eds) *Adaptive Radiations in Prehistoric Panama*. Peabody Museum Monographs 5. Cambridge: Harvard University, pp. 44–55.

Linares OF, Sheets PD and Rosenthal EJ (1975) Prehistoric agriculture in tropical highlands. *Science* 187:137–145.

Liu W and Huang Y (2005) Compound specific *D*/*H* ratios and molecular distributions of higher plant leaf waxes as novel paleoenvironmental indicators in the Chinese Loess Plateau. *Organic Geochemistry* 26: 851–860.

Luzzadder-Beach S, Beach TP and Dunning NP (2012) Wetland fields as mirrors of drought and the Maya abandonment. *PNAS* 109(10): 3646–3651.

Marzi R, Torkelson BE and Olson RK (1993) A revised carbon preference index. *Organic Geochemistry* 20(8): 1303–1306.

Medina-Elizalde M, Burns SJ, Lea DW, Asmerom Y, von Gunten L, Polyak V, Vuille M and Karmalkar A (2010) High resolution stalagmite climate record from the Yucatán Peninsula spanning the Maya terminal classic period. *Earth and Planetary Science Letters* 298: 255–262.

Meyers PA (2003) Applications of organic geochemistry to paleolimnological reconstructions: a summary of examples from the Laurentian Great Lakes. *Organic Geochemistry* 34: 261–289.

Palumbo SD (2009) *The development of complex society in the Volcán Barú region of western Panama*. PhD Thesis, University of Pittsburgh, USA.

Peterson LC and Haug GH (2006) Variability in the mean latitude of the Atlantic Intertropical Convergence Zone as recorded by riverine input of sediments to the Cariaco Basin (Venezuela). *Palaeogeography, Palaeoclimatology, Palaeoecology* 234: 97–113.

Polissar PJ and D'Andrea WJ (2014) Uncertainty in paleohydrologic reconstructions from molecular δ*D* values. *Geochimica et Cosmochimica Acta* 129: 146–156.

Polissar PJ and Freeman KH (2010) Effects of aridity and vegetation on plant-wax δD in modern lake sediments. *Geochimica et Cosmochimica Acta* 74: 5785–5797.

Poveda G, Waylen PR and Pulwarty RS (2006) Annual and inter-annual variability of the present climate in northern South America and southern Mesoamerica. *Palaeogeography, Palaeoclimatology, Palaeoecology* 234: 3–27.

Poynter J and Eglinton G (1990) Molecular composition of three sediments from Hole 717C: the Bengal Fan. *Proceedings of the Ocean Drilling Program, Scientific Results* 116: 155–161.

Poynter JG, Farrimond P, Robinson N and Eglinton (1989) Aeolian-derived higher plant lipids in the marine sedimentary record: links with palaeoclimate. In: Leinen M and Sarnthein M (eds) *Paleoclimatology and Paleometerology: Modern and Past Patterns of Global Atmospheric Transport*. Dordrecht: Kluwer Academic Publishers, pp. 435–462.

Ranere AJ (1980) Preceramic shelters in the Talamancan Range. In: Linares OF and Ranere AJ (eds) *Adaptive Radiations in Prehistoric Panama*. Peabody Museum Monographs 5. Cambridge: Harvard University, pp. 16–43.

Quintanilla I (1990) *Ocupaciones precolumbinas en el bosque tropical lluvioso: evaluación arqueológica de la Estación Biológica La Selva*. Unpublished report on file at the La Selva Biological Station, Puerto Viejo de Sarapiquí, Costa Rica.

R Core Team (2019) R: a language and environment for statistical computing. R Foundation for Statistical Computing, Vienna. Available at: https://www.r-project.org (accessed 23 January 2019).

Reimer PJ, Bard E, Bayliss A, Beck JW, Blackwell PG, Ramsey CB, Buck CE, Cheng H, Edwards RL, Friedrich M, Grootes PM, Guilderson TP, Haflidason H, Hajdas I, Hatté C, Heaton TJ, Hoffmann DL, Hogg AG, Hughen KA, Kaiser KF, Kromer B, Manning SW, Niu M, Reimer RW, Richards DA, Scott EM, Southon JR, Staff RA, Turney CSM and van der Plicht J (2013) IntCal13 and Marine13 radiocarbon age calibration curves 0-50,000 years cal BP. *Radiocarbon* 55(4): 1869–1887.

Sachse D and Gleixner G (2004) Hydrogen isotope ratios of recent lacustrine sedimentary *n*-alkanes record modern climate variability. *Geochimica et Cosmochimica Acta* 68(23): 4877–4889.

Sachse D, Billault I, Bowen GJ, Chikaraishi Y, Dawson TE, Feakins SJ, Freeman KH, Magill CR, McInerney FA, van der Meer MTJ, Polissar P, Robins RJ, Sachs JP, Schmidt H-L, Sessions AL, White JWC, West JB and Kahmen A (2012) Molecular paleohydrology: interpreting the hydrogen-isotopic composition of lipid biomarkers from photosynthesizing organisms. *Annual Review of Earth and Planetary Sciences* 40: 221–249.

Sachse D, Gleixner G, Wilkes H and Kahmen A (2010) Leaf wax *n*-alkane δD values of field-grown barley reflect leaf water δD values at the time of leaf formation. *Geochimica et Cosmochimica Acta* 74: 6741–6750.

Sachse D, Radke J and Gleixner G (2006) *δ*D values of individual *n*-alkanes from terrestrial plants along a climate gradient – implications for the sedimentary biomarker record. *Organic Geochemistry* 37: 469–483.

Sánchez M and Rojas P (2002) Asentamientos humanos antiguos en las tierras intermedias del Cantón de Coto Brus. *Cuadernos de Antropología* 12: 87–106.

Sheets PD (1980) The Volcán Barú region: a site survey. In: Linares OF and Ranere AJ (eds) *Adaptive Radiations in Prehistoric Panama*. Peabody Museum Monographs. Cambridge: Harvard University, pp. 267–275.

Sheets PD (1992) The pervasive pejorative in Intermediate Area studies. In: Lange FW (ed) *Wealth and Hierarchy in the Intermediate Area*. Washington DC: Dumbarton Oaks, pp. 15–41.

Sheets PD (2001) The effects of explosive volcanism on simple to complex societies in ancient Middle America. In: Markgraf V (ed) *Interhemispheric Climate Linkages*. San Diego: Academic Press, pp. 73–86.

Smalley J and Blake M (2003) Sweet beginnings: stalk sugar and the domestication of maize. *Current Anthropology* 44(5): 675–703.

Smith CE (1980) Plant remains from the Chiriquí sites and ancient vegetational patterns. In: Linares OF and Ranere AJ (eds) *Adaptive Radiations in Prehistoric Panama*. Peabody Museum Monographs 5. Cambridge: Harvard University, pp. 151–174.

Snarskis MJ (1981) The archaeology of Costa Rica. In: Benson EP (ed) *Between Continents/Between Seas: Precolumbian Art of Costa Rica*. New York: Harry N Abrams, pp. 15–84.

Stansell ND, Steinman BA, Abbott MB, Rubinov M and Roman-Lacayo M (2013) Lacustrine stable isotope record of precipitation changes in Nicaragua during the Little Ice Age and the Medieval Climate Anomaly. *Geology* 41(2): 151–154.

Stuiver M (1970) Oxygen and carbon isotope ratios of fresh-water carbonates as climatic indicators. *Journal of Geophysical Research* 75(27): 5247–5257.

Taylor ZP, Horn SP and Finkelstein DB (2013) Pre-Hispanic agricultural decline prior to the Spanish Conquest in southern Central America. *Quaternary Science Reviews* 73: 196–200.

Wahl D, Byrne R and Anderson L (2014) An 8700 year paleoclimate reconstruction from the southern Maya lowlands. *Quaternary Science Reviews* 103: 19–25.

Webster JW, Brook GA, Railsback LB, Cheng H, Edwards RL, Alexander C and Reeder PP (2007) Stalagmite evidence from Belize indicating significant droughts at the time of the Preclassic Abandonment, the Maya Hiatus, and the Classic Maya collapse. *Palaeogeography, Palaeoclimatology, Palaeoecology* 250: 1–17.

Wu J, Porinchu DF and Horn SP (2017) A chironomid-based reconstruction of late-Holocene climate and environmental change for southern Pacific Costa Rica. *The Holocene* 27(1): 73–84.

Wu J, Porinchu DF and Horn SP (2019) Late Holocene hydroclimate variability in Costa Rica: signature of the Terminal Classic Drought and the Medieval Climate Anomaly in the northern tropical Americas. *Quaternary Science Reviews* 215: 144–159.

Xia Z-H, Xu B-Q, Mügler I, Wu G-J, Gleixner G, Sachse D and Zhu L-P (2008) Hydrogen isotope ratios of terrigenous *n*-alkanes in lacustrine surface sediment of the Tibetan Plateau record the precipitation signal. *Geochemical Journal* 42: 331–338.

X.10 Appendix

Table 4.1. Greater Chiriquí cultural chronology. Following Corrales (2000) and others.

Period	Dates (BP)	Key cultural features and developments
Chiriquí	1150–450	• Consolidated regional centers in lowland alluvial areas near major rivers (Linares et al. 1975; Sheets 1980; Snarskis 1981; Drolet 1983, 1984, 1988, 1992) • Major changes in material culture and social organization, influx of culture or people from South America (Snarskis 1981) • Distinct, more elaborate ceramics (Drolet 1992) • Metallurgy flourishes (Snarskis 1981; Drolet 1992) • Larger, more complex sites (Corrales et al. 1988; Drolet 1992) • Increased importance of maize (Corrales et al. 1988) • Hierarchical organization and ranked societies, chiefdom-level organization (Corrales et al. 1988; Drolet 1988, 1992) • Lavish burials in cemeteries, gold artifacts (Snarskis 1981) • Warfare, palisaded villages (Corrales 2000)
Aguas Buenas	2250–1150	• Sites on mid- to high elevation terraces near secondary rivers, small streams, and lakes (Linares and Sheets 1980; Snarskis 1981; Drolet 1992) • Dispersed hamlets of 5–8 houses (Drolet 1992) • Large ceremonial centers with mounds, terraces, or platforms, e.g., Barriles in Panama and Bolas in Diquís (Snarskis 1981) • First archaeological evidence of maize (Galinat 1980; Smith 1980; Drolet 1992) • Maize and bean farming + gathered wild resources, hunting, fishing (Linares and Sheets 1980; Drolet 1988, Corrales 2000) • Stone grinding tools for maize or manioc (Haberland 1984) • Ceremonial metates, some lapidary work (Snarskis 1981) • Ritual burials beneath dwellings, few cemeteries (Snarskis 1981) • Early social stratification and warfare (Linares et al. 1975)
Sinancrá	3450–2250	• Arrival of ceramic technology (Corrales 2000) • Transition to sedentary agriculture (Corrales 2000) • Adoption of maize seen in lake sediments (Clement and Horn 2001; Horn 2006; Johanson et al. forthcoming) • Role of maize unclear (Hoopes 1991, 1996)
Archaic	4250–3450	• Not well-represented in archaeology • Stone grinding implements (Corrales 2000) • Early horticulture based on tubers, fruits, and seeds with limited forest alteration (Ranere 1980) • Preceramic, pre-maize(?)[a]

[a] Timing of the introduction of maize in the Diquís is debated (Anchukaitis and Horn 2005).

Table 4.2. Radiocarbon determinations for the Laguna Santa Elena sediment core.[a]

Lab Number[b]	Material Dated	Depth (cm)	$\delta^{13}C$ (‰)	Uncalibrated ^{14}C Age (^{14}C yr BP)	±2σ Age Range (cal yr BP)	Probability
Beta-158436	wood	156.5	–28.1	150 ±40	42–(–1)	16.6
					154–59	32.3
					234–167	28.7
					284–236	17.2
OS-138420	plant material	261.5	–25.2	205 ±15	12–0	18.6
					187–149	49.9
					297–270	26.4
Beta-150706	plant material	312.0	–26.3	640 ±60	677–539	95.0
Beta-145347	plant material	434.5	–14.5	1240 ±40	1270–1070	95.0
Beta-145348	charcoal	530.5	–25.5	1510 ±40	1424–1315	66.1
					1443–1429	3.3
					1521–1455	25.4
Beta-141242	wood	580.5	–30.6	1880 ±30	1883–1730	95.0
Beta-141243	wood	682.5	–27.9	1950 ±30	1950–1825	91.6
					1970–1960	2.6
					1983–1980	0.8

[a] Dates calibrated using the 'clam' package (v. 2.3.2; Blaauw 2019) for the R Statistical Environment (v. 3.5.3; R Core Team 2019) and the IntCal13 radiocarbon calibration curve (Reimer et al. 2013).

[b] Analyses were performed by Beta Analytic, Inc. (Beta #) and the National Ocean Sciences Accelerator Mass Spectrometry Lab (OS #).

Table 4.3. Plant taxa represented in the Santa Elena pollen assemblages. Categorized by most likely life form at our research site.[a]

Taxon[b]	Life Form Category[c]
Anacardiaceae	Angiosperm tree + shrub
Araliaceae	Angiosperm tree + shrub
Arecaceae	Angiosperm tree + shrub
Begoniaceae	Angiosperm tree + shrub
Bignoniaceae	Angiosperm tree + shrub
Elaeocarpaceae	Angiosperm tree + shrub
Ericaceae	Angiosperm tree + shrub
Malpighiaceae	Angiosperm tree + shrub
Melastomataceae/Combretaceae	Angiosperm tree + shrub
Myrtaceae	Angiosperm tree + shrub
Rhamnaceae	Angiosperm tree + shrub
Sapindaceae	Angiosperm tree + shrub
Sapotaceae/Meliaceae	Angiosperm tree + shrub
Tiliaceae	Angiosperm tree + shrub
Urticales (di- + triporate)	Angiosperm tree + shrub
Vochysiaceae	Angiosperm tree + shrub
Acalypha	Angiosperm tree + shrub
Alchornea	Angiosperm tree + shrub
Alfaroa	Angiosperm tree + shrub
Alnus	Angiosperm tree + shrub
Bocconia	Angiosperm tree + shrub
Bursera	Angiosperm tree + shrub
Cecropia	Angiosperm tree + shrub
Celtis	Angiosperm tree + shrub
Ficus	Angiosperm tree + shrub
Hedyosmum	Angiosperm tree + shrub
Ilex	Angiosperm tree + shrub
Myrica	Angiosperm tree + shrub
Myrsine	Angiosperm tree + shrub
Piper	Angiosperm tree + shrub
Quercus	Angiosperm tree + shrub
Sapium	Angiosperm tree + shrub
Tournefortia	Angiosperm tree + shrub
Trema	Angiosperm tree + shrub
Ulmus	Angiosperm tree + shrub
Weinmannia	Angiosperm tree + shrub
Zanthoxylum	Angiosperm tree + shrub
Alismataceae	Forb
Amaranthaceae	Forb
Apiaceae	Forb
Asteraceae	Forb

Table 4.3. Continued.

Taxon	Life Form Category
Lamiaceae	Forb
Rubiaceae	Forb
Scrophulariaceae	Forb
Solanaceae	Forb
Chamaesyce	Forb
Cyperaceae	Graminoid
Poaceae	Graminoid
Zea mays subsp. *mays*	Graminoid
Prumnopitys (formerly *Podocarpus*)	Gymnosperm
Mono- and trilete fern spores	Pteridophytes

[a] Pollen identification and taxonomy follows Anchukaitis and Horn (2005). We excluded indeterminate pollen grains and spores and taxa that could not be readily classified.

[b] In many cases, pollen can only be identified to the family level or to the order for some pollen types in the Urticales group.

[c] Many taxa listed include species with more than one life form. Here we categorize plants into the life forms that are most likely represented at the Laguna Santa Elena site. We combined angiosperm trees and shrubs because many taxa in the list are found as both in forests of the Pacific slope in southern Costa Rica.

Table 4.4. Global average apparent fractionation factors (ε) for Santa Elena. Fractionation between plants and meteoric water for $C_{27–31}$ odd *n*-alkanes. Compiled from the supplementary data in Sachse et al. (2012).

Plant Type	C_{27}	C_{29}	C_{31}
Gymnosperms	–112‰	–110‰	–103‰
Angiosperm trees and shrubs	–107‰	–111‰	–107‰
C_3 Graminoids	–127‰	–149‰	–157‰
C_4 Graminoids	–131‰	–132‰	–136‰
Forbs	–124‰	–128‰	–130‰
Pteridophytes	–103‰	–108‰	–114‰

Table 4.5. Expected δD values for modern precipitation at Santa Elena. Location: 8.9290 °N, 82.9257 °W, 1055 m elevation. From the Online Isotopes in Precipitation Calculator (OIPC v.3.1; Bowen 2019).

	Jan	Feb	Mar	Apr	May	Jun	Jul	Aug	Sep	Oct	Nov	Dec	Year
δD (‰)	–23	–23	–21	–32	–49	–67	–44	–54	–53	–55	–47	–36	–57

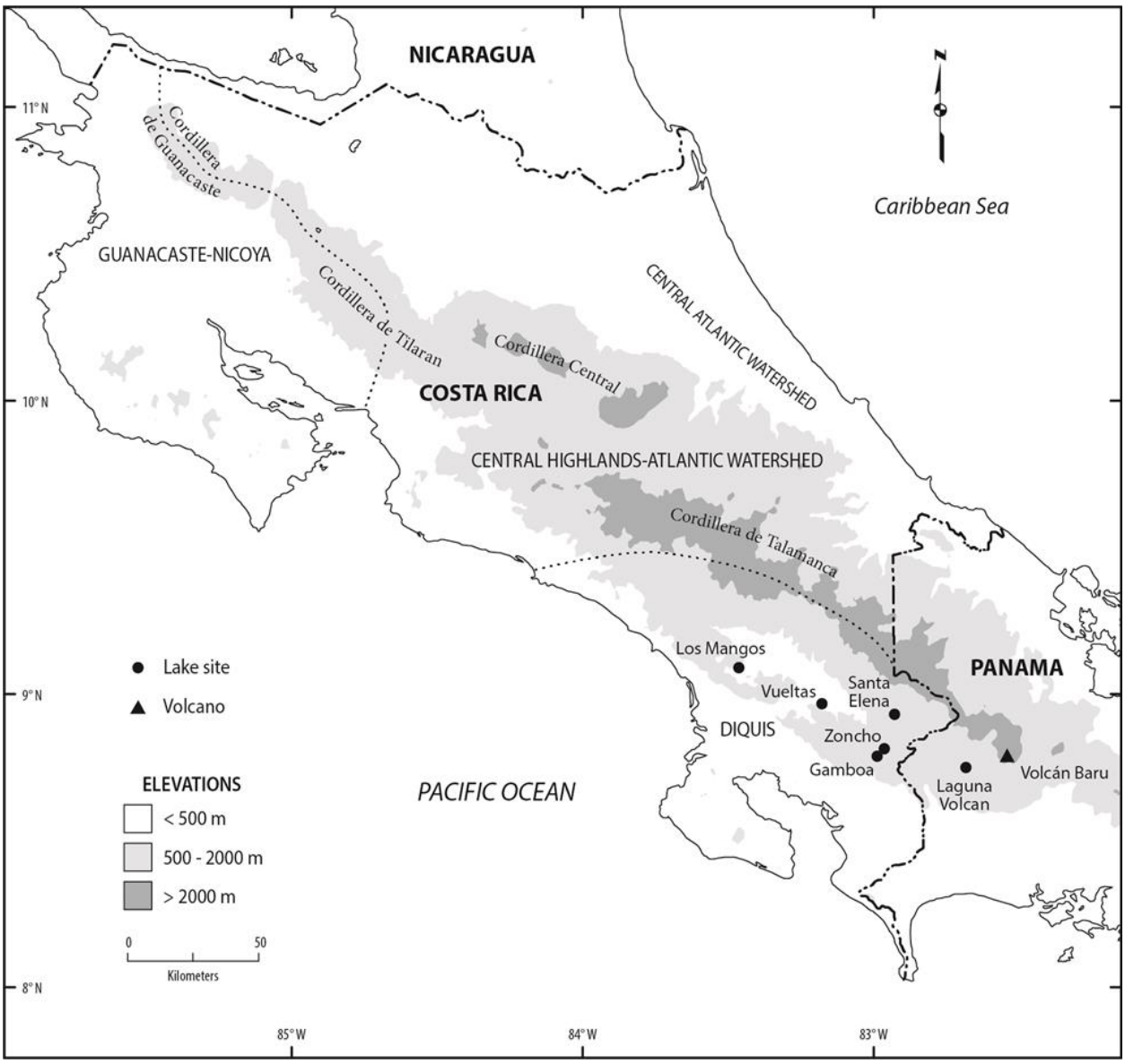

Fig. 4.1. Location of Laguna Santa Elena. Includes other sites in Costa Rica and Panama mentioned in the text. Archaeological region boundaries follow Snarskis (1981). Map modified from Fig. 27-1 in Horn (2006).

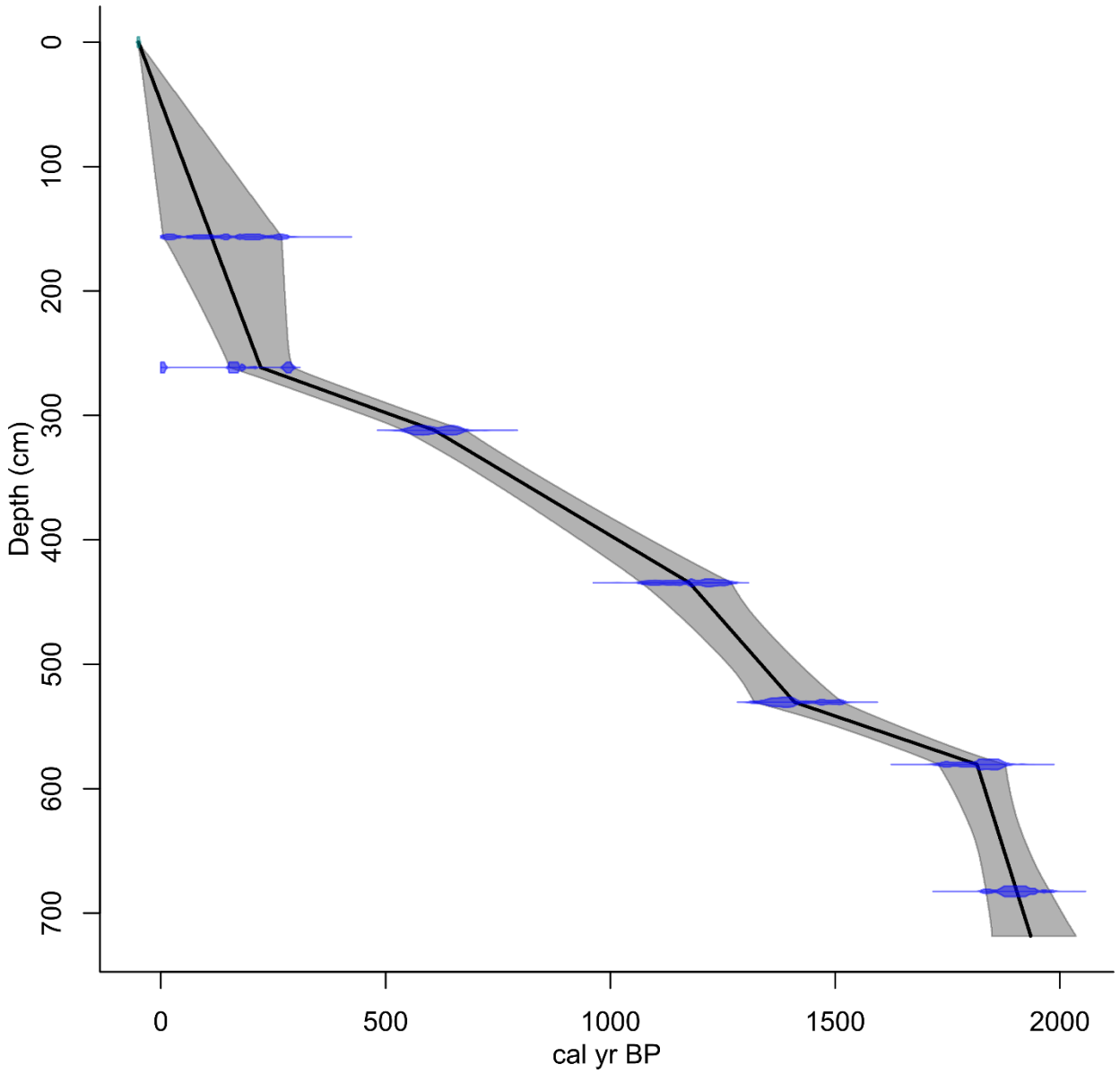

Fig. 4.2. Age-depth model for Laguna Santa Elena. Blue marks represent the ^{14}C probability distributions of the dates. Black line is the best fit model. Gray shading is the 95% confidence interval. Model was created using linear interpolation with the 'clam' package (Blaauw 2019) for the R Statistical Environment (R Core Team 2019) and the IntCal13 radiocarbon calibration curve (Reimer et al. 2013).

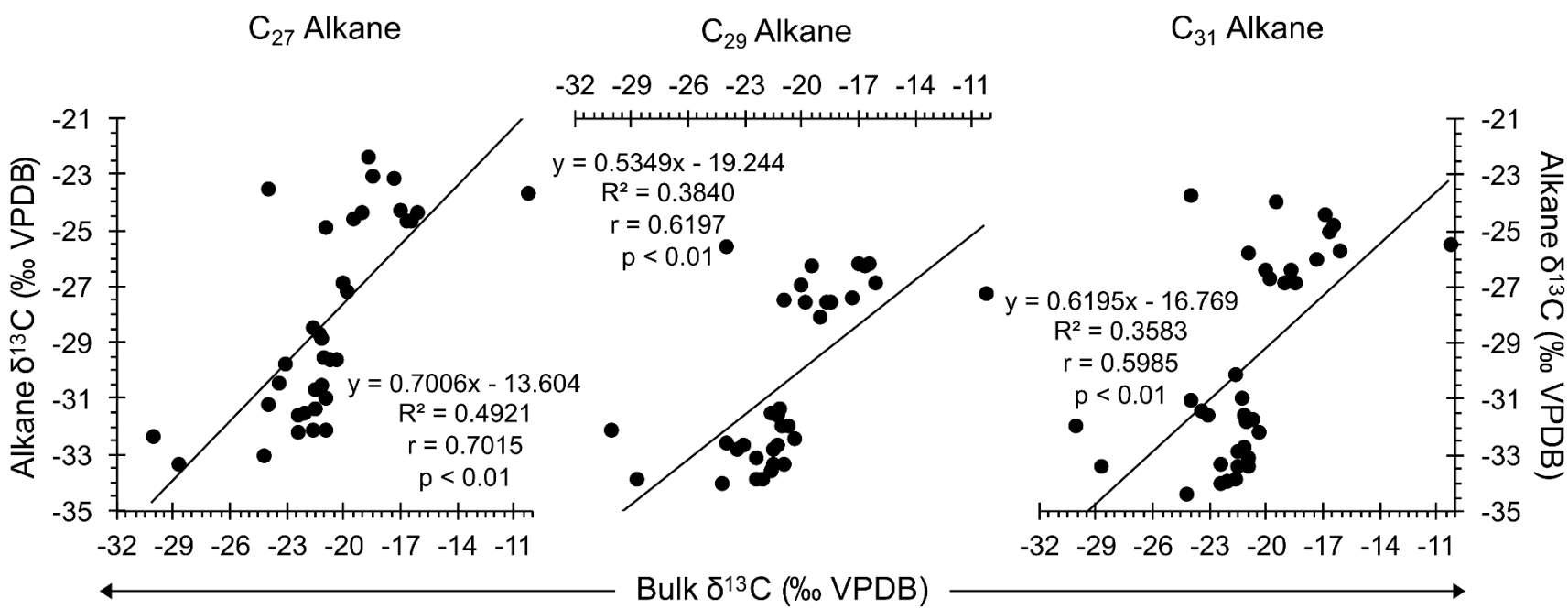

Fig. 4.3. Regression analyses of stratigraphically coeval bulk $\delta^{13}C$ and *n*-alkane $\delta^{13}C$.

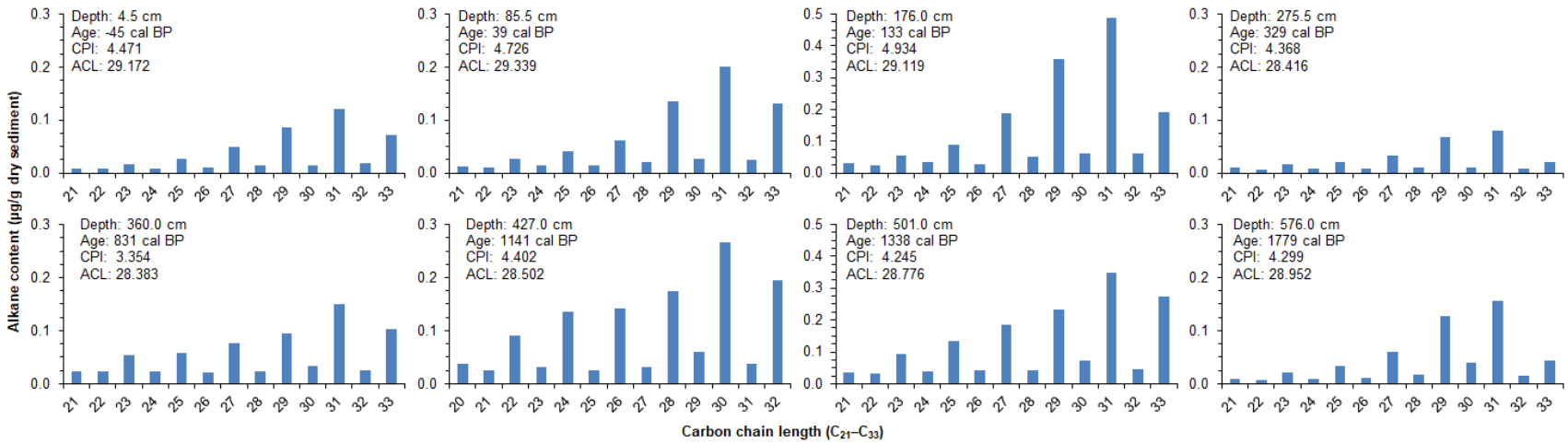

Fig. 4.4. Alkane distributions, CPI, and ACL for selected samples. Note changes in scale on the y-axes.

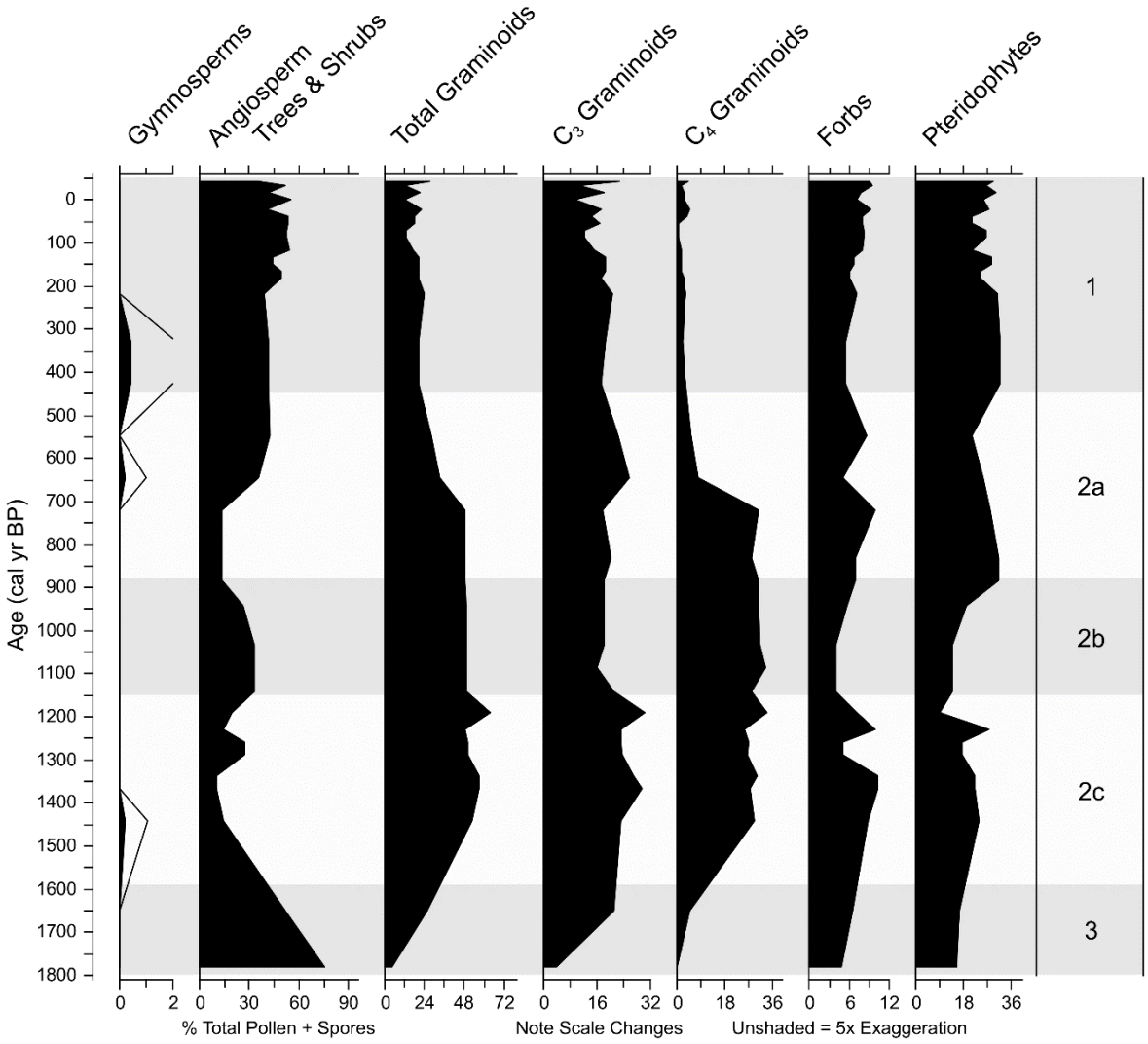

Fig. 4.5. Plants represented in the Santa Elena pollen record. Categorized by taxonomy and life form following Feakins (2013). Percentages for gymnosperms, angiosperm trees and shrubs, total graminoids, forbs (non-graminoid herbaceous taxa), and pteridophytes are calculated based on a sum of pollen and spore counts for all included taxa. Percentages for C_3 and C_4 graminoids are calculated from total graminoids using a two-endmember mixing model (see text) representing an average of $C_{27–31}$ odd numbered *n*-alkane homologues. Zones are informally delineated based on changes in proxy data following Anchukaitis and Horn (2005) and Kerr et al. (forthcoming).

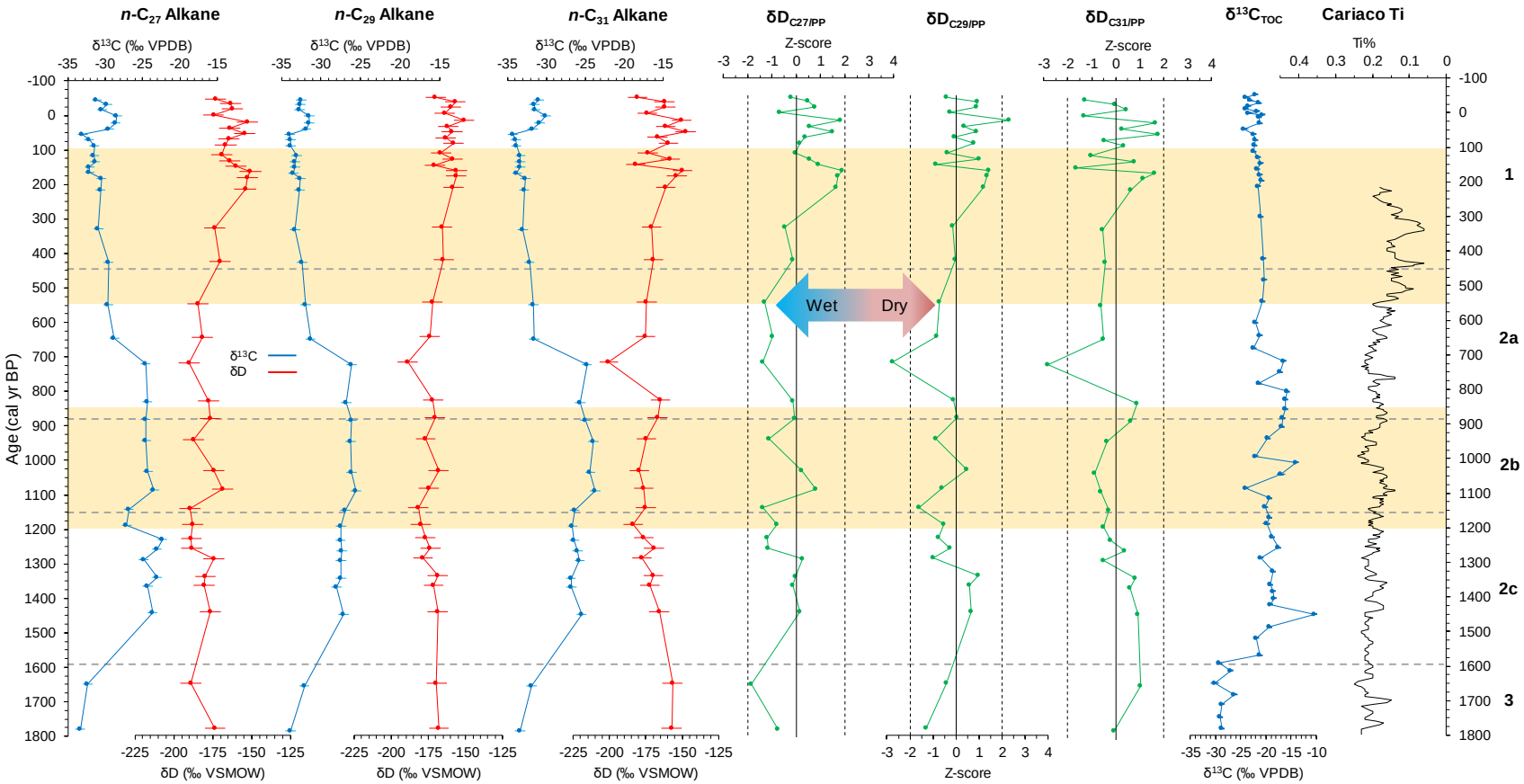

Fig. 4.6. Santa Elena isotope data. Includes leaf wax δD and $\delta^{13}C$ data and z-scores for δD_{PP} for odd numbered *n*-alkanes $C_{27–31}$. Bulk $\delta^{13}C_{TOC}$ data are from Kerr et al. (forthcoming). Cariaco basin titanium values are from the dataset tuned by Kennett et al. (2012). Note scale changes on the x-axes. Zones shown by horizontal gray dashed lines follow the informal zonation delineated by Anchukaitis and Horn (2005) and Kerr et al. (forthcoming) based on changes in the proxy data, as labeled at right. The upper shaded band covers the interval of the Little Ice Age (ca. 550–100 cal yr BP) and the lower shaded band covers the Terminal Classic Drought (ca. 1200–850 cal yr BP). VPDB = Vienna Pee Dee Belemnite. VSMOW = Vienna Standard Mean Ocean Water.

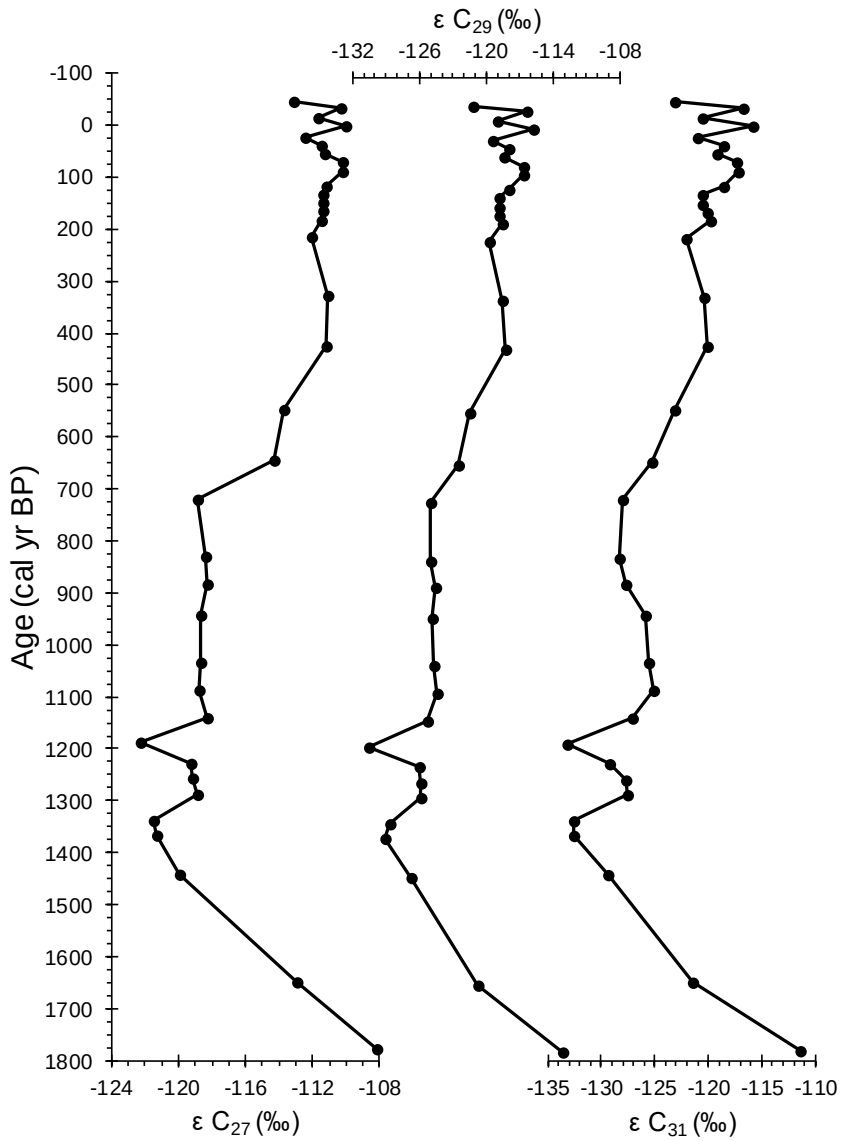

Fig. 4.7. Fractionation factors (ε) between plants and precipitation. Note changes in scale on the x-axes.

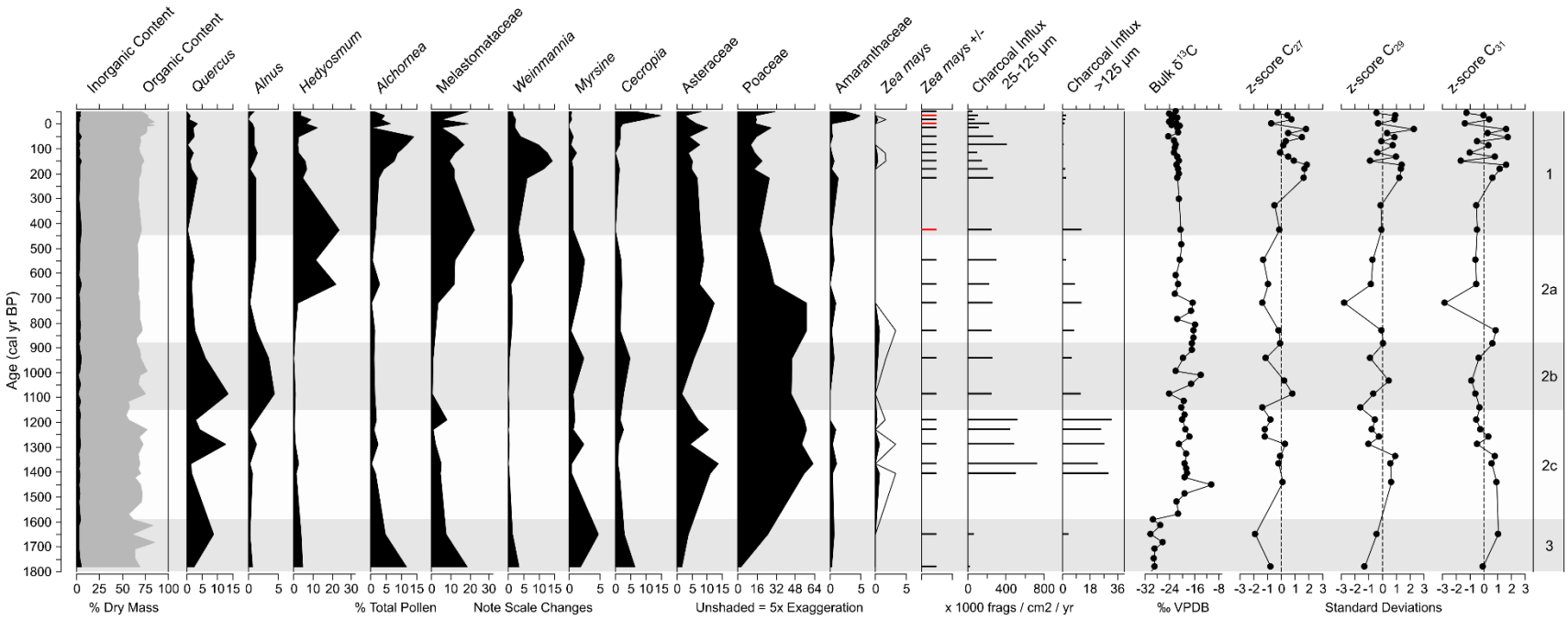

Fig. 4.8. Select proxy data for Laguna Santa Elena. Includes sediment composition (black curve = % carbonate) from Kerr et al. (forthcoming), select pollen data, microscopic and macroscopic charcoal influx from Anchukaitis and Horn (2005), bulk $\delta^{13}C$ data from Kerr et al. (forthcoming), and z-scores for δD_{PP} for odd numbered *n*-alkanes C_{27-31} (this study) for Laguna Santa Elena. Red lines in the *Zea mays* +/- column represent the absence of maize pollen at three sampled levels. Note scale changes. VPDB = Vienna Pee Dee Belemnite. Zones delineated at right follow Anchukaitis and Horn (2005) and Kerr et al. (forthcoming).

4.11 Supplemental Information

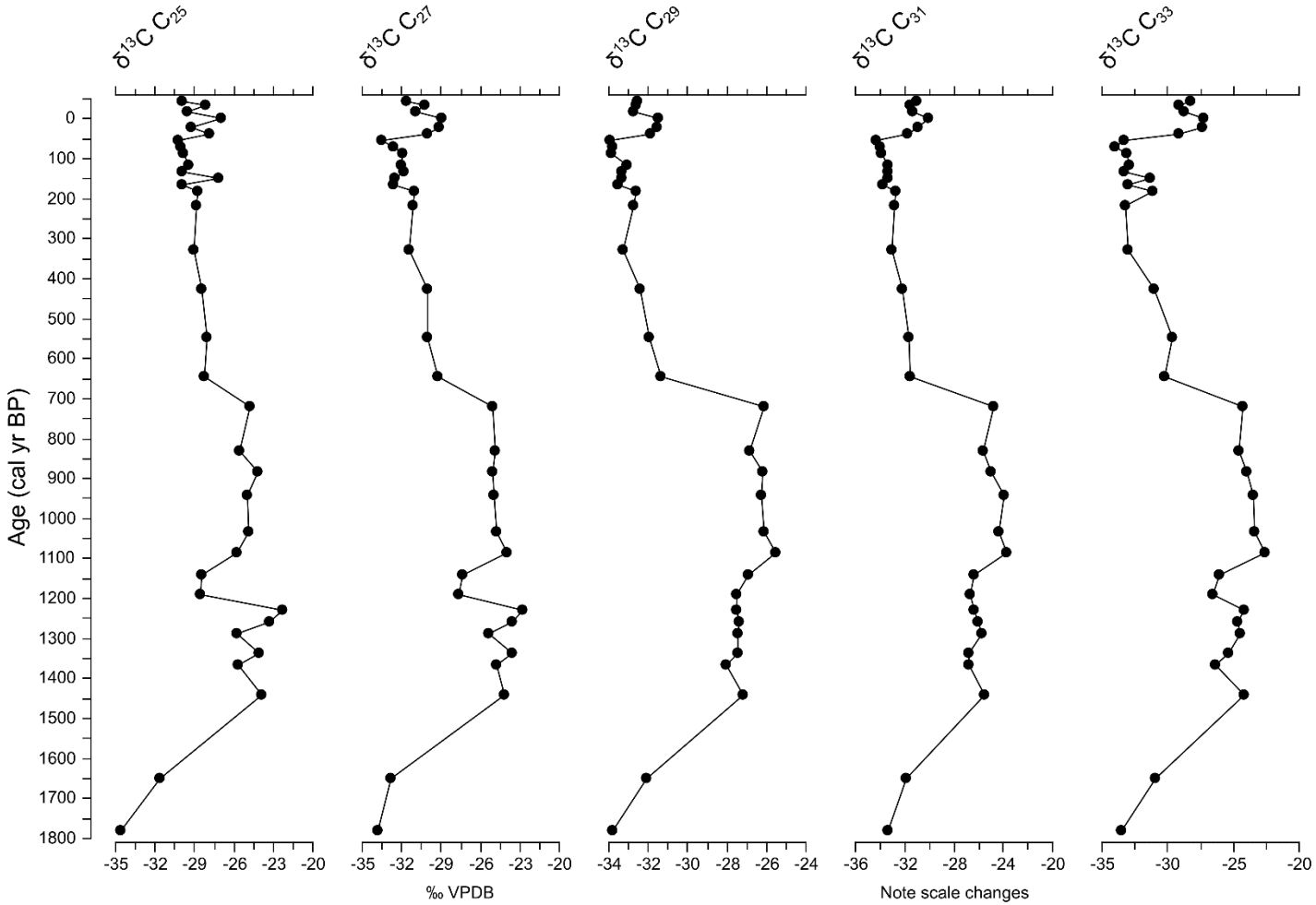

Fig. S4.1. *n*-alkane $\delta^{13}C$ values for odd numbered homologues C_{25} to C_{33}. Note changes to scale on the x-axes.

CHAPTER 5

SUMMARY AND CONCLUSIONS

5.1 Summary of Research

The dissertation research presented here (1) used compound-specific stable hydrogen (δD) isotope analysis of *n*-alkanes from terrestrial leaf waxes preserved in sediment cores to reconstruct variations in Holocene paleohydrology at three small lakes in Costa Rica; (2) developed paleoenvironmental reconstructions that unambiguously reflect climate in order to better understand relationships between climate, environment, and human activity in prehistory; and (3) developed some of the first long records of paleoprecipitation from Costa Rica and compared those records with paired evidence of vegetation change and fire history from the same sediment cores and with archaeological records of prehistoric human activity.

5.2 Major Conclusions

5.2.1 Hydrogen Isotope Analysis of Holocene Paleohydrology on Cerro Chirripó

At Lago de las Morrenas 1, this research revealed millennial-scale patterns and variations in hydroclimate over nearly 10,000 years on Costa Rica's highest peak. Conditions during the Early Holocene were characterized by dry climate, frequent fires, increased C_4 plants, and high lake levels. The Middle Holocene was marked by relatively wetter climate with little fire and continued high lake levels, followed by gradual drying and variable climate, low lake levels, and considerably more frequent fires. The Late Holocene was a time of dry climate with low lake levels and frequent fires. The Morrenas sediment core records local manifestations of several global-scale extreme climate events, including the 8200 yr BP event, the 5200 yr BP event, the Terminal Classic Drought, and the Little Ice Age. In general, Holocene hydroclimate at Morrenas 1 matches patterns seen in the broader circum-Caribbean and supports the idea that

climate in highland Costa Rica is intimately linked to forcing mechanisms and drivers of climate change on the Atlantic side of the Panamanian Isthmus.

5.2.2 Precipitation and Maize Agriculture in the Caribbean Lowlands of Costa Rica

At Laguna Bonillita, this research provides a 2700-year history of paleohydrology in the Central Atlantic Watershed of the Caribbean Lowlands. Bonillita experienced multiple episodes of significantly wetter and significantly drier than average hydroclimate during the Late Holocene, the timing of which match with other records from Costa Rica, Central America, and the wider circum-Caribbean. The Terminal Classic Drought and the Little Ice Age are both well-represented in the Bonillita record. The TCD was a time of climate instability in the watershed and was marked by multiple episodes of dry conditions, while the LIA was marked by a multi-century sustained period of dry conditions, matching other records from the circum-Caribbean. Although Bonillita saw episodes of both agricultural intensification and decline, the site was never abandoned and was inhabited by native maize agriculturalists moving inland under pressure from Spanish settlement along the coast during the Little Ice Age. As at the Morrenas site, the record from Bonillita shows that climate in the Caribbean lowlands was responding to Atlantic-side forcing mechanisms and drivers of change. Contrary to declines in culture and maize agriculture to the north in the Yucatan, the Caribbean lowlands of Costa Rica saw increases in maize agriculture during drying events, demonstrating that some drying is good for maize in generally wet tropical environments.

5.2.3 Precipitation and Maize Agriculture in Southern Pacific Costa Rica

At Laguna Santa Elena, this research demonstrates an 1800-year history of climate and environmental change that is temporally linked to major changes in cultural complexity in the Diquís archaeological subregion. As at our other sites, Santa Elena experienced multiple episodes of significantly wetter and significantly drier hydroclimate over the Late Holocene, including local manifestations of the Terminal Classic Drought and the Little Ice Age. Unlike at other sites in this dissertation and in research reported for the wider circum-Caribbean, the Santa Elena site was not extremely dry during the TCD and, in fact, experienced multiple episodes of wetter than average conditions during the interval of ca. 1200–850 cal yr BP. The first half of the LIA at Santa Elena was marked by average moisture conditions, while the second half was marked by unpredictability, with swings between wet and dry conditions. As at Bonillita, some drying was good for maize agriculture at Santa Elena. Declines in population and maize agriculture at Santa Elena took place during wetter than average conditions. Contrary to hypothesized teleconnections from the Atlantic side of Central America, hydroclimate forcing in southern Pacific Costa Rica appears to be somewhat out of sync with the broader circum-Caribbean, which may be due to a strong connection with Pacific-side climate dynamics that remains poorly understood.

5.3 Future Work

Ongoing and future work building on this project involves compound-specific isotope analysis on sediments from other lakes in Costa Rica and the wider circum-Caribbean. The goal is to build a network of sites using the same δD proxy to enable regional reconstruction of precipitation patterns and their comparison with paleoenvironmental and archaeological evidence

of human activity across the Holocene. These studies would be enhanced by continued and new work on the archaeology of the lake watersheds, as well as further examination of the δD proxy itself and its response to vegetation change. We also plan to write larger synthesis papers including other sites in our NSF project that are being investigated by other researchers.

VITA

Matthew T. Kerr was born in Seneca, Pennsylvania on February 19, 1979. He graduated from Cranberry Area High School in Seneca in 1997. He enlisted in the United States Army in May of 2001 and served two combat tours of duty in Operation Iraqi Freedom. He was honorably discharged from active duty in May of 2006.

He then attended the University of North Carolina Wilmington, where he graduated in 2012 *summa cum laude* with a Bachelor of Arts degree in Anthropology, a concentration in Archaeology, a minor in history, and honors in Anthropology. He became interested in archaeogeochemistry, stable isotope biogeochemistry, mass spectrometry, and prehistoric human-environment interactions during his studies. Matthew's undergraduate research, published in the *Journal of Archaeological Science*, focused on the Black Drink of the Southeastern Native Americans and caffeine in archaeological pottery residues.

Matthew entered the graduate program in geography at the University of Tennessee in 2012 and graduated in 2014 with a Master of Science degree, specializing in stable isotope analysis, prehistoric human-environment interactions, and paleoclimate. Matthew entered the PhD program in geography at Tennessee in 2014. His PhD specialty fields were Quaternary Environments and Prehistoric Human-Environment Interactions. Matthew completed his PhD in Geography in August of 2019. Throughout his years at Tennessee, Matthew was supported by research assistantships from the UT Initiative for Quaternary Paleoclimate Research and the National Science Foundation, and as a graduate teaching assistant and associate in the Department of Geography.

Matthew's dissertation research was supported by a Doctoral Dissertation Research Improvement grant from the National Science Foundation, the Oscar Roy Ashley Graduate

Fellowship from the University of Tennessee, a Phi Kappa Phi Dissertation Fellowship, multiple awards from the Stewart K. McCroskey Memorial Fund in the UT Department of Geography, and the Biogeography Specialty Group of the American Association of Geographers.